

FINAL REPORT
TO
GREAT LAKES NATIONAL PROGRAM OFFICE
UNITED STATE ENVIRONMENTAL PROTECTION AGENCY

MODELING THE BEHAVIOR AND FATE OF NUTRIENTS
AND TRACE CONTAMINANTS IN THE UPPER GREAT
LAKES CONNECTING CHANNELS

NOVEMBER 1987

INTERAGENCY AGREEMENT DW 13931213-01-0

BETWEEN

GREAT LAKES ENVIRONMENTAL RESEARCH LABORATORY
NATIONAL OCEANIC AND ATMOSPHERIC ADMINISTRATION
ANN ARBOR, MICHIGAN

AND

GREAT LAKES NATIONAL PROGRAM OFFICE
UNITED STATES ENVIRONMENTAL PROTECTION AGENCY
CHICAGO, ILLINOIS

U.S. Environmental Protection Agency
GLNPO Library Collection (PL-12J)
77 West Jackson Boulevard,
Chicago, IL 60604-3590

TABLE OF CONTENTS

	PAGE
EXECUTIVE SUMMARY	1
INTRODUCTION	6
REPORTS	
Unsteady Flow Model of Entire St. Clair River	8
J. A. Derecki, L. L. Makuch, and J. R. Brook	
St. Clair and Detroit River Current Measurements	92
J. A. Derecki, K. A. Darr, and R. N. Kelley	
Development of a Shallow Water Numerical Wave Model for Lake St. Clair .	135
D. J. Schwab and P. C. Liu	
Modeling Particle Transport in Lake St. Clair	145
D. J. Schwab and A. H. Clites	
Total Phosphorus Budget for Lake St. Clair: 1975 - 1980	161
G. A. Lang, J. A. Morton, and T. D. Fontaine, III	
Phosphorus Release from Sediments and Mussels in Lake St. Clair, with Notes on Mussel Abundance and Biomass	190
T. F. Nalepa, W. S. Gardner, and J. M. Malczyk	
Sediment Transport in Lake St. Clair	213
N. Hawley and B. Lesht	
Accumulation of Fallout Cesium-137 and Chlorinated Organic Contaminants in Recent Sediments of Lake St. Clair	289
J. A. Robbins and B. G. Oliver	
Toxicokinetics of Selected Xenobiotics in <u>Hexagenia limbata</u> : Laboratory Studies and Simulation Model	357
P. F. Landrum and R. Poore	
Modeling the Fate and Transport of Contaminants in Lake St. Clair . . .	386
G. A. Lang and T. D. Fontaine, III	

EXECUTIVE SUMMARY

The following points summarize the findings of our research:

Unsteady Flow Model of Entire St. Clair River

- This is the only flow model for the entire St. Clair River, including its extensive delta.
- Model provides for flow separation around islands in the upper river and through the main delta channels in the lower river.
- Three model versions provide information on river stages (profile), discharge, or velocities along preselected portions or the entire river. Daily or monthly tabulations of data with corresponding means can be furnished to users.
- The model furnishes hydrological data needed to compute contaminant mass balances.

St. Clair and Detroit River Current Measurements

- The measurements represent a unique time series of long-term, continuous velocity measurements in the Great Lakes connecting channels in the lake.
- The measurements permit evaluation of winter ice effects and weed effects during most of the year on the flows of the St. Clair and Detroit Rivers.
- The measurements permit evaluation of different types of current meters. Single-point, contact sensors (electromagnetic meters) present problems because of weed clogging effects; remote sensors (acoustic Doppler-shift meters) are ideally suited for use in the river but are expensive. The acoustic Doppler current profiler measures velocity distribution in the overhead vertical water column, which could not be duplicated with a string of point-measuring meters because of ice and navigation problems.
- The measurements provide data for adjusting winter flows in the St. Clair and Detroit Rivers.

Shallow Water Wave Model for Lake St. Clair

- A shallow water version of our deepwater wave model tends to underestimate the highest waves at all stations in the lake.
- The deep water version of the model provides quite acceptable estimates of waveheight, even for the largest waves at the shallowest stations and is therefore quite acceptable in Lake St. Clair.

- The wave model can be used to drive sediment resuspension in contaminant fate models.

Particle Transport Model for Lake St. Clair

- Although the average hydraulic residence time for Lake St. Clair is about nine days, residence times of water from individual tributaries range from 4 to over 30 days in the absence of wind.
- East winds greatly decrease the expected residence time of water from the Thames River, while northwest winds increase the residence time of water entering from the St. Clair Cutoff and St. Clair Flats.
- Based on circulation patterns generated by 6 months of real wind conditions, water entering the lake from the Thames River or one of the 3 lower St. Clair River channels has a large probability of mixing with waters of the eastern two-thirds of the lake.
- Flows from the upper St. Clair River channels and the Clinton River follow well-defined routes that are restricted to the western third of the lake.
- Circulation model predictions compare favorably with current measurements made by drifters and current meters in Lake St. Clair in 1985, although the model appears to be underestimating the current speeds.

Lake St. Clair Phosphorus Budget 1975 - 1980

- Lake Huron was the major source of phosphorus to Lake St. Clair, accounting for approximately 52% of the total annual load. Hydrologic area loads (diffuse and indirect point sources) contributed 43% of the total load. The remaining 5% came from the atmosphere, shoreline erosion, and direct point sources.
- The Thames and Sydenham areas of Ontario contributed 75% of the total hydrologic area load (92% of the total Canadian hydrologic area load). The Clinton and Black areas of the U.S. contributed 15% of the total hydrologic area load (83% of the total U.S. hydrologic area load). Eighty-five percent of the total hydrologic area load was from diffuse sources.
- Averaged over the six-year study period, estimated external loads were not significantly different from estimated outflow losses. Therefore, there does not appear to be a significant net internal source or sink of phosphorus in Lake St. Clair during 1975-80.

Sediment Phosphorus Dynamics and Mussel Populations

- Soluble reactive phosphorus release from Lake St. Clair sediments averaged 19 ugP/m²/day. This represents about 1% of the total bioavailable phosphorus load that annually enters the lake from other

sources. Mean maximum release was 47 ugP/m²/day, or about 2% of the annual bioavailable load from other sources.

- Mean mussel density was 2/m² and mean biomass was 4.3 gDW/m². Of the 20 species collected, Lampsilis radiata siliquodea and Leptodea fragilaris were the dominant forms, accounting for 45% and 13% of the total population. The former species was dominated by older individuals, which may indicate the population is declining.
- The mean excretion rate of phosphorus by mussels was 1.4 ugP/gDW/h. On a lake-wide basis, this amounts to 5% of the bioavailable load from other sources.

Sediment Transport in Lake St. Clair

- Sediment resuspension in Lake St. Clair is due primarily to wave action.
- The initiation of sediment resuspension can be predicted using a simple model with wave orbital velocity as the forcing function.
- Critical values of wave orbital velocity for resuspension range from 0.1 cm/s to 0.9 cm/s when calculated one meter above the bed.
- Variations in the critical orbital velocity may be related to substrate characteristics, but this cannot be proven with the data available.
- The orbital velocities are calculated from the wave field produced by the GLERL wave model. This model requires over-lake wind velocity measurements as input.

Cesium-137 and Chlorinated Organics in Lake St. Clair Sediments

- Eight percent of atomic fallout Cs-137 that entered Lake St. Clair mainly in the mid 1960s is still present in sediments 20 years later (1985).
- Comparison of total Cs-137 loading with 1985 Cs-137 storage indicates a sediment residence time of about 5 years. This is consistent with previously studied loss rates of mercury with chlorinated organics from the bottom. Changes in total storage of the radionuclide between 1976 and 1985, however, implies a longer residence time of about 15 years.
- Probably because of mixing and burial mechanisms, the residence time of this tracer and other contaminants appears to increase over time.
- Resuspension of sediments is continuing to supply radiocesium to the water where it is exported from the lake.
- Chlorinated organic compounds, like Cs-137, are associated with fine sediments and preferentially deposit in the deepest water.

- The sediments presently contain nearly 1 metric ton of HCB and PCBs and 0.2 metric tons of OCS, far higher contaminant masses than those found in the St. Clair River.
- Based on the behavior of Cs-137, crude estimates of total particle-associated contaminant loads to Lake St. Clair are: HCB, 15 MT; QCB, 2.8 MT; HCBd, 3.3 MT; OCS, 4.3 MT; PCBs, 20 MT; total DDT, 5.4 MT.

Hexagenia and Contaminants

- Hexagenia are an important food source for fish in the connecting waterways of the Great Lakes. Because of Hexagenia's position in the foodweb, their losses due to toxic effects of contaminants, or their bioaccumulation of contaminants and subsequent transfer to fish, are important topics to study.
- Contaminant uptake and depuration rates of Lake St. Clair Hexagenia limbata vary seasonally. A simulation model suggests that temperature mediated changes in the depuration rate constant is the term responsible for most of the seasonal variation.
- The contaminant accumulation rate constant of Hexagenia limbata is similar to that of other Great Lakes invertebrates, but its depuration rate constant is much larger.
- Hexagenia limbata obtain a greater percentage of their contaminant body burden from the sediment than do other Great Lakes invertebrates.

Generic Contaminant Fate and Transport Modeling

- A multi-segment model to simulate the distribution and transport of contaminants in Lake St. Clair was developed based on the EPA's Chemical Transport and Fate Model TOXIWASP. The model segmented Lake St. Clair into 126 well-mixed segments: 42 water segments, 42, active sediment layer segments, and 42 deep sediment layer segments.
- Simulations of the fate and behavior of chloride, cesium-137, and the organic contaminants octachlorostyrene (OCS) and polychlorinated biphenyls (PCB) were carried out.
- The ability of the model to accurately predict the movement and concentrations of a conservative tracer was substantiated using chloride data gathered during four, 1974 cruises.
- The ability of the model to accurately predict the distribution and concentrations of highly partitioned contaminants was tested with Cesium-137 data. Through calibration of the spatially-varying organic carbon content of the sediments, the model matched the magnitude and distribution of observed 1976 cesium-137 in surficial (0-2 cm) sediments. The calibrated sediment organic carbon content values ranged from 0.14% to 5% (areal mean = 1.27%) and are well within the range and spatial distribution of observed values. Simulations were continued out to 1985

for model verification purposes. The predicted distribution of sediment-bound Cs-137 in the active layer compared well with the observed 1985 values.

- Using an estimated load (1.9 lbs/d) of OCS to Lake St. Clair, the model was run until simulated OCS levels in the active layer (0-10 cm) agreed with observed 1983 values. This occurred at 4500 days and implies that OCS loadings began in the latter part of 1970. This result is consistent with speculation that OCS was introduced to the lower Great Lakes beginning in the 1970s. The model predicted 1983 mean and maximum OCS sediment concentrations of 3.8 and 23.1 $\mu\text{g/kg}$, respectively. These compare with observed values of 2.7 and 26.2 $\mu\text{g/kg}$. The model predicted 1983 active layer bio-bound OCS levels of 0-96 $\mu\text{g/kg}$ dry weight, with a mean concentration of 20 $\mu\text{g/kg}$. The observed range was 2-154 $\mu\text{g/kg}$ dry weight (mean = 43 $\mu\text{g/kg}$) measured in whole clam tissue collected in 1983.
- Using observed 1970 PCB levels as initial conditions and an estimated PCB load (5.1 lb/d), the model accurately predicted the 1974 PCB sediment (0-2 cm) concentrations in Anchor Bay and open-lake sediments. However, the model tended to overpredict the PCB values along the eastern and western segments of the main lake, which may indicate additional or increased PCB sources in these areas. The data showed a decline in mean lake-wide sediment concentration of total PCB from 19 $\mu\text{g/kg}$ (max. = 40 $\mu\text{g/kg}$) in 1970 to 10 $\mu\text{g/kg}$ (max. = 28 $\mu\text{g/kg}$) in 1974. The model simulated a similar 4 year decline in mean sediment concentration from 19.8 to 8.7 $\mu\text{g/kg}$ (max. from 39 to 26 $\mu\text{g/kg}$). The model predicted a 1974 mean active layer bio-bound PCB concentration of 97 $\mu\text{g/kg}$ dry wt. (range = 31-212 $\mu\text{g/kg}$). This compares with observed mean values of 90.6 and 44.2 $\mu\text{g/kg}$ dry wt. (Aroclors 1254 and 1260, respectively) measured in whole clam tissue in 1983.

INTRODUCTION

The Upper Great Lakes Connecting Channels Study (UGLCCS) is a multi-agency, multi-national study of the St. Marys River, the St. Clair River, Lake St. Clair, and the Detroit River. The goals of the study include:

1. Determining the present environmental status of the study area;
2. Identifying and quantifying sources of ecosystem degradation in the study area;
3. Assessing the adequacy of existing or planned control programs;
4. Developing long-term monitoring programs for assessing the effectiveness of control programs;
5. Facilitating the development of remedial action plans by the the Province of Ontario and the State of Michigan.

Towards accomplishing these goals, the Great Lakes Environmental Research Laboratory (GLERL) of the National Oceanic and Atmospheric Administration (NOAA) designed modeling, field, and laboratory studies of the connecting channels study area and processes therein. Through the Activities Integration Committee or other less formal avenues, GLERL's studies were carefully coordinated with proposed or ongoing studies of other agencies in order to maximize scientific insights. A cross reference showing the correspondence between GLERL's studies and UGLCCS activity numbers is provided in Table 1. In some cases the GLERL studies were associated with more than one of the UGLCCS activities.

As part of the NOAA - EPA interagency agreement, GLERL provided the Great Lakes National Program Office (GLNPO) with written quarterly reports describing progress towards meeting the goals of the study, and oral presentations summarizing each year's work. Scientists at GLERL are presently submitting the results of their work to professional scientific journals. This draft final report documents research conducted during the entire interagency agreement period, December 1, 1984 through November 30, 1987

Table 1. Correspondence of GLERL Activities with UGLCCS Activities.

GLERL Activity	UGLCCS Activity No.
Unsteady Flow Model of Entire St. Clair River	C.5
St. Clair and Detroit River Current Measurements	C.5
Development of a Shallow Water Numerical Wave Model for Lake St. Clair	C.2
Modeling Particle Transport in Lake St. Clair	C.2
Total Phosphorus Budget for Lake St. Clair: 1975 - 1980	C.1
Phosphorus Release from Sediments and Mussels in Lake St. Clair with Notes on Mussel Abundance and Biomass	H.20
Sediment Transport in Lake St. Clair	G.3
Accumulation of Fallout Cesium-137 and Chlorinated Organic Contaminants in Recent Sediments of Lake St. Clair	G.1,G.2
Toxicokinetics of Organic Xenobiotics in the <u>Hexagenia limbata</u> : Laboratory Studies and Simulation Model	H.16
Modeling the Fate and Transport of Contaminants in Lake St. Clair .	C.1,C.2,C.3

UNSTEADY FLOW MODEL OF ENTIRE ST. CLAIR RIVER

Jan A. Derecki, Laura L. Makuch, and Jeffrey R. Brook

ABSTRACT

This report describes the development and calibration of an unsteady flow model for the entire St. Clair River, from Lake Huron to Lake St. Clair, to simulate hourly and daily flow rates. Unlike previous St. Clair River hydraulic models that are limited to the upper single-stem river channel, the present model versions (hourly or daily) provide flow separation around Stag and Fawn Islands in the upper and middle river, and through the main delta channels (North, Middle, South, and Cutoff) in the lower river. The model provides three options for simulation of the river stages (profile), discharge, or velocities, respectively. This information is needed in order to predict the fate and transport of pollutants in the entire river channel, including the island and delta obstructions to its flow. The model can be run for the entire river or any preselected river reach bounded by water level gages.

INTRODUCTION

A series of hydrodynamic models have been developed and used extensively at the Great Lakes Environmental Research Laboratory (GLERL) to

Consequently, interest in and applications of model-simulated flows are expanding from total flow rates to flow distribution and localized effects.

The principal goal of this Upper Great Lakes Connecting Channels Study (UGLCCS) activity was to develop the hydrodynamic models for selected upper connecting channels of the Great Lakes. The St. Clair River was selected because it forms the upper portion of the outlet through the St. Clair River - Lake St. Clair - Detroit River system from the upper Great Lakes (Superior, Michigan, and Huron). This unsteady flow model of the entire St. Clair River, from Lake Huron to Lake St. Clair, provides flow separation around Stag and Fawn Islands in the upper and middle river, and through the main delta channels of the North, Middle, and South Channels and the St. Clair Cutoff in the lower river (Figure 1). The forcing functions in the model are the river stages recorded at the water level gages enclosing preselected river reaches (entire river or longitudinal segments). These water levels from the extreme gage locations form the model's boundary conditions.

MODEL DEVELOPMENT

The present unsteady flow model for the entire St. Clair River is an extension and modification of the existing GLERL upper river model versions. All these models are driven by water level data taken from appropriate water level gages along the river. The present model also uses the St. Clair Shores gage in Lake St. Clair to indicate water levels at the mouth of the

river. To permit near real-time model applications only the official National Oceanic and Atmospheric Administration (NOAA) water level gage data available at GLERL are used in the model.

Unsteady Flow Equations

The unsteady flow model is based on complete one-dimensional partial differential equations of continuity and momentum. The momentum equation includes the effects of motion but neglects the effects of wind stress and ice. Except for short periods associated with storms, the wind stress effects were found to be generally insignificant on the St. Clair River flows in a previous study (Derecki and Kelley, 1981) and the wind data are normally not available for real-time applications. The effects of transient ice flows and resulting ice jams in the lower river are significant and may be substantial during winter and early spring in the St. Clair River. However, no tested method for including these effects is presently available.

Expressed in terms of flow Q and stage Z above a fixed datum, the equations of continuity and motion are as follows:

$$\frac{\partial Z}{\partial t} + \frac{1}{T} \frac{\partial Q}{\partial X} = 0 \quad (1)$$

$$\frac{1}{A} \frac{\partial Q}{\partial t} - \frac{2QT}{A^2} \frac{\partial Z}{\partial t} + \left(g - \frac{Q^2 T}{A^3} \right) \frac{\partial Z}{\partial X} + \frac{g n^2 Q / Q}{2.208 A^2 R^{4/3}} = 0 \quad (2)$$

where X = discharge in the positive flow direction

t = time

A = channel cross-sectional area

T = top width of the channel at the water surface

g = acceleration due to gravity

R = hydraulic radius

n = Manning's roughness coefficient

∂ = partial derivative function

// = absolute value.

Channel definition is shown in Figure 2. Equations (1) and (2) were placed in finite difference form at point M in an X-t grid (Figure 3) to yield respectively,

$$\frac{Z_u' + Z_d' - Z_u - Z_d}{2 \Delta t} - \frac{\theta (Q_d' - Q_u') + (1-\theta) (Q_d - Q_u)}{T \Delta X} = 0 \quad (3)$$

$$\frac{Q_u' + Q_d' - Q_u - Q_d}{2 \bar{A} \Delta t} - \frac{\bar{Q} T (Z_u' + Z_d' - Z_u - Z_d)}{\bar{A}^2 \Delta t} +$$

$$\frac{(g - \bar{Q}^2 T)}{\bar{A}^3} - \frac{\theta [(Z_d' - Z_u') + (1-\theta)(Z_d - Z_u)]}{\Delta X} +$$

$$\frac{gn^2 \bar{Q} / \bar{Q}}{2.208 \frac{\bar{Q}^{4/3}}{A R}} = 0 \quad (4)$$

where a prime indicates location and overbars indicate mean, such that

$$\theta = \frac{\Delta t'}{\Delta t} \quad (5)$$

$$Q = 0.5 [\theta (Q_u' + Q_d') + (1-\theta) (Q_u + Q_d)] \quad (6)$$

$$\bar{A} = 0.5 [\theta (A_u' + A_d') + (1-\theta) (A_u + A_d)] \quad (7)$$

Solution of equations (3) and (4) by the implicit method forms the basis of the numerical unsteady flow model. A stable solution for these equations is provided by the weighting coefficient θ , which was selected empirically (Quinn and Wylie, 1972) to be 0.75. Application of the equations at the river's cross-sections selected to define the actual river channel produces a set of nonlinear equations that are solved simultaneously with linear approximations by the Newton-Raphson numerical iteration procedure. In the initial St. Clair River model version an idealized river channel, based on averaged river cross-sections for selected reaches, was used. The use of idealized river channel simplifies simulation of discharge but prevents valid velocity determination. Description of the initial St. Clair River model, including calibration, sensitivity analysis, program listings, and output samples, are given by Quinn and Hagman (1977). The initial model has been revised by Derecki and Kelley (1981) to replace the idealized river channel with the actual configurations of the river and to include wind stress effects.

Mathematical Solution

A schematic diagram for the entire St. Clair River model, including its delta, is shown in Figure 4. The model can be run for any river reach containing at least three NOAA water level gages by specifying gage locations for the beginning and ending boundaries of the reach; the mid-gage

is used to check the accuracy of the computed river profile by comparing deviations between computed and measured water levels. In the previous St. Clair River models the mathematical solution of the model equations was provided by using banded matrix, which is most efficient for solving single-channel configurations.

However, this matrix is impractical for solving flow separations and was replaced with sparse matrix in the present model. The Yale Sparse Matrix package available in the GLERL computer library is used in the model. All the St. Clair River model versions are the hydraulic transient models, which differ from standard profile or backwater computations; the hydraulic transient models include time dependent terms of mass continuity and momentum, which allows the simulation of wave propagation as well as profiles along the river.

Initial work on the new delta-model development included extending the existing single-stem upper river model through the middle river (St. Clair to Algonac), with modification to provide flows around the Stag and Fawn Islands.

Computations for continuity and momentum around an island start at the downstream channel junction or node, proceed along one side of the island to a breakpoint section just below the upstream node, then return to the other side of the island and proceed to its breakpoint; the breakpoints are then combined at the upstream node and the computations continue upstream in the single-stem channel (Figure 5). Because of mass continuity at the nodal

points, representing channel separation or confluence, the water level is the same for the joint and separate channels, and the flow in the joint channel is the sum of flows in separate channels. This provides additional continuity equations for the water surface and flows at the nodes, which are listed below.

$$WS_n = WS_{s1} = WS_{s2} \quad (8)$$

$$Q_n = Q_{s1} + Q_{s2} \quad (9)$$

The island-model version was extended to Lake St. Clair by treating the upper delta as an island and the lower delta as a composite of two islands with separate channels. The composite delta islands are terminated with short imaginary channels in the lake. This treatment of delta flow distribution provides separation of flows through the North Channel and South Channel in the upper delta, and consequent respective separation through the lower North and Middle Channels, and the lower South and St. Clair Cutoff Channels in the lower delta, covering all the main delta channels. To help the program converge on a solution more quickly, the initial flow values around the islands and the delta are provided in the model. These initial flows are the fixed percentages of the normal total flow, based on existing measurements. Nearly all gages used in the model were moved at various times and some with more recent moves may have different numbers specified in the model. Occasionally, a gage in the same location may have experienced a vertical movement, due to some corrective measure performed on the gage; such corrections for the vertical movement

are also specified in the model. These corrections are based on results determined in previous studies and are included in previous model versions, where appropriate. Because all physical and hydraulic input data are in English system, the basic model computations are performed in the English units and the final result-output converted to the SI system of units, if desired.

To initialize the computations the model is operated until a steady state is achieved, prior to simulation of actual data. This is accomplished by successive iterations of the continuity and momentum equations in their discrete form (finite difference) until an acceptable tolerance is attained.

Based on previous models, the number of this "steady state" iterations is preset at 12. Occasionally, the water level gages break down providing erroneous or no water level records. However, these records are necessary for the gages forming the model's boundary conditions. To permit initiation of computations the missing data are estimated from long-term means (or previous values within the run), which most likely would not be sufficiently accurate. Initiation of computations in such cases may require unreasonably large number of iterations to achieve "fictitious" steady state (with erroneous results), and the preset number of 12 iterations eliminates such possibility. To make the user aware of possible inaccuracies (along with causes), all partial or missing/estimated water level inputs are flagged in the model outputs.

Model computations are performed for each river reach between successive sections used to define the river channel. For the entire river, with the delta, this involves 180 cross-sections of the river channel. Input data for these computational reaches are obtained by averaging records of the successive bounding sections. Except for the starting and ending reaches, each reach contains four unknowns, which are the upstream and downstream water surfaces and flows. The starting and ending model reaches contain three unknowns because the upstream and downstream sections in these reaches, respectively, correspond to the water level gages with known water surfaces (model's boundary conditions). The model equations are set-up in the sparse matrix as alternating rows of continuity (odd rows) and momentum (even rows) equations, as shown in Figure 6. The matrix non-zero values are indicated by X's and are the partial derivatives of the equations for indicated rows with respect to the variables in indicated columns. The partial derivatives of the continuity and momentum equations with respect to water surface and flow are listed below.

$$\frac{\partial C}{\partial Z_u'} = \frac{1}{2 \Delta t} \quad (10)$$

$$\frac{\partial C}{\partial Z_d'} = \frac{\partial C}{\partial Z_u'} \quad (11)$$

$$\frac{\partial C}{\partial Q_u'} = \frac{\theta}{T \Delta X} \quad (12)$$

$$\frac{\partial C}{\partial Q_d'} = - \frac{\theta}{T \Delta X} \quad (13)$$

$$\frac{\partial M}{\partial Z_{u'}} = \frac{\bar{Q} T}{\bar{A} \Delta t} + (g - \frac{\bar{Q} T}{\bar{A}}) \cdot \frac{\theta}{\Delta X} \quad (14)$$

$$\frac{\partial M}{\partial Z_{d'}} = \frac{\bar{Q} T}{\bar{A} \Delta t} - (g - \frac{\bar{Q} T}{\bar{A}}) \cdot \frac{\theta}{\Delta X} \quad (15)$$

$$\frac{\partial M}{\partial Q_{u'}} = \frac{1}{2 \bar{A} \Delta t} - \frac{\theta T (Z_{u'} + Z_{d'} - Z_u - Z_d)}{2 \bar{A} \Delta t}$$

$$\frac{\theta \bar{Q} T [\theta (Z_{u'} - Z_{d'}) + (1 - \theta)(Z_u - Z_d)]}{\bar{A} \Delta X} +$$

$$\frac{\theta g n \bar{Q}^2}{2.208 \bar{A} R^{4/3}} \quad (16)$$

$$\frac{\partial M}{\partial Q_{d'}} = \frac{\partial M}{\partial Q_{u'}} \quad (17)$$

MODEL CALIBRATION

Model Scope

As mentioned in the preceding discussion, the model has two versions (with separate programs) for the simulation of hourly or daily river profiles and resulting flows. The model can be operated for the entire river, with separation of flows around the upper river islands and through the main delta channels in the lower river, or for any river reach bounded

by NOAA water level gages, which form the model's boundary conditions (a minimum of three gages are employed, with the mid-gage used to provide a check on simulation accuracy). Because all river profile and flow information for the entire river will not fit on a computer page, three separate options are provided for the river stages, discharge, and velocities, respectively.

Hydraulic Parameters

The hydraulic parameters needed to operate the model are the river stations, the top channel widths, the datum reference elevations, and the base areas below the datum for each section used to define the river channel. Because of the large number of sections (180), printout of this information is normally suppressed in the model output but is contained in the program and can be easily reinstated. Other hydraulic parameters needed to run the model are the water surface elevations for the water level gages and the roughness coefficients for the river reaches bounded by successive water level gages (8). All other data needed in the computations (total channel area, hydraulic radius, length of river reaches, etc.) are determined from the above data.

Model Calibration

Calibration of the model consisted of adjusting the roughness coefficients of the river channel, which is the unknown in the flow equation during periods of flow measurement. The channel roughness coefficients

were determined for each river reach bounded by successive water level gages, with separate coefficients for the North and South delta channels, for a total of 8. The roughness coefficients were derived from 14 sets of flow measurements on the St. Clair River conducted by the Corps of Engineers during 1959-77. The equation used to compute the roughness coefficients is the Manning equation, which is

$$n = \frac{1.486 A R^{2/3}}{Q} \cdot \left(\frac{Z_u - Z_d}{L} + \frac{Q \Delta A}{g L A^3} \right) \quad (18)$$

The relationships between computed roughness coefficients for the 8 successive river reaches and either upstream or downstream river stages are shown in Figures 7-14. These relationships normally represent the best-fit lines derived by regression (least squares) for graphs indicating slope or the arithmetic means for graphs in which plotted data did not indicate any slope.

Thus, the roughness coefficient graphs for the upstream reaches (FG-DP and DP-MBR) indicate positive slope; those for most of the single-channel river (MBR-DD, DD-MV, MV-SC, and SC-AL) indicate no slope or change in channel roughness with water level elevation; both delta reaches are between AL-SCS but are designated AL-ND and AL-SD to indicate north and south delta channels, respectively, and show negative slopes. In the lower delta four separate channels are actually used but there were insufficient data to derive separate roughness coefficients. The downstream river channel, from the St. Clair City through the delta, was affected by regimen changes

between 1959-63, when extensive dredging was conducted for navigation improvements. For these downstream reaches separate roughness coefficients were derived for each regime, representing pre-project conditions (through 1963) and current conditions (starting in 1964). These and other St. Clair River regimen changes are extensively analyzed and documented in various studies (Derecki, 1985). The computed roughness coefficients actually represent channel roughness and combined effect of possible errors, such as those in flow measurements and determination of channel parameters, and the computed coefficients for some reaches were modified somewhat when such change was strongly indicated during the model calibration process. Thus, calibrated roughness does not always represent the best-fit line for plotted data (Figures 9 and 11). The calibrated roughness coefficients for the 8 river reaches are summarized in Table 1.

The Ft. Gratiot and St. Clair water level gages were moved in 1970, with apparent uncompensated hydraulic effects. These effects were determined from a comparison study as a 0.055 m (0.18 ft) reduction for the Ft. Gratiot gage levels and a 0.027 m (0.09 ft) increase for the St. Clair gage levels (Quinn, 1976). The Ft. Gratiot gage was modified again in 1981, following blockage of its intake by silt, with apparent uncompensated hydraulic effect which was determined as an increase in its elevation of 0.037 m (0.12 ft) from the preceding period (Derecki, 1982). Thus, effective Ft. Gratiot uncompensated hydraulic effect was decreased in 1981 to a reduction of 0.018 m (0.06 ft) in the gage levels. These vertical gage-record corrections are included in the model to provide unbiased continuation of the water levels at the gages.

Computer Programs

The St. Clair River model for the entire river, with flow separation around islands and through main delta channels, uses water level data from GLERL computer disk pack files (VAX), as did preceding models. Two generalized versions of the model for simulating hourly and daily flow rates, respectively, were prepared and stored in the computer files. These model versions operate on hourly or daily computational time scales and provide summary tables for daily or monthly data, respectively. Each model version has three options for the output of simulated river stages at the gage locations and the total discharge or average velocities at selected points, as well as separate values around islands and through the delta. Separate output options were provided since all this information would not fit on a single computer page. A check of model accuracy is provided in a form of water level deviations between computed and measured water levels at the water level gage sites. Basic model computations are listed in the program in English units; the final results are printed in either English or SI units, as specified in the output option. The hourly and daily model versions are listed in the Appendix as Figures A-15 and A-16, respectively. Examples of model outputs for the water levels, discharge, and velocity options are shown in the Appendix Tables A-1 through A-3 for the hourly model, and Tables A-4 through A-6 for the daily model, respectively.

CONCLUSIONS

This model was developed to correct or eliminate the shortcomings of previous model versions. It simulates the St. Clair River profile either for the entire length of the river or for selected segments, and provides an accuracy check for the computed profile at the water-level-gage locations. The model simulates flows (discharge or velocity) in all the more important river channels, providing flow separation around the islands in the upper and middle river, and through the main delta channels in the lower river. As such, it should become a valuable tool for both hydraulic and other water resource studies in the upper Great Lakes basin.

ACKNOWLEDGEMENT

The authors gratefully acknowledge work performed by D. L. Schultz in the initial phases of model development.

LITERATURE CITED

- Derecki, J.A., 1982. Effect of the 1981 Fort Gratiot gage modifications on the hydraulic regime of the St. Clair River. GLERL Open File Report, NOAA, Great Lakes Environmental Research Laboratory, Ann Arbor, MI, 3pp.
- Derecki, J.A., 1985. Effect of channel changes in the St. Clair River during the present century. Journal of Great Lakes Research, 11(3):201-207.
- Derecki, J.A., and R.N. Kelley, 1981. Improved St. Clair River dynamic flow models and comparison analysis. NOAA Tech. Memo. ERL GLERL-34, NOAA Great Lakes Environmental Research Laboratory, Ann Arbor, MI, 36 pp.
- Quinn, F.H., 1976. Effect of Fort Gratiot and St. Clair gage relocations on the apparent hydraulic regime of the St. Clair River. GLERL Open File Report, NOAA Great Lakes Environmental Research Laboratory, Ann Arbor, MI, 7pp.
- Quinn, F.H., and J.C. Hagman, J.C., 1977. Detroit and St. Clair River transient models. NOAA Tech. Memo. ERL GLERL-14, NOAA Great Lakes Environmental Research Laboratory, Ann Arbor, MI, 45 pp.

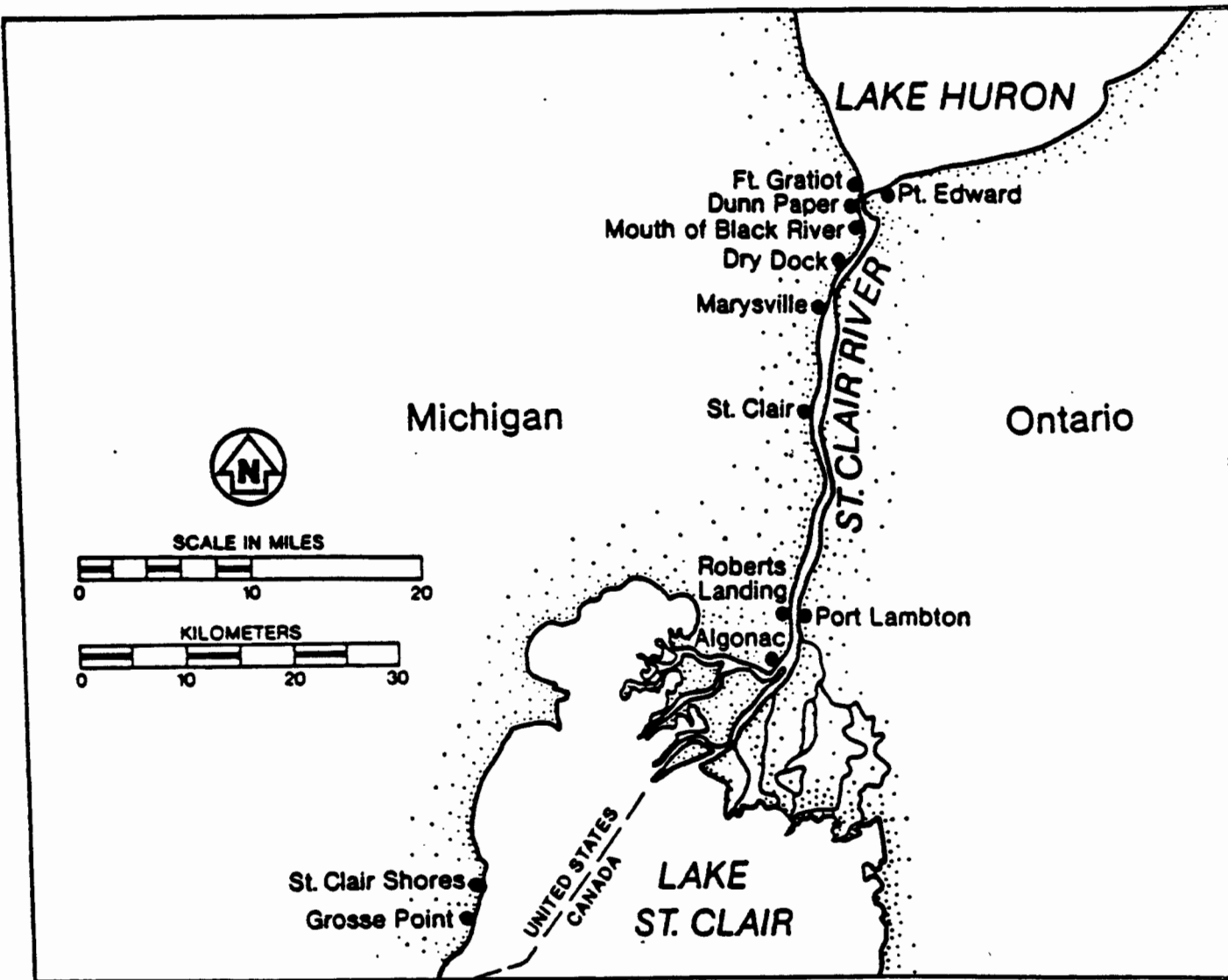
Quinn, F.H., and E.B. Wylie, 1972. Transient analysis of the Detroit River by the implicit method. Water Resources Research, 8(6):1461-1469.

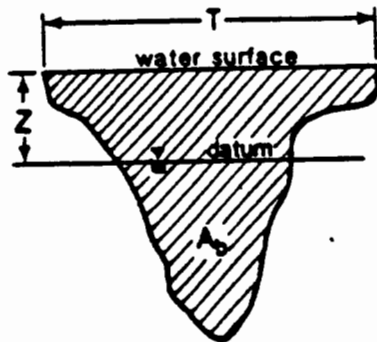
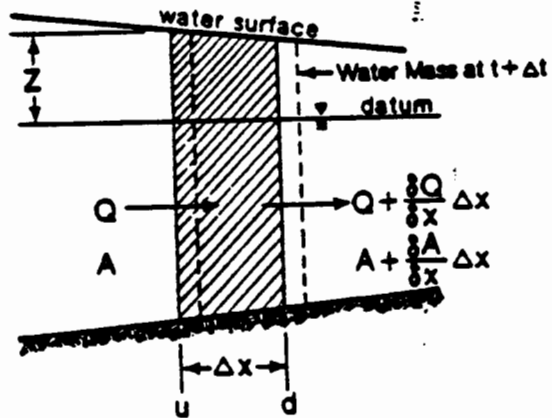
TABLE 1. Roughness coefficients for the St. Clair River reaches.

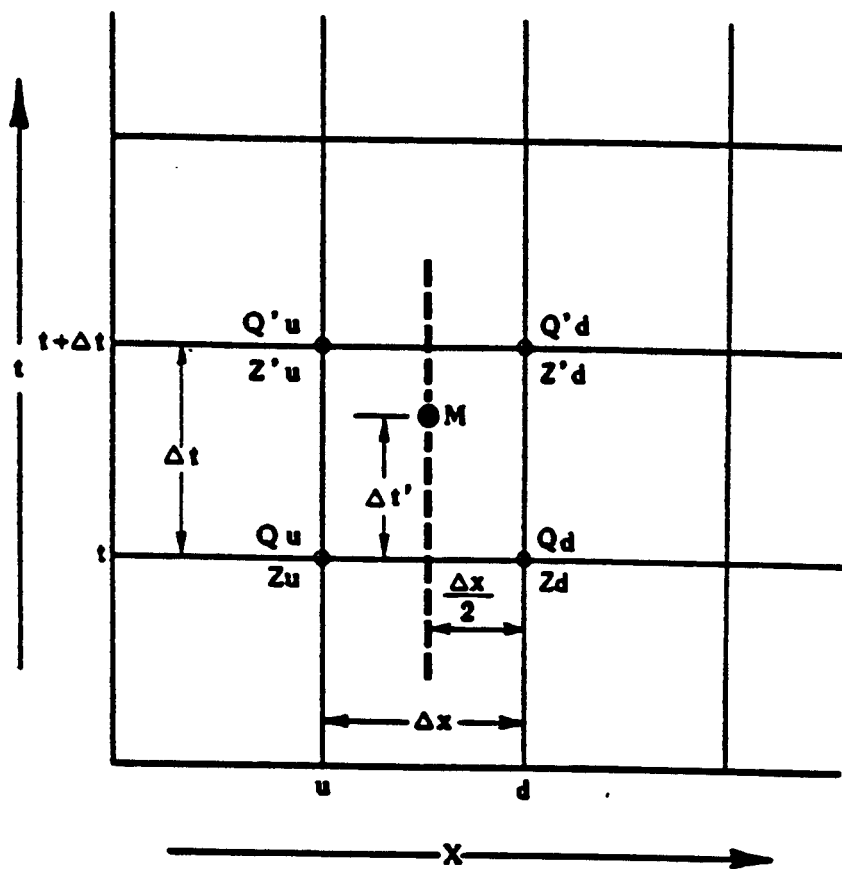
Reach	Roughness coefficients (n)
FR-DP	n = 0.0033947 (FG) - 1.92253
DP-MBR	n = 0.0002708 (DP) - 0.12683
MBR-DD	n = 0.0221
DD-MV	n = 0.0250
MV-SC	a. Current regime (starting 1964): n = 0.0240 b. Pre-project regime (through 1963): n = 0.0260
SC-AL	a. Current regime: n = 0.0230 b. Pre-project regime: n = 0.0235
AL-ND	a. Current regime: n = -0.0017647 (SCS) + 1.04729 b. Pre-project regime: n = -0.0053707 (SCS) + 3.11427
AL-SD	a. Current regime: n = -0.0011146 (SCS) + 0.66250 b. Pre-project regime: n = -0.0032907 (SCS) + 1.90968

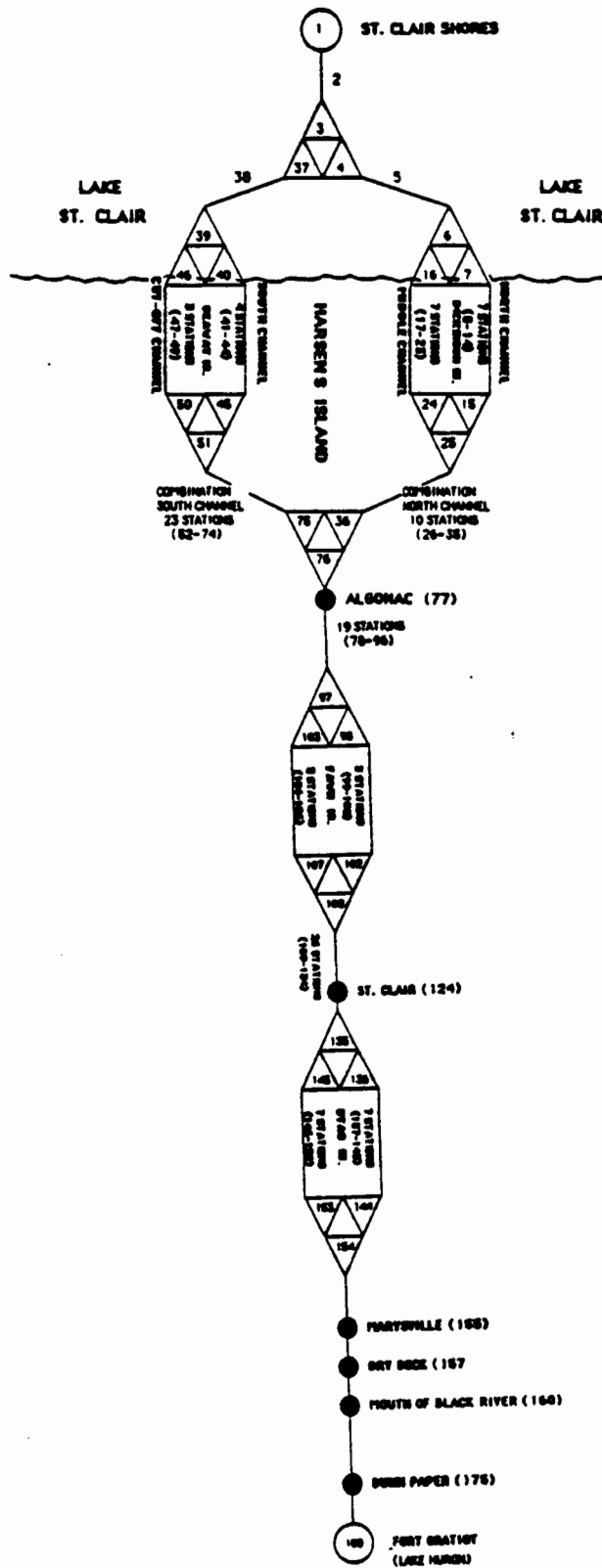
LIST OF FIGURES

1. St. Clair River with location of water level gages.
2. Channel definition sketch.
3. X-t grid for the implicit method.
4. Schematic model diagram.
5. Representation of an island.
6. Sparse matrix.
7. Roughness coefficient for FG-DP reach.
8. Roughness coefficient for DP-MBR reach.
9. Roughness coefficient for MBR-DD reach.
10. Roughness coefficient for DD-MV reach.
11. Roughness coefficient for MV-SC reach.
12. Roughness coefficient for SC-AL reach.
13. Roughness coefficient for AL-ND reach.
14. Roughness coefficient for AL-SD reach.

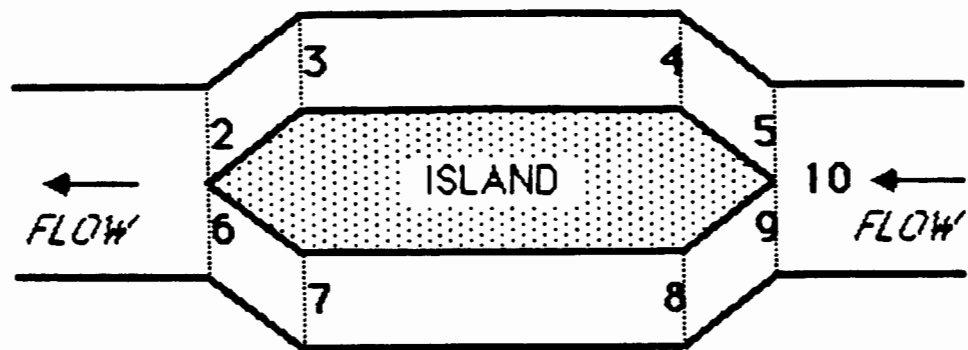




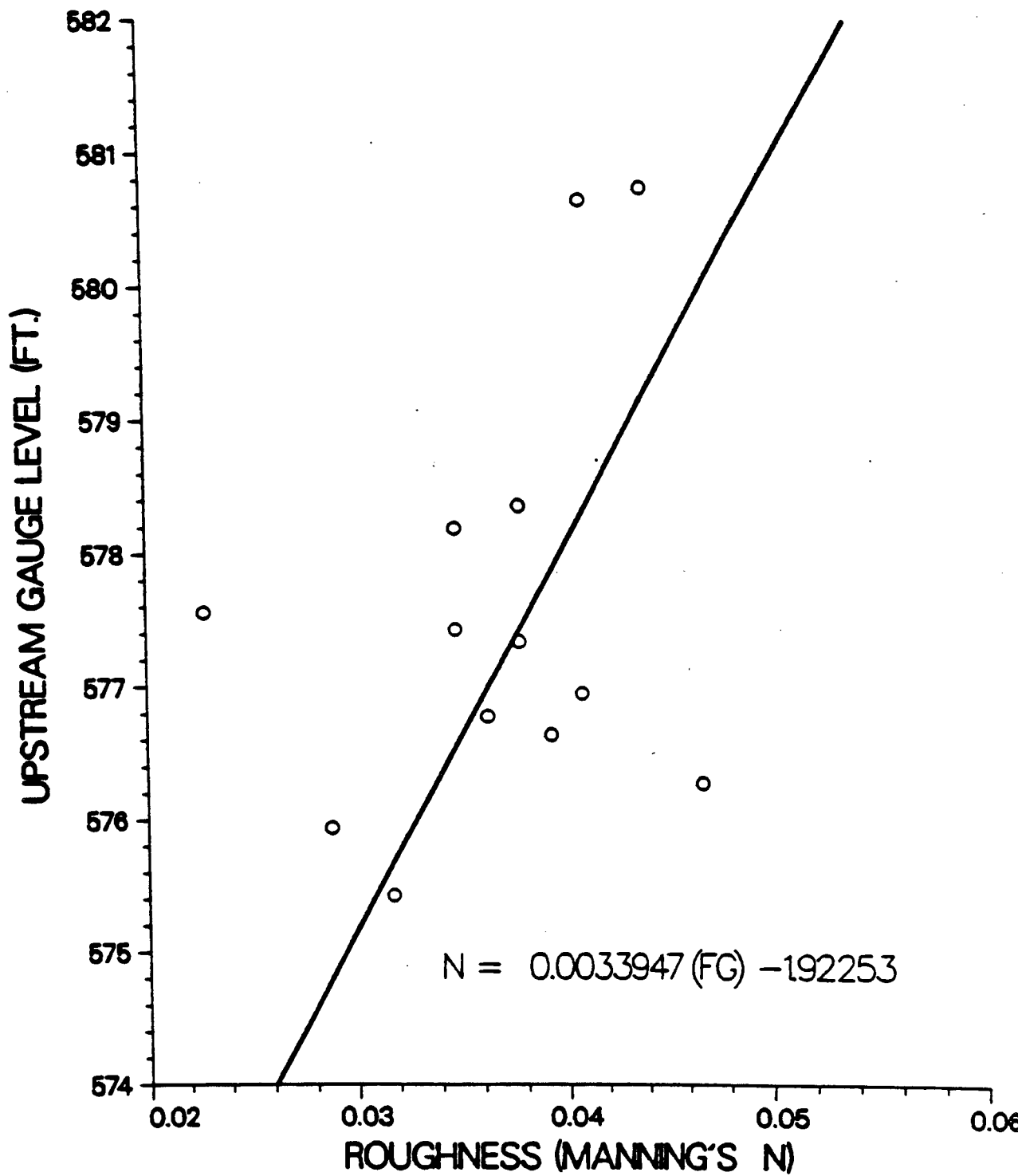


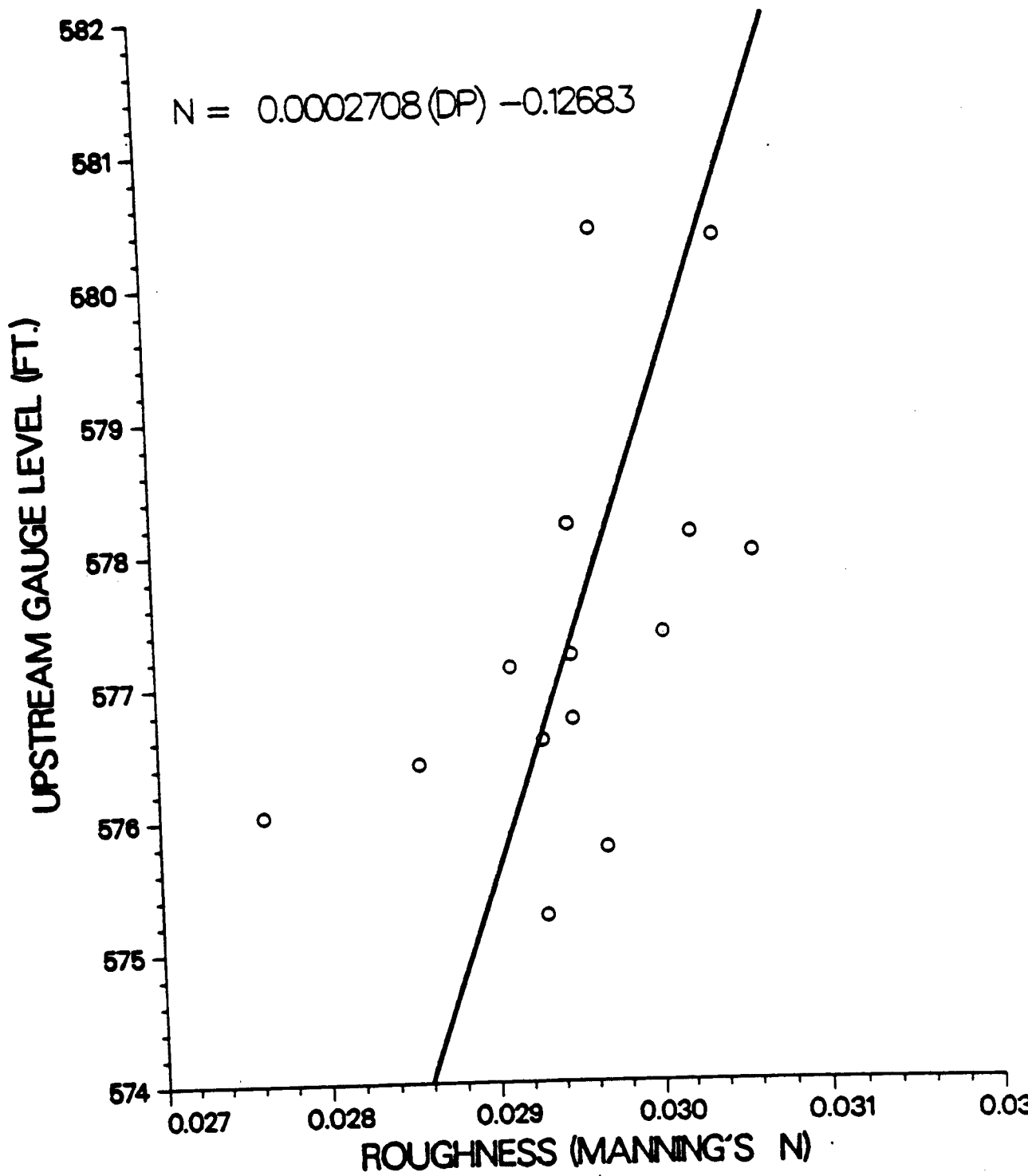


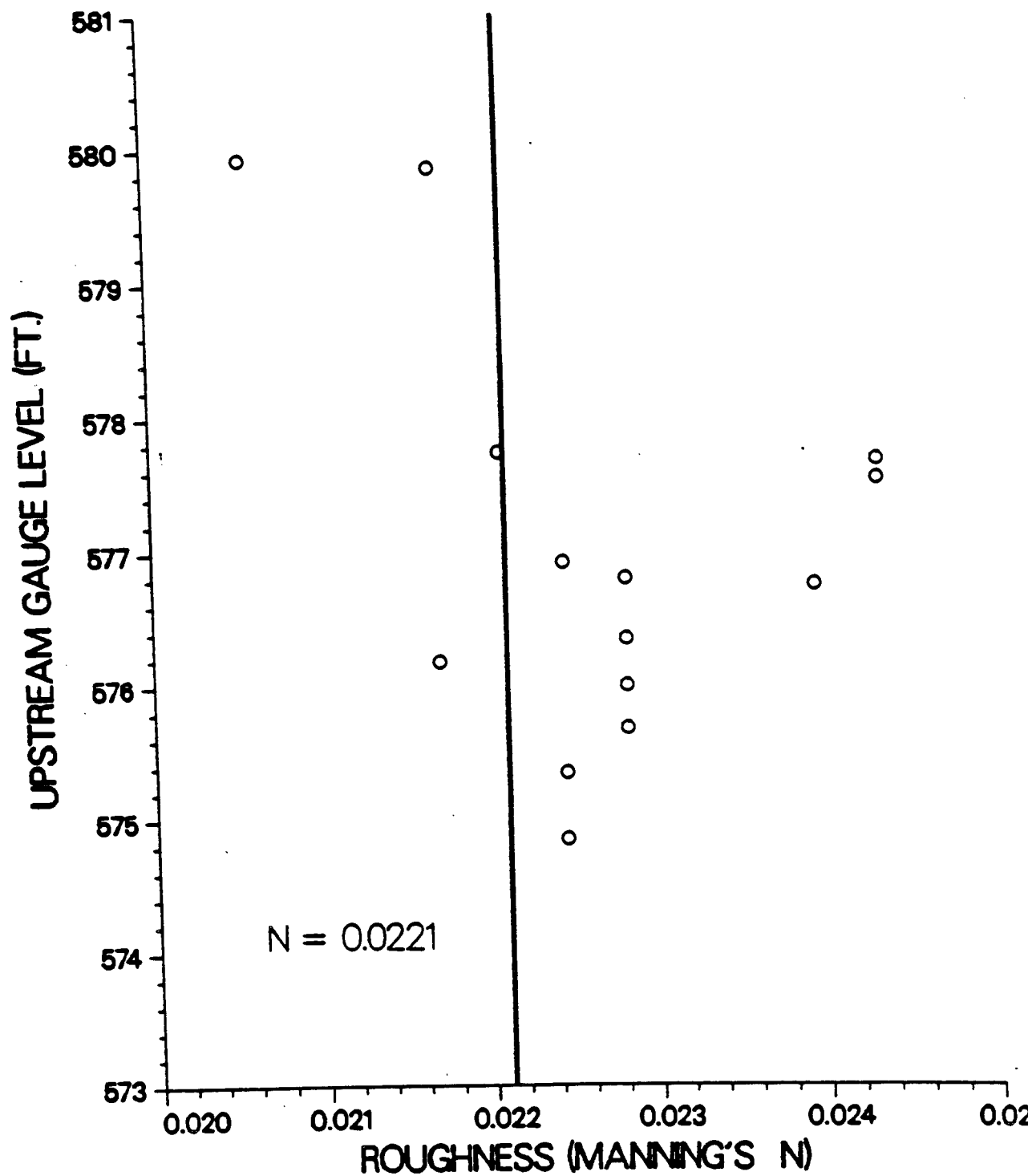
ST CLAIR RIVER SCHEMATIC REPRESENTATION

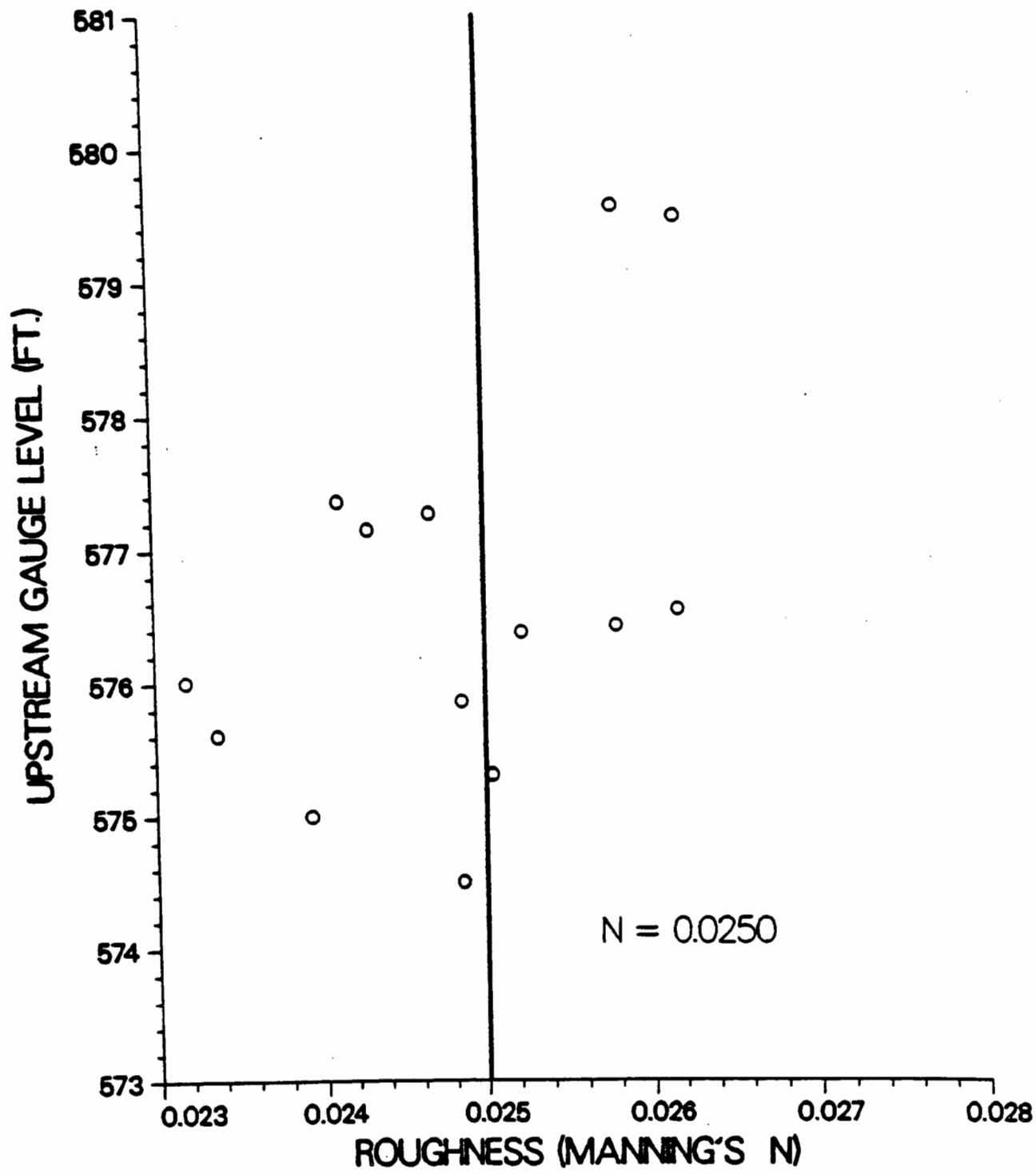


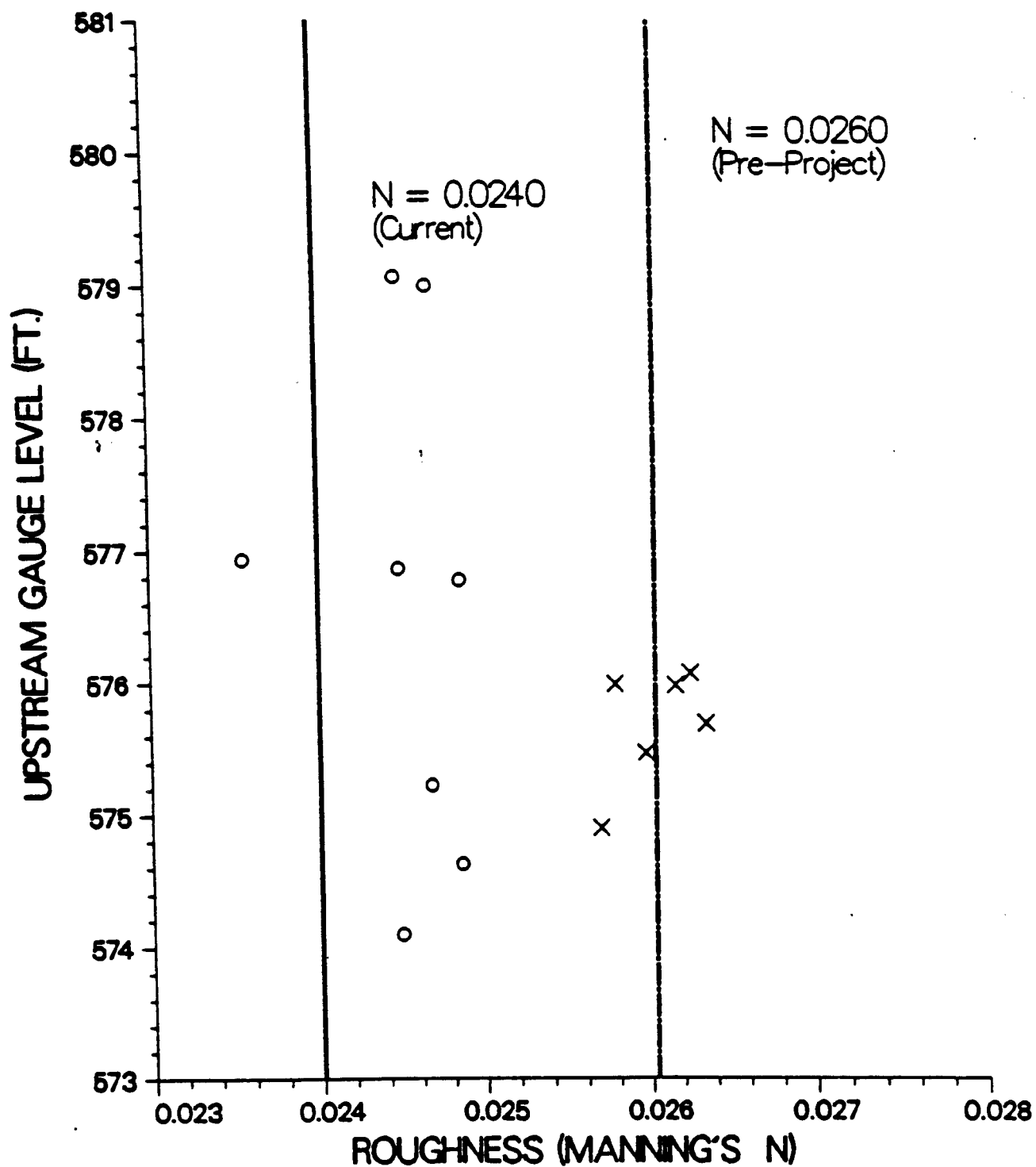
		Q1	WS2	Q2	WS3	Q3	WS4	Q4
<hr/>									
c	1-2	x	x	x					
■	1-2	x	x	x					
c	2-3		x	x	x	x			
■	2-3		x	x	x	x			
c	2-4				x	x	x	x	
■	2-4				x	x	x	x

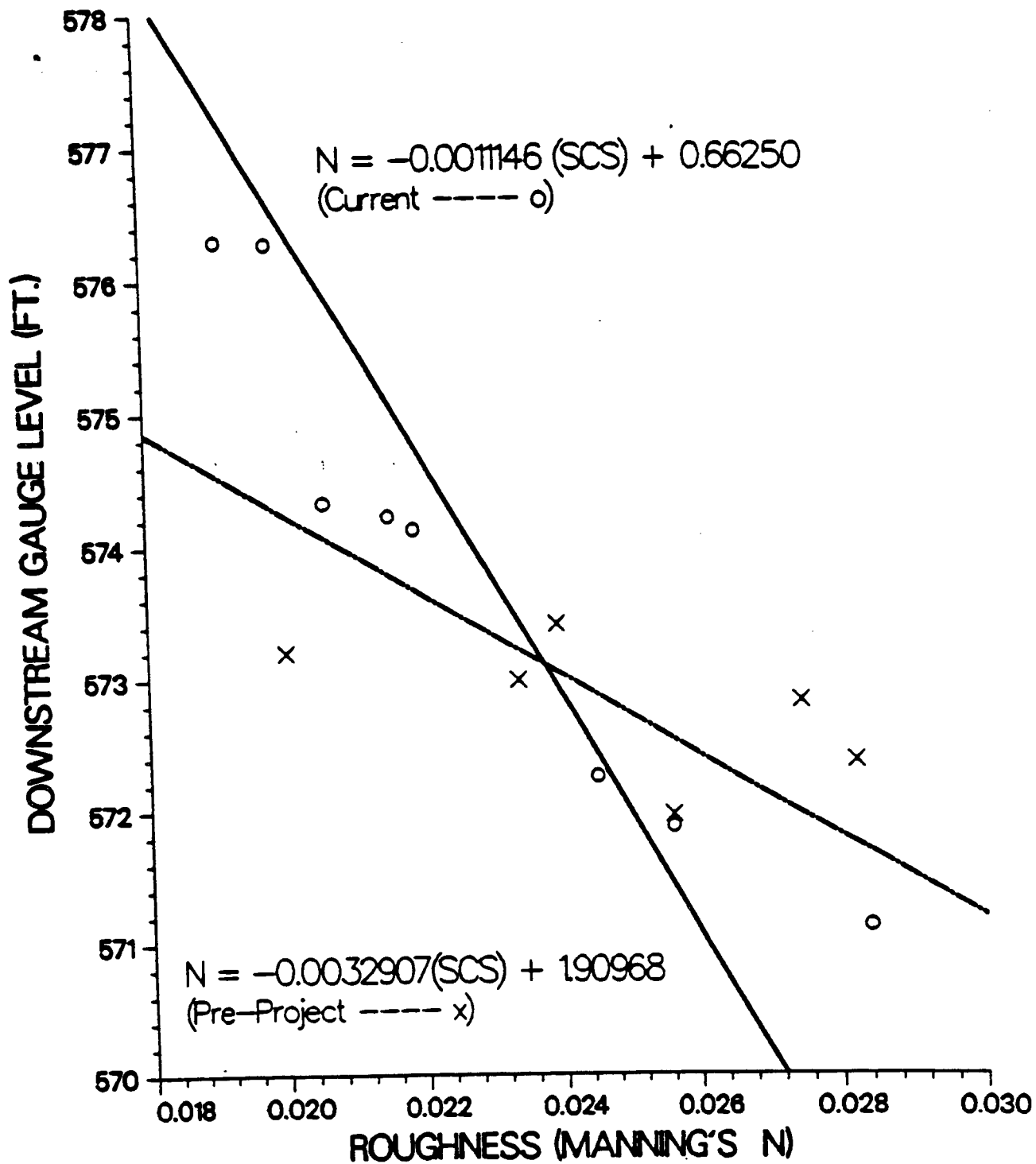












APPENDIX A.

HOURLY AND DAILY UNSTEADY FLOW MODELS:

1. Model Programs (Appendix Figures A-15 and A-16).
2. Model Outputs (Appendix Tables A-1 through A-6).

Program [HYDRO.JDSTCLR]HDELTA.FOR

This is the St Clair River Transient Model - Hourly Version.

It is set to run in BATCH MODE...

To run the program...

1. Set desired parameters in file [HYDRO.JDSTCLR]HDELTA.PAR

Line 1 - Starting and ending day, month and yr.

DA MO YR DA MO YR (I2,I2,I2,I2,I2,I2,I2,I2,I2,I2)

Line 2 - Starting and ending points of model. (I1,I1,I1)

- 1 - Fort Gratiot
- 2 - Dunn Paper
- 3 - Mouth of Black River
- 4 - Dry Dock
- 5 - Marysville
- 6 - St Clair
- 7 - Algonac
- 8 - Lake St Clair

Line 3 - Output Option (I1)

- 1 - Water levels and deviations.
- 2 - Total discharge and discharge around islands and, if included, discharge in the delta channels.
- 3 - Velocity near the starting, ending and midpoint of the simulated river and velocities around islands and, if included, velocities in the delta channels.

Line 4 - Units Option (I1)

- 0 - Metric units
- 1 - English units

2. Make sure that file [HYDRO.JDSTCLR]HDELTA.DAT is available.
3. Type: SUBMIT HDELTA/NOTIFY
4. When your request is completed the output will appear in file:
[HYDRO.JDSTCLR]ZHDELTA.OUT
Note: this file is 132 characters wide.

PROGRAM ST_DELTA_HOURLY

```

c
C.....This is an hourly version of PROGRAM ST_DELTA_DAILY.
C.....Programmers  QUINN  LLM  JRB
C
C . . . THIS VERSION USES ROUGHNESS COEFFICIENTS CALCULATED FROM
C . . . '59-'77 VIA GUESSN.FOR, AND COMPARES ALL INTERMEDIATE GAGES.
C . . . IT WAS ADAPTED FROM XX2.FOR, AND THEREFORE ZYX AND SCDQMOD TO
C . . . ALLOW FOR ISLANDS; ie SPARCE MATRIX AND NON-CONSEC. STATIONING.
C . . . FOR005) HRISLE.DAT:  PHYSICAL DATA (STA,ABAS,DATU,&AT)
C . . . FOR006) THE OUTPUT FILE HRDEL.OUT
C . . . FOR007) SYSS$OUTPUT
C . . . FOR010) TT
      IMPLICIT DOUBLE PRECISION (A-H,O-Z)
      REAL NPERC,MPERC,PERC
      LOGICAL NEWROW,MONFLAG
      INTEGER RR(358),CC(358),ESP,PATH,FLAG
      CHARACTER*9 NAMMON(12),NAME(8)*20,NMM(8)*3,NOTE(8,24)*1,MARK(181)
>*2
      COMMON /WAT001/IHOUR(24,31),MEAN(31),MEM,MAXV(31),MAXD(31),IFLAG,
> MINH(31),MIND(31),MAXM(4),MINM(4),IC,IGEAGE,MONAA,IYRR,IDUM(142)
      DIMENSION AA(180),ABAS(180),DATU(180),AT(180),X(180),STA(180),
> WS(50,180),Q(55,180),YVECT(358),XMTRX(358,358),T(180),AN(180),
> A(180),U(180),R(180),QA(180),SUM(44),AVE(44),ADJ(8),IGAGE(8),
> OLD(8),LOC(8),DEV(8),WSSAV(50,8),A1(8),B1(8),NODE(10),NBR(5),
> IA(359),AVECT(1378),JA(1378),ICC(358),YV(358),RSP(5722),ISP(5722)
>,VEL(180)
      EQUIVALENCE (ISP,RSP)
      DATA NAMMON/' JANUARY',' FEBRUARY',' MARCH',' APRIL',
> ' MAY',' JUNE',' JULY',' AUGUST',
> 'SEPTEMBER',' OCTOBER',' NOVEMBER',' DECEMBER'/
      DATA NAME/' FT. GRATIOT ',' DUNN PAPER ',
> 'MOUTH OF BLACK RIVER',' DRY DOCK ',
> ' MARYSVILLE ',' ST CLAIR ',
> ' ALGONAC ','LAKE ST. CLAIR (SCS)'/
      DATA NMM/' FG',' DP',' MBR',' DD',' MV',' SC',' AL','SCS'/
      DATA LOC/180,178,160,157,155,129,77,1/
      DATA IGAGE/14098,14096,14090,14087,14084,14080,14070,14052/
      DATA OLD/580.92,580.43,580.09,579.53,579.01,578.16,576.60,576.23/
C      A1 IS SLOPE AND B1 IS INTERCEPT OF MANNINGS N'S FOR ALL REACHES
c      this is for years 1959-1977
      DATA A1/0.0033947,0.0002708,0.,0.,0.,-0.0011146,-0.0017647/
      DATA B1/-1.92253,-0.12683,0.0221,0.0250,0.0240,0.0230,
>0.66250,1.04729/
C
C . . . ISLAND/DELTA SPECIFIC VARIABLE ASSIGNMENTS
      DATA NODE/3,6,25,39,51,76,97,108,135,154/
      DATA NBR/15,36,45,102,144/
      EPERC1=.253
      WPERC1=1.-EPERC1
      EPERC2=.376

```

```

WPERC2=1.-EPERC2
NPERC=.35
MPERC=.21
CNPERC=.56
FNPERC=.56
SPERC=.21
COPERC=.23
CSPERC=.44
FSPERC=.44
NSP=5722
NISLANDS=5
ICOUNT=0
LRATIO=2
IFLAG=0

C
C . . . PHYSICAL DATA ACCESSED
DO 10 I=1,LOC(1)
10 READ(5,1020) STA(I),ABAS(I),DATU(I),AT(I)
C
C . . . PROMPT FOR AND READ BEGINNING AND ENDING DATES
C WRITE(7,2000)
READ (10,1000) MONA,IDAYA,IYRA,MONB,IDAYB,IYRB
IF(MONA.LE.0) THEN
    MONA=12
    IYRA=IYRA-1
END IF
IYRA=IYRA+1900
IYRB=IYRB+1900
C
C . . . PROMPT FOR LOCATION OF UPPER AND LOWER LIMITS TO BE RUN
C 9 WRITE(7,2020) (I,NAME(I), I=1,8)
9 READ(10,1010) IUP,IDN
IIDN=IDN-1
IIUP=IUP+1
IF(IUP.GE.IIDN) GO TO 9
C
C . . . PROMPT FOR OPTION NUMBER
C 616 WRITE(7,8001)
616 READ(10,8002)NOPT
IF(NOPT.GT.3.OR.NOPT.LT.1) GO TO 616
C
READ(10,8002) MUNITS
C
C . . . DEFINE AND ADJUST PARAMETERS, BASED UPON LIMITS FROM ABOVE
NRM=LOC(IUP)-LOC(IDN)
NMR=NRM+1
IF(LOC(IDN).EQ.1) GO TO 27
DO 24 I=1,NMR
STA(I)=STA(I-1+LOC(IDN))
ABAS(I)=ABAS(I-1+LOC(IDN))
DATU(I)=DATU(I-1+LOC(IDN))
24 AT(I)=AT(I-1+LOC(IDN))

```

```

NODE(1)=NODE(1)-LOC(IDN)+1
NODE(2)=NODE(2)-LOC(IDN)+1
NODE(3)=NODE(3)-LOC(IDN)+1
NODE(4)=NODE(4)-LOC(IDN)+1
NODE(5)=NODE(5)-LOC(IDN)+1
NODE(6)=NODE(6)-LOC(IDN)+1
NODE(7)=NODE(7)-LOC(IDN)+1
NODE(8)=NODE(8)-LOC(IDN)+1
NODE(9)=NODE(9)-LOC(IDN)+1
NODE(10)=NODE(10)-LOC(IDN)+1
NBR(1)=NBR(1)-LOC(IDN)+1
NBR(2)=NBR(2)-LOC(IDN)+1
NBR(3)=NBR(3)-LOC(IDN)+1
NBR(4)=NBR(4)-LOC(IDN)+1
NBR(5)=NBR(5)-LOC(IDN)+1
DO 25 I=IUP,IDN
25 LOC(I)=LOC(I)-LOC(IDN)+1
C
C . . . CALCULATE DISTANCES BETWEEN SECTIONS
27 DO 30 I=1,NRM
  X(I)=STA(I+1)-STA(I)
30 IF(I.EQ.NBR(1).OR.I.EQ.NBR(2).OR.I.EQ.NBR(3).OR.I.EQ.
  >NBR(4).OR.I.EQ.NBR(5)) X(I)=0.0
C
C . . . The following lines which, have been COMMENTED with "cO", will
C . . . WRITE the BASIC PHYSICAL DATA. Should the user desire to see
C . . . this data, the "cO's" would have to be eliminated and the
C . . . program re-compiled/linked etc. TO RE-COMPILE submit HCDelta.
C
cO      WRITE (6,3000)
cO      WRITE (6,3010)
cO      DO 40 I=1,NMR
cO        MARK(I)=' '
cO        IF(I.EQ.NODE(3).OR.I.EQ.NODE(5).OR.I.EQ.NODE(6)
cO        >.OR.I.EQ.NODE(7).OR.I.EQ.NODE(8).OR.I.EQ.NODE(9).OR.
cO        >I.EQ.NODE(10)) MARK(I)='<'
cO        IF(I.GT.NODE(2).AND.I.LE.NBR(1))MARK(I)='N '
cO        IF(I.GT.NBR(1).AND.I.LT.NODE(3))MARK(I)='M '
cO        IF(I.GT.NODE(3).AND.I.LE.NBR(2))MARK(I)='UN'
cO        IF(I.GT.NODE(4).AND.I.LE.NBR(3))MARK(I)='S '
cO        IF(I.GT.NBR(3).AND.I.LT.NODE(5))MARK(I)='CO'
cO        IF(I.GT.NODE(5).AND.I.LT.NODE(6))MARK(I)='US'
cO        IF(I.GT.NODE(7).AND.I.LE.NBR(4).OR.I.GT.NODE(9).AND.I
cO        >.LE.NBR(5))MARK(I)='W '
cO        IF(I.GT.NBR(4).AND.I.LT.NODE(8).OR.I.GT.NBR(5).AND.I
cO        >.LT.NODE(10))MARK(I)='E '
cO        IF(I.LE.NODE(2).OR.I.GT.NBR(2).AND.I.LE.NODE(4)) GO TO 40
cO        WRITE(6,3020) STA(I),ABAS(I),DATU(I),AT(I),MARK(I)
cO        DO 40 IJ=IUP,IDN
cO      40 IF(I.EQ.LOC(IJ)) WRITE(6,3030) NAME(IJ)
C
C      THESE NEXT 2 MANNINGS N PRINTOUTS ARE HARDWIRED. IF THE

```

```

C      NUMBER OF STATIONS CHANGES, CHANGE THESE!
C
C0      IF(IDN.EQ.8) WRITE(6,3040) A1(8),NMM(8),B1(8),STA(7),STA(36)
C0      IF(IDN.EQ.8) WRITE(6,3040) A1(7),NMM(8),B1(7),STA(40),STA(77)
C0      DO 45 I=IIDN,IUP,-1
C0  45 IF(I.LT.7)WRITE(6,3040) A1(I),NMM(I),B1(I),STA(LOC(I+1)),
C0      >STA(LOC(I))
C
C . . . INITIALIZE AND ASSIGN ADDITIONAL VARIABLES
      DO 50 I=1,4
50 ADJ(I)=0.
      NVAR=NRM*2
      ANC=1.
      DT=ANC*3600.
      DO 56 I=1,42
56 SUM(I)=0.
      TH=.75
      TH1=.25
      MM=0
      M=13
      istart=13
      iend=36
      KDK=IDAYA
      kkz=11
      MON=MONA
      IYR=IYRA
      MONFLAG=.FALSE.
      JRB=(IUP+IDN)/2
C
C
C      Routine to read all of the water level data from the disk and
C      store it in another tempory file. This way the disk is not tied
C      up for long periods of time when running the program.
C
C . . . READ WATER LEVELS FROM DISC.
C
52 CALL NODAYS( IYR,MON,1,NDM,NDY,JD)
      DO 55 JJ=IUP,IDN
      IW=1
      IC=IGAGE(JJ)/10000
      IGAG=IGAGE(JJ)-IC*10000
      CALL GAGEIO( IW,IC,IGAG ,MON,IYR,IB,IT,IDA,IDB,IDC,IER)
      IF(IER.NE.0) THEN
          WRITE(6,3110) NAMMON(MON),IYR,IER
          CALL EXIT
      END IF
      DO 54 J=1,NDM
      DO 53 I=1,24
          WRITE(9,1050) IHOURL(I,J)
53 CONTINUE
      WRITE(9,1050) MEAN(J)
54 CONTINUE

```

```

55 CONTINUE
C
  IF(IYR-IYRB) 58,57,65
57 IF(MON-MONB) 58,65,65
58 CONTINUE
  IF(MON-12) 60,59,59
59 IYR=IYR+1
60 CONTINUE
C . . . UPDATE MONTH AND YEAR AND RECHECK IF MORE DATA SHOULD BE USED
  MON=MON+1
  IF(MON-13) 62,61,61
61 MON=1
62 IF(IYR-IYRB) 64,63,65
63 IF(MON-MONB) 64,64,65
64 CONTINUE
C
  GO TO 52
65 CALL DISMOUNTPACK('WATER_LEVELS')
  MON=MONA
  IYR=IYRA
  REWIND 9
C . . . COME HERE EACH DAY AND PRINT TITLES AND HEADINGS FOR
C                                     EACH OPTION
70 continue
  if(Nopt.eq.1.and.iup.eq.1) iiup=iiup+1
C*****OPTION FOR WATER LEVELS*****
  IF(NOPT.EQ.1) THEN
    WRITE(6,3000)
    WRITE(6,3050) NAMMON(MON),kdk,IYR,NAME(IUP),NAME(IDN)
    WRITE(6,3060) ANC,NRM
    WRITE(6,3070) NMM(IDN),NMM(IUP),
  >   NMM(IUP),(NMM(I),I=IIDN,IIUP,-1)
    WRITE(6,3071) (NMM(I),I=IIDN,IIUP,-1)
    IF(NOPT.EQ.1.AND.IUP.EQ.1)IIUP=IIUP-1
C
C *****OPTION FOR FLOWS WITHOUT DELTA*****
C
  ELSE IF(NOPT.EQ.2 .AND. IDN.NE.8) THEN
    WRITE(6,3000)
    WRITE(6,8051)NAMMON(MON),kdk,IYR,NAME(IUP),NAME(IDN)
    WRITE(6,3060)ANC,NRM
    WRITE(6,7020)
    WRITE(6,7030)NMM(IDN),NMM(JRB),NMM(IUP),NMM(IIDN),NMM(JRB),
  >   NMM(IUP),NMM(JRB)
    WRITE(6,7040)
C
C *****OPTION FOR FLOWS WITH DELTA*****
C
  ELSE IF(NOPT.EQ.2 .AND. IDN.EQ.8) THEN
    WRITE(6,3000)
    WRITE(6,8051)NAMMON(MON),kdk,IYR,NAME(IUP),NAME(IDN)
    WRITE(6,3060)ANC,NRM

```

```

        WRITE(6,8020)
        WRITE(6,8030)NMM(IDN),NMM(IIDN-1),NMM(IUP),NMM(IUP),NMM(IIDN),
> NMM(IIDN-1)
        WRITE(6,8040)

C
C *****OPTION FOR VELOCITIES WITHOUT DELTA*****
C
        ELSE IF(NOPT.EQ.3 .AND. IDN.NE.8) THEN
            WRITE(6,3000)
            WRITE(6,9051)NAMMON(MON),kdk,IYR,NAME(IUP),NAME(IDN)
            WRITE(6,3060)ANC,NRM
            WRITE(6,9025)
            WRITE(6,7030)NMM(IDN),NMM(JRB),NMM(IUP),NMM(IIDN),NMM(JRB),
> NMM(IUP),NMM(JRB)
            WRITE(6,9041)

C
C *****OPTION FOR VELOCITIES WITH DELTA*****
C
        ELSE IF(NOPT.EQ.3 .AND. IDN.EQ.8) THEN
            WRITE(6,3000)
            WRITE(6,9051)NAMMON(MON),kdk,IYR,NAME(IUP),NAME(IDN)
            WRITE(6,3060)ANC,NRM
            WRITE(6,9020)
            WRITE(6,9030)NMM(IDN),NMM(IIDN-1),NMM(IUP),NMM(IUP),NMM(IIDN),
> NMM(IIDN-1)
            WRITE(6,9040)
            END IF
71      Continue

C
C . . . ADJUST GAGE-SPECIFIC VARIABLES BASED UPON YEARS STUDIED
        IF(IYR.LT.1970) IGAGE(1)=14099
        IF(IYR.LT.1971) IGAGE(6)=14080
        IF(IYR.GT.1970) ADJ(1)=.18
        IF(IYR.GT.1981) ADJ(1)=.06
        IF(IYR.LT.1971) ADJ(6)=.09

C
C . . . READ WATER LEVELS FROM UNIT 9. . .
C
        CALL NODAYS( IYR,MON,1,NDM,NDY,JD)

C
        DO 110 JJ=IUP,IDN

C
        DO 77 J=1,NDM
            DO 75 I=1,24
75          READ(9,1050,END=78) IHOURL(I,J)
77          READ(9,1050,END=78) MEAN(J)

C
C      THE BLOCK OF CODE FOR READING THE WATER LEVELS DISC
C      IS DIFFERENT FROM THE DAILY VERSION OF THE PROGRAM.
C
78      CONTINUE

```



```

DO 110 J=istart,iend
  IF(KKZ.EQ.11) THEN
    I=J-12
  ELSE
    I=J-1
  END IF
C
C . . . FLAG MISSING DATA AND ASSIGN GAGE LEVELS TO WSSAV
IF( I HOUR(I,KDK).GT.0) THEN
  NOTE(JJ,KDK)=' '
ELSE
  NOTE(JJ,KDK)='E'
END IF
if(1hour(i,kdk).le.0) then
  wssav(j,jj)=old(jj)
else
  wssav(j,jj)=(1hour(i,kdk)+ib)/100.+adj(jj)
end if
old(jj)=wssav(j,jj)
IF(JJ.EQ.IUP.OR.JJ.EQ.IDN) WS(J,LOC(JJ))=WSSAV(J,JJ)
110 CONTINUE
IF(MONFLAG) GO TO 200
C
C . . . SET WS FOR 12 PREVIOUS TIME STEPS, TO ACHIEVE 'STEADY STATE'.
DO 120 I=1,12
  DO 120 J=1,8
    WSSAV(I,J)=WSSAV(13,J)
120 IF(J.EQ.IUP .OR. J.EQ.IDN) WS(I,LOC(J))=WSSAV(13,J)
C
C . . . ZERO MATRIX, SET CHANNEL PARAMETERS, & SET INITIAL CONDITIONS.
DO 130 I = 1,NVAR
  YVECT(I)=0.
  DO 130 J = 1,NVAR
130 XMTRX(J,I)=0.
  XSUM=STA(LOC(IUP))-STA(LOC(IDN))
  SLOPE=(WSSAV(1,IUP)-WSSAV(1,IDN))/XSUM
  AA(1)=ABAS(1)+AT(1)*(WS(1,1)-DATU(1))
  DO 150 I=1,NRM
    IF(I.NE.NRM) THEN
      WS(1,I+1)=WS(1,I)+SLOPE*X(I)
      IF(I.EQ.NBR(1)) WS(1,I+1)=WS(1,NODE(2))
      IF(I.EQ.NBR(2)) WS(1,I+1)=WS(1,NODE(1))
      IF(I.EQ.NBR(3)) WS(1,I+1)=WS(1,NODE(4))
      IF(I.EQ.NBR(4)) WS(1,I+1)=WS(1,NODE(7))
      IF(I.EQ.NBR(5)) WS(1,I+1)=WS(1,NODE(9))
      WS(2,I+1)=WS(1,I+1)
    END IF
    AA(I+1)= ABAS(I+1)+AT(I+1)*(WS(1,I+1)-DATU(I+1))
    A(I)=(AA(I)+AA(I+1))/2.
    T(I)=(AT(I)+AT(I+1))/2.
150 R(I)=A(I)/T(I)
    AN(1)= A1(IIDN)*WSSAV(M,IIDN)+B1(IIDN)

```

```

      QSTART=1.486*A(1)*R(1)**(2./3.)*(WS(1,2)-WS(1,1))**.5/AN(1)
    > /X(1)**.5
C
C . . . SPLIT FLOW INITIALLY AROUND THE ISLANDS FOR FASTER CONVERGENCE
DO 190 I=1,NMR
  PERC=1.
  IF(I.GT.NODE(1) .AND. I.LE.NODE(2)) PERC=FNPERC
  IF(I.GT.NODE(2) .AND. I.LE.NBR(1)) PERC=NPERC
  IF(I.GT.NBR(1) .AND. I.LT.NODE(3)) PERC=MPERC
  IF(I.GE.NODE(3) .AND. I.LE.NBR(2)) PERC=CNPERC
  IF(I.GT.NBR(2) .AND. I.LE.NODE(4)) PERC=FSPERC
  IF(I.GT.NODE(4) .AND. I.LE.NBR(3)) PERC=SPERC
  IF(I.GT.NBR(3) .AND. I.LT.NODE(5)) PERC=COPERC
  IF(I.GE.NODE(5) .AND. I.LT.NODE(6)) PERC=CSPERC
  IF(I.GT.NODE(7) .AND. I.LE.NBR(4)) PERC=WPERC1
  IF(I.GT.NBR(4) .AND. I.LT.NODE(8)) PERC=EPERC1
  IF(I.GT.NODE(9) .AND. I.LE.NBR(5)) PERC=WPERC2
  IF(I.GT.NBR(5) .AND. I.LT.NODE(10)) PERC=EPERC2
  Q(1,I)=QSTART*PERC
190  Q(2,I)=Q(1,I)
     kb=36
     M=1
200  CONTINUE
     N=M+1
     ITER=1
210  YVMAX=0.
     DO 230 I=1,NRM
       QA(I)=TH/2.*(Q(N,I)+Q(N,I+1))+TH1/2.*(Q(M,I)+Q(M,I+1))
       U(I)=ABS(QA(I))
       DO 230 J=IUP,IDN
         IF(I.LT.LOC(J)) AN(I)=A1(J)*WSSAV(M,J)+B1(J)
230   IF(IDN.EQ.8.AND.I.GT.3.AND.I.LE.36) AN(I)=A1(8)*WSSAV(M,J)
       > +B1(8)
C
C . . . COMPUTE AREAS AND HYDRAULIC RADII
c   i made a change here...i replaced the i's in the eqn. below w/l's
      AA(1)=ABAS(1)+AT(1)*(TH*WS(N,1)+TH1*WS(M,1)-DATU(1))
      DO 250 I=1,NRM
        AA(I+1)= ABAS(I+1)+AT(I+1)*(TH*WS(N,I+1)+TH1*WS(M,I+1)-DATU(I+1))
        A(I)=(AA(I)+AA(I+1))/2.
        T(I)=(AT(I)+AT(I+1))/2.
250  R(I)=A(I)/T(I)
C      IF(IDN.EQ.8.AND.ITER.EQ.1) THEN
C        DO 343 I=54,LOC(IUP)
C          Q(N,I)=Q(N,I)+.04*Q(N,I)
C      343  Q(M,I)=Q(N,I)
C        END IF
C
C . . . CONTINUITY EQUATIONS
      NRD=NVAR-1
      DO 260 I=1,NRD,2
        ID=I/2+1

```

```

IU-ID+1
DO 255 J=1,5
  JJ=NBR(J)
  KK=NODE(2*J)
  LL=NODE(2*J-1)
  IF(IDN.NE.8.AND.ID.EQ.LL.OR.IDN.NE.8.AND.IU.EQ.KK.OR.
> IDN.EQ.8.AND.I.GT.106.AND.ID.EQ.LL.OR.IDN.EQ.8.AND.I.GT.106
> .AND.IU.EQ.KK.OR.IDN.EQ.8.AND.ID.EQ.6.OR.IDN.EQ.8.AND.ID.EQ.
> 24.OR.IDN.EQ.8.AND.ID.EQ.39.OR.IDN.EQ.8.AND.ID.EQ.50.OR.
> IDN.EQ.8.AND.ID.EQ.3) THEN
    YVECT(I)=-(WS(N,IU)+WS(M,IU)-WS(N,ID)-WS(M,ID))/2.
    XMTRX(I,I-1)=-0.5
    XMTRX(I,I+1)=+0.5
    GO TO 260
  ELSE IF(ID.EQ.JJ.AND.IDN.NE.8.OR.ID.EQ.JJ.AND.IDN.EQ.8
> .AND.J.GE.4) THEN
    YVECT(I)=-(WS(N,KK)+WS(M,KK)-WS(N,JJ)-WS(M,JJ))/2.
    XMTRX(I,I-1)=-0.5
    XMTRX(I,2*KK-2)=+0.5
    GO TO 260
  ELSE IF(IDN.EQ.8.AND.ID.EQ.NBR(1)) THEN
    YVECT(I)=-(WS(N,ID)+WS(M,ID)-WS(N,NODE(3))-WS(M,NODE(3)))/2.
    XMTRX(I,28) = +.5
    XMTRX(I,48) = -.5
    GO TO 260
  ELSE IF(IDN.EQ.8.AND.ID.EQ.NBR(2)) THEN
    YVECT(I)=-(WS(N,ID)+WS(M,ID)-WS(N,NODE(6))-WS(M,NODE(6)))/2.
    XMTRX(I,70)= +.5
    XMTRX(I,150)= -.5
    GO TO 260
  ELSE IF(IDN.EQ.8.AND.ID.EQ.NBR(3)) THEN
    YVECT(I)=-(WS(N,ID)+WS(M,ID)-WS(N,NODE(5))-WS(M,NODE(5)))/2.
    XMTRX(I,88)= +.5
    XMTRX(I,100)= -.5
    GO TO 260
  END IF
255 CONTINUE
  YVECT(I)=-(WS(N,ID)+WS(N,IU)-WS(M,ID)-WS(M,IU))/(2.*DT)+
> (TH*(Q(N,ID)-Q(N,IU))+TH1*(Q(M,ID)-Q(M,IU)))/(T(ID)*X(ID))
  XMTRX(I,I)=TH/(T(ID)*X(ID))
  XMTRX(I,I+2)=XMTRX(I,I)
  IF(I.EQ.1) THEN
    XMTRX(I,2)=1./(2.*DT)
  ELSE
    XMTRX(I,I-1)=1./(2.*DT)
    XMTRX(I,I+1)=1./(2.*DT)
    IF(I.EQ.NRD) XMTRX(I,I+1)=XMTRX(I,I+2)
    IF(I.EQ.NRD) XMTRX(I,I+2)=0.
  END IF
260 CONTINUE

```

```

C
C . . . MOMENTUM EQUATIONS

```

```

DO 280 I=2,NVAR,2
  ID=I/2
  IU=ID+1
  DO 265 J=1,5
    JJ=NBR(J)
    KK=NODE(2*J)
    LL=NODE(2*J-1)
    IF(IDN.NE.8.AND.ID.EQ.LL.OR.IDN.EQ.8.AND.J.GE.4.AND.
> ID.EQ.LL) THEN
      YVECT(I)--(Q(N,JJ+1)+Q(M,JJ+1)+Q(N,IU)+Q(M,IU)-Q(N,ID)-Q(M,ID))
> /2.
      XMTRX(I,I-1)--0.5
      XMTRX(I,I+1)--0.5
      XMTRX(I,2*JJ+1)--0.5
      GO TO 280
    ELSE IF(IDN.NE.8.AND.ID.EQ.JJ.OR.IDN.EQ.8.AND.J.GE.4.AND.
> ID.EQ.JJ) THEN
      YVECT(I)--(WS(N,IU)+WS(M,IU)-WS(N,LL)-WS(M,LL))/2.
      XMTRX(I,2*LL-2)--0.5
      XMTRX(I,I)--0.5
      GO TO 280
    ELSE IF(IDN.NE.8.AND.IU.EQ.KK.OR.IDN.EQ.8.AND.J.GE.4.AND.
> IU.EQ.KK) THEN
      YVECT(I)--(Q(N,KK)+Q(M,KK)-Q(N,ID)-Q(M,ID)-Q(N,JJ)-Q(M,JJ))/2.
      XMTRX(I,2*JJ-1)--0.5
      XMTRX(I,I-1)--0.5
      XMTRX(I,I+1)--0.5
      GO TO 280
    ELSE IF(IDN.EQ.8.AND.ID.EQ.NODE(1)) THEN
      YVECT(I)= -(Q(N,NODE(1))+Q(M,NODE(1))-Q(N,NODE(1)+1)
> -Q(M,NODE(1)+1)-Q(N,NBR(2)+1)-Q(M,NBR(2)+1))/2.
      XMTRX(I,I-1)= +.5
      XMTRX(I,I+1)= -.5
      XMTRX(I,73)= -.5
      GO TO 280
    ELSE IF(IDN.EQ.8.AND.ID.EQ.NODE(2)) THEN
      YVECT(I)= -(Q(N,NODE(2))+Q(M,NODE(2))-Q(N,NODE(2)+1)
> -Q(M,NODE(2)+1)-Q(N,NBR(1)+1)-Q(M,NBR(1)+1))/2.
      XMTRX(I,I-1)= +.5
      XMTRX(I,I+1)= -.5
      XMTRX(I,31)= -.5
      GO TO 280
    ELSE IF(IDN.EQ.8.AND.ID.EQ.NODE(4)) THEN
      YVECT(I)= -(Q(N,NODE(4))+Q(M,NODE(4))-Q(N,NODE(4)+1)
> -Q(M,NODE(4)+1)-Q(N,NBR(3)+1)-Q(M,NBR(3)+1))/2.
      XMTRX(I,I-1)= +.5
      XMTRX(I,I+1)= -.5
      XMTRX(I,91)= -.5
      GO TO 280
    ELSE IF(IDN.EQ.8.AND.ID.EQ.NBR(1)) THEN
      YVECT(I)= -(WS(N,NBR(1)+1)+WS(M,NBR(1)+1)-WS(N,NODE(2))
> -WS(M,NODE(2)))/2.

```

```

      XMTRX(I,I)=+.5
      XMTRX(I,10)=-.5
      GO TO 280
    ELSE IF(IDN.EQ.8.AND.IU.EQ.NODE(3)) THEN
      YVECT(I)--(Q(N,NODE(3))+Q(M,NODE(3))-Q(N,NODE(3)-1)
> -Q(M,NODE(3)-1)-Q(N,NBR(1))-Q(M,NBR(1)))/2.
      XMTRX(I,I+1)=+.5
      XMTRX(I,I-1)=-.5
      XMTRX(I,29)=-.5
      GO TO 280
    ELSE IF(IDN.EQ.8.AND.ID.EQ.NBR(2)) THEN
      YVECT(I)--(WS(N,NODE(1))+WS(M,NODE(1))-WS(N,NBR(2)+1)
> -WS(M,NBR(2)+1))/2.
      XMTRX(I,72)=-.5
      XMTRX(I,4)=+.5
      GO TO 280
    ELSE IF(IDN.EQ.8.AND.ID.EQ.NBR(3)) THEN
      YVECT(I)--(WS(N,NODE(4))+WS(M,NODE(4))-WS(N,NBR(3)+1)
> -WS(M,NBR(3)+1))/2.
      XMTRX(I,76)=+.5
      XMTRX(I,90)=-.5
      GO TO 280
    ELSE IF(IDN.EQ.8.AND.IU.EQ.NODE(5)) THEN
      YVECT(I)--(Q(N,NODE(5))+Q(M,NODE(5))-Q(N,NODE(5)-1)
> -Q(M,NODE(5)-1)-Q(N,NBR(3))-Q(M,NBR(3)))/2.
      XMTRX(I,101)=+.5
      XMTRX(I,99)=-.5
      XMTRX(I,89)=-.5
      GO TO 280
    ELSE IF(IDN.EQ.8.AND.IU.EQ.NODE(6)) THEN
      YVECT(I)--(Q(N,NODE(6))+Q(M,NODE(6))-Q(N,NODE(6)-1)
> -Q(M,NODE(6)-1)-Q(N,NBR(2))-Q(M,NBR(2)))/2.
      XMTRX(I,151)=+.5
      XMTRX(I,71)=-.5
      XMTRX(I,149)=-.5
      GO TO 280
    END IF
265 CONTINUE
      Z41--QA(ID)*T(ID)*(WS(N,IU)+WS(N,ID)-WS(M,IU)-WS(M,ID))/
> (2.*DT*A(ID)**2.)*2.
      Z61=(Q(N,ID)+Q(N,IU)-Q(M,ID)-Q(M,IU))/(2.*DT*A(ID))
      Z11=32.17*AN(ID)**2.*QA(ID)*U(ID)/(2.21*A(ID)**2.*R(ID)**(4./3.))
      Z21=32.17*(TH*(WS(N,ID)-WS(N,IU))+TH1*(WS(M,ID)-WS(M,IU)))/X(ID)
      Z31--(QA(ID)**2.*(AA(ID)-AA(IU)))/(A(ID)**3.*X(ID))
      YVECT(I)--(Z11+Z21+Z31+Z41+Z61)
      XMTRX(I,I)--(32.2-QA(ID)**2.*T(ID)/(A(ID)**3.))/X(ID)*TH-QA(ID)
> *T(ID)/(DT*A(ID)**2.)
      IF(I.LT.4) GO TO 270
      XMTRX(I,I-2)=(32.2-QA(ID)**2.*T(ID)/(A(ID)**3.))/X(ID)*TH-QA(ID)
> *T(ID)/(DT*A(ID)**2.)
270 ZZZ1=ABS(QA(ID))
      P1=32.2*AN(ID)**2.*ZZZ1*TH/(2.2082*A(ID)**2.*R(ID)**(4./3.))

```

```

        IF (YV(I).LT.-20.) YV(I)=-20.
        II=I/2+1
        WS(N,II)=WS(N,II)+YV(I)
310 CONTINUE
C
C . . . ASSIGN MAXIMUM DELTA VALUE, AND TEST FOR EXCESSIVE ITERATIONS
DO 319 I=2,NNR,2
319 IF(ABS(YV(I)).GT.YVMAX) YVMAX=YV(I)
DO 320 I=2,NNR,2
    IF(ABS(YV(I)).GT..002) THEN
        IF(ITER.GT.20) THEN
            WRITE(6,1133) ITER,YVMAX,I/2
1133     FORMAT(' ',I2,' ITERATIONS.  YVMAX =',E10.3,' AT I=',I2,/)
            GO TO 500
        END IF
        ITER=ITER+1
        GO TO 210
    END IF
320 CONTINUE
C
C . . . DETERMINE THE DEVIATION OF CALCULATED FROM MEASURED LEVELS
JB=N+1
DO 330 IJ=IIUP,IIDN
    IF(WSSAV(N,IJ).LT.50.) WSSAV(N,IJ)=WS(N,LOC(IJ)).0001
330 DEV(IJ)=WS(N,LOC(IJ))-WSSAV(N,IJ)
    MM=MM+1
    NM=MM-kkz
    IF(NM.LE.0) GO TO 340
    IF(NOPT.EQ.3) THEN
        DO 6262 I=1,NRM+1
6262    VEL(I)=Q(N,I)/AA(I)
    END IF
C
C . . . METRIC OPTION FOR OUTPUT . . .
IF(MUNITS.EQ.0)THEN
    DO 6700 MC = IUP,IDN
6700    WSSAV(N,MC) = WSSAV(N,MC)/3.28083
    DO 6720 MC = IIUP,IIDN
        WS(N,LOC(MC)) = WS(N,LOC(MC))/3.28083
6720    DEV(MC) = DEV(MC)/3.28083
C
    Q(N,LOC(IUP)) = Q(N,LOC(IUP))*0.02832
    Q(N,LOC(IIDN)) = Q(N,LOC(IIDN))*0.02832
    Q(N,NBR(5)+5) = Q(N,NBR(5)+5)*0.02832
    Q(N,NBR(5)-4) = Q(N,NBR(5)-4)*0.02832
    Q(N,NODE(10)+1) = Q(N,NODE(10)+1)*0.02832
    Q(N,NBR(4)+3) = Q(N,NBR(4)+3)*0.02832
    Q(N,NBR(4)-2) = Q(N,NBR(4)-2)*0.02832
    Q(N,NODE(8)+1) = Q(N,NODE(8)+1)*0.02832
    Q(N,NBR(1)-3) = Q(N,NBR(1)-3)*0.02832
    Q(N,NBR(1)+6) = Q(N,NBR(1)+6)*0.02832
    Q(N,NBR(3)-3) = Q(N,NBR(3)-3)*0.02832

```

```

Q(N,NBR(3)+3) = Q(N,NBR(3)+3)*0.02832
Q(N,LOC(JRB)) = Q(N,LOC(JRB))*0.02832
C
VEL(LOC(IUP)) = VEL(LOC(IUP))/3.28083
VEL(LOC(IIDN)) = VEL(LOC(IIDN))/3.28083
VEL(NBR(5)+5) = VEL(NBR(5)+5)/3.28083
VEL(NBR(5)-4) = VEL(NBR(5)-4)/3.28083
VEL(NBR(4)+3) = VEL(NBR(4)+3)/3.28083
VEL(NBR(4)-2) = VEL(NBR(4)-2)/3.28083
VEL(NBR(1)-3) = VEL(NBR(1)-3)/3.28083
VEL(NBR(1)+6) = VEL(NBR(1)+6)/3.28083
VEL(NBR(3)-3) = VEL(NBR(3)-3)/3.28083
VEL(NBR(3)+3) = VEL(NBR(3)+3)/3.28083
VEL(LOC(JRB)) = VEL(LOC(JRB))/3.28083
END IF
C
C
C . . . PRINT OUTPUT.
      if(NOPT.EQ.1.and.iup.eq.1) iiup=iiup+1
C*****OPTION FOR WATER LEVELS*****
C
      IF(NOPT.EQ.1) THEN
        WRITE(6,3120) nm,WSSAV(N,IDN),NOTE(IDN,KDK),
      > (WS(N,LOC(I)),I-IIDN,IIUP,-1)
        WRITE(6,3121) WSSAV(N,IUP),NOTE(IUP,KDK),
      > Q(N,LOC(IUP)),
      > (WSSAV(N,I),NOTE(I,KDK),DEV(I), I-IIDN,IIUP,-1)
C
C *****OPTION FOR FLOW WITHOUT DELTA*****
C
      ELSE IF(NOPT.EQ.2.AND.IDN.NE.8) THEN
        WRITE(6,7050)NM,WSSAV(N,IDN),NOTE(IDN,KDK),WS(N,LOC(JRB)),
      >WSSAV(N,IUP),NOTE(IUP,KDK),Q(N,LOC(IIDN)),Q(N,LOC(JRB)),
      >Q(N,LOC(IUP)),Q(N,NBR(5)+5),Q(N,NBR(5)-4),Q(N,NBR(4)+3),
      >Q(N,NBR(4)-2),WSSAV(N,JRB),NOTE(JRB,KDK),DEV(JRB)
C
C *****OPTION FOR FLOW WITH DELTA*****
C
      ELSE IF(NOPT.EQ.2 .AND. IDN.EQ.8) THEN
        WRITE(6,8050)NM,WSSAV(N,IDN),NOTE(IDN,KDK),WS(N,LOC(IIDN-1)),
      >WSSAV(N,IUP),NOTE(IUP,KDK),Q(N,LOC(IUP)),Q(N,LOC(IIDN)),
      >Q(N,NBR(5)+5),Q(N,NBR(5)-4),Q(N,NBR(4)+3),Q(N,NBR(4)-2),
      >Q(N,NBR(1)-3),Q(N,NBR(1)+6),Q(N,NBR(3)-3),Q(N,NBR(3)+3),
      >WSSAV(N,IIDN-1),NOTE(IIDN-1,KDK),DEV(IIDN-1)
C
C *****OPTION FOR VELOCITIES WITH DELTA*****
C
      ELSE IF(NOPT.EQ.3 .AND. IDN.EQ.8) THEN
C
        WRITE(*,*)'NM= ',NM
        WRITE(6,9050) NM,WSSAV(N,IDN),NOTE(IDN,KDK),WS(N,LOC(IIDN-1)),
      >WSSAV(N,IUP),NOTE(IUP,KDK),VEL(LOC(IUP)),VEL(LOC(IIDN)),
      >VEL(NBR(5)+5),VEL(NBR(5)-4),VEL(NBR(4)+3),VEL(NBR(4)-2),

```

```

      >VEL(NBR(1)-3),VEL(NBR(1)+6),VEL(NBR(3)-3),VEL(NBR(3)+3),
      >WSSAV(N,IIDN-1),NOTE(IIDN-1,KDK),DEV(IIDN-1)
C
C *****OPTION FOR VELOCITIES WITHOUT DELTA*****
C
      ELSE IF(NOPT.EQ.3 .AND. IDN.NE.8) THEN
        WRITE(6,9055)NM,WSSAV(N,IDN),NOTE(IDN,KDK),WS(N,LOC(JRB)),
        >WSSAV(N,IUP),NOTE(IUP,KDK),VEL(LOC(IIDN)),VEL(LOC(JRB)),
        >VEL(LOC(IUP)),VEL(NBR(5)+5),VEL(NBR(5)-4),VEL(NBR(4)+3),
        >VEL(NBR(4)-2),WSSAV(N,JRB),NOTE(JRB,KDK),DEV(JRB)
C
      END IF
C
      if(Nopt.eq.1.and.iup.eq.1) iiup=iiup-1
331  continue
C
C . . . SHOW HOUR ON TERMINAL SCREEN AND COMPUTE MEAN VALUES.
      WRITE(7,2030)MON,KDK,IYR-1900,NM
      SUM(1)=SUM(1)+WSSAV(N,IUP)
      DO 334 I=2,7
334  SUM(I)=SUM(I)+WS(N,LOC(I))
      SUM(8)=SUM(8)+WSSAV(N,IDN)
      DO 335 I=1,6
335  SUM(I+8)=SUM(I+8)+WSSAV(N,I+1)
      DO 336 I=1,6
336  SUM(I+14)=SUM(I+14)+DEV(I+1)
C
C
C . . . THESE ARE THE CALCULATIONS FOR FLOW AVERAGES
      SUM(21)=SUM(21)+Q(N,LOC(IUP))
      SUM(22)=SUM(22)+Q(N,NBR(5)+5)
      SUM(23)=SUM(23)+Q(N,NBR(5)-4)
      SUM(24)=SUM(24)+Q(N,NODE(10)+1)
      SUM(25)=SUM(25)+Q(N,NBR(4)+3)
      SUM(26)=SUM(26)+Q(N,NBR(4)-2)
      SUM(27)=SUM(27)+Q(N,NODE(8)+1)
      SUM(28)=SUM(28)+Q(N,LOC(IIDN))
      SUM(29)=SUM(29)+Q(N,NBR(1)-3)
      SUM(30)=SUM(30)+Q(N,NBR(1)+6)
      SUM(31)=SUM(31)+Q(N,NBR(3)-3)
      SUM(32)=SUM(32)+Q(N,NBR(3)+3)
      SUM(43)=SUM(43)+Q(N,LOC(JRB))
      SUM(33)=SUM(33)+VEL(LOC(IUP))
      SUM(34)=SUM(34)+VEL(LOC(IIDN))
      SUM(35)=SUM(35)+VEL(NBR(5)+5)
      SUM(36)=SUM(36)+VEL(NBR(5)-4)
      SUM(37)=SUM(37)+VEL(NBR(4)+3)
      SUM(38)=SUM(38)+VEL(NBR(4)-2)
      SUM(39)=SUM(39)+VEL(NBR(1)-3)
      SUM(40)=SUM(40)+VEL(NBR(1)+6)
      SUM(41)=SUM(41)+VEL(NBR(3)-3)
      SUM(42)=SUM(42)+VEL(NBR(3)+3)

```



```

SUM(44)=SUM(44)+VEL(LOC(JRB))
C
C . . . CONVERT FROM METRIC BACK TO ENGLISH UNITS . .
IF(MUNITS.EQ.0)THEN
DO 6730 MC = IUP, IDN
6730 WSSAV(N,MC) = WSSAV(N,MC)*3.28083
DO 6740 MC = IIUP, IIDN
WS(N,LOC(MC)) = WS(N,LOC(MC))*3.28083
6740 DEV(MC) = DEV(MC)*3.28083
C
Q(N,LOC(IUP)) = Q(N,LOC(IUP))/0.02832
Q(N,LOC(IIDN)) = Q(N,LOC(IIDN))/0.02832
Q(N,NBR(5)+5) = Q(N,NBR(5)+5)/0.02832
Q(N,NBR(5)-4) = Q(N,NBR(5)-4)/0.02832
Q(N,NODE(10)+1) = Q(N,NODE(10)+1)/0.02832
Q(N,NBR(4)+3) = Q(N,NBR(4)+3)/0.02832
Q(N,NBR(4)-2) = Q(N,NBR(4)-2)/0.02832
Q(N,NODE(8)+1) = Q(N,NODE(8)+1)/0.02832
Q(N,NBR(1)-3) = Q(N,NBR(1)-3)/0.02832
Q(N,NBR(1)+6) = Q(N,NBR(1)+6)/0.02832
Q(N,NBR(3)-3) = Q(N,NBR(3)-3)/0.02832
Q(N,NBR(3)+3) = Q(N,NBR(3)+3)/0.02832
Q(N,LOC(JRB)) = Q(N,LOC(JRB))/0.02832
C
VEL(LOC(IUP)) = VEL(LOC(IUP))*3.28083
VEL(LOC(IIDN)) = VEL(LOC(IIDN))*3.28083
VEL(NBR(5)+5) = VEL(NBR(5)+5)*3.28083
VEL(NBR(5)-4) = VEL(NBR(5)-4)*3.28083
VEL(NBR(4)+3) = VEL(NBR(4)+3)*3.28083
VEL(NBR(4)-2) = VEL(NBR(4)-2)*3.28083
VEL(NBR(1)-3) = VEL(NBR(1)-3)*3.28083
VEL(NBR(1)+6) = VEL(NBR(1)+6)*3.28083
VEL(NBR(3)-3) = VEL(NBR(3)-3)*3.28083
VEL(NBR(3)+3) = VEL(NBR(3)+3)*3.28083
VEL(LOC(JRB)) = VEL(LOC(JRB))*3.28083
END IF
C
C
340 DO 350 I=1,NMR
350 Q(JB,I)=2.*Q(N,I)-Q(M,I)
DO 360 I=2,NRM
360 WS(JB,I)=2.*WS(N,I)-WS(M,I)
write(7,2030)mon,KDK,iyr-1900,NM
M=M+1
C
IF(M-kb)2333,2333,370
2333 continue
C
C . . . HOURLY RETURN LOOP
IF(nM-24.Lt.0) GO TO 200
370 DO 380 I=1,44
380 AVE(I)=SUM(I)/NM

```

```

C
C . . . PRINT DAILY MEAN VALUES
      if(Nopt.eq.1.and.iup.eq.1) iiup=iiup+1
C
C *****OPTION FOR WATER LEVELS*****
C
      IF(NOPT.EQ.1) THEN
        WRITE(6,3130) AVE(8),(AVE(1),I-IIDN,IIUP,-1)
        WRITE(6,3131) AVE(1),AVE(21),
      > (AVE(I+7),AVE(I+13), I-IIDN,IIUP,-1)
        if(Nopt.eq.1.and.iup.eq.1) iiup=iiup-1
C
C *****OPTION FOR FLOW WITHOUT DELTA*****
C
      ELSE IF(NOPT.EQ.2.AND.IDN.NE.8) THEN
        WRITE(6,7060) AVE(8),AVE(3),AVE(1),AVE(28),AVE(43),AVE(21),
      > AVE(22),AVE(23),AVE(25),AVE(26),AVE(10),AVE(JRB+13)
C
C *****OPTION FOR FLOW WITH DELTA*****
C
      ELSE IF(NOPT.EQ.2 .AND. IDN.EQ.8) THEN
        WRITE(6,8060) AVE(8),AVE(IIDN-1),AVE(1),AVE(21),AVE(28),AVE(22),
      > AVE(23),AVE(25),AVE(26),AVE(29),AVE(30),AVE(31),AVE(32),
      > AVE(IIDN+6),AVE(IIDN+12) ;
C
C *****OPTION FOR VELOCITIES WITH DELTA*****
C
      ELSE IF(NOPT.EQ.3 .AND. IDN.EQ.8) THEN
        WRITE(6,9060) AVE(8),AVE(IIDN-1),AVE(1),AVE(33),AVE(34),AVE(35),
      > AVE(36),AVE(37),AVE(38),AVE(39),AVE(40),AVE(41),AVE(42),
      > AVE(IIDN+6),AVE(IIDN+12)
C
C *****OPTION FOR VELOCITIES WITHOUT DELTA*****
C
      ELSE IF(NOPT.EQ.3 .AND. IDN.NE.8) THEN
        WRITE(6,9065) AVE(8),AVE(10),AVE(1),AVE(34),AVE(44),AVE(33),
      > AVE(35),AVE(36),AVE(37),AVE(38),AVE(3),AVE(JRB+13)
C
      END IF
C
381 continue
      MONFLAG=.TRUE.
      IF(IYR-IYRB) 388,386,500
386 IF(MON-MONB) 388,387,500
387 IF(KDK-IDAYB) 388,500,500
388 CONTINUE
      if(kdk-ndm) 390,333,333
333 IF(MON-12) 390,389,389
389 IYR=IYR+1
      mon=0
390 CONTINUE
      DO 392 I=1,42

```

```

392 SUM(I)=0.
    DO 400 I=1,NMR
      WS(1,I)=WS(M,I)
      Q(1,I)=Q(M,I)
400 Q(2,I)=Q(JB,I)
    DO 410 I=2,NRM
410 WS(2,I)=WS(JB,I)
C
C . . . UPDATE MONTH AND YEAR AND RECHECK IF MORE DATA SHOULD BE USED
414 IF(IYR-IYRB) 418,416,500
416 IF(MON-MONB) 418,418,500
418 CONTINUE
C
C This is for running the model for the end of the month
C to the beginning of the next month.
C
    if(kdk-ndm)421,420,420
420 mon=mon+1
    kdk=0
421 kkz=0
    kb=25
    istart=2
    iend=25
    MM=0
    M=1
    KDK=KDK+1
C
C . . . MONTHLY RETURN LOOP AND END PROGRAM LOCATION
GO TO 70
500 CALL EXIT
C
C . . . FORMAT STATEMENTS.
1000 FORMAT(I2,5(LX,I2))
1010 FORMAT(I1,LX,I1)
1020 FORMAT(F8.0,F8.0,F8.2,F8.0)
1050 FORMAT(I6)
C2000 FORMAT('/' ENTER BEGINNING AND ENDING DATES '/' MM/DD/YY-MM/DD/YY')
C2020 FORMAT('/' ENTER STARTING AND ENDING STATIONS: '/8(I2,' ' ,A20/))
2030 FORMAT(' ',I2,2('/','I3),' HOUR= ',I3)
3000 FORMAT(1H1)
3010 FORMAT(///,26X,'ST. CLAIR RIVER HOURLY TRANSIENT MODEL',/,36X,
  > 'BASIC DATA'///,23X,'STATION',5X,'ABASE',5X,'DATUM',5X,'WIDTH',/)
3020 FORMAT(20X,F10.0,F10.0,F9.2,F8.0,LX,A2)
3030 FORMAT('+',62X,A20)
3040 FORMAT(/,12X,' MANNING n =',F11.8,' * WS@',A3,' +'
  > ,F10.7,' FOR STATIONS',F7.0,' THRU ',F7.0)
3050 FORMAT(///,45X,'ST. CLAIR RIVER HOURLY TRANSIENT MODEL',///,52X,A9,
  > 1X,I2,',',15,/,10X,A20,' to ',A20,40X,'WATER LEVELS VERSION',/)
3060 FORMAT(36X,F5.1,LX,'HOUR TIME INCREMENTS',11X,I3,LX,'REACHES',/)
3070 FORMAT(6X,A3,4X,'|-----COMPUTED LEVELS-----|',2X,A3,5X,A3,
  > 4X,'|-----MEASURED LEVELS AND COMPUTED DEVIATIONS (C-M)-----
  > ---|'/LX,'HR',3X,'MEAS.',5(4X,A3))

```

```

3071 FORMAT('+',T50,'MEAS. COMP.Q',1X,4(1X,'|-----',A3,'---|'),1X,
>'|-----',A3,'---|',/)
3110 FORMAT(1X,A9,1X,I4,1X,' ERROR OF TYPE ',12)
3120 FORMAT(1X,I2,F8.2,A1,5(F7.2))
3121 FORMAT('+',T48,F7.2,A1,F8.0,5(F7.2,A1,1X,F4.2))
3130 FORMAT(/,1X,'AVE ',F6.2,1X,5(F7.2))
3131 FORMAT('+',T48,F7.2,F8.0,1X,5(F7.2,2X,F4.2))
6190 FORMAT(' FLAG=',15,' ESP=',15,' PATH=',15)
C7000 FORMAT('/' ENTER OPTION NUMBER/' 1. OUTPUT SHOWS WATER LEVELS
C > AND DEVIATIONS/' 2. OUTPUT SHOWS FLOWS AROUND ISLANDS')
7010 FORMAT(I1)
C8001 FORMAT(' Enter option for delta output:/' 1. Output shows Water
C > Levels and Deviations/' 2. Output shows flows around delta and i
C > slands/' 3. Output shows velocities around delta and islands'/)
8002 FORMAT(I1)
8051 FORMAT(///,45X,'ST.CLAIR RIVER HOURLY TRANSIENT MODEL',//,52X,A9,
>1X,I2,',',15,/,10X,A20,' to ',A20,40X,'RIVER DISCHARGE VERSION',/
>/)
8020 FORMAT(//,5X,'|----RIVER PROFILE-----|',2X,'|--TOTAL FLOW--|',3X,
>'|-----ISLAND FLOWS-----|',3X,'|-----DELTA FLOWS-----
>----|',2X,'|---DEV----|',//)
8030 FORMAT(' HR',4X,2(A3,5X),A3,6X,A3,6X,A3,6X,'STAG E',3X,'STAG W'
>,4X,'FAWN E',3X,'FAWN W',3X,'N.CH.',3X,'M.CH.',3X,'S.CH.',3X,
>'CUTOFF',3X,A3,4X,'DEV')
8040 FORMAT(6X,'MEAS.',4X,'COMP.',3X,'MEAS.',4X,'FLOW',5X,'FLOW',8X,'Q
>',8X,'Q',8X,'Q',8X,'Q',8X,'Q',7X,'Q',7X,'Q',8X,'Q',5X,'MEAS.',2X,
>'C-M',/)
8050 FORMAT(1X,I2,F8.2,A1,1X,F7.2,F8.2,A1,1X,F8.0,1X,F8.0,2X,F8.0,2X,
>F7.0,1X,F8.0,2X,F8.0,1X,F7.0,1X,F7.0,1X,F7.0,1X,F7.0,
>1X,F7.2,A1,F5.2)
8060 FORMAT(/,1X,'AVE',F7.2,2X,F7.2,F8.2,2X,F8.0,1X,F8.0,2X,F8.0,2X,
>F7.0,1X,F8.0,2X,F8.0,1X,F7.0,1X,F7.0,1X,F7.0,1X,F7.0,1X,F7.2,1X,
>F5.2)
9020 FORMAT(//,5X,'|----RIVER PROFILE----|',3X,'|--TOT. VEL.--|',4X,
>'|-----MID ISLAND VELOCITIES-----|',3X,'|---MID DELTA VELOCITIES-
>---|',2X,'|---DEV----|',//)
9030 FORMAT(' HR',4X,2(A3,5X),A3,6X,A3,6X,A3,6X,'STAG E',3X,'STAG W'
>,4X,'FAWN E',3X,'FAWN W',3X,'N.CH.',3X,'M.CH.',3X,'S.CH.',2X,
>'CUTOFF',3X,A3,5X,'DEV')
9040 FORMAT(6X,'MEAS.',4X,'COMP.',3X,'MEAS.',4X,'VEL.',5X,'VEL.',8X,
>'V',8X,'V',8X,'V',8X,'V',8X,'V',7X,'V',7X,'V',7X,'V',5X,'MEAS.',
>3X,'C-M',/)
9050 FORMAT(1X,I2,F8.2,A1,1X,F7.2,F8.2,A1,1X,F6.2,3X,F6.2,4X,F6.2,4X,
>F5.2,4X,F6.2,3X,F6.2,3X,F5.2,3X,F5.2,3X,F5.2,3X,F5.2,2X,F7.2,A1,
>1X,F5.2)
9051 FORMAT(///,45X,'ST.CLAIR RIVER HOURLY TRANSIENT MODEL',//,52X,A9,
>1X,I2,',',15,/,10X,A20,' TO ',A20,40X,'RIVER VELOCITIES VERSION'
>,//)
9060 FORMAT(/,' AVE',F7.2,2X,F7.2,F8.2,2X,F6.2,3X,F6.2,4X,F6.2,4X,
>F5.2,4X,F6.2,3X,F6.2,3X,F5.2,3X,F5.2,3X,F5.2,3X,F5.2,2X,F7.2,2X,
>F5.2)
7020 FORMAT(//,17X,'|----- RIVER PROFILE -----|',4X,'|--- TOTAL DISCHA

```

```

>RGE ---| |----- ISLAND FLOWS -----| |---- DEV ----|',/)
7030 FORMAT(8X,'DAY',7X,A3,8X,A3,8X,A3,8X,A3,6X,A3,6X,A3,3X,
>'STAG E',2X,'STAG W',2X,'FAWN E',2X,'FAWN W',4X,A3,7X,'DEV')
7040 FORMAT(18X,'MEAS.',6X,'COMP.',6X,'MEAS.',6X,2('FLOW',5X),'FLOW',3X
>,4('FLOW',4X),1X,'MEAS.',4X,'(C-M)',/)
7050 FORMAT(9X,I2,6X,F6.2,A1,4X,F6.2,5X,F6.2,A1,1X,3(2X,F7.0),
>4(1X,F7.0),2X,F6.2,A1,2X,F6.2)
7060 FORMAT(/,8X,'AVE',6X,F6.2,5X,F6.2,5X,F6.2,2X,3(2X,F7.0),4(1X,F7.0)
>,2X,F6.2,4X,F5.2)
9025 FORMAT(/,17X,'|----- RIVER PROFILE -----|',5X,'|-- TOTAL VELOCIT
>IES --| |-- MID ISLAND VELOCITIES ---| |---- DEV ----|'/)
9041 FORMAT(18X,'MEAS.',6X,'COMP.',6X,'MEAS.',2X,3(5X,'VEL.'),2X,
>'VEL.',3(4X,'VEL.'),5X,'MEAS.',4X,'(C-M)',/)
9055 FORMAT(9X,I2,6X,F6.2,A1,3X,F6.2,6X,F6.2,A1,3(5X,F4.2),3X,F4.2,
>3(4X,F4.2),4X,F6.2,A1,2X,F6.2)
9065 FORMAT(/,8X,'AVE',6X,F6.2,4X,F6.2,6X,F6.2,1X,3(5X,F4.2),3X,F4.2,
>3(4X,F4.2),4X,F6.2,4X,F5.2)

```

C
C

END

Program [HYDRO.JDSTCLR]DDELTA.FOR

This is the St Clair River Transient Model - Daily Version.

It is set to run in BATCH MODE...

To run the program...

1. Set desired parameters in file [HYDRO.JDSTCLR]DDELTA.PAR

Line 1 - Starting and ending month and yr.

MO YR MO YR (I2,IX,I2,IX,I2,IX,I2)

Line 2 - Starting and ending points of model. (I1,IX,I1)

- 1 - Fort Gratiot**
- 2 - Dunn Paper**
- 3 - Mouth of Black River**
- 4 - Dry Dock**
- 5 - Marysville**
- 6 - St Clair**
- 7 - Algonac**
- 8 - Lake St Clair**

Line 3 - Output Option (I1)

- 1 - Water levels and deviations.**
- 2 - Total discharge and discharge around islands and, if included, discharge in the delta channels.**
- 3 - Velocity near the starting, ending and midpoint of the simulated river and velocities around islands and, if included, velocities in the delta channels.**

Line 4 - Units Option (I1)

- 0 - Metric units**
- 1 - English units**

2. Make sure that file [HYDRO.JDSTCLR]DDELTA.DAT is available.

3. Type: SUBMIT DDELTA/NOTIFY

4. When your request is completed the output will appear in file:

[HYDRO.JDSTCLR]ZDELTA.OUT

Note: this file is 132 characters wide.

```

>IA(359),AVECT(1378),JA(1378),ICC(358),YV(358),RSP(5722),ISP(5722)
>,VEL(180)
  EQUIVALENCE (ISP,RSP)
  DATA NAMMON/' JANUARY',' FEBRUARY',' MARCH',' APRIL',
>              ' MAY',' JUNE',' JULY',' AUGUST',
>              ' SEPTEMBER',' OCTOBER',' NOVEMBER',' DECEMBER'/
  DATA NAME/' FT. GRATIOT ' DUNN PAPER '
>              ' MOUTH OF BLACK RIVER' ' DRY DOCK '
>              ' MARYSVILLE ' ST CLAIR '
>              ' ALGONAC ' ' LAKE ST. CLAIR (SCS)'/
  DATA NMM/' FG',' DP',' MBR',' DD',' MV',' SC',' AL',' SCS'/
  DATA LOC/180,178,160,157,155,129,77,1/
  DATA IGAGE/14098,14096,14090,14087,14084,14080,14070,14052/
  DATA OLD/580.92,580.43,580.09,579.53,579.01,578.16,576.60,576.23/
C  A1 IS SLOPE AND B1 IS INTERCEPT OF MANNINGS N'S FOR ALL REACHES
  DATA A1/0.0033947,0.0002708,0.,0.,0.,0.,-0.0011146,-0.0017647/
  DATA B1/-1.92253,-0.12683,.0221,.0250,.0240,.0230,
>0.66250,1.04729/

C
C . . . ISLAND/DELTA SPECIFIC VARIABLE ASSIGNMENTS
C
  DATA NODE/3,6,25,39,51,76,97,108,135,154/
  DATA NBR/15,36,45,102,144/

C
  EPERC1=.253
  WPERC1=1.-EPERC1
  EPERC2=.376
  WPERC2=1.-EPERC2
  NPERC=.35
  MPERC=.21
  CNPERC=.56
  FNPERC=.56
  SPERC=.21
  COPERC=.23
  CSPERC=.44
  FSPERC=.44
  NSP=5722
  ICOUNT=0
  LRATIO=2
  IFLAG=0

C
C . . . PHYSICAL DATA ACCESSED
C
  DO 10 I=1,LOC(1)
  10 READ(5,1020) STA(I),ABAS(I),DATU(I),AT(I)

C
C . . . PROMPT FOR AND READ BEGINNING AND ENDING DATES
C
C  WRITE(7,2000)
  READ (10,1000) MONA,IYRA,MONB,IYRB
  IF(MONA.LE.0) THEN
    MONA=12

```

```

        IYRA-IYRA-1
    END IF
    IYRA-IYRA+1900
    IYRB-IYRB+1900
C
C . . . PROMPT FOR LOCATION OF UPPER AND LOWER LIMITS TO BE RUN
C
C     9 WRITE(7,2020) (I,NAME(I), I=1,8)
C     9 READ(10,1010) IUP,IDN
C       IIDN=IDN-1
C       IIUP=IUP+1
C       IF(IUP.GE.IIDN) GO TO 9
C
C . . . PROMPT FOR OPTION NUMBER
C
C     616 WRITE(7,8001)
C     616 READ(10,8002)NOPT
C       IF(NOPT.GT.3.OR.NOPT.LT.1) GO TO 616
C
C       READ(10,8005) MUNITS
C
C . . . DEFINE AND ADJUST PARAMETERS, BASED UPON LIMITS FROM ABOVE
C     NRM=LOC(IUP)-LOC(IDN)
C     NMR=NRM+1
C     IF(LOC(IDN).EQ.1) GO TO 27
C     DO 24 I=1,NMR
C       STA(I)=STA(I-1+LOC(IDN))
C       ABAS(I)=ABAS(I-1+LOC(IDN))
C       DATU(I)=DATU(I-1+LOC(IDN))
C     24 AT(I)=AT(I-1+LOC(IDN))
C       NODE(1)=NODE(1)-LOC(IDN)+1
C       NODE(2)=NODE(2)-LOC(IDN)+1
C       NODE(3)=NODE(3)-LOC(IDN)+1
C       NODE(4)=NODE(4)-LOC(IDN)+1
C       NODE(5)=NODE(5)-LOC(IDN)+1
C       NODE(6)=NODE(6)-LOC(IDN)+1
C       NODE(7)=NODE(7)-LOC(IDN)+1
C       NODE(8)=NODE(8)-LOC(IDN)+1
C       NODE(9)=NODE(9)-LOC(IDN)+1
C       NODE(10)=NODE(10)-LOC(IDN)+1
C       NBR(1)=NBR(1)-LOC(IDN)+1
C       NBR(2)=NBR(2)-LOC(IDN)+1
C       NBR(3)=NBR(3)-LOC(IDN)+1
C       NBR(4)=NBR(4)-LOC(IDN)+1
C       NBR(5)=NBR(5)-LOC(IDN)+1
C       DO 25 I=IUP,IDN
C     25 LOC(I)=LOC(I)-LOC(IDN)+1
C
C . . . CALCULATE DISTANCES BETWEEN SECTIONS
C     27 DO 30 I=1,NRM
C       X(I)=STA(I+1)-STA(I)
C     30 IF(I.EQ.NBR(1).OR.I.EQ.NBR(2).OR.I.EQ.NBR(3).OR.I.EQ.

```



```

      >NBR(4).OR.I.EQ.NBR(5)) X(I)=0.0
C
C . . . The following lines which, have been COMMENTED with "c0", will
C . . . WRITE the BASIC PHYSICAL DATA. Should the user desire to see
C . . . this data, the "c0's" would have to be eliminated and the
C . . . program re-compiled/linked etc. TO RE-COMPILE submit DCDELTA.
C
c0      WRITE (6,3000)
c0      WRITE (6,3010)
c0      DO 40 I=1,NMR
c0          MARK(I)=' '
c0          IF(I.EQ.NODE(3).OR.I.EQ.NODE(5).OR.I.EQ.NODE(6)
c0      >.OR.I.EQ.NODE(7).OR.I.EQ.NODE(8).OR.I.EQ.NODE(9).OR.
c0      >I.EQ.NODE(10)) MARK(I)='<'
c0          IF(I.GT.NODE(2).AND.I.LE.NBR(1))MARK(I)='N '
c0          IF(I.GT.NBR(1).AND.I.LT.NODE(3))MARK(I)='M '
c0          IF(I.GT.NODE(3).AND.I.LE.NBR(2))MARK(I)='UN'
c0          IF(I.GT.NODE(4).AND.I.LE.NBR(3))MARK(I)='S '
c0          IF(I.GT.NBR(3).AND.I.LT.NODE(5))MARK(I)='CO'
c0          IF(I.GT.NODE(5).AND.I.LT.NODE(6))MARK(I)='US'
c0          IF(I.GT.NODE(7).AND.I.LE.NBR(4).OR.I.GT.NODE(9).AND.I
c0      >.LE.NBR(5))MARK(I)='W '
c0          IF(I.GT.NBR(4).AND.I.LT.NODE(8).OR.I.GT.NBR(5).AND.I
c0      >.LT.NODE(10))MARK(I)='E '
c0          IF(I.LE.NODE(2).OR.I.GT.NBR(2).AND.I.LE.NODE(4)) GO TO 40
c0          WRITE(6,3020) STA(I),ABAS(I),DATU(I),AT(I),MARK(I)
c0          DO 40 IJ=IUP,IDN
c0      40 IF(I.EQ.LOC(IJ)) WRITE(6,3030) NAME(IJ)
C
C      THESE NEXT 2 MANNINGS N PRINTOUTS ARE HARDWIRED. IF THE
C      NUMBER OF STATIONS CHANGES, CHANGE THESE!
C
c0      IF(IDN.EQ.8) WRITE(6,3040) A1(8),NMM(8),B1(8),STA(7),STA(36)
c0      IF(IDN.EQ.8) WRITE(6,3040) A1(7),NMM(8),B1(7),STA(40),STA(77)
c0      DO 45 I=IIDN,IUP,-1
c0      45 IF(I.LT.7)WRITE(6,3040) A1(I),NMM(I),B1(I),STA(LOC(I+1)),
c0      >STA(LOC(I))
C
C . . . INITIALIZE AND ASSIGN ADDITIONAL VARIABLES
      DO 50 I=1,4
50 ADJ(I)=0.
      NVAR=NRM*2
      ANC=24.
      DT=ANC*3600.
      DO 51 I=1,42
51 SUM(I)=0.
      TH=.75
      TH1=.25
      MM=0
      M=13
      istart=13
      iend=43

```

```

      kkr=11
      MON=MONA
      IYR=IYRA
      MONFLAG=.FALSE.
      JRB=(IUP+IDN)/2

C
C   Routine to read all of the water level data from the disk and
C   store it in another tempory file. This way the disk is not tied
C   up for long periods of time when running the program.
C
C . . . READ WATER LEVELS FROM DISC.
C
52  CALL NODAYS( IYR,MON,1,NDM,NDY,JD)
    DO 55 JJ=IUP,IDN
      IW=1
      IC=IGAGE(JJ)/10000
      IGAG=IGAGE(JJ)-IC*10000
      CALL GAGEIO( IW,IC,IGAG ,MON,IYR,IB,IT,IDA,IDB,IDC,IER)
      IF(IER.NE.0) THEN
        WRITE(6,3110) NAMMON(MON),IYR,IER
        CALL EXIT
      END IF
      DO 54 J=1,NDM
        DO 53 I=1,24
          WRITE(9,56) I,HOURL(I,J)
53  CONTINUE
        WRITE(9,56) MEAN(J)
54  CONTINUE
55  CONTINUE
56  FORMAT(I6)
C
      IF(IYR-IYRB) 58,57,65
57  IF(MON-MONB) 58,65,65
58  CONTINUE
      IF(MON-12) 60,59,59
59  IYR=IYR+1
60  CONTINUE
C . . . UPDATE MONTH AND YEAR AND RECHECK IF MORE DATA SHOULD BE USED
      MON=MON+1
      IF(MON-13) 62,61,61
61  MON=1
62  IF(IYR-IYRB) 64,63,65
63  IF(MON-MONB) 64,64,65
64  CONTINUE
C
      GO TO 52
65  CALL DISMOUNTPACK('WATER_LEVELS')
      MON=MONA
      IYR=IYRA
      REWIND 9
C
C . . . COME HERE EACH MONTH AND PRINT TITLES AND HEADINGS FOR

```

```

C      EACH OPTION
70  continue
    if(Nopt.eq.1.and.iup.eq.1) iiup=iiup+1
C
C *****OPTION FOR WATER LEVELS*****
C
    IF(NOPT.EQ.1) THEN
        WRITE(6,3000)
        WRITE(6,3050) NAMMON(MON),IYR,NAME(IUP),NAME(IDN)
        WRITE(6,3060) ANC,NRM
        WRITE(6,3070) NMM(IDN),NMM(IUP),
    >  NMM(IUP),(NMM(I),I-IIDN,IIUP,-1)
        WRITE(6,3071) (NMM(I),I-IIDN,IIUP,-1)
        IF(NOPT.EQ.1.AND.IUP.EQ.1)IIUP=IIUP-1
C
C *****OPTION FOR FLOWS WITHOUT DELTA*****
C
    ELSE IF(NOPT.EQ.2 .AND. IDN.NE.8) THEN
        WRITE(6,3000)
        WRITE(6,8051)NAMMON(MON),IYR,NAME(IUP),NAME(IDN)
        WRITE(6,3060)ANC,NRM
        WRITE(6,7020)
        WRITE(6,7030)NMM(IDN),NMM(JRB),NMM(IUP),NMM(IIDN),NMM(JRB),
    >  NMM(IUP),NMM(JRB)
        WRITE(6,7040)
C
C *****OPTION FOR FLOWS WITH DELTA*****
C
    ELSE IF(NOPT.EQ.2 .AND. IDN.EQ.8) THEN
        WRITE(6,3000)
        WRITE(6,8051)NAMMON(MON),IYR,NAME(IUP),NAME(IDN)
        WRITE(6,3060)ANC,NRM
        WRITE(6,8020)
        WRITE(6,8030)NMM(IDN),NMM(IIDN-1),NMM(IUP),NMM(IUP),NMM(IIDN),
    >  NMM(IIDN-1)
        WRITE(6,8040)
C
C *****OPTION FOR VELOCITIES WITHOUT DELTA*****
C
    ELSE IF(NOPT.EQ.3 .AND. IDN.NE.8) THEN
        WRITE(6,3000)
        WRITE(6,9051)NAMMON(MON),IYR,NAME(IUP),NAME(IDN)
        WRITE(6,3060)ANC,NRM
        WRITE(6,9025)
        WRITE(6,7030)NMM(IDN),NMM(JRB),NMM(IUP),NMM(IIDN),NMM(JRB),
    >  NMM(IUP),NMM(JRB)
        WRITE(6,9041)
C
C *****OPTION FOR VELOCITIES WITH DELTA*****
C
    ELSE IF(NOPT.EQ.3 .AND. IDN.EQ.8) THEN
        WRITE(6,3000)

```

```

        WRITE(6,9051)NAMMON(MON),IYR,NAME(IUP),NAME(IDN)
        WRITE(6,3060)ANC,NRM
        WRITE(6,9020)
        WRITE(6,9030)NMM(IDN),NMM(IIDN-1),NMM(IUP),NMM(IUP),NMM(IIDN),
> NMM(IIDN-1)
        WRITE(6,9040)
        END IF
C
71  continue
C . . . ADJUST GAGE-SPECIFIC VARIABLES BASED UPON YEARS STUDIED
        IF(IYR.LT.1970) IGAGE(1)=14099
        IF(IYR.LT.1971) IGAGE(6)=14080
        IF(IYR.GT.1970) ADJ(1)--.18
        IF(IYR.GT.1981) ADJ(1)--.06
        IF(IYR.LT.1971) ADJ(6)--.09
C
C . . . READ WATER LEVELS FROM UNIT 9 . . .
C
        CALL NODAYS( IYR,MON,1,NDM,NDY,JD)
C
        DO 110 JJ=IUP,IDN
C
        DO 77 J=1,NDM
            DO 75 I=1,24
75      READ(9,1050,END=78) IHOURL(I,J)
77      READ(9,1055,END=78) MEAN(J)
C
78      CONTINUE
        KK = 1
        DO 100 J=ISTART,IEND
            DO 80 I=1,24
C
C . . . FLAG MISSING DATA AND ASSIGN GAGE LEVELS TO WSSAV
        IF(IHOURL(I,KK).GT.0) THEN
            NOTE(JJ,KK)=' '
        ELSE
            NOTE(JJ,KK)='*'
            GO TO 90
        END IF
80      CONTINUE
90      WSSAV(J,JJ)=0.0
        IF(MEAN(KK).LE.0) THEN
            WSSAV(J,JJ)=OLD(JJ)
            NOTE(JJ,KK)='E'
        ELSE
            WSSAV(J,JJ)=(MEAN(KK)+IB)/100.0+ADJ(JJ)
        END IF
        OLD(JJ) = WSSAV(J,JJ)
        IF(JJ.EQ.IUP.OR.JJ.EQ.IDN) WS(J,LOC(JJ))=WSSAV(J,JJ)
100     KK = KK+1
110     CONTINUE
        IF(MONFLAG) GO TO 200

```

```

C
C . . . SET WS FOR 12 PREVIOUS TIME STEPS, TO ACHIEVE 'STEADY STATE'.
DO 120 I=1,12
  DO 120 J=1,8
    WSSAV(I,J)=WSSAV(13,J)
120  IF(J.EQ.IUP .OR. J.EQ.IDN) WS(I,LOC(J))=WSSAV(13,J)
C
C . . . ZERO MATRIX, SET CHANNEL PARAMETERS, & SET INITIAL CONDITIONS.
DO 130 I = 1,NVAR
  YVECT(I)=0.
  DO 130 J = 1,NVAR
130  XMTRX(J,I)=0.
  XSUM=STA(LOC(IUP))-STA(LOC(IDN))
  SLOPE=(WSSAV(1,IUP)-WSSAV(1,IDN))/XSUM
  AA(1)=ABAS(1)+AT(1)*(WS(1,1)-DATU(1))
  DO 150 I=1,NRM
    IF(I.NE.NRM) THEN
      WS(1,I+1)=WS(1,I)+SLOPE*X(I)
      IF(I.EQ.NBR(1)) WS(1,I+1)=WS(1,NODE(2))
      IF(I.EQ.NBR(2)) WS(1,I+1)=WS(1,NODE(1))
      IF(I.EQ.NBR(3)) WS(1,I+1)=WS(1,NODE(4))
      IF(I.EQ.NBR(4)) WS(1,I+1)=WS(1,NODE(7))
      IF(I.EQ.NBR(5)) WS(1,I+1)=WS(1,NODE(9))
      WS(2,I+1)=WS(1,I+1)
    END IF
    AA(I+1)= ABAS(I+1)+AT(I+1)*(WS(1,I+1)-DATU(I+1))
    A(I)=(AA(I)+AA(I+1))/2.
    T(I)=(AT(I)+AT(I+1))/2.
150  R(I)=A(I)/T(I)
    AN(1)= A1(IIDN)*WSSAV(M,IIDN)+B1(IIDN)
    QSTART=1.486*A(1)*R(1)**(2./3.)*(WS(1,2)-WS(1,1))**.5/AN(1)
    > /X(1)**.5
C
C . . . SPLIT FLOW INITIALLY AROUND THE ISLANDS FOR FASTER CONVERGENCE
DO 190 I=1,NMR
  PERC=1.
  IF(I.GT.NODE(1) .AND. I.LE.NODE(2)) PERC=FNPERC
  IF(I.GT.NODE(2) .AND. I.LE.NBR(1)) PERC=NPERC
  IF(I.GT.NBR(1) .AND. I.LT.NODE(3)) PERC=MPERC
  IF(I.GE.NODE(3) .AND. I.LE.NBR(2)) PERC=CNPERC
  IF(I.GT.NBR(2) .AND. I.LE.NODE(4)) PERC=FSPERC
  IF(I.GT.NODE(4) .AND. I.LE.NBR(3)) PERC=SPERC
  IF(I.GT.NBR(3) .AND. I.LT.NODE(5)) PERC=COPERC
  IF(I.GE.NODE(5) .AND. I.LT.NODE(6)) PERC=CSPERC
  IF(I.GT.NODE(7) .AND. I.LE.NBR(4)) PERC=WPERC1
  IF(I.GT.NBR(4) .AND. I.LT.NODE(8)) PERC=EPERC1
  IF(I.GT.NODE(9) .AND. I.LE.NBR(5)) PERC=WPERC2
  IF(I.GT.NBR(5) .AND. I.LT.NODE(10)) PERC=EPERC2
  Q(1,I)=QSTART*PERC
190  Q(2,I)=Q(1,I)
  kb=48
  M=1

```

```

200 CONTINUE
    N=M+1
    ITER=1
210 YVMAX=0.
    DO 230 I=1,NRM
        QA(I)=TH/2.*(Q(N,I)+Q(N,I+1))+TH1/2.*(Q(M,I)+Q(M,I+1))
        U(I)=ABS(QA(I))
        DO 230 J=IUP,IDN
            IF(I.LT.LOC(J)) AN(I)=A1(J)*WSSAV(M,J)+B1(J)
230    IF(IDN.EQ.8.AND.I.GT.3.AND.I.LE.36) AN(I)=A1(8)*WSSAV(M,J)
        > +B1(8)
C
C . . . COMPUTE AREAS AND HYDRAULIC RADII
    AA(1)=ABAS(1)+AT(1)*(TH*WS(N,I)+TH1*WS(M,I)-DATU(I))
    DO 250 I=1,NRM
        AA(I+1)= ABAS(I+1)+AT(I+1)*(TH*WS(N,I+1)+TH1*WS(M,I+1)-DATU(I+1))
        A(I)=(AA(I)+AA(I+1))/2.
        T(I)=(AT(I)+AT(I+1))/2.
250 R(I)=A(I)/T(I)
C
C . . . CONTINUITY EQUATIONS
    NRD=NVAR-1
    DO 260 I=1,NRD,2
        ID=I/2+1
        IU=ID+1
        DO 255 J=1,5
            JJ=NBR(J)
            KK=NODE(2*J)
            LL=NODE(2*J-1)
            IF(IDN.NE.8.AND.ID.EQ.LL.OR.IDN.NE.8.AND.IU.EQ.KK.OR.
> IDN.EQ.8.AND.I.GT.106.AND.ID.EQ.LL.OR.IDN.EQ.8.AND.I.GT.106
> .AND.IU.EQ.KK.OR.IDN.EQ.8.AND.ID.EQ.6.OR.IDN.EQ.8.AND.ID.EQ.
> 24.OR.IDN.EQ.8.AND.ID.EQ.39.OR.IDN.EQ.8.AND.ID.EQ.50.OR.
> IDN.EQ.8.AND.ID.EQ.3) THEN
                YVECT(I)=-(WS(N,IU)+WS(M,IU)-WS(N,ID)-WS(M,ID))/2.
                XMTRX(I,I-1)=-0.5
                XMTRX(I,I+1)=+0.5
                GO TO 260
            ELSE IF(ID.EQ.JJ.AND.IDN.NE.8.OR.ID.EQ.JJ.AND.IDN.EQ.8
> .AND.J.GE.4) THEN
                YVECT(I)=-(WS(N,KK)+WS(M,KK)-WS(N,JJ)-WS(M,JJ))/2.
                XMTRX(I,I-1)=-0.5
                XMTRX(I,2*KK-2)=+0.5
                GO TO 260
            ELSE IF(IDN.EQ.8.AND.ID.EQ.NBR(1)) THEN
                YVECT(I)=-(WS(N,ID)+WS(M,ID)-WS(N,NODE(3))-WS(M,NODE(3)))/2.
                XMTRX(I,28) = +.5
                XMTRX(I,48) = -.5
                GO TO 260
            ELSE IF(IDN.EQ.8.AND.ID.EQ.NBR(2)) THEN
                YVECT(I)=-(WS(N,ID)+WS(M,ID)-WS(N,NODE(6))-WS(M,NODE(6)))/2.
                XMTRX(I,70)=+.5

```

```

        XMTRX(I,150)=- .5
        GO TO 260
    ELSE IF(IDN.EQ.8.AND.ID.EQ.NBR(3)) THEN
        YVECT(I)--(WS(N,ID)+WS(M,ID)-WS(N,NODE(5))-WS(M,NODE(5)))/2.
        XMTRX(I,88)=+.5
        XMTRX(I,100)=-.5
        GO TO 260
    END IF
255 CONTINUE
    YVECT(I)--((WS(N,ID)+WS(N,IU)-WS(M,ID)-WS(M,IU))/(2.*DT)+
> (TH*(Q(N,ID)-Q(N,IU))+TH1*(Q(M,ID)-Q(M,IU)))/(T(ID)*X(ID)))
    XMTRX(I,I)=TH/(T(ID)*X(ID))
    XMTRX(I,I+2)--XMTRX(I,I)
    IF(I.EQ.1) THEN
        XMTRX(I,2)=1./(2.*DT)
    ELSE
        XMTRX(I,I-1)=1./(2.*DT)
        XMTRX(I,I+1)=1./(2.*DT)
        IF(I.EQ.NRD) XMTRX(I,I+1)=XMTRX(I,I+2)
        IF(I.EQ.NRD) XMTRX(I,I+2)=0.
    END IF
260 CONTINUE
C
C . . . MOMENTUM EQUATIONS
DO 280 I=2,NVAR,2
    ID=I/2
    IU=ID+1
    DO 265 J=1,5
        JJ=NBR(J)
        KK=NODE(2*J)
        LL=NODE(2*J-1)
        IF(IDN.NE.8.AND.ID.EQ.LL.OR.IDN.EQ.8.AND.J.GE.4.AND.
> ID.EQ.LL) THEN
            YVECT(I)--(Q(N,JJ+1)+Q(M,JJ+1)+Q(N,IU)+Q(M,IU)-Q(N,ID)-Q(M,ID))
> /2.
            XMTRX(I,I-1)=-0.5
            XMTRX(I,I+1)=+0.5
            XMTRX(I,2*JJ+1)=+0.5
            GO TO 280
        ELSE IF(IDN.NE.8.AND.ID.EQ.JJ.OR.IDN.EQ.8.AND.J.GE.4.AND.
> ID.EQ.JJ) THEN
            YVECT(I)--(WS(N,IU)+WS(M,IU)-WS(N,LL)-WS(M,LL))/2.
            XMTRX(I,2*LL-2)=-0.5
            XMTRX(I,I)=+0.5
            GO TO 280
        ELSE IF(IDN.NE.8.AND.IU.EQ.KK.OR.IDN.EQ.8.AND.J.GE.4.AND.
> IU.EQ.KK) THEN
            YVECT(I)--(Q(N,KK)+Q(M,KK)-Q(N,ID)-Q(M,ID)-Q(N,JJ)-Q(M,JJ))/2.
            XMTRX(I,2*JJ-1)=-0.5
            XMTRX(I,I-1)=-0.5
            XMTRX(I,I+1)=+0.5
            GO TO 280

```

```

ELSE IF(IDN.EQ.8.AND.ID.EQ.NODE(1)) THEN
  YVECT(I)= -(Q(N,NODE(1))+Q(M,NODE(1))-Q(N,NODE(1)+1)
> -Q(M,NODE(1)+1)-Q(N,NBR(2)+1)-Q(M,NBR(2)+1))/2.
  XMTRX(I,I-1)= +.5
  XMTRX(I,I+1)= -.5
  XMTRX(I,73)= -.5
  GO TO 280
ELSE IF(IDN.EQ.8.AND.ID.EQ.NODE(2)) THEN
  YVECT(I)= -(Q(N,NODE(2))+Q(M,NODE(2))-Q(N,NODE(2)+1)
> -Q(M,NODE(2)+1)-Q(N,NBR(1)+1)-Q(M,NBR(1)+1))/2.
  XMTRX(I,I-1)= +.5
  XMTRX(I,I+1)= -.5
  XMTRX(I,31)= -.5
  GO TO 280
ELSE IF(IDN.EQ.8.AND.ID.EQ.NODE(4)) THEN
  YVECT(I)= -(Q(N,NODE(4))+Q(M,NODE(4))-Q(N,NODE(4)+1)
> -Q(M,NODE(4)+1)-Q(N,NBR(3)+1)-Q(M,NBR(3)+1))/2.
  XMTRX(I,I-1)= +.5
  XMTRX(I,I+1)= -.5
  XMTRX(I,91)= -.5
  GO TO 280
ELSE IF(IDN.EQ.8.AND.ID.EQ.NBR(1)) THEN
  YVECT(I)= -(WS(N,NBR(1)+1)+WS(M,NBR(1)+1)-WS(N,NODE(2))
> -WS(M,NODE(2)))/2.
  XMTRX(I,I)= +.5
  XMTRX(I,10)= -.5
  GO TO 280
ELSE IF(IDN.EQ.8.AND.IU.EQ.NODE(3)) THEN
  YVECT(I)= -(Q(N,NODE(3))+Q(M,NODE(3))-Q(N,NODE(3)-1)
> -Q(M,NODE(3)-1)-Q(N,NBR(1))-Q(M,NBR(1)))/2.
  XMTRX(I,I+1)= +.5
  XMTRX(I,I-1)= -.5
  XMTRX(I,29)= -.5
  GO TO 280
ELSE IF(IDN.EQ.8.AND.ID.EQ.NBR(2)) THEN
  YVECT(I)= -(WS(N,NODE(1))+WS(M,NODE(1))-WS(N,NBR(2)+1)
> -WS(M,NBR(2)+1))/2.
  XMTRX(I,72)= -.5
  XMTRX(I,4)= +.5
  GO TO 280
ELSE IF(IDN.EQ.8.AND.ID.EQ.NBR(3)) THEN
  YVECT(I)= -(WS(N,NODE(4))+WS(M,NODE(4))-WS(N,NBR(3)+1)
> -WS(M,NBR(3)+1))/2.
  XMTRX(I,76)= +.5
  XMTRX(I,90)= -.5
  GO TO 280
ELSE IF(IDN.EQ.8.AND.IU.EQ.NODE(5)) THEN
  YVECT(I)= -(Q(N,NODE(5))+Q(M,NODE(5))-Q(N,NODE(5)-1)
> -Q(M,NODE(5)-1)-Q(N,NBR(3))-Q(M,NBR(3)))/2.
  XMTRX(I,101)= +.5
  XMTRX(I,99)= -.5
  XMTRX(I,89)= -.5

```



```

      GO TO 280
    ELSE IF(IDN.EQ.8.AND.IU.EQ.NODE(6)) THEN
      YVECT(I)=-(Q(N,NODE(6))+Q(M,NODE(6))-Q(N,NODE(6)-1)
> -Q(M,NODE(6)-1)-Q(N,NBR(2))-Q(M,NBR(2)))/2.
      XMTRX(I,151)=+.5
      XMTRX(I,71)=-.5
      XMTRX(I,149)=-.5
      GO TO 280
    END IF
265 CONTINUE
    Z41=-QA(ID)*T(ID)*(WS(N,IU)+WS(N,ID)-WS(M,IU)-WS(M,ID))/
> (2.*DT*A(ID)**2.)*2.
    Z61=(Q(N,ID)+Q(N,IU)-Q(M,ID)-Q(M,IU))/(2.*DT*A(ID))
    Z11=32.17*AN(ID)**2.*QA(ID)*U(ID)/(2.21*A(ID)**2.*R(ID)**(4./3.))
    Z21=32.17*(TH*(WS(N,ID)-WS(N,IU))+TH1*(WS(M,ID)-WS(M,IU)))/X(ID)
    Z31=- (QA(ID)**2.*(AA(ID)-AA(IU))/(A(ID)**3.*X(ID)))
    YVECT(I)=-(Z11+Z21+Z31+Z41+Z61)
    XMTRX(I,I)=-(32.2-QA(ID)**2.*T(ID)/(A(ID)**3.))/X(ID)*TH-QA(ID)
> *T(ID)/(DT*A(ID)**2.)
    IF(I.LT.4) GO TO 270
    XMTRX(I,I-2)=(32.2-QA(ID)**2.*T(ID)/(A(ID)**3.))/X(ID)*TH-QA(ID)
> *T(ID)/(DT*A(ID)**2.)
270 ZZZ1=ABS(QA(ID))
    P1=32.2*AN(ID)**2.*ZZZ1*TH/(2.2082*A(ID)**2.*R(ID)**(4./3.))
> -QA(ID)/A(ID)**3.*(AA(ID)-AA(IU))*TH/X(ID)-TH*T(ID)*(WS(N,ID)
> +WS(N,IU)-WS(M,ID)-WS(M,IU))/(2.*DT*A(ID)**2.)
    XMTRX(I,I-1)=1./(2.*A(ID)*DT)+P1
    XMTRX(I,I+1)=XMTRX(I,I-1)
    IF(I.EQ.NVAR) XMTRX(I,I)=XMTRX(I,I+1)
    IF(I.EQ.NVAR) XMTRX(I,I+1)=0.
280 CONTINUE
C
C . . .SET UP AVECT, JA, AND IA, AND ACCESS SPARCE MATRIX SOLVER
DO 290 I=1,NVAR
290 IA(I)=0.
DO 291 I=1,900
  AVECT(I)=0.
291 JA(I)=0.
  K=0
DO 292 I=1,NVAR
  RR(I)=I
  CC(I)=I
  ICC(I)=I
  NEWROW=.TRUE.
DO 292 J=1,NVAR
  IF(XMTRX(I,J).NE.0.) THEN
    K=K+1
    AVECT(K)=XMTRX(I,J)
    JA(K)=J
    IF(NEWROW) THEN
      IA(I)=K
      NEWROW=.FALSE.

```

```

        END IF
        END IF
292 CONTINUE
    IA(NVAR+1)=K+1
    NSP=100+8*NVAR+2+2*K
    PATH=2
    IF(ICOUNT.EQ.0) PATH=1
    ICOUNT=ICOUNT+1
    CALL CDRV(NVAR,RR,CC,ICC,IA,JA,AVECT,YVECT,YV,NSP,ISP,RSP,ESP,
> PATH,FLAG)
    IF(FLAG.NE.0) THEN
        WRITE(6,6190) FLAG,ESP,PATH
        GO TO 500
    END IF

C
C . . . DETERMINE NEW FLOWS AND LEVELS
    NNR=NVAR+1
    DO 300 I=1,NNR,2
        II=I/2+1
        Q(N,II)=Q(N,II)+YV(I)
        IF(II=NNR.EQ.0) Q(N,NNR)=Q(N,NNR)+YV(NVAR)
300 CONTINUE
    NNR=NVAR-2
    DO 310 I=2,NNR,2
        IF (YV(I).LT.-20.) YV(I)--20.
        II=I/2+1
        WS(N,II)=WS(N,II)+YV(I)
310 CONTINUE

C
C . . . ASSIGN MAXIMUM DELTA VALUE, AND TEST FOR EXCESSIVE ITERATIONS
    DO 319 I=2,NNR,2
319 IF(ABS(YV(I)).GT.YVMAX) YVMAX=YV(I)
    DO 320 I=2,NNR,2
        IF(ABS(YV(I)).GT..002) THEN
            IF(ITER.GT.20) THEN
                WRITE(6,1133) ITER,YVMAX,I/2
1133     FORMAT(' ',I2,' ITERATIONS.  YVMAX =',E10.3,' AT I=',I2,/)
                GO TO 500
            END IF
            ITER=ITER+1
            GO TO 210
        END IF
320 CONTINUE

C
C . . . DETERMINE THE DEVIATION OF CALCULATED FROM MEASURED LEVELS
    JB=N+1
    DO 330 IJ=IIUP,IIDN
        IF(WSSAV(N,IJ).LT.50.) WSSAV(N,IJ)=WS(N,LOC(IJ))- .0001
330 DEV(IJ)=WS(N,LOC(IJ))-WSSAV(N,IJ)
        MM=MM+1
        NM=NM+kkz
        IF(NM.LE.0) GO TO 340

```

```

      IF(NOPT.EQ.3) THEN
        DO 6262 I=1,NRM+1
6262  VEL(I)=Q(N,I)/AA(I)
      END IF
C
C . . . METRIC OPTION FOR OUTPUT . .
      IF(MUNITS.EQ.0) THEN
        DO 6700 MC = IUP, IDN
6700  WSSAV(N,MC) = WSSAV(N,MC)/3.28083
        DO 6720 MC= IIUP, IIDN
          WS(N,LOC(MC)) = WS(N,LOC(MC))/3.28083
6720  DEV(MC) = DEV(MC)/3.28083
C
          Q(N,LOC(IUP)) = Q(N,LOC(IUP))*0.02832
          Q(N,LOC(IIDN)) = Q(N,LOC(IIDN))*0.02832
          Q(N,NBR(5)+5) = Q(N,NBR(5)+5)*0.02832
          Q(N,NBR(5)-4) = Q(N,NBR(5)-4)*0.02832
          Q(N,NODE(10)+1) = Q(N,NODE(10)+1)*0.02832
          Q(N,NBR(4)+3) = Q(N,NBR(4)+3)*0.02832
          Q(N,NBR(4)-2) = Q(N,NBR(4)-2)*0.02832
          Q(N,NODE(8)+1) = Q(N,NODE(8)+1)*0.02832
          Q(N,NBR(1)-3) = Q(N,NBR(1)-3)*0.02832
          Q(N,NBR(1)+6) = Q(N,NBR(1)+6)*0.02832
          Q(N,NBR(3)-3) = Q(N,NBR(3)-3)*0.02832
          Q(N,NBR(3)+3) = Q(N,NBR(3)+3)*0.02832
          Q(N,LOC(JRB)) = Q(N,LOC(JRB))*0.02832
C
          VEL(LOC(IUP)) = VEL(LOC(IUP))/3.28083
          VEL(LOC(IIDN)) = VEL(LOC(IIDN))/3.28083
          VEL(NBR(5)+5) = VEL(NBR(5)+5)/3.28083
          VEL(NBR(5)-4) = VEL(NBR(5)-4)/3.28083
          VEL(NBR(4)+3) = VEL(NBR(4)+3)/3.28083
          VEL(NBR(4)-2) = VEL(NBR(4)-2)/3.28083
          VEL(NBR(1)-3) = VEL(NBR(1)-3)/3.28083
          VEL(NBR(1)+6) = VEL(NBR(1)+6)/3.28083
          VEL(NBR(3)-3) = VEL(NBR(3)-3)/3.28083
          VEL(NBR(3)+3) = VEL(NBR(3)+3)/3.28083
          VEL(LOC(JRB)) = VEL(LOC(JRB))/3.28083
        END IF
C
C . . . PRINT OUTPUT.
      IF(NOPT.EQ.1.and.iup.eq.1) iiup=iiup+1
C
C *****OPTION FOR WATER LEVELS*****
C
      IF(NOPT.EQ.1) THEN
        WRITE(6,3120) NM,WSSAV(N,IDN),NOTE(IDN,NM),
        > (WS(N,LOC(I)),I-IIDN,IIUP,-1)
        WRITE(6,3121) WSSAV(N,IUP),NOTE(IUP,NM),
        > Q(N,LOC(IUP)),
        > (WSSAV(N,I),NOTE(I,NM),DEV(I), I-IIDN,IIUP,-1)
C

```

C *****OPTION FOR FLOW WITHOUT DELTA*****

C

```
ELSE IF(NOPT.EQ.2.AND.IDN.NE.8) THEN
  WRITE(6,7050)NM,WSSAV(N,IDN),NOTE(IDN,NM),WS(N,LOC(JRB)),
  >WSSAV(N,IUP),NOTE(IUP,NM),Q(N,LOC(IIDN)),Q(N,LOC(JRB)),
  >Q(N,LOC(IUP)),Q(N,NBR(5)+5),Q(N,NBR(5)-4),Q(N,NBR(4)+3),
  >Q(N,NBR(4)-2),WSSAV(N,JRB),NOTE(JRB,NM),DEV(JRB)
```

C

C *****OPTION FOR FLOW WITH DELTA*****

C

```
ELSE IF(NOPT.EQ.2.AND.IDN.EQ.8) THEN
  WRITE(6,8050)NM,WSSAV(N,IDN),NOTE(IDN,NM),WS(N,LOC(IIDN-1)),
  >WSSAV(N,IUP),NOTE(IUP,NM),Q(N,LOC(IUP)),Q(N,LOC(IIDN)),
  >Q(N,NBR(5)+5),Q(N,NBR(5)-4),Q(N,NBR(4)+3),Q(N,NBR(4)-2),
  >Q(N,NBR(1)-3),Q(N,NBR(1)+6),Q(N,NBR(3)-3),Q(N,NBR(3)+3),
  >WSSAV(N,IIDN-1),NOTE(IIDN-1,NM),DEV(IIDN-1)
```

C

C *****OPTION FOR VELOCITIES WITHOUT DELTA*****

C

```
ELSE IF(NOPT.EQ.3.AND.IDN.NE.8) THEN
  WRITE(6,9055)NM,WSSAV(N,IDN),NOTE(IDN,NM),WS(N,LOC(JRB)),
  >WSSAV(N,IUP),NOTE(IUP,NM),VEL(LOC(IIDN)),VEL(LOC(JRB)),
  >VEL(LOC(IUP)),VEL(NBR(5)+5),VEL(NBR(5)-4),VEL(NBR(4)+3),
  >VEL(NBR(4)-2),WSSAV(N,JRB),NOTE(JRB,NM),DEV(JRB)
```

C

C *****OPTION FOR VELOCITIES WITH DELTA*****

C

```
ELSE IF(NOPT.EQ.3.AND.IDN.EQ.8) THEN
  WRITE(6,9050) NM,WSSAV(N,IDN),NOTE(IDN,NM),WS(N,LOC(IIDN-1)),
  >WSSAV(N,IUP),NOTE(IUP,NM),VEL(LOC(IUP)),VEL(LOC(IIDN)),
  >VEL(NBR(5)+5),VEL(NBR(5)-4),VEL(NBR(4)+3),VEL(NBR(4)-2),
  >VEL(NBR(1)-3),VEL(NBR(1)+6),VEL(NBR(3)-3),VEL(NBR(3)+3),
  >WSSAV(N,IIDN-1),NOTE(IIDN-1,NM),DEV(IIDN-1)
  END IF
```

```
  if(Nopt.eq.1.and.iup.eq.1) iiup=iiup-1
```

333 continue

C

C . . . COMPUTE MEAN VALUES.

```
SUM(1)=SUM(1)+WSSAV(N,IUP)
```

```
DO 334 I=2,7
```

334 SUM(I)=SUM(I)+WS(N,LOC(I))

```
SUM(8)=SUM(8)+WSSAV(N,IDN)
```

```
DO 335 I=1,6
```

```
SUM(I+8)=SUM(I+8)+WSSAV(N,I+1)
```

335 SUM(I+14)=SUM(I+14)+DEV(I+1)

C

C . . . THESE ARE THE CALCULATIONS FOR FLOW AVERAGES

```
SUM(21)=SUM(21)+Q(N,LOC(IUP))
```

```
SUM(22)=SUM(22)+Q(N,NBR(5)+5)
```

```
SUM(23)=SUM(23)+Q(N,NBR(5)-4)
```

```
SUM(24)=SUM(24)+Q(N,NODE(10)+1)
```

```
SUM(25)=SUM(25)+Q(N,NBR(4)+3)
```

```

SUM(26)=SUM(26)+Q(N,NBR(4)-2)
SUM(27)=SUM(27)+Q(N,NODE(8)+1)
SUM(28)=SUM(28)+Q(N,LOC(IIDN))
SUM(29)=SUM(29)+Q(N,NBR(1)-3)
SUM(30)=SUM(30)+Q(N,NBR(1)+6)
SUM(31)=SUM(31)+Q(N,NBR(3)-3)
SUM(32)=SUM(32)+Q(N,NBR(3)+3)
SUM(43)=SUM(43)+Q(N,LOC(JRB))
SUM(33)=SUM(33)+VEL(LOC(IUP))
SUM(34)=SUM(34)+VEL(LOC(IIDN))
SUM(35)=SUM(35)+VEL(NBR(5)+5)
SUM(36)=SUM(36)+VEL(NBR(5)-4)
SUM(37)=SUM(37)+VEL(NBR(4)+3)
SUM(38)=SUM(38)+VEL(NBR(4)-2)
SUM(39)=SUM(39)+VEL(NBR(1)-3)
SUM(40)=SUM(40)+VEL(NBR(1)+6)
SUM(41)=SUM(41)+VEL(NBR(3)-3)
SUM(42)=SUM(42)+VEL(NBR(3)+3)
SUM(44)=SUM(44)+VEL(LOC(JRB))

```

C

C . . CONVERT BACK TO ENGLISH UNITS . .

IF(MUNITS.EQ.0)THEN

DO 6730 MC = IUP, IDN

6730 WSSAV(N,MC) = WSSAV(N,MC)*3.28083

DO 6740 MC = IIUP, IIDN

WS(N,LOC(MC)) = WS(N,LOC(MC))*3.28083

6740 DEV(MC) = DEV(MC)*3.28083

C

Q(N,LOC(IUP)) = Q(N,LOC(IUP))/0.02832

Q(N,LOC(IIDN)) = Q(N,LOC(IIDN))/0.02832

Q(N,NBR(5)+5) = Q(N,NBR(5)+5)/0.02832

Q(N,NBR(5)-4) = Q(N,NBR(5)-4)/0.02832

Q(N,NODE(10)+1) = Q(N,NODE(10)+1)/0.02832

Q(N,NBR(4)+3) = Q(N,NBR(4)+3)/0.02832

Q(N,NBR(4)-2) = Q(N,NBR(4)-2)/0.02832

Q(N,NODE(8)+1) = Q(N,NODE(8)+1)/0.02832

Q(N,NBR(1)-3) = Q(N,NBR(1)-3)/0.02832

Q(N,NBR(1)+6) = Q(N,NBR(1)+6)/0.02832

Q(N,NBR(3)-3) = Q(N,NBR(3)-3)/0.02832

Q(N,NBR(3)+3) = Q(N,NBR(3)+3)/0.02832

Q(N,LOC(JRB)) = Q(N,LOC(JRB))/0.02832

C

VEL(LOC(IUP)) = VEL(LOC(IUP))*3.28083

VEL(LOC(IIDN)) = VEL(LOC(IIDN))*3.28083

VEL(NBR(5)+5) = VEL(NBR(5)+5)*3.28083

VEL(NBR(5)-4) = VEL(NBR(5)-4)*3.28083

VEL(NBR(4)+3) = VEL(NBR(4)+3)*3.28083

VEL(NBR(4)-2) = VEL(NBR(4)-2)*3.28083

VEL(NBR(1)-3) = VEL(NBR(1)-3)*3.28083

VEL(NBR(1)+6) = VEL(NBR(1)+6)*3.28083

VEL(NBR(3)-3) = VEL(NBR(3)-3)*3.28083

VEL(NBR(3)+3) = VEL(NBR(3)+3)*3.28083

```

      VEL(LOC(JRB)) = VEL(LOC(JRB))*3.28083
      END IF
C
340 DO 350 I=1,NMR
350 Q(JB,I)=2.*Q(N,I)-Q(M,I)
      DO 360 I=2,NRM
360 WS(JB,I)=2.*WS(N,I)-WS(M,I)
      write(7,2030)mon,nm,iyr-1900
      M=M+1
      IF(M-kb)2333,2333,370
2333 continue
C
C . . . DAILY RETURN LOOP.
      IF(NM-NDM.LT.0) GO TO 200
370 DO 380 I=1,44
380 AVE(I)=SUM(I)/NM
C
C . . . PRINT MONTHLY MEAN VALUES
C
      if(Nopt.eq.1.and.iup.eq.1) iiup=iiup+1
C
C *****OPTION FOR WATER LEVELS*****
C
      IF(NOPT.EQ.1) THEN
        WRITE(6,3130) AVE(8),(AVE(I),I=IIDN,IIUP,-1)
        WRITE(6,3131) AVE(1),AVE(21),
      > (AVE(I+7),AVE(I+13), I=IIDN,IIUP,-1)
        if(Nopt.eq.1.and.iup.eq.1) iiup=iiup-1
C
C *****OPTION FOR FLOW WITHOUT DELTA*****
C
      ELSE IF(NOPT.EQ.2.AND.IDN.NE.8) THEN
        WRITE(6,7060) AVE(8),AVE(3),AVE(1),AVE(28),AVE(43),AVE(21),
      > AVE(22),AVE(23),AVE(25),AVE(26),AVE(10),AVE(JRB+13)
C
C *****OPTION FOR FLOW WITH DELTA*****
C
      ELSE IF(NOPT.EQ.2.AND.IDN.EQ.8) THEN
        WRITE(6,8060) AVE(8),AVE(IIDN-1),AVE(1),AVE(21),AVE(28),AVE(22),
      > AVE(23),AVE(25),AVE(26),AVE(29),AVE(30),AVE(31),AVE(32),
      > AVE(IIDN+6),AVE(IIDN+12)
C
C *****OPTION FOR VELOCITIES WITHOUT DELTA*****
C
      ELSE IF(NOPT.EQ.3.AND.IDN.NE.8) THEN
        WRITE(6,9065) AVE(8),AVE(10),AVE(1),AVE(34),AVE(44),AVE(33),
      > AVE(35),AVE(36),AVE(37),AVE(38),AVE(3),AVE(JRB+13)
C
C *****OPTION FOR VELOCITIES WITH DELTA*****
C
      ELSE IF(NOPT.EQ.3.AND.IDN.EQ.8) THEN
        WRITE(6,9060) AVE(8),AVE(IIDN-1),AVE(1),AVE(33),AVE(34),AVE(35),

```

```

>AVE(36),AVE(37),AVE(38),AVE(39),AVE(40),AVE(41),AVE(42),
>AVE(IIDN+6),AVE(IIDN+12)
END IF

```

C

```

381 continue
    MONFLAG=.TRUE.
    IF(IYR-IYRB) 388,386,500
386 IF(MON-MONB) 388,500,500
388 CONTINUE
    IF(MON-12) 390,389,389
389 IYR=IYR+1
390 CONTINUE
    DO 392 I=1,42
392 SUM(I)=0.
    DO 400 I=1,NMR
    WS(1,I)=WS(M,I)
    Q(1,I)=Q(M,I)
400 Q(2,I)=Q(JB,I)
    DO 410 I=2,NRM
410 WS(2,I)=WS(JB,I)

```

C

```

C . . . UPDATE MONTH AND YEAR AND RECHECK IF MORE DATA SHOULD BE USED
    MON=MON+1
    IF(MON-13) 414,412,412
412 MON=1
414 IF(IYR-IYRB) 418,416,500
416 IF(MON-MONB) 418,418,500
418 CONTINUE
    kkz=0
    kb=36
    istart=2
    iend=32
    MM=0
    M=1

```

C

```

C . . . MONTHLY RETURN LOOP AND END PROGRAM LOCATION
    GO TO 70
500 CALL EXIT

```

C

```

C . . . FORMAT STATEMENTS.
1000 FORMAT(I2,3(1X,I2))
1010 FORMAT(I1,1X,I1)
1020 FORMAT(F8.0,F8.0,F8.2,F8.0)
1050 FORMAT(I6)
1055 FORMAT(I6)
C2000 FORMAT('/' ENTER BEGINNING AND ENDING DATES '/' MM/YY-MM/YY')
C2020 FORMAT('/' ENTER STARTING AND ENDING STATIONS:'/8(I2,') ',A20/)
2030 FORMAT(' ',I2,2('/ ',I3))
3000 FORMAT(1H1)
3010 FORMAT(///,26X,'ST. CLAIR RIVER TRANSIENT MODEL',/,36X,
    > 'BASIC DATA'///,23X,'STATION',5X,'ABASE',5X,'DATUM',5X,'WIDTH',/)

```

```

3020 FORMAT(20X,F10.0,F10.0,F9.2,F8.0,1X,A2)
3030 FORMAT('+',62X,A20)
3040 FORMAT(/,12X,' MANNING n =',F11.8,' * WS2',A3,' +',
> ,F10.7,' FOR STATIONS',F7.0,' THRU ',F7.0)
3050 FORMAT(///45X,'ST.CLAIR RIVER TRANSIENT MODEL',//,52X,A9,I5,/,
> 10X,A20,' to ',A20,40X,'WATER LEVELS VERSION',/)
3060 FORMAT(36X,F5.1,1X,'HOUR TIME INCREMENTS',11X,I3,1X,'REACHES',/)
3070 FORMAT(6X,A3,4X,'1-----COMPUTED LEVELS-----1',2X,A3,5X,A3,4
> X,'1-----MEASURED LEVELS AND COMPUTED DEVIATIONS (C-M)-----
> 1'/6X,'MEAS.',5(4X,A3))
3071 FORMAT('+',T50,'MEAS. COMP.Q',1X,4(1X,'1-----',A3,'-----1'),1X,
> '1-----',A3,'-----1',/)
3110 FORMAT(1X,A9,1X,I4,1X,' ERROR OF TYPE ',I2)
3120 FORMAT(1X,I2,F8.2,A1,5(F7.2))
3121 FORMAT('+',T48,F7.2,A1,F8.0,5(F7.2,A1,1X,F4.2))
3130 FORMAT(/,1X,'AVE ',F6.2,1X,5(F7.2))
3131 FORMAT('+',T48,F7.2,F8.0,1X,5(F7.2,2X,F4.2))
6190 FORMAT(' FLAG=',I5,' ESP=',I5,' PATH=',I5)
C7000 FORMAT('/' ENTER OPTION NUMBER '/' 1. OUTPUT SHOWS WATER LEVELS
C > AND DEVIATIONS '/' 2. OUTPUT SHOWS FLOWS AROUND ISLANDS')
7010 FORMAT(I1)
7020 FORMAT(//,17X,'1----- RIVER PROFILE -----1',4X,'1----- TOTAL DISCHA
> RGE -----1 1----- ISLAND FLOWS -----1 1----- DEV -----1',/)
7030 FORMAT(8X,'DAY',7X,A3,8X,A3,8X,A3,8X,A3,6X,A3,6X,A3,3X,
> 'STAG E',2X,'STAG W',2X,'FAWN E',2X,'FAWN W',4X,A3,7X,'DEV')
7040 FORMAT(18X,'MEAS.',6X,'COMP.',6X,'MEAS.',6X,2('FLOW',5X),'FLOW',3X
> ,4('FLOW',4X),1X,'MEAS.',4X,'(C-M)',/)
7050 FORMAT(9X,I2,6X,F6.2,A1,4X,F6.2,5X,F6.2,A1,1X,3(2X,F7.0),
> 4(1X,F7.0),2X,F6.2,A1,2X,F6.2)
7060 FORMAT(/,8X,'AVE',6X,F6.2,5X,F6.2,5X,F6.2,2X,3(2X,F7.0),4(1X,F7.0)
> ,2X,F6.2,4X,F5.2)
C8001 FORMAT(' Enter option for delta output: '/' 1. Output shows Water
C > Levels and Deviations '/' 2. Output shows flows around delta and 1
C > islands '/' 3. Output shows velocities around delta and islands '/')
8002 FORMAT(I1)
8005 FORMAT(I1)
8020 FORMAT(//,5X,'1-----RIVER PROFILE-----1',2X,'1-----TOTAL FLOW-----1',3X,
> '1-----ISLAND FLOWS-----1',3X,'1-----DELTA FLOWS-----
> -----1',3X,'1-----DEV-----1',/)
8030 FORMAT(7X,2(A3,5X),A3,6X,A3,6X,A3,6X,'STAG E',3X,'STAG W',4X,'FAWN
> E',3X,'FAWN W',3X,'N.CH.',3X,'M.CH.',3X,'S.CH.',3X,'CUTOFF',4X,
> A3,5X,'DEV')
8040 FORMAT(6X,'MEAS.',4X,'COMP.',3X,'MEAS.',4X,'FLOW',5X,'FLOW',8X,'Q
> ',8X,'Q',8X,'Q',8X,'Q',8X,'Q',7X,'Q',7X,'Q',8X,'Q',6X,'MEAS.',3X,
> 'C-M',/)
8050 FORMAT(1X,I2,F8.2,A1,1X,F7.2,F8.2,A1,F8.0,1X,F8.0,2X,F8.0,2X,
> F7.0,1X,F8.0,2X,F8.0,1X,F7.0,1X,F7.0,1X,F7.0,2X,F7.0,
> 2X,F7.2,A1,1X,F5.2)
8051 FORMAT(///,45X,'ST.CLAIR RIVER TRANSIENT MODEL',//,52X,A9,I5,/,
> 10X,A20,' to ',A20,40X,'RIVER DISCHARGE VERSION',/)
8060 FORMAT(/,1X,'AVE',F7.2,2X,F7.2,F8.2,1X,F8.0,1X,F8.0,2X,F8.0,2X,
> F7.0,1X,F8.0,2X,F8.0,1X,F7.0,1X,F7.0,1X,F7.0,2X,F7.0,2X,F7.2,2X,

```



```

>F5.2)
9020 FORMAT(/,5X,'1-----RIVER PROFILE-----1',3X,'1--TOT. VEL.--1',4X,
>'1-----MID ISLAND VELOCITIES-----1',3X,'1--MID DELTA VELOCITIES-
>-----1',2X,'1-----DEV-----1',/)
9025 FORMAT(/,17X,'1----- RIVER PROFILE -----1',5X,'1-- TOTAL VELOCIT
>IES --1 1-- MID ISLAND VELOCITIES --1 1-- DEV --1'/)
9030 FORMAT(7X,2(A3,5X),A3,6X,A3,6X,A3,6X,'STAG E',3X,'STAG W',4X,'FAWN
> E',3X,'FAWN W',3X,'N.CH.',3X,'M.CH.',3X,'S.CH.',2X,'CUTOFF',3X,
>A3,5X,'DEV')
9040 FORMAT(6X,'MEAS.',4X,'COMP.',3X,'MEAS.',4X,'VEL.',5X,'VEL.',8X,
>'V',8X,'V',8X,'V',8X,'V',8X,'V',7X,'V',7X,'V',7X,'V',5X,'MEAS.',
>3X,'C-M',/)
9041 FORMAT(18X,'MEAS.',6X,'COMP.',6X,'MEAS.',2X,3(5X,'VEL. '),2X,
>'VEL.',3(4X,'VEL. '),5X,'MEAS.',4X,'(C-M)',/)
9050 FORMAT(1X,I2,F8.2,A1,1X,F7.2,F8.2,A1,1X,F6.2,3X,F6.2,4X,F6.2,4X,
>F5.2,4X,F6.2,3X,F6.2,3X,F5.2,3X,F5.2,3X,F5.2,3X,F5.2,2X,F7.2,A1,
>1X,F5.2)
9051 FORMAT(///,45X,'ST.CLAIR RIVER TRANSIENT MODEL',//,52X,A9,I5,/,
>10X,A20,' to ',A20,40X,'RIVER VELOCITY VERSION',/)
9055 FORMAT(9X,I2,6X,F6.2,A1,3X,F6.2,6X,F6.2,A1,3(5X,F4.2),3X,F4.2,
>3(4X,F4.2),4X,F6.2,A1,2X,F6.2)
9060 FORMAT(/,' AVE',F7.2,2X,F7.2,F8.2,2X,F6.2,3X,F6.2,4X,F6.2,4X,
>F5.2,4X,F6.2,3X,F6.2,3X,F5.2,3X,F5.2,3X,F5.2,3X,F5.2,2X,F7.2,2X,
>F5.2)
9065 FORMAT(/,8X,'AVE',6X,F6.2,4X,F6.2,6X,F6.2,1X,3(5X,F4.2),3X,F4.2,
>3(4X,F4.2),4X,F6.2,4X,F5.2)

```

C

END

C

TABLES

1. Roughness coefficients for the St. Clair River reaches.
- A-2. Hourly model output - water levels option.
- A-3. Hourly model output - river discharge option.
- A-4. Hourly model output - river velocities option.
- A-5. Daily model output - water levels option.
- A-6. Daily model output - river discharge option.
- A-7. Daily model output - river velocities option.

Table A-1. Hourly model output - water levels option.

ST. CLAIR RIVER HOURLY TRANSIENT MODEL																
FT. GRATIOT to LAKE ST. CLAIR (SCS)							MAY 8, 1987									
1.0 HOUR TIME INCREMENTS							179 REACHES									
HR	SCS MEAS.	-----COMPUTED LEVELS-----					FG MEAS.	FG COMP.Q	-----MEASURED LEVELS AND COMPUTED DEVIATIONS (C-M)-----							
		AL	SC	MV	DD	MBR			AL	SC	MV	DD	MBR			
1	176.46	176.62	176.01	176.29	176.42	176.53	176.76	6150.	176.60	0.01	176.02	-0.01	176.27	0.02	176.41	0.01
2	176.47	176.62	176.02	176.30	176.43	176.55	176.77	6214.	176.59	0.03	176.03	-0.01	176.27	0.03	176.42	0.01
3	176.47	176.63	176.02	176.30	176.43	176.54	176.76	6162.	176.60	0.02	176.03	-0.01	176.26	0.04	176.39	0.04
4	176.47	176.63	176.03	176.31	176.44	176.56	176.79	6275.	176.61	0.02	176.03	-0.01	176.26	0.04	176.41	0.03
5	176.47	176.63	176.03	176.31	176.45	176.56	176.78	6217.	176.61	0.02	176.05	-0.02	176.29	0.03	176.42	0.02
6	176.44	176.61	176.02	176.31	176.44	176.55	176.77	6186.	176.61	0.00	176.04	-0.02	176.28	0.03	176.41	0.03
7	176.47	176.62	176.02	176.31	176.44	176.56	176.78	6270.	176.61	0.01	176.04	-0.02	176.28	0.03	176.41	0.03
8	176.46	176.62	176.02	176.31	176.44	176.56	176.78	6245.	176.61	0.01	176.03	-0.01	176.29	0.02	176.42	0.02
9	176.47	176.62	176.02	176.31	176.44	176.55	176.77	6219.	176.61	0.01	176.04	-0.02	176.28	0.02	176.41	0.02
10	176.47	176.63	176.04	176.33	176.47	176.59	176.83	6450.	176.60	0.03	176.07	-0.03	176.31	0.02	176.46	0.01
11	176.48	176.64	176.05	176.33	176.48	176.58	176.79	6245.	176.62	0.02	176.06	-0.01	176.30	0.04	176.43	0.04
12	176.48	176.64	176.04	176.32	176.44	176.56	176.77	6162.	176.61	0.03	176.06	-0.02	176.29	0.02	176.42	0.02
13	176.47	176.63	176.04	176.33	176.46	176.59	176.82	6359.	176.62	0.01	176.05	-0.01	176.30	0.03	176.43	0.03
14	176.48	176.63	176.04	176.32	176.45	176.56	176.77	6139.	176.62	0.02	176.07	-0.03	176.29	0.02	176.42	0.03
15	176.47	176.63	176.03	176.31	176.44	176.56	176.78	6240.	176.62	0.01	176.01	0.02	176.29	0.02	176.41	0.03
16	176.48	176.63	176.03	176.32	176.45	176.57	176.79	6266.	176.61	0.02	176.05	-0.02	176.29	0.02	176.43	0.02
17	176.46	176.63	176.03	176.31	176.43	176.55	176.76	6143.	176.62	0.01	176.06	-0.03	176.29	0.02	176.36	0.06
18	176.45	176.62	176.03	176.32	176.45	176.57	176.81	6344.	176.60	0.01	176.04	-0.01	176.29	0.03	176.42	0.03
19	176.46	176.62	176.03	176.32	176.45	176.57	176.79	6272.	176.61	0.01	176.05	-0.02	176.30	0.02	176.43	0.02
20	176.45	176.61	176.02	176.31	176.44	176.55	176.78	6222.	176.62	0.00	176.05	-0.03	176.29	0.01	176.42	0.02
21	176.46	176.61	176.02	176.31	176.44	176.56	176.79	6289.	176.61	0.00	176.04	-0.02	176.29	0.02	176.42	0.03
22	176.45	176.61	176.02	176.30	176.44	176.55	176.77	6230.	176.63	-0.02	176.07	-0.05	176.29	0.01	176.42	0.02
23	176.45	176.61	176.01	176.29	176.42	176.53	176.74	6124.	176.62	-0.01	176.07	-0.06	176.30	-0.01	176.43	-0.02
24	176.46	176.61	176.00	176.28	176.41	176.52	176.74	6152.	176.61	-0.01	176.04	-0.04	176.28	0.00	176.40	0.01
AVE	176.47	176.62	176.03	176.31	176.44	176.56	176.78	6233.	176.61	0.01	176.05	-0.02	176.29	0.02	176.42	0.02

Table A-2. Hourly model output - river discharge option.

ST. CLAIR RIVER HOURLY TRANSIENT MODEL

MAY 8, 1987

FT. GRATIOT

to LAKE ST. CLAIR (SCS)

RIVER DISCHARGE VERSION

1.0 HOUR TIME INCREMENTS

179 REACHES

----RIVER PROFILE-----				--TOTAL FLOW--		-----ISLAND FLOWS-----				-----DELTA FLOWS-----				---DEV---	
HR	SCS MEAS.	SC COMP.	FG MEAS.	FG FLOW	AL FLOW	STAG E Q	STAG W Q	FAWN E Q	FAWN W Q	N.CH. Q	M.CH. Q	S.CH. Q	CUTOFF Q	SC MEAS.	DEV C-M
1	176.46	176.01	176.76	6158.	6156.	2457.	3700.	777.	5380.	1973.	828.	1000.	2349.	176.02	-0.01
2	176.47	176.02	176.77	6214.	6146.	2467.	3716.	777.	5380.	1982.	822.	997.	2340.	176.03	-0.01
3	176.47	176.02	176.76	6162.	6160.	2466.	3711.	778.	5380.	1977.	830.	1009.	2347.	176.03	-0.01
4	176.47	176.03	176.79	6275.	6184.	2480.	3736.	782.	5406.	1982.	832.	1010.	2352.	176.03	-0.01
5	176.47	176.03	176.78	6217.	6217.	2487.	3745.	786.	5433.	1995.	838.	1020.	2369.	176.05	-0.02
6	176.44	176.02	176.77	6186.	6299.	2480.	3733.	793.	5471.	2043.	859.	1061.	2413.	176.04	-0.02
7	176.47	176.02	176.78	6270.	6234.	2493.	3754.	789.	5459.	1973.	826.	996.	2362.	176.04	-0.02
8	176.46	176.02	176.78	6245.	6227.	2496.	3758.	786.	5447.	2001.	840.	1031.	2391.	176.03	-0.01
9	176.47	176.02	176.77	6219.	6234.	2486.	3742.	786.	5447.	1991.	834.	1010.	2377.	176.04	-0.02
10	176.47	176.04	176.83	6450.	6240.	2524.	3805.	790.	5488.	1992.	835.	1014.	2382.	176.07	-0.03
11	176.48	176.05	176.79	6245.	6259.	2519.	3792.	793.	5488.	1998.	838.	1011.	2379.	176.06	-0.01
12	176.48	176.04	176.77	6162.	6266.	2480.	3728.	788.	5488.	2011.	845.	1024.	2400.	176.06	-0.02
13	176.47	176.04	176.82	6359.	6266.	2502.	3769.	789.	5468.	2014.	846.	1025.	2400.	176.05	-0.01
14	176.48	176.04	176.77	6139.	6258.	2490.	3747.	790.	5469.	2001.	839.	1014.	2395.	176.07	-0.03
15	176.47	176.03	176.78	6240.	6247.	2481.	3732.	786.	5452.	2004.	841.	1019.	2399.	176.01	0.02
16	176.48	176.03	176.79	6266.	6227.	2494.	3756.	786.	5445.	1989.	834.	1004.	2387.	176.05	-0.02
17	176.46	176.03	176.76	6143.	6240.	2477.	3726.	786.	5445.	2006.	842.	1022.	2390.	176.06	-0.03
18	176.45	176.03	176.81	6344.	6201.	2499.	3764.	792.	5471.	2021.	848.	1033.	2410.	176.04	-0.01
19	176.46	176.03	176.79	6272.	6284.	2514.	3787.	796.	5495.	2007.	841.	1020.	2396.	176.05	-0.02
20	176.45	176.02	176.78	6222.	6303.	2499.	3760.	795.	5490.	2026.	850.	1041.	2415.	176.05	-0.03
21	176.46	176.02	176.79	6289.	6272.	2501.	3766.	791.	5481.	1999.	837.	1016.	2396.	176.04	-0.02
22	176.45	176.02	176.77	6230.	6269.	2498.	3760.	790.	5474.	2011.	843.	1032.	2409.	176.07	-0.05
23	176.45	176.01	176.74	6124.	6251.	2471.	3716.	787.	5452.	1997.	836.	1010.	2399.	176.07	-0.06
24	176.46	176.00	176.74	6152.	6173.	2457.	3698.	777.	5399.	1983.	821.	994.	2374.	176.04	-0.04
AVE	176.47	176.03	176.78	6233.	6237.	2488.	3746.	787.	5449.	1997.	838.	1018.	2385.	176.05	-0.02

Table A-3. Hourly model putout - river velocities option.

ST.CLAIR RIVER HOURLY TRANSIENT MODEL

MAY 8, 1987

FT. GRATIOT

TO LAKE ST. CLAIR (SCS)

RIVER VELOCITIES VERSION

1.0 HOUR TIME INCREMENTS

179 REACHES

----RIVER PROFILE----				--TOT. VEL.--		-----MID ISLAND VELOCITIES-----				---MID DELTA VELOCITIES---				----DEV-----	
HR	SCS MEAS.	SC COMP.	FG MEAS.	FG VEL.	AL VEL.	STAG E V	STAG W V	FAWN E V	FAWN W V	N.CH. V	M.CH. V	S.CH. V	CUTOFF V	SC MEAS.	DEV C-M
1	175.48	176.01	176.76	1.06	0.67	0.98	0.86	0.49	0.93	0.78	0.52	0.35	0.76	176.02	-0.01
2	175.47	176.02	176.77	1.06	0.68	0.98	0.86	0.49	0.93	0.78	0.52	0.35	0.76	176.03	-0.01
3	175.47	176.02	176.76	1.06	0.67	0.98	0.86	0.49	0.93	0.78	0.52	0.35	0.76	176.03	-0.01
4	175.47	176.03	176.79	1.07	0.67	0.99	0.86	0.49	0.93	0.79	0.53	0.36	0.77	176.03	-0.01
5	175.47	176.03	176.78	1.06	0.67	0.99	0.86	0.49	0.93	0.79	0.53	0.36	0.77	176.05	-0.02
6	175.44	176.02	176.77	1.06	0.68	0.99	0.86	0.50	0.94	0.81	0.54	0.37	0.79	176.04	-0.02
7	175.47	176.02	176.78	1.06	0.68	0.99	0.87	0.49	0.94	0.78	0.52	0.36	0.77	176.04	-0.02
8	175.46	176.02	176.78	1.06	0.67	0.99	0.87	0.49	0.94	0.80	0.53	0.36	0.78	176.03	-0.01
9	175.47	176.02	176.77	1.06	0.67	0.99	0.86	0.49	0.94	0.79	0.53	0.36	0.77	176.04	-0.02
10	175.47	176.04	176.83	1.09	0.67	1.00	0.88	0.49	0.94	0.79	0.53	0.36	0.78	176.07	-0.03
11	175.48	176.05	176.79	1.06	0.68	1.00	0.87	0.49	0.94	0.79	0.53	0.36	0.77	176.06	-0.01
12	175.48	176.04	176.77	1.06	0.68	0.98	0.86	0.49	0.94	0.80	0.53	0.36	0.78	176.06	-0.02
13	175.47	176.04	176.82	1.08	0.68	0.99	0.87	0.49	0.94	0.80	0.53	0.36	0.78	176.06	-0.01
14	175.48	176.04	176.77	1.04	0.68	0.99	0.86	0.49	0.94	0.79	0.53	0.36	0.78	176.07	-0.03
15	175.47	176.03	176.78	1.06	0.68	0.99	0.86	0.49	0.94	0.79	0.53	0.36	0.78	176.01	0.02
16	175.48	176.03	176.79	1.06	0.67	0.99	0.87	0.49	0.94	0.79	0.53	0.36	0.78	176.05	-0.02
17	175.46	176.03	176.76	1.04	0.67	0.98	0.86	0.49	0.94	0.80	0.53	0.36	0.78	176.06	-0.03
18	175.45	176.03	176.81	1.08	0.68	0.99	0.87	0.49	0.94	0.80	0.54	0.36	0.79	176.04	-0.01
19	175.46	176.03	176.79	1.06	0.68	1.00	0.87	0.50	0.94	0.80	0.53	0.36	0.78	176.05	-0.02
20	175.46	176.02	176.78	1.06	0.68	0.99	0.87	0.50	0.95	0.81	0.54	0.36	0.79	176.05	-0.03
21	175.46	176.02	176.79	1.07	0.68	0.99	0.87	0.49	0.94	0.80	0.53	0.36	0.78	176.04	-0.02
22	175.46	176.02	176.77	1.06	0.68	0.99	0.87	0.49	0.94	0.80	0.53	0.36	0.79	176.07	-0.05
23	175.45	176.01	176.74	1.04	0.68	0.98	0.86	0.49	0.94	0.79	0.53	0.36	0.78	176.07	-0.06
24	175.46	176.00	176.74	1.06	0.67	0.98	0.86	0.49	0.93	0.78	0.52	0.36	0.77	176.04	-0.04
AVE	175.47	176.03	176.78	1.06	0.67	0.99	0.87	0.49	0.94	0.79	0.53	0.36	0.78	176.05	-0.02

Table A-4. Daily model output - water levels option.

ST. CLAIR RIVER TRANSIENT MODEL

JUNE 1988

FT. GRATIOT

to LAKE ST. CLAIR (SCS)

WATER LEVELS VERSION

24.0 HOUR TIME INCREMENTS

179 REACHES

SCS MEAS.		-----COMPUTED LEVELS-----					FG MEAS.	FG COMP.Q	-----MEASURED LEVELS AND COMPUTED DEVIATIONS (C-M)-----									
		AL	SC	MV	DD	MBR			AL	SC	MV	DD	MBR					
1	175.66	175.82	176.25	176.55	176.69	176.81	177.06	6690.	175.78	0.04	176.27	-0.02	176.52	0.03	176.66	0.03	176.79	0.02
2	175.66	175.82	176.25	176.55	176.69	176.81	177.06	6690.	175.77	0.05	176.26	0.00	176.51	0.04	176.65	0.04	176.78	0.03
3	175.66	175.81	176.23	176.52	176.65	176.77	177.01	6539.	175.79	0.02	176.25	-0.02	176.49	0.03	176.63	0.02	176.75	0.02
4	175.64	175.80	176.22	176.52	176.66	176.78	177.02	6604.	175.79	0.01	176.26	-0.03	176.49	0.02	176.63	0.02	176.76	0.02
5	175.68	175.83	176.26	176.55	176.69	176.81	177.05	6647.	175.81	0.02	176.28	-0.02	176.52	0.03	176.67	0.02	176.79	0.02
6	175.70	175.85	176.26	176.55	176.68	176.80	177.03	6552.	175.83	0.02	176.28	-0.02	176.52	0.03	176.66	0.02	176.78	0.02
7	175.69	175.84	176.24	176.53	176.66	176.77	177.01	6485.	175.82	0.01	176.28	-0.03	176.50	0.02	176.64	0.02	176.76	0.01
8	175.69	175.84	176.26	176.55	176.69	176.81	177.05	6638.	175.83	0.01	176.29	-0.03	176.53	0.03	176.67	0.02	176.80	0.01
9	175.69	175.84	176.26	176.55	176.68	176.80	177.04	6582.	175.82	0.02	176.29	-0.03	176.52	0.03	176.67	0.02	176.79	0.01
10	175.69	175.83	176.24	176.52	176.65	176.77	177.00	6488.	175.82	0.01	176.27	-0.03	176.50	0.02	176.64	0.02	176.76	0.01
11	175.71	175.86	176.26	176.54	176.67	176.79	177.02	6488.	175.85	0.01	176.30	-0.04	176.53	0.02	176.65	0.02	176.78	0.00
12	175.74	175.87	176.26	176.52	176.65	176.76	176.98	6319.	175.91	-0.03	176.32	-0.07	176.53	-0.01	176.65	0.00	176.78	-0.01
13	175.75	175.89	176.30	176.59	176.72	176.84	177.07	6590.	175.90	-0.01	176.35	-0.05	176.58	0.01	176.71	0.01	176.84	0.00
14	175.77	175.91	176.31	176.59	176.72	176.83	177.06	6507.	175.90	0.01	176.35	-0.04	176.57	0.02	176.70	0.01	176.83	0.01
15	175.78	175.91	176.31	176.58	176.71	176.82	177.05	6454.	175.91	0.01	176.34	-0.03	176.56	0.02	176.69	0.01	176.82	0.01
16	175.74	175.88	176.30	176.59	176.73	176.85	177.09	6684.	175.92	-0.04	176.35	-0.05	176.59	0.01	176.72	0.01	176.84	0.01
17	175.76	175.90	176.32	176.61	176.75	176.87	177.11	6686.	175.89	0.02	176.35	-0.03	176.59	0.02	176.72	0.02	176.85	0.02
18	175.75	175.89	176.29	176.57	176.70	176.82	177.06	6527.	175.89	0.00	176.33	-0.04	176.56	0.01	176.69	0.01	176.81	0.01
19	175.75	175.89	176.30	176.58	176.71	176.83	177.06	6502.	175.90	-0.01	176.33	-0.04	176.57	0.01	176.71	0.01	176.82	0.01
20	175.78	175.92	176.33	176.62	176.75	176.87	177.11	6658.	175.90	0.02	176.36	-0.03	176.60	0.02	176.73	0.02	176.86	0.02
21	175.77	175.90	176.29	176.57	176.69	176.81	177.03	6414.	175.90	0.01	176.32	-0.02	176.55	0.02	176.68	0.01	176.80	0.00
22	175.74	175.88	176.28	176.56	176.69	176.81	177.04	6500.	175.90	-0.02	176.32	-0.04	176.55	0.01	176.68	0.01	176.81	0.00
23	175.74	175.88	176.30	176.59	176.72	176.84	177.08	6633.	175.89	-0.01	176.34	-0.04	176.58	0.01	176.71	0.02	176.83	0.01
24	175.73	175.88	176.32	176.62	176.76	176.89	177.14	6815.	175.88	0.00	176.35	-0.03	176.60	0.02	176.75	0.01	176.87	0.02
25	175.74	175.88	176.31	176.60	176.73	176.85	177.10	6071.	175.88	0.01	176.34	-0.04	176.58	0.01	176.72	0.01	176.85	0.01
26	175.72	175.86	176.27	176.55	176.68	176.80	177.03	6497.	175.88	-0.02	176.32	-0.06	176.56	-0.01	176.68	0.00	176.80	0.00
27	175.71	175.86	176.28	176.58	176.71	176.83	177.08	6603.	175.88	-0.02	176.34	-0.06	176.57	0.00	176.70	0.01	176.84	0.00
28	175.73	175.88	176.30	176.60	176.73	176.86	177.10	6704.	175.87	0.00	176.35	-0.04	176.59	0.01	176.72	0.01	176.85	0.01
29	175.73	175.88	176.32	176.62	176.76	176.89	177.14	6812.	175.86	0.02	176.35	-0.03	176.60	0.02	176.74	0.02	176.87	0.02
30	175.73	175.88	176.31	176.61	176.75	176.87	177.12	6740.	175.87	0.01	176.34	-0.03	176.59	0.02	176.73	0.02	176.85	0.02
AVE	175.72	175.87	176.28	176.57	176.70	176.82	177.06	6593.	175.86	0.01	176.32	-0.03	176.55	0.02	176.69	0.02	176.81	0.01

Table A-5. Daily model output - river discharge option.

ST.CLAIR RIVER TRANSIENT MODEL

JUNE 1986

FT. GRATIOT

to LAKE ST. CLAIR (SCS)

RIVER DISCHARGE VERSION

24.0 HOUR TIME INCREMENTS

179 REACHES

	----RIVER PROFILE----			--TOTAL FLOW--		-----ISLAND FLOWS-----				-----DELTA FLOWS-----				----DEV----	
	SCS MEAS.	SC COMP.	FG MEAS.	FG FLOW	AL FLOW	STAG E Q	STAG W Q	FAWN E Q	FAWN W Q	N.CH. Q	M.CH. Q	S.CH. Q	CUTOFF Q	SC MEAS.	DEV C-M
1	175.68	176.25	177.06	6690.	6690.	2675.	4015.	838.	5852.	2119.	901.	912.	2758.	176.27	-0.02
2	175.68	176.25	177.06	6690.	6690.	2675.	4015.	838.	5852.	2119.	901.	912.	2758.	176.28	-0.00
3	175.68	176.23	177.01	6539.	6551.	2616.	3928.	820.	5730.	2077.	883.	897.	2695.	176.25	-0.02
4	175.64	176.22	177.02	6604.	6602.	2639.	3963.	828.	5773.	2087.	886.	895.	2735.	176.26	-0.03
5	175.68	176.26	177.05	6647.	6631.	2656.	3987.	830.	5805.	2090.	889.	890.	2756.	176.28	-0.02
6	175.70	176.26	177.03	6552.	6557.	2621.	3934.	820.	5737.	2069.	881.	849.	2758.	176.28	-0.02
7	175.69	176.24	177.01	6485.	6490.	2593.	3893.	812.	5677.	2047.	872.	828.	2744.	176.28	-0.03
8	175.69	176.26	177.05	6638.	6627.	2652.	3980.	830.	5798.	2091.	890.	857.	2789.	176.29	-0.03
9	175.69	176.26	177.04	6582.	6587.	2633.	3952.	824.	5763.	2074.	883.	843.	2786.	176.29	-0.03
10	175.69	176.24	177.00	6480.	6487.	2592.	3891.	812.	5674.	2048.	872.	836.	2732.	176.27	-0.03
11	175.71	176.26	177.02	6488.	6476.	2593.	3892.	810.	5669.	2040.	869.	829.	2734.	176.30	-0.04
12	175.74	176.26	176.98	6319.	6325.	2529.	3795.	790.	5535.	1988.	849.	771.	2715.	176.32	-0.07
13	175.75	176.30	177.07	6590.	6585.	2631.	3947.	821.	5747.	2049.	876.	728.	2910.	176.35	-0.05
14	175.77	176.31	177.06	6507.	6513.	2605.	3907.	812.	5702.	2038.	872.	714.	2887.	176.35	-0.04
15	175.78	176.31	177.05	6454.	6454.	2582.	3873.	805.	5649.	2024.	867.	708.	2855.	176.34	-0.03
16	175.74	176.30	177.09	6664.	6665.	2664.	3997.	833.	5830.	2094.	895.	746.	2935.	176.35	-0.05
17	175.76	176.32	177.11	6666.	6657.	2666.	3998.	831.	5829.	2078.	885.	715.	2902.	176.35	-0.03
18	175.75	176.29	177.06	6527.	6544.	2613.	3920.	817.	5724.	2061.	881.	748.	2859.	176.33	-0.04
19	175.75	176.30	177.06	6582.	6553.	2623.	3935.	819.	5736.	2053.	877.	750.	2865.	176.33	-0.04
20	175.78	176.33	177.11	6658.	6643.	2661.	3991.	829.	5817.	2077.	889.	734.	2940.	176.36	-0.03
21	175.77	176.29	177.03	6414.	6438.	2570.	3854.	803.	5632.	2022.	865.	709.	2844.	176.32	-0.02
22	175.74	176.28	177.04	6500.	6497.	2598.	3899.	812.	5684.	2040.	872.	735.	2853.	176.32	-0.04
23	175.74	176.30	177.08	6633.	6626.	2652.	3970.	828.	5799.	2074.	886.	754.	2912.	176.34	-0.04
24	175.73	176.32	177.14	6815.	6800.	2724.	4086.	851.	5957.	2135.	912.	788.	2974.	176.35	-0.03
25	175.74	176.31	177.10	6671.	6681.	2671.	4006.	834.	5847.	2094.	894.	779.	2913.	176.34	-0.04
26	175.72	176.27	177.03	6497.	6511.	2600.	3902.	813.	5696.	2046.	873.	765.	2829.	176.32	-0.06
27	175.71	176.28	177.08	6663.	6651.	2662.	3995.	832.	5820.	2086.	890.	791.	2885.	176.34	-0.06
28	175.73	176.30	177.10	6784.	6699.	2681.	4022.	837.	5864.	2097.	895.	789.	2917.	176.35	-0.04
29	175.73	176.32	177.14	6812.	6806.	2724.	4085.	850.	5956.	2138.	913.	809.	2946.	176.35	-0.03
30	175.73	176.31	177.12	6740.	6745.	2698.	4046.	842.	5903.	2119.	905.	808.	2912.	176.34	-0.03
AVE	175.72	176.28	177.06	6593.	6592.	2637.	3950.	824.	5769.	2072.	884.	797.	2839.	176.32	-0.03

Table A-6. Daily model output - river velocities option.

ST. CLAIR RIVER TRANSIENT MODEL

JUNE 1988

FT. GRATIOT

to LAKE ST. CLAIR (SCS)

RIVER VELOCITY VERSION

24.0 HOUR TIME INCREMENTS

179 REACHES

----RIVER PROFILE----			--TOT. VEL.--		-----MID ISLAND VELOCITIES-----				---MID DELTA VELOCITIES---				----DEV----	
SCS MEAS.	SC COMP.	FG MEAS.	FG VEL.	AL VEL.	STAG E V	STAG W V	FAWN E V	FAWN W V	N.CH. V	M.CH. V	S.CH. V	CUTOFF V	SC MEAS.	DEV C-M
1	176.66	176.26	177.06	1.11	0.71	1.03	0.90	0.61	0.99	0.82	0.66	0.31	0.88	176.27 -0.02
2	176.66	176.26	177.06	1.11	0.71	1.03	0.90	0.61	0.99	0.82	0.66	0.31	0.88	176.26 0.00
3	176.66	176.23	177.01	1.09	0.69	1.01	0.89	0.60	0.97	0.80	0.64	0.31	0.86	176.26 -0.02
4	176.64	176.22	177.02	1.10	0.70	1.02	0.89	0.60	0.97	0.81	0.66	0.31	0.87	176.26 -0.03
5	176.68	176.28	177.06	1.10	0.70	1.03	0.90	0.60	0.98	0.81	0.66	0.30	0.88	176.26 -0.02
6	176.70	176.26	177.03	1.09	0.69	1.01	0.89	0.60	0.96	0.80	0.64	0.29	0.88	176.26 -0.02
7	176.69	176.24	177.01	1.08	0.69	1.00	0.88	0.49	0.96	0.79	0.63	0.28	0.87	176.26 -0.03
8	176.69	176.26	177.06	1.10	0.70	1.02	0.90	0.60	0.98	0.80	0.64	0.29	0.89	176.29 -0.03
9	176.69	176.26	177.04	1.09	0.70	1.02	0.89	0.60	0.97	0.80	0.64	0.29	0.88	176.29 -0.03
10	176.69	176.24	177.00	1.08	0.69	1.00	0.88	0.49	0.96	0.79	0.63	0.28	0.87	176.27 -0.03
11	176.71	176.26	177.02	1.08	0.68	1.00	0.88	0.49	0.96	0.78	0.63	0.28	0.87	176.30 -0.04
12	176.74	176.26	176.90	1.06	0.67	0.98	0.86	0.48	0.93	0.76	0.62	0.26	0.86	176.32 -0.07
13	176.75	176.30	177.07	1.09	0.69	1.01	0.89	0.60	0.96	0.78	0.63	0.26	0.92	176.35 -0.06
14	176.77	176.31	177.06	1.08	0.68	1.00	0.87	0.49	0.96	0.78	0.63	0.24	0.91	176.35 -0.04
15	176.78	176.31	177.06	1.07	0.68	0.99	0.87	0.48	0.94	0.77	0.62	0.24	0.90	176.34 -0.03
16	176.74	176.30	177.09	1.10	0.70	1.02	0.89	0.60	0.98	0.80	0.64	0.26	0.93	176.35 -0.06
17	176.76	176.32	177.11	1.10	0.70	1.02	0.89	0.60	0.97	0.79	0.64	0.24	0.94	176.35 -0.03
18	176.76	176.29	177.06	1.08	0.69	1.01	0.88	0.49	0.96	0.79	0.63	0.26	0.90	176.33 -0.04
19	176.76	176.30	177.06	1.09	0.69	1.01	0.88	0.49	0.96	0.78	0.63	0.26	0.90	176.33 -0.04
20	176.78	176.33	177.11	1.10	0.70	1.02	0.89	0.60	0.97	0.79	0.64	0.26	0.93	176.36 -0.03
21	176.77	176.29	177.03	1.08	0.67	0.99	0.86	0.48	0.94	0.77	0.62	0.24	0.89	176.32 -0.02
22	176.74	176.26	177.04	1.08	0.68	1.00	0.88	0.49	0.96	0.78	0.63	0.26	0.90	176.32 -0.04
23	176.74	176.30	177.08	1.10	0.70	1.02	0.89	0.60	0.97	0.79	0.64	0.26	0.92	176.34 -0.04
24	176.73	176.32	177.14	1.12	0.72	1.04	0.91	0.61	1.00	0.82	0.66	0.27	0.94	176.36 -0.03
25	176.74	176.31	177.10	1.10	0.70	1.03	0.90	0.60	0.98	0.80	0.64	0.26	0.92	176.34 -0.04
26	176.72	176.27	177.03	1.08	0.69	1.00	0.88	0.49	0.96	0.78	0.63	0.26	0.89	176.32 -0.06
27	176.71	176.28	177.08	1.10	0.70	1.03	0.90	0.60	0.98	0.80	0.64	0.27	0.91	176.34 -0.06
28	176.73	176.30	177.10	1.11	0.70	1.03	0.90	0.61	0.98	0.80	0.64	0.27	0.92	176.36 -0.04
29	176.73	176.32	177.14	1.12	0.72	1.04	0.91	0.61	1.00	0.82	0.66	0.27	0.93	176.36 -0.03
30	176.73	176.31	177.12	1.11	0.71	1.03	0.90	0.61	0.99	0.81	0.66	0.27	0.92	176.34 -0.03
AVE	176.72	176.28	177.06	1.09	0.69	1.02	0.89	0.60	0.97	0.79	0.64	0.27	0.90	176.32 -0.03

ST. CLAIR AND DETROIT RIVER CURRENT MEASUREMENTS

Jan A. Derecki, Kathleen A. Darr, and Raymond N. Kelley

ABSTRACT

Velocities in the unregulated Great Lakes connecting channels, the St. Clair and Detroit Rivers, were continuously measured with current meters during an experimental field program. The program was initiated to improve determination of winter flows, when the accuracy of normal flow determinations is affected by ice. This study describes the experimental results of continuous flow measurements using electromagnetic current meters and an acoustic Doppler current profiler meter during the 1983-87 period of data collection. Verification of current meter results was provided by model-simulated flows during open-water periods and flow transfer between the rivers during winter, when at least one of the rivers was ice-free. Results indicate that accurate estimates of mean river velocities (and consequently discharge) can be obtained with a single well-placed current meter. However, the electromagnetic current meters are a direct-contact single-point sensors that are affected by frazil ice during winter and weed effects during most of the year, producing frequently questionable or erroneous data. The acoustic profiler is a remote sensor of velocities in the overhead water column and is not affected by the frazil ice and weed problems, producing superior data.

INTRODUCTION

Flows in the unregulated Great Lakes connecting channels, the St. Clair and Detroit Rivers (Figure 1), are normally determined by either stage-fall-discharge equations or unsteady flow numerical models. The calibration of both the equations and models is based on periodic discharge measurements taken over the years by the Corps of Engineers (COE) during the open-water seasons (spring, summer, and fall). Consequently, the calculated flows normally exhibit good accuracy during ice-free periods, but may contain large errors during winter months with extensive ice cover. The St. Clair River is particularly prone to large ice jams because of practically unlimited ice flow supply provided by Lake Huron and an extensive river delta that retards the passage of these ice flows. Large ice retardation of flows in the St. Clair River is relatively frequent during winter months. The magnitude of larger ice retardations generally approaches about 20% of normal flow (1,100 c3/s), but in extreme cases has been observed to approach 50%. The ice conditions in the St. Clair and Detroit Rivers are different, because of large difference in the upstream lakes and ice supplies, and the ice problem also contributes to large discrepancies in the simulated flows for these rivers. In some cases, these flow discrepancies exceed 20% of total flow, which exceeds acceptable errors by an order of magnitude.

The St. Clair and Detroit River flows are determined at the Great Lakes Environmental Research Laboratory (GLERL) with unsteady flow models, with the current model versions described by Derecki and Kelley (1981) for the

St. Clair River, and Quinn and Hagman (1977) for the Detroit River. These rivers generally do not freeze over and are frequently free of ice during winter. During such ice-free periods the models are adequate for the simulation of winter flow rates. However, the models are not calibrated for additional flow resistance due to ice, because of lack of proper data, and tend to greatly overestimate the river flows during heavy ice accumulations. The ice covers in these rivers are transient in nature, formed by the consolidation of ice flows supplied by the upstream lakes due to ice break-up by winter storms or spring thawing. In both instances proper meteorological conditions are required to produce heavy ice concentrations in the rivers. Generally southern storms are needed to destroy ice bridges (Figure 2) which normally form at the heads of the rivers and help keep the rivers free of ice, with subsequent shift to northerly winds that can force large amounts of ice flows into the river channels.

Knowledge of accurate flows during both open-water and ice-covered periods in the St. Clair and Detroit Rivers is needed for a variety of scientific and water resource studies, ranging from water balance and chemical/biological loadings to lake regulation, lake level forecasts, and winter navigation. Large discrepancies in winter flows are associated with abnormal river profile on the St. Clair and/or Detroit Rivers that exist during ice conditions. A lack of measured data on river velocities and water levels at critical interim points makes it impossible to determine whether one or both river models are in error during winter. To address this problem, a field measurement program was implemented in the St. Clair and Detroit Rivers. The program tests the applicability of using

continuously recording current meters to provide accurate velocity measurements on an ongoing basis, independent of river ice conditions.

FIELD MEASUREMENT PROGRAM

The velocity and thus flow (discharge) of the upper St. Clair and Detroit Rivers were continuously measured using current meters. Practical requirements dictated the use of current meters without moving parts (to avoid clogging), that are capable of prolonged operation (six months) at frequent sampling rates. The initial phase of the field program on the St. Clair River contained a pilot study, started in 1981, which provided for familiarization and field testing of equipment. The actual data collection program started in 1983, following additional resolution of encountered problems. During the Upper Great Lakes Connecting Channels Study (UGLCCS) activities, begun in 1985, the field program was in its second phase, started in 1984, with simultaneous measurements of point-velocities in both rivers and selective measurements of vertical velocity profiles in one of the rivers. The current-meter stations were located in the upper portions of both rivers, close to the COE flow measurement sections. These sections of the rivers have fairly steep hydraulic gradients and are normally free from consolidated ice cover. The meters were permanently deployed at the river bottom and connected by cable to shore-located data recording stations. This arrangement permitted remote access by telephone via teletype-recorder to both the meters and their individual data records. The operation of the current meters was monitored daily to detect and correct

any instrument problems in order to eliminate or reduce data gaps. Ice conditions in the rivers were also monitored during winter and checked as needed by periodic ice surveys conducted by car or plane. Collected velocity data were stored in computer files and subjected to routine preliminary analysis, including comparison with model-simulated flows.

Point Measurements

After examination of the types of meters available, an electromagnetic (EM) current meter was selected (Marsh McBirney, Model 585) for the first phase of the program limited to the St. Clair River. The standard meter was modified to include an externally located recording system (Figure 3), which provided unlimited continuous operational capacity at a cable-connected recording system (cassette tapes) located on the shore. After field testing and several meter modifications, the in situ field operations were started in September 1981, with the deployment of two EM current meters in the upper St. Clair River, near the head of the river at Port Huron, MI (Figure 2). The meters were installed on the United States side of the river, outside of navigation channel about 50 and 70 m from shore, in 13 and 15 m of water. Meter sensors were positioned 2 m above the bottom. Deployment and subsequent removal of meters took place with the assistance of the USCGC Bramble and a commercial diver, who guided the underwater operation. The Detroit District of COE also participated in the project by making discharge measurements during the open-water seasons. These measurements were intended to provide data for calibration of the point-velocities measured by the meters with the mean river velocity at the meter location. They were

not used in this study, because several conducted measurements either encountered operational problems or indicated considerable discrepancy in the data.

The EM current meters in this study sampled ambient river velocity at one-second intervals for Y- and X-axis velocity components, and an azimuth angle. These raw data were converted to the north and east velocity components, which were recorded with an accompanying azimuth angle at 15-minute intervals. The 15-minute input data were stored in a computer file and converted to hourly and/or daily resultant velocity magnitude and direction. The field seasons during the first phase of the program normally covered late fall, winter, and spring months (November-June). The meters were redeployed for the 1982-83 and 1983-84 winter seasons. However, velocity measurements during the first two seasons contained some unresolved problems and questionable data, and were excluded from this study. High quality river velocity measurements during the 1983-84 season (obtained with one of the meters) coincided with the record St. Clair River ice jam of April 1984. This jam, which lasted nearly the entire month (April 5-29), established records for both magnitude and lateness of occurrence, and provided an excellent opportunity for testing the current-meter program. This record ice jam and other aspects of the field measurement experiment are discussed in previously published papers (Derecki and Quinn, 1986a, 1986b, and 1987).

The second phase of the study included simultaneous velocity measurements in both rivers, starting in November 1984, with redeployment of

meters in the St. Clair River for the 1984-85 winter season. The Detroit River installation consists of two EM current meters, which were deployed in August and tested during the summer of 1984 in the upper portion of the river at Fort Wayne COE Boatyard (Figure 4). The two meters were installed outside of navigation channel about 60 and 90 m from the United States shore. Meters were placed in 12 and 14 m of water with upward positioned sensors 2 m above the bottom. Similar operation and deployment procedures were used on both rivers, with the USCGC Mariposa or the USCGC Bristol Bay providing assistance in the Detroit River. During this phase of the study the meters were not removed for the summer but were left operating throughout the year to test the effects of weed transport and accumulation on the velocity measurements.

Vertical Profile Measurements

Initial point-velocity measurements indicated a need for vertical distribution of velocities, and recent advances in acoustical instrumentation (Doppler-shift sensors) made such measurements practical. Consequently, the St. Clair River installation was augmented during the November 1984 redeployment with one acoustic Doppler current profiler (ADCP) meter (RD Instruments, Model 1200 RDDR), which permits measurements of velocities at approximately 1 m intervals in almost the entire vertical water column (Figure 5). The ADCP meter was installed between the two EM current meters, about 60 m from shore in 14 m of water (Figure 3). The meter housing was oriented horizontally and the upward-looking sensor was connected by a 90-degree elbow about 0.5 m above the bottom. The ADCP meter

samples remotely vertical velocities in the overhead water column with continuous sound waves (pings) from four beams at a rate of five times per second, starting about 1 m above the sensor. The raw data from the four beams are averaged to produce Y- and X-axis velocity components, along with an azimuth angle, for approximately 1 m increments of depth to the surface. These data are converted to the north and east velocity components for the 1-m progressive data segments, and indicate velocities at the mid-points of each vertical segment. In a total water depth of about 14 m, this procedure provided vertical velocity and direction values for 11 levels between approximately 2.5 m above the bottom and 0.5 m below the surface. The surface readings are eliminated because of large data scatter at the air-water interface (sound speed is about 5 times faster in water than in air). The data were recorded at a cable-connected shore station at 15-minute intervals (similar to the EM current meters).

These remote-sensing instruments are expensive but provide continuous measurement capability that can not be duplicated with a string of point-measuring meters because of navigation and ice problems near the surface. The ADCP meter was removed from the St. Clair River in April 1986. It was used during summer on the Detroit River in a demonstration of moving-boat measurements (in June), and later (November) deployed in a normal-bottom position on that river in place of the outer EM meter, 90 m from shore (Figure 4). The ADCP meter change was made to provide vertical velocity profile measurements in both rivers. Additional requirement for such data in the Detroit River are the reversals of its flow, which occur occasionally

because of the combined effects of storms on Lake Erie and ice jams in the St. Clair River.

ST. CLAIR RIVER DATA

Electromagnetic Current Meter Records

During the period of study, data were collected from the EM current meters for nearly three and a half years on the St. Clair River. These data underwent preliminary analysis and comparison with model simulated flows. The meters' operation was monitored daily to detect and correct any instrument problems in order to eliminate or reduce data gaps. The water level gages on the river were also monitored daily to detect ice effects on the river's profile and several ice surveys were conducted, when ice problems were indicated by this process.

Operation of the current meter program and monitoring of the meter records indicated that frazil ice affects the operation of the EM current meters. Although frazil ice episodes in the St. Clair River (later confirmed on the Detroit River) are relatively infrequent (about 5 to 10 occurrences on each river per winter), they drastically affect the meter data, which have to be corrected by elimination of bad data records. The formation of frazil ice is a supercooling phenomenon, with distinct characteristics, and can be easily identified. During cold spells in the winter months (December-February), an additional sudden drop in temperatures

causes the formation of frazil ice. This jelly-like ice formation is sticky and adheres to objects; it coats the meter sensors, reducing their sensitivity and producing low readings, at times approaching zero. The sudden drop in the EM meter velocities associated with frazil ice normally starts after sunset (before midnight) and disappears rapidly after sunrise (before noon). However, severe episodes of frazil ice may last continuously for a few days at a time.

Serious weed effects on the EM current meter operations were not at first apparent during the initial phase of the program, limited to the St. Clair River, because the meters were deployed in late fall (November), the Lake Huron water is relatively clean, and the water velocity is high in the upper river. These factors contributed to reduced weed accumulation around the sensors. However, definite weed problems were encountered during the subsequent prolonged operations, particularly in the summer and fall seasons during continuous annual operations of the meter program. Weed accumulation reduces meter readings and requires divers to inspect and clean the sensors at frequent intervals for reliable data records. The EM current meter velocity records taken immediately before and after cleaning of sensors by divers (on both rivers) indicate that weed accumulation may reduce meter velocities by as much as 25-50%. The records also show that this weed accumulation may occur in only a few days, following deployment or cleaning of meters. However, weed accumulation is generally gradual and difficult to identify during initial stages. Since diver operations are expensive and at times not feasible, this type of meter is not generally suitable for

prolonged/continuous operations in rivers with high weed content, particularly during the high weed transport season.

Discussion and presentation of the EM current meter results in this report are limited to selected episodes which illustrate the nature and quality of data. The first drastic episode of this type is the record April 1984 ice jam on the St. Clair River. This jam vividly demonstrates the effectiveness of the in situ current meter velocity measurements in estimating the river flows. The collection of high quality-current meter data during the ice jam represents a major accomplishment and invaluable information on the winter flow regime of the St. Clair River. Results from one of the current meters in operation at that time are indicated in Figure 6, which shows the effect of the ice jam on the upper river flows (velocity and direction). The meter velocity was reduced by about 50% during most of April, changing near the river bottom at the meter location from about 1.0 to 0.5 m s⁻¹. Higher velocities at the beginning of May, following the jam breakup, were produced by the increased head (water level difference) between Lakes Michigan-Huron and St. Clair. Records from the second meter during this period showed other/additional effects, which were later determined as weed effects.

Verification of the current meter results on the St. Clair River during the ice jam episode is provided by flow transfer from the Detroit River, which was free of ice during April and provided accurate flow simulation with a numerical model. Conversely, good agreement in derived flows by two independent methods demonstrates that the St. Clair-Detroit River flow

transfer method is a very useful technique, provided that one of the rivers is free of ice problems. Comparison of flows transferred from the Detroit River with the St. Clair River flows derived from the current meter measurements is shown in Figure 7. Extrapolation of the average river velocity and discharge from the current-meter point-measurements is discussed in the following paragraphs. The transfer factor, shown in the figure, represents a summation of the hydrologic factors that determine the difference between the flows in the St. Clair and Detroit Rivers, namely, the precipitation on Lake St. Clair plus tributary runoff minus evaporation from the lake and the storage of water on the lake. The agreement between the meter and transferred flows is good during most of the March-May period, particularly during the ice jam in April. In the few instances when the two sets of flows deviate substantially, it is probably the transferred flows that are in error. Thus, the high peak in transferred flow at the beginning of May is caused by an extremely high storage of water on Lake St. Clair, which appears to be overestimated. Larger deviations at the beginning and during the second week of March appear to be caused by model oversimulation of the Detroit River flows, probably due to the presence of some ice in the river (March ice cover was not observed).

Comparison of the current meter velocities with the St. Clair River numerical model results during the first deployment period (November 1983 -July 1984 field season), expressed as a ratio of model to meter velocity, is shown in Figure 8. As expected, the figure shows a complete breakdown of the St. Clair River model following the development of the ice jam in April. During other times, the normal model-meter relationship is reasonably

consistent and first-cut estimates of the average river velocity at the meter location could be obtained by applying the velocity ratio to the point-measurements of the meter (CM#1). The other meter (CM#2) shows weed effects during March-June period, with reduced meter readings and exaggerated model ice effects in April. The relationship between the normal model and the weed-free meter velocities for the 1983-84 deployment period, after elimination of the bad model results in April, is indicated in Figure 9. The two equations shown in the figure are for a linear regression of the data points (least squares) and for a velocity forced through a zero-intercept. The equations agree closely and either one could be used to produce acceptable average river velocities. The equation constant from the zero-intercept equation also agree very closely with the reciprocal of the average model-to-meter ratio (Figure 8). The high correlation coefficient (0.94) indicates that over 88% (R^2) of the variation between the average river velocity (simulated by model) and the current-meter velocity measured at a single point near the river bottom is explained by a simple regression.

Determination of river discharge, based on measurements (Figure 7), was made by multiplying derived average river velocities from current meters by the corresponding cross-section areas, obtained from model computations. These areas were readily available, since in either velocity extrapolation method (ratio or regression) the flows (discharge or velocity) were also simulated by the models. At the meter location, most changes in the river discharge are produced by corresponding changes in velocity, and errors introduced in the derived discharge due to omission of the corresponding

cross-section area changes are relatively small. In the most extreme cases, connected with prolonged-massive ice jams, the velocity and corresponding discharge changes (reduction) could exceed 50%; similar cross-section area and corresponding discharge changes would be under 5%. During large ice jams, to which the St. Clair River is particularly prone, the above meter-derived flows represent a tremendous improvement over uncorrected model results, which may oversimulate actual flows by a factor of two (CM#1 in Figure 8). Availability of similar measurements during such ice jam episodes (provided meter readings are not affected by weeds), especially in conjunction with flow transfers (if feasible), may provide acceptable flow estimates.

Simultaneous operation of the current meter program on both rivers throughout the year and monitoring of the meter records indicated the seriousness of weed effects on the EM current meters. Severe weed effects, especially after storms or other sudden surges, can be as dramatic as those of frazil ice, but generally weed accumulation is gradual and may fluctuate in severity. An attempt was made to keep the EM current meters free of weed problems with periodic cleaning of meter sensors by divers, but was generally unsuccessful. Primarily because of weeds, the EM current meter field program was generally unsuccessful on the St. Clair River for prolonged periods during the second continuous deployment spanning several field seasons and a few meter changes because of instrument problems (November 1984-June 1987). This is indicated by the model-meter velocity ratios shown in Figure 10. Drastic weed-effect problems during a summer season (May-October, 1986) are indicated in Figure 11, which shows the

effects of small but gradually increasing weed accumulation during May and June, some recovery in July, and a massive-sudden weed clogging of the meters' sensors in mid-August that remained in effect until the cleaning of meters in November.

Acoustic Current Profiler Records

The ADCP meter was deployed in the St. Clair River in November 1984 and operated until April 1986, for nearly a year and a half long data period. Data collected with this instrument are unaffected by the frazil ice and weed problems, most likely because of the meters' physical characteristics. Both the outgoing and reflected sound waves travel through any frazil ice coating the sensor. The same applies to weed accumulation. Meter characteristics also permit its deployment in a low-profile horizontal position on a support structure designed to reduce weed accumulation. Very little weed accumulation was actually observed by divers during inspections. This eliminates data gaps during winter and questionable or outright erroneous data periods during heavy weed transport/accumulation (summer-fall and after storms). The upper St. Clair River vertical velocity profile measurements obtained with this meter represent high quality, unique data not previously available on the Great Lakes connecting channels. The profiler is expensive but produces a data set which could not be duplicated with a dozen of the EM current meters, since they could not be deployed at 1 m intervals and operated continuously near the surface throughout the year (navigation and ice problems). The quality of ADCP meter data is also better. The following discussion and presentation of the profiler results

is limited to a few data samples that illustrate the nature and quality of collected data.

The vertical distribution of velocity in the water column measured with the profiler during June 1985 is indicated in Figure 12. It gives the progression of daily velocities at 11 levels with 1-m depth increments between approximately 2.5 m above the bottom and 0.5 m below the surface, the practical limits of vertical measurements for the water depth of about 14 m. The figure shows a high degree of consistency between velocities at different depths throughout the month. This consistency indicates that good estimates of velocities in the entire water column or at different depth levels could be obtained with single point-measurements, such as those made with the EM current meters (provided problems are eliminated). Highest velocities normally occur near the surface, with a smooth progression of increasing velocities from the bottom towards the surface, unless surface flow is opposed by substantial wind shear. With strong counter-current winds (southerly), which are generally limited to relatively short periods, the velocity near the surface is occasionally retarded sufficiently so that the highest velocity occurs 2-3 m below the surface. A more frequent occurrence is the nearly uniform velocity in the top water layer spanning a few (occasionally several) meters.

The smooth transition of velocities between progressive water layers is indicated even more vividly in Figure 13, which shows two vertical velocity profiles. A typical high-velocity profile is shown by June 10, 1985, which was selected because of sharp increase in velocities on that day (Figure

12); the March 5, 1985, profile was added to show a typical low-velocity profile. Despite rapid change in velocities on June 10, the graph shows an extremely smooth transition in the vertical distribution of velocities. The use of daily velocities provided some smoothing of the graphs, but generally similar profiles are obtained for shorter periods (hourly and 15-minute data). To extend the profiles to the bottom and the surface, where velocities could not be measured, these points were estimated and incorporated in the graphs. The surface point was estimated by extending the curve indicated by the preceding three measured points to the surface. The bottom point was estimated by forcing a similar curve near the bottom through a maximum-depth and zero-velocity intercept. The profiles show that the vertical velocity distribution is definitely exponential (logarithmic), which agrees with theoretical derivations for turbulent flow (Prandtl, 1925; von Karman, 1934). This includes most of the depth but excludes the boundary layer, where the distribution can not be logarithmic because of theoretical considerations.

Verification of the high consistency of velocities at different levels, indicated in the preceding figure, is shown in Figure 14 by a statistical relationship between profiler velocities near the bottom (bin 1) and the integrated average velocities (11 bins) for the eighteen-month period (November 1984 - April 1986). The two equations shown in the figure are for a linear regression of the measured data points (least squares) and for a velocity forced through zero-intercept, which are nearly identical. Either equation could be used to provide good estimates of the average vertical velocity. The extremely high correlation coefficient for the least squares

linear regression ($R=0.99$) indicates that almost all (nearly 99%) of the variation between the average vertical velocity and a single point measurement near the river bottom is explained by a simple regression.

Comparison of the profiler velocities (near-bottom and integrated average) with the St. Clair River average values (at this location), derived with the unsteady flow numerical model for the November 1984 - April 1986 period and expressed as ratios of these velocities, is shown in Figure 15. Larger variations or disagreements are seen during January and February, when the model results contain substantial errors because of ice effects. During other times the agreement is reasonably good and first-cut estimates of the average river velocity (or eventually discharge) could be obtained by applying the velocity ratios to the profiler measurements. The relationship between normal model and profiler velocities (excluding the bad ice-affected model results) for the same period is shown in Figure 16. Comparison of results presented in Figures 14 and 16 indicates a considerable loss of accuracy (23%) for the estimates of average river velocity. However, the correlation coefficient for these estimates is still reasonably high ($R=0.87$). Even these estimates, obtained with a single meter, represent a large improvement over the model-simulated results during winter months with significant ice problems. The 1984-85 and 1985-86 winter seasons were relatively uneventful (without large ice jams) and the ice effect indicated in Figure 15 for the model-simulated flows represents approximately average ice conditions.

DETROIT RIVER DATA

Electromagnetic Current Meter Records

The period of record for the EM current meter data on the Detroit River covered about 3 years (August 1984-June 1987). Problems with weed accumulation for the EM current meters became readily apparent on the Detroit River during the second phase of the program, when continuous meter operation throughout the year were begun in the summer of 1984. The weed content in the Detroit River is higher and the river velocities are lower than in the St. Clair River, contributing to more weed accumulation and higher weed effects. With the higher weed content, more problems were encountered in the operation of the EM current meters on the Detroit River. Primarily because of weeds, the EM current meter field program was generally unsuccessful on the St. Clair River during most of the year (summer and fall), but at least partially successful during winter, while on the Detroit River it was completely unsuccessful throughout the three annual periods. This is indicated in Figure 17, showing the model-meter velocity ratios for the period of record. Generally, these ratios are not stable for any extended period of time.

Acoustic Current Profiler Records

The quality of the ADCP meter data collected on the Detroit River remained high, similarly to that from the St. Clair River. Profiler operations were similar on both rivers, with about the same water depths and

the vertical velocity measured at 11 levels or bins approximately 1 m in depth. The quality of the Detroit River profiler data is indicated in Figure 18, showing the model-profiler velocity ratios for the period of study (November 1986 - June 1987). The figure shows small ice-effect problems affecting model-simulated velocities during winter, which is typical for the Detroit River. Large ice jams occurred during this winter on the St. Clair River, but its EM current meters were generally affected by weeds and indicate biased ice effect.

The current meter field experiment was terminated in June 1987 with the removal of the EM current meters in both rivers. The ADCP meter was left in place in the Detroit River to continue the study of its flow reversals. More detailed data analysis from the experimental field program will be conducted next year. Its primary purpose will be to develop a method for correcting the unsteady flow model simulation during winter periods with substantial ice problems.

SUMMARY AND RECOMMENDATIONS

Flows in the St. Clair-Detroit River system, the outlet from the upper Great Lakes, are needed for a variety of hydraulic and water resource studies. Applications include hydrologic water balance, lake regulation, lake level forecasts, navigation, transport of pollutants, recreation, and consumptive water use. During the open-water season, acceptably accurate estimates for these flows are provided with available mathematical unsteady-

flow models. However, these models may produce large errors during winter months when rapid transport of ice flows causes formation of ice jams in the lower river reaches. The St. Clair River is particularly prone to large ice jams because of the potentially large ice flow supply from Lake Huron and an extensive river delta which retards the passage of these ice flows. Flow estimates during ice conditions can best be obtained from in situ current meter measurements.

Analysis of data collected during the 1983-87 period indicates that acceptable estimates of river flows can be obtained with a single, well-placed current meter. However, the EM current meters are susceptible to frazil ice problems during winter, and to weed effects during most of the year, making them of dubious value on rivers with high weed content, such as the Detroit River. These problems can be avoided with the ADCP meter, which is not affected by the frazil ice and weed effects and produces better quality data for nearly the entire water column. The vertical velocity profiles measured with the ADCP meter show a high consistency in an exponential vertical distribution of velocities.

Because of the high quality of data for the overhead water column, deployment of the ADCP meters should be considered by agencies responsible for flow measurements in large rivers, such as COE for the Great Lakes connecting channels. Data from such meters could be collected either continuously or on demand. With proper calibration, the ADCP meters may provide a suitable substitute for the labor-intensive periodic measurements

now conducted by these agencies. The quality of such measurements would also be higher.

ACKNOWLEDGEMENTS

From the beginning of the current-meter field experiment a number of people contributed to the successful operation of the project. The authors express their thanks to all the contributors and acknowledge specifically their contributions. Several people from GLERL Instrument Lab, namely, H.K. Soo, R.D. Kistler, R.W. Muzzi, T.C. Miller, and J.E. Dungan are acknowledged for their extensive involvement in instrumentation and field operations throughout the project or its portions. The study was conducted by GLERL's Lake Hydrology Group with Dr. F.H. Quinn as Head, initially by A.J. Potok with assistance from J.J. Kolodziejczak. The initial program was extensively modified and field tested prior to data collection phase. At different times throughout the study assistance in data analysis was provided by M. Moliassa, S.R. Bonema, W.P. Moore, B.M. Slizewski, B.E. Short, and D.A. Buckwald, all part-time temporary employees. Finally, the authors thank the U.S. Ninth Coast Guard District for the deployment support provided on both rivers, without which this project would not have been possible.

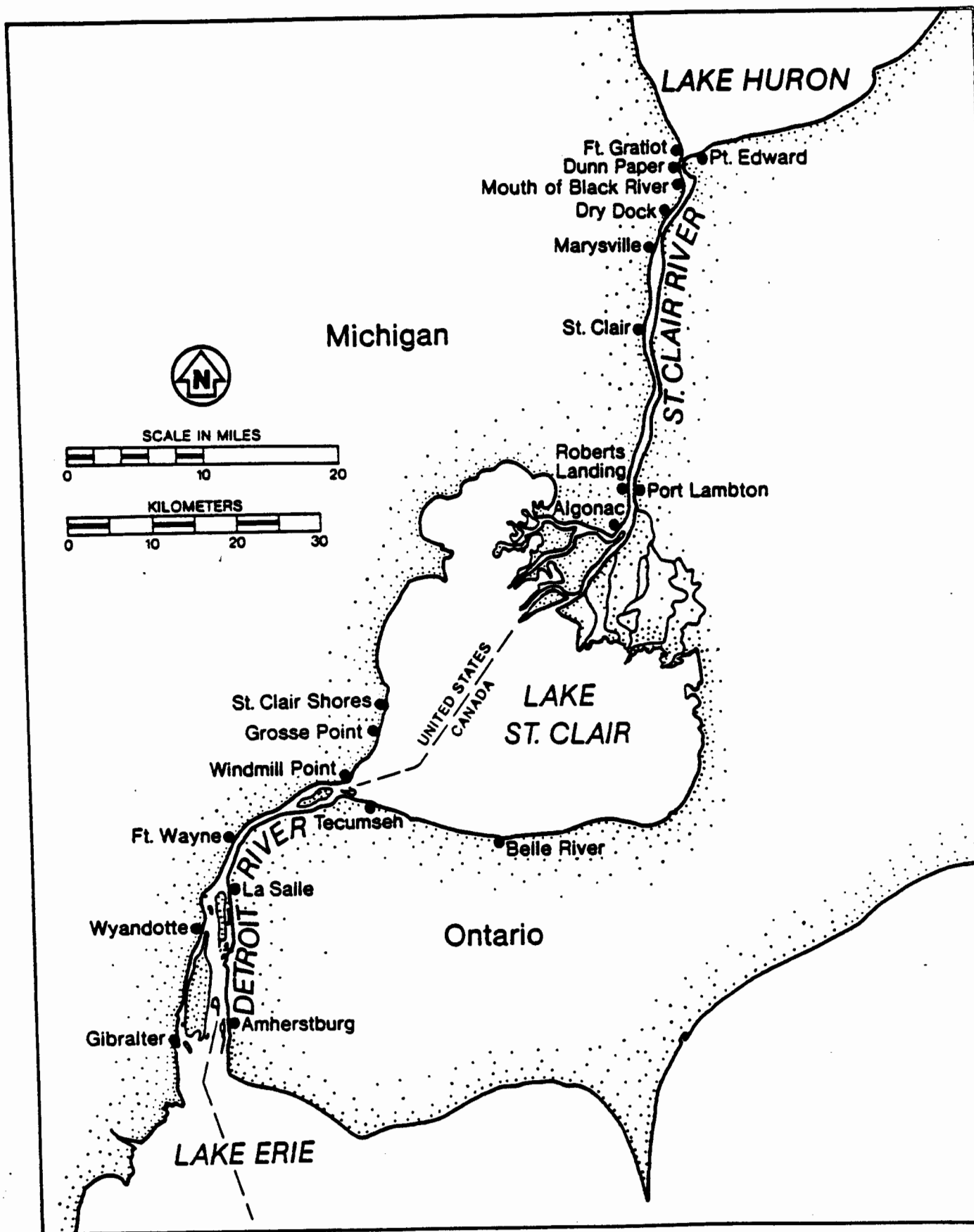
LITERATURE CITED

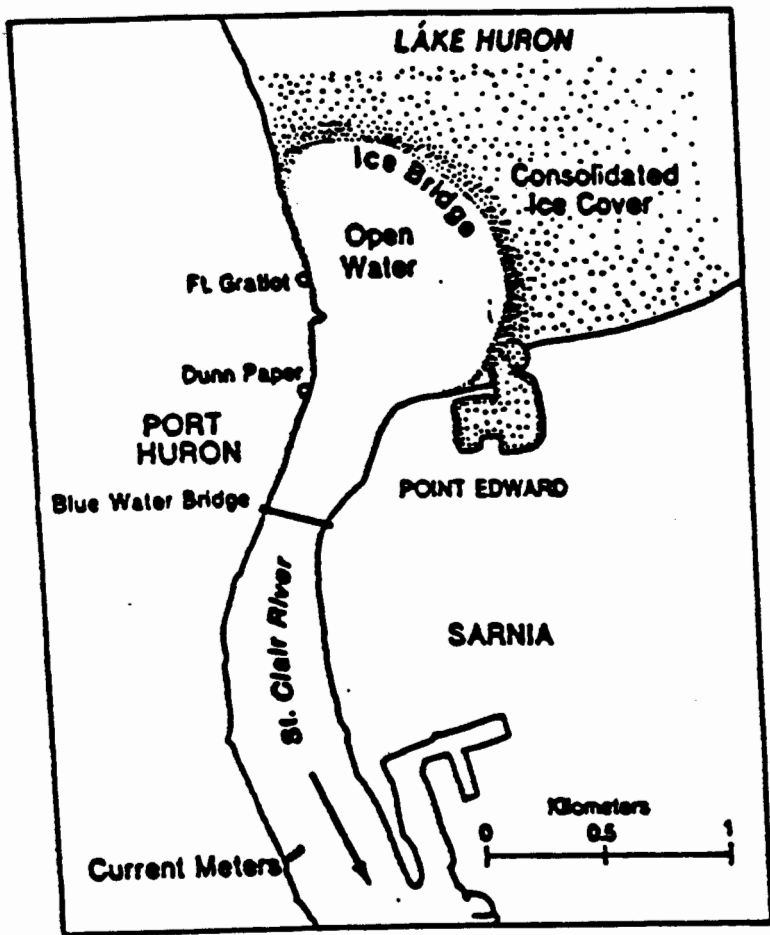
- Derecki, J.A., and R.N. Kelley. 1981. Improved St. Clair River dynamic flow models and comparison analysis, NOAA Tech. Memo. ERL GLERL-34.
- Derecki, J.A., and F.H. Quinn. 1986a. Natural regulation of the Great Lakes by ice jams: a case study. Proceedings, 4th Workshop on Hydraulics of River Ice, Service Hydraulique, Ecole Polytechnique de Montreal, Quebec, June 19-20, Vol. 1, pp. F4.1-F4.24.
- Derecki, J.A., and F.H. Quinn. 1986b. The record St. Clair River ice jam of 1984, J. Hyd. Eng., 112(12):1182-1194.
- Derecki, J.A., and F.H. Quinn. 1987. Use of current meters for continuous measurement of flows in large rivers. Water Resour. Res., 23(9):1751-1756.
- Prandtl, L. 1925. Bericht uber untersuchungen zur ausgenbildeten turbulenz, Z. angew. Math. u. Mech., 5(2):136.
- Quinn, F.H., and J.C. Hagman. 1977. Detroit and St. Clair River transient models, NOAA Tech. Memo. ERL GLERL-14.
- von Karman, Th. 1934. Turbulence and skin friction, J. Aeronaut. Sci., 1(1):1.

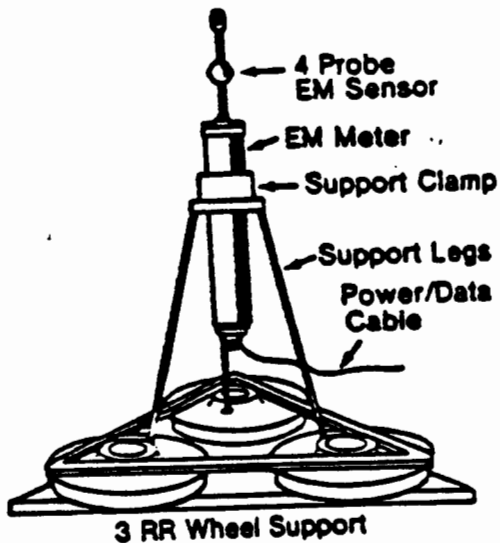
LIST OF FIGURES

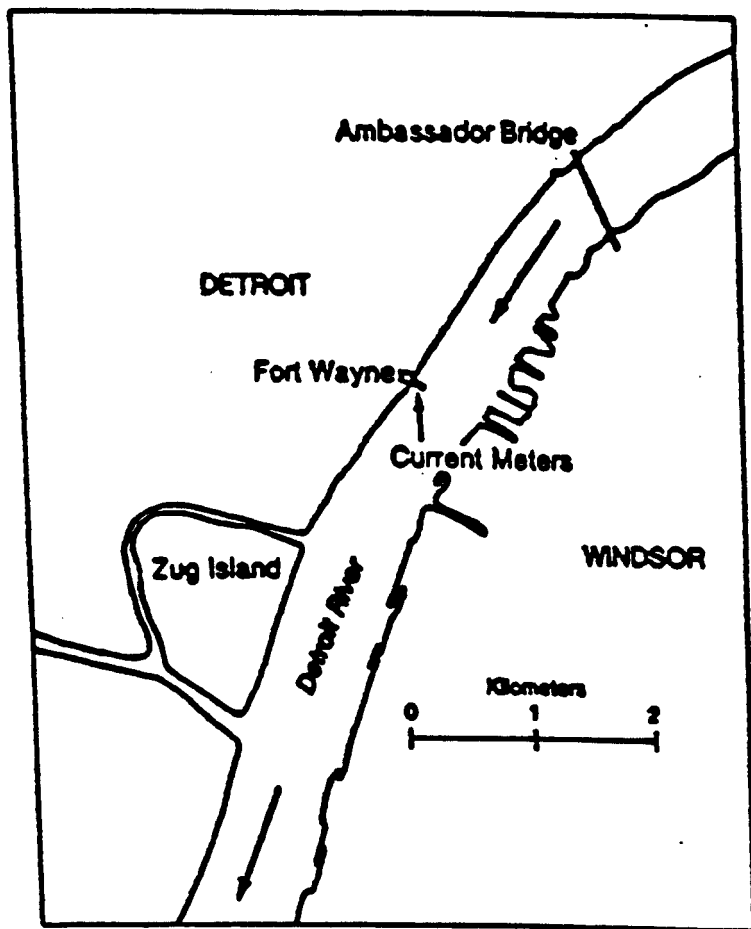
1. St. Clair-Detroit River system with location of water level gages.
2. The point-measuring EM current meter and support.
3. Locations of St. Clair River current meters and ice bridge.
4. Location of Detroit River current meters.
5. The ADCP meter with diagram showing its remote-sensing operation.
6. St. Clair River EM meter data centered around ice jam, March-May, 1984.
7. St. Clair and Detroit River flows, March-May, 1984.
8. St. Clair River ratios of model to EM meter velocity during first deployment period, November 1983 - July 1984.
9. St. Clair River ratios of model to EM meter velocity during second deployment period, November 1984 - June 1987.
10. Relationships between St. Clair River normal model and EM meter velocity, November 1983 - July 1984.
11. St. Clair River EM meter and model velocities showing weed-effect problems, May - October 1986.
12. Vertical distribution of daily velocity, June 1985.
13. Vertical velocity profiles, March 5 and June 10, 1985.
14. St. Clair River profiler relationship between near-bottom and average vertical velocity, November 1984 - April 1986.
15. St. Clair River ratios of model to profiler velocity during deployment period, November 1984 - April 1986.
16. Relationship between St. Clair River normal model and profiler velocity, November 1984 - April 1986.

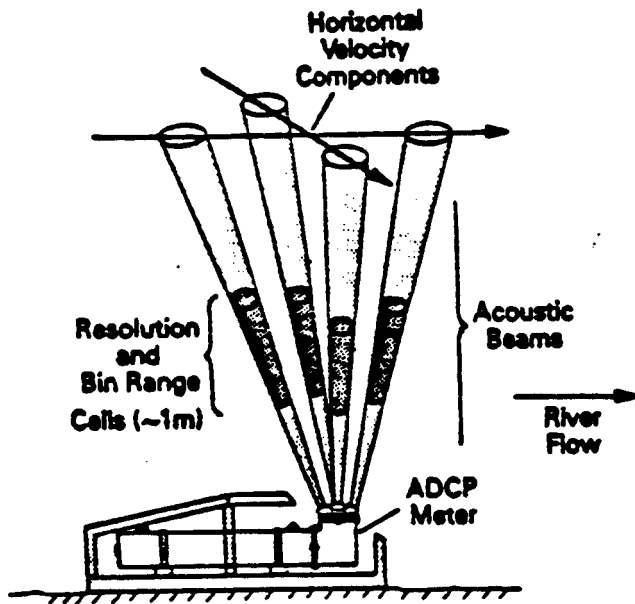
17. Detroit River ratios of model to EM meter velocity during deployment period, August 1984 - June 1987.
18. Detroit River ratios of model to profiler velocity during the period of study, November 1986 - June 1987.

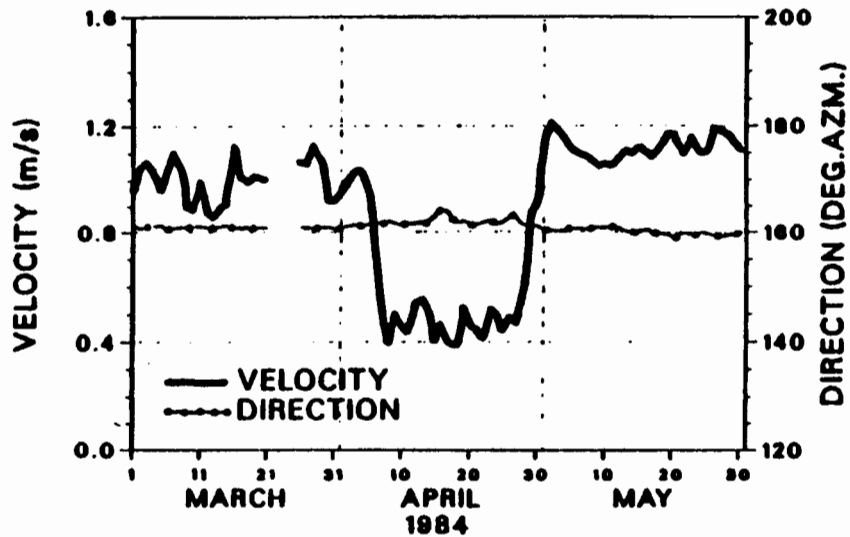


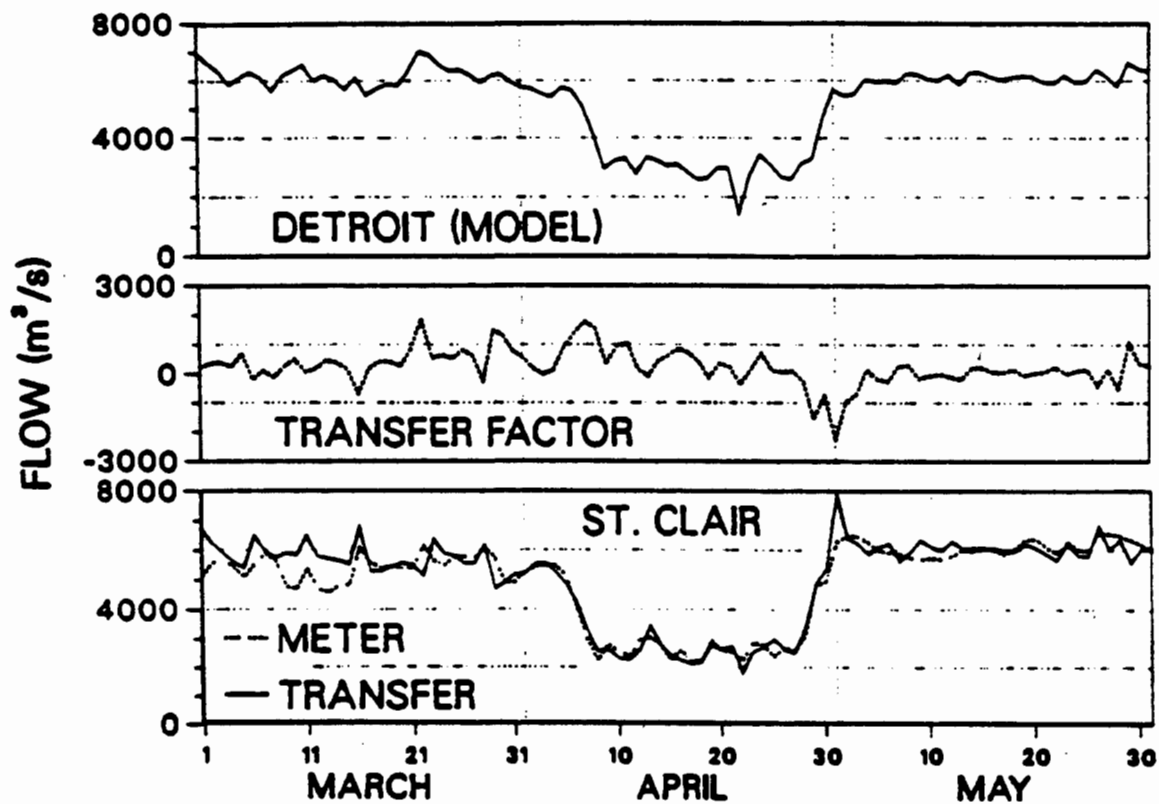


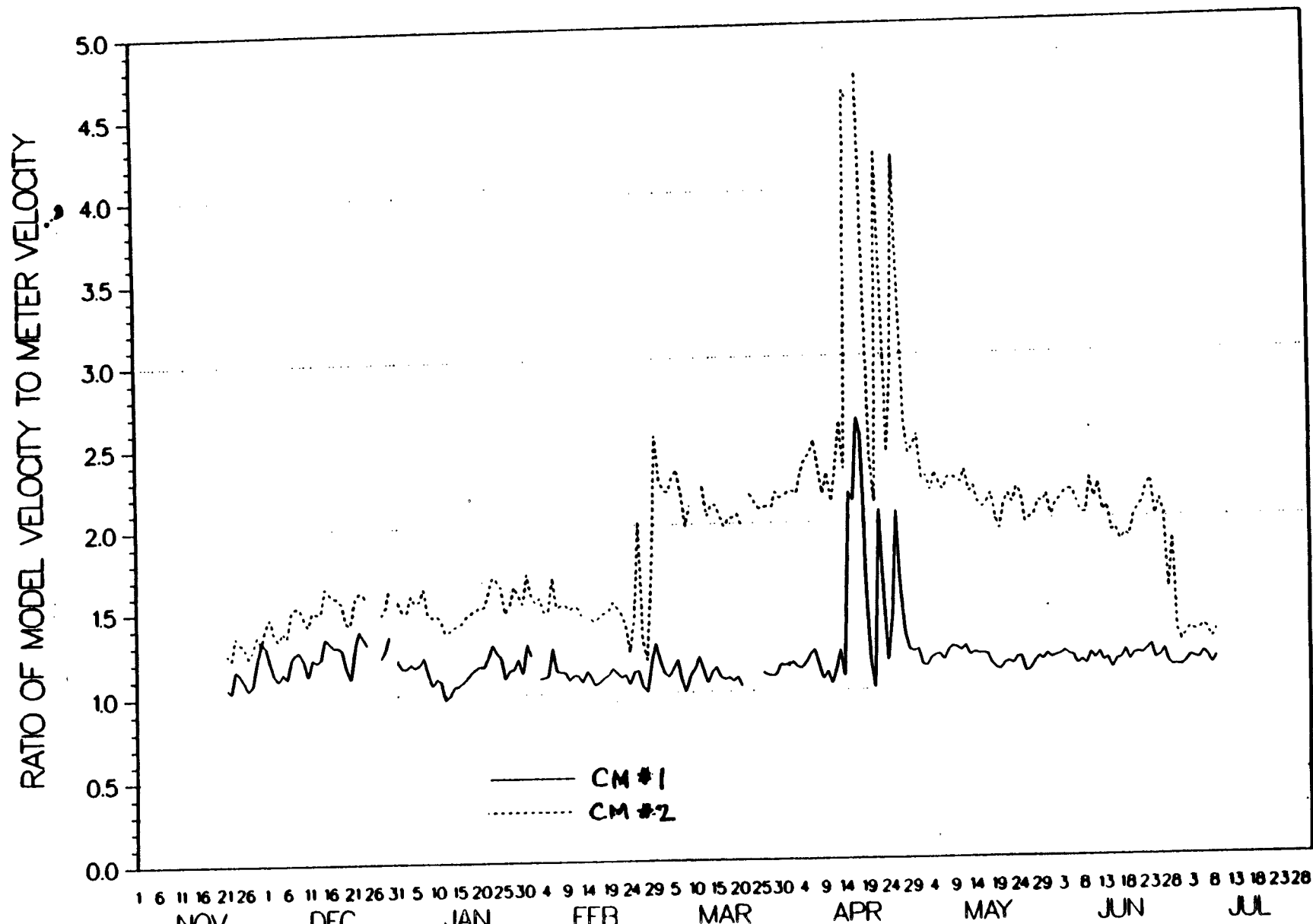


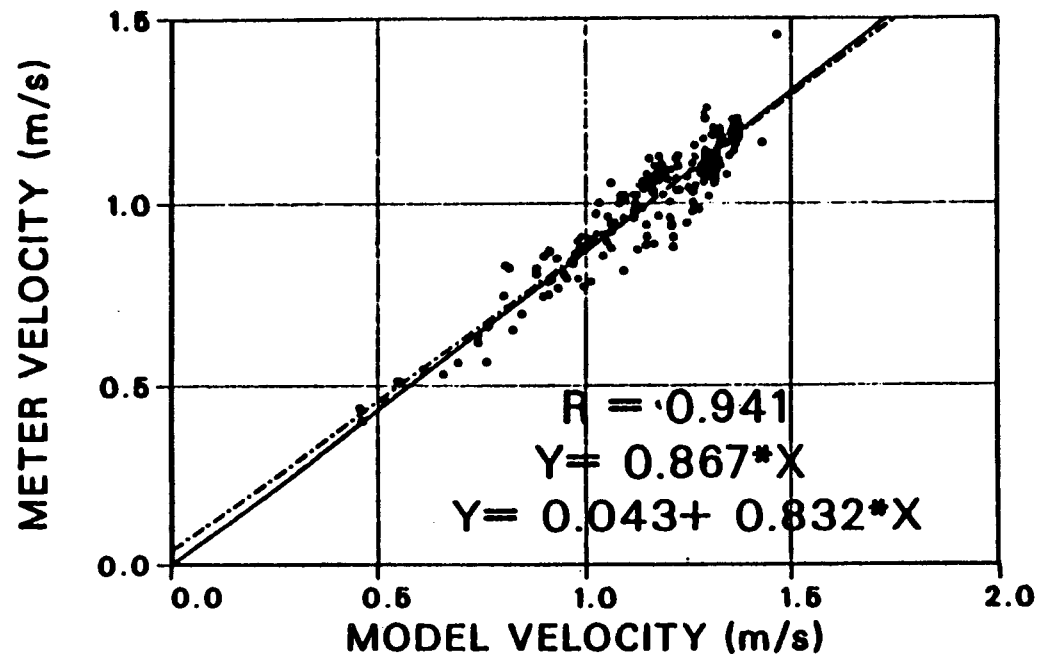


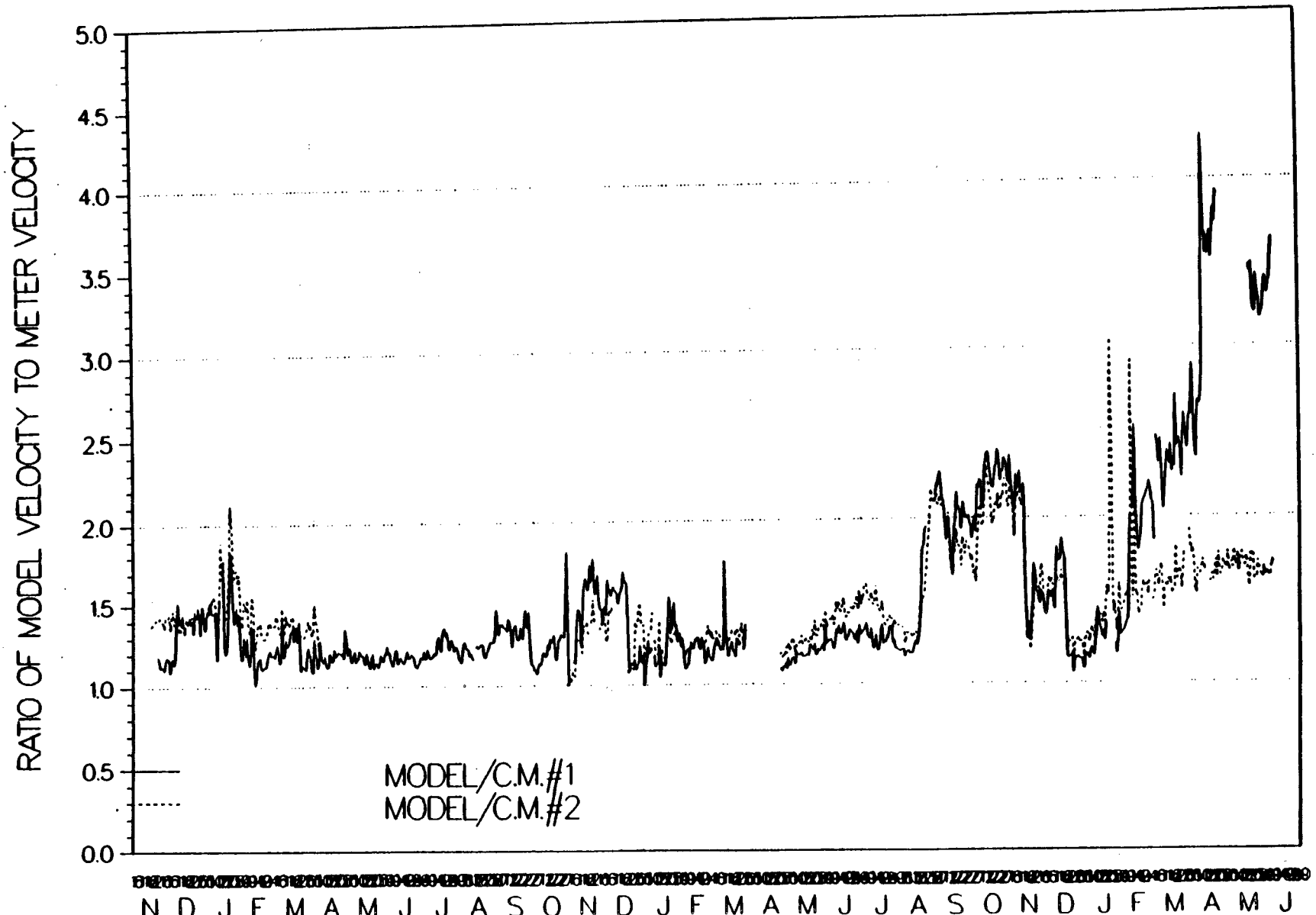


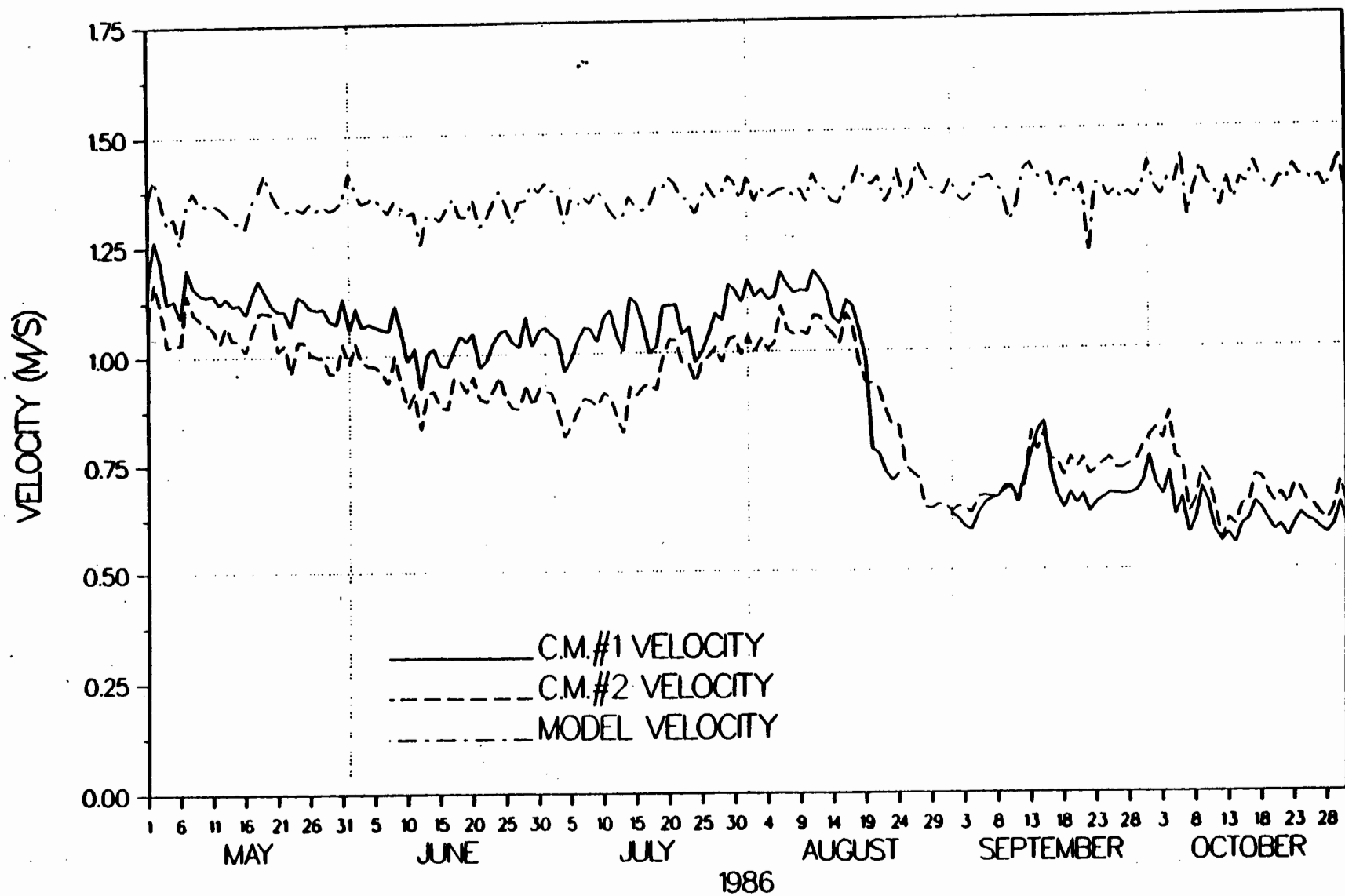


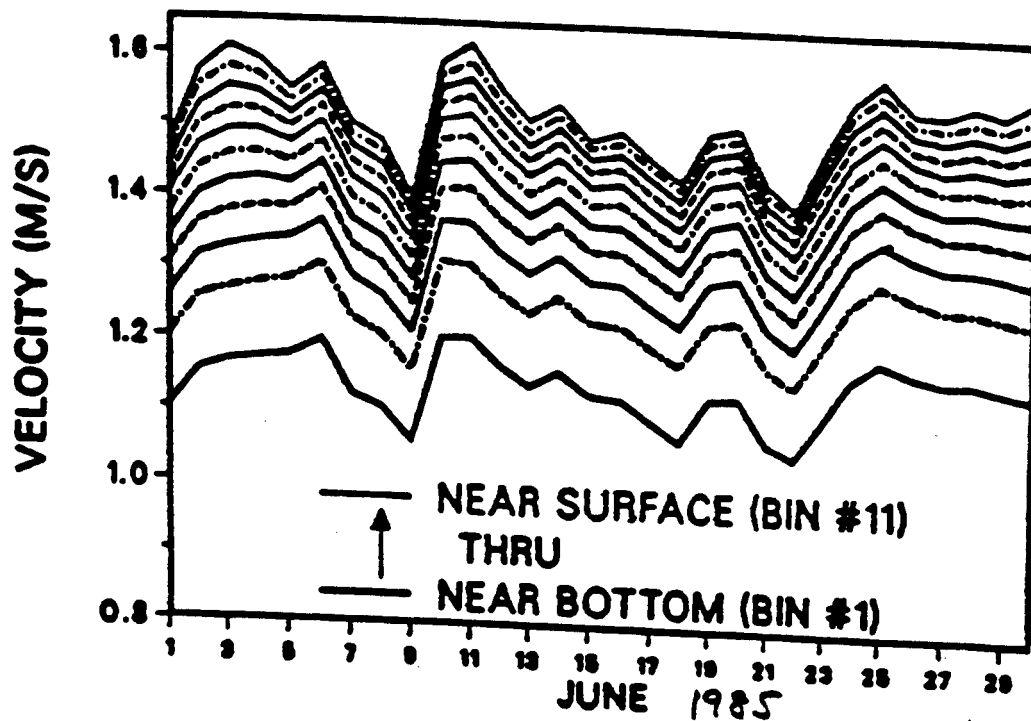


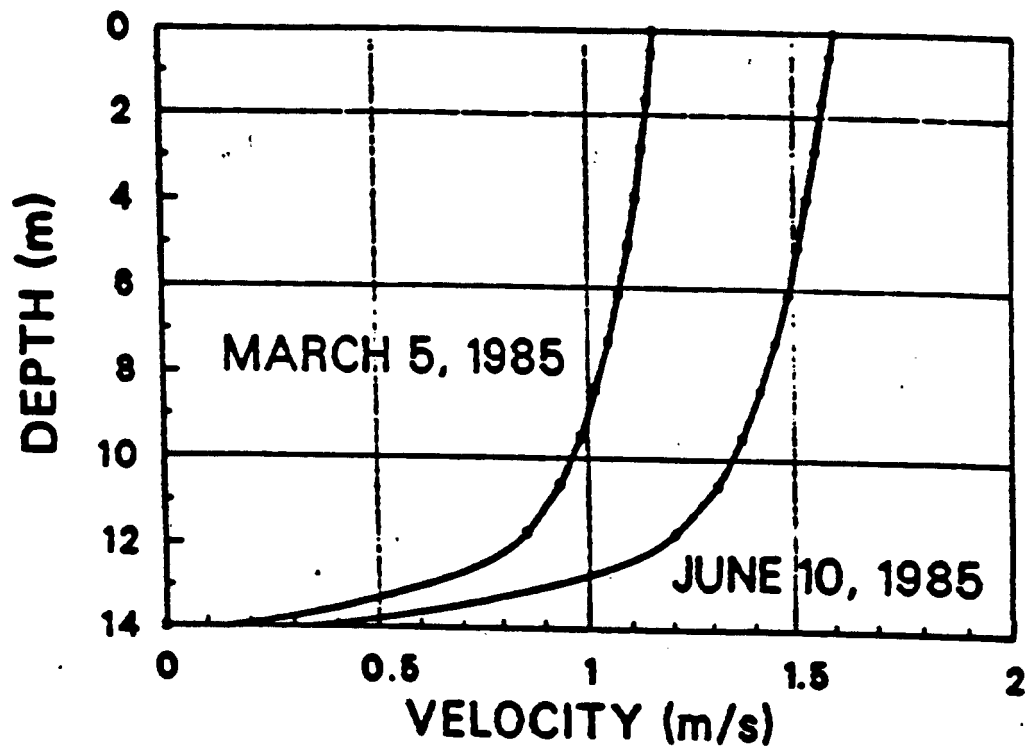


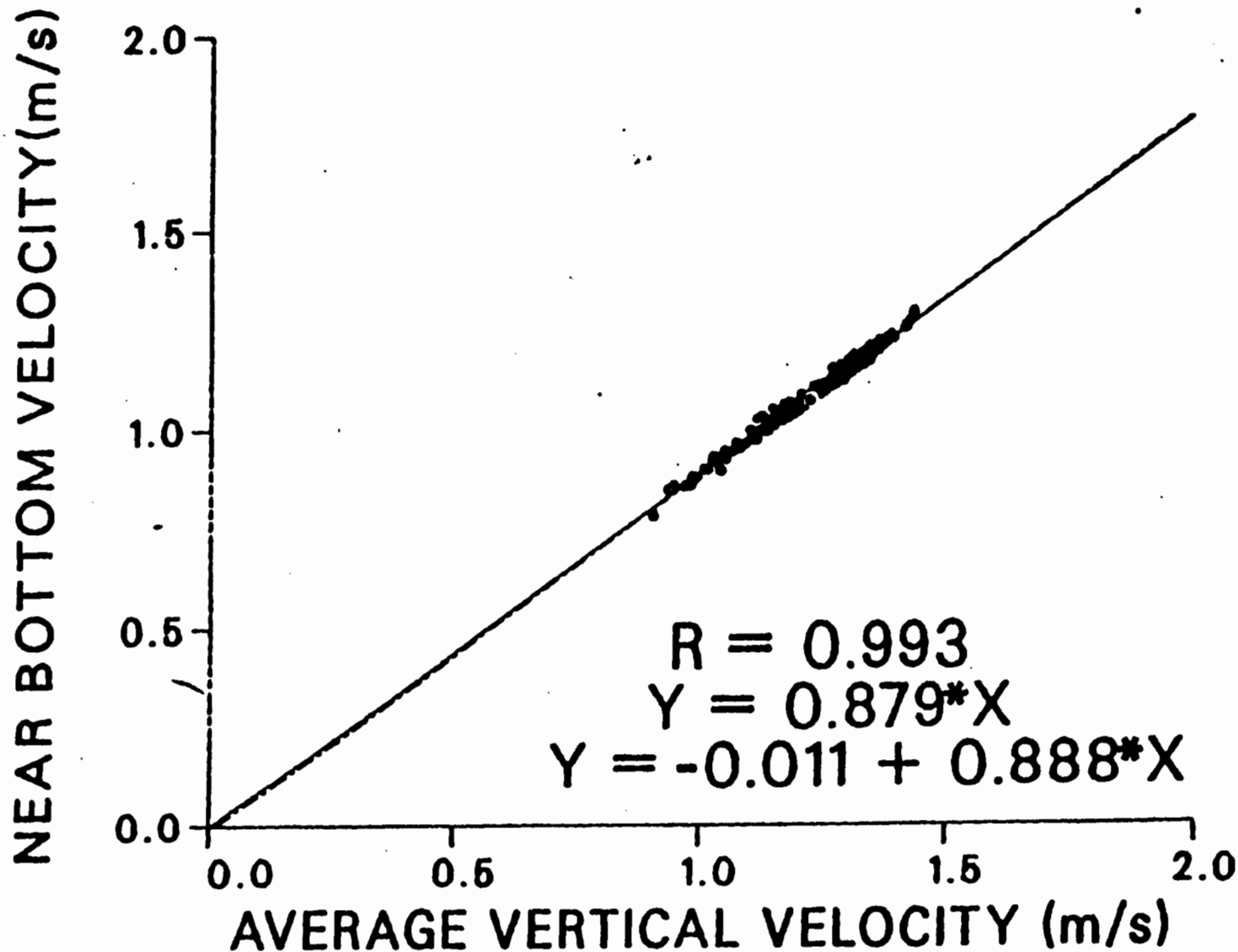




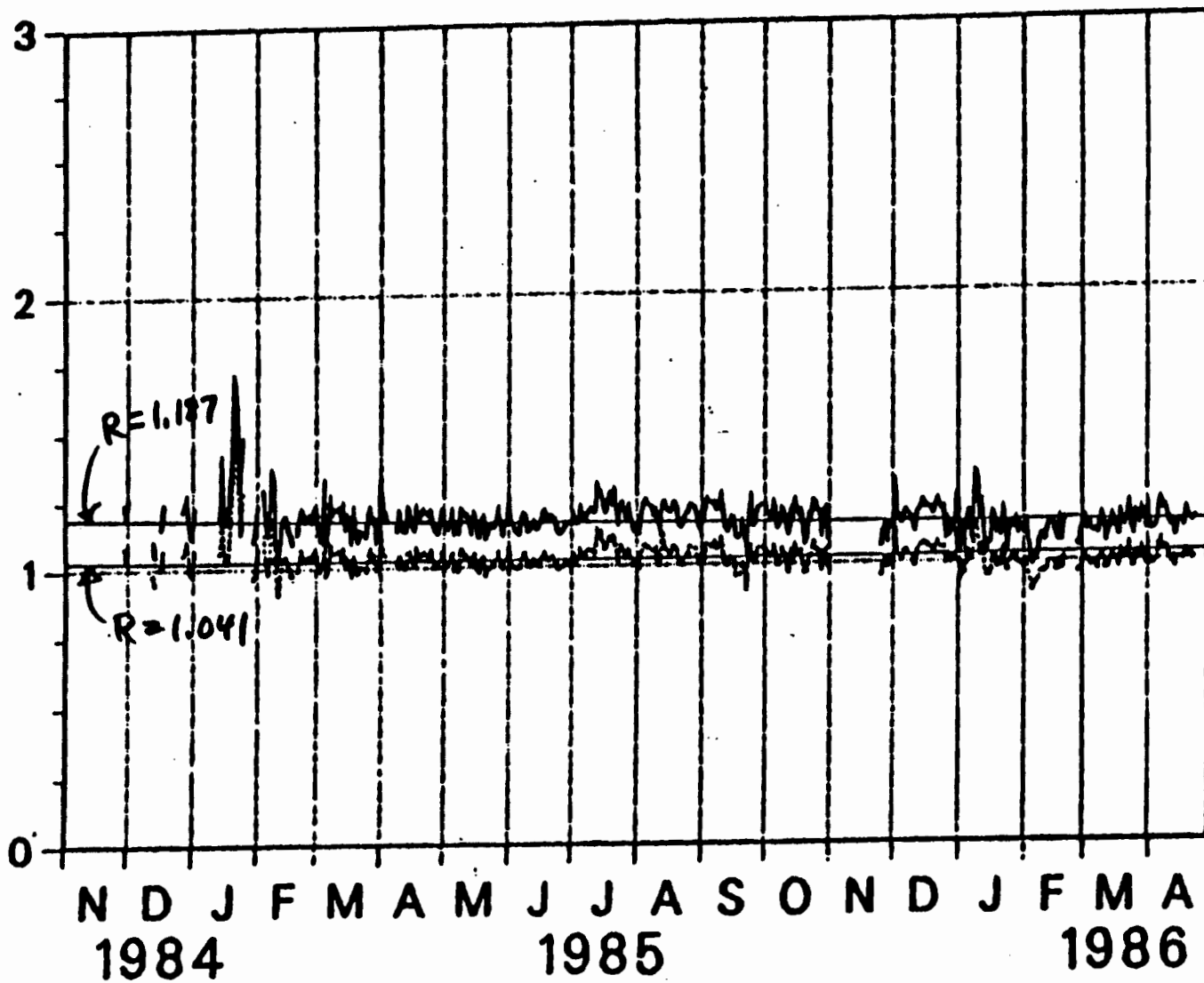




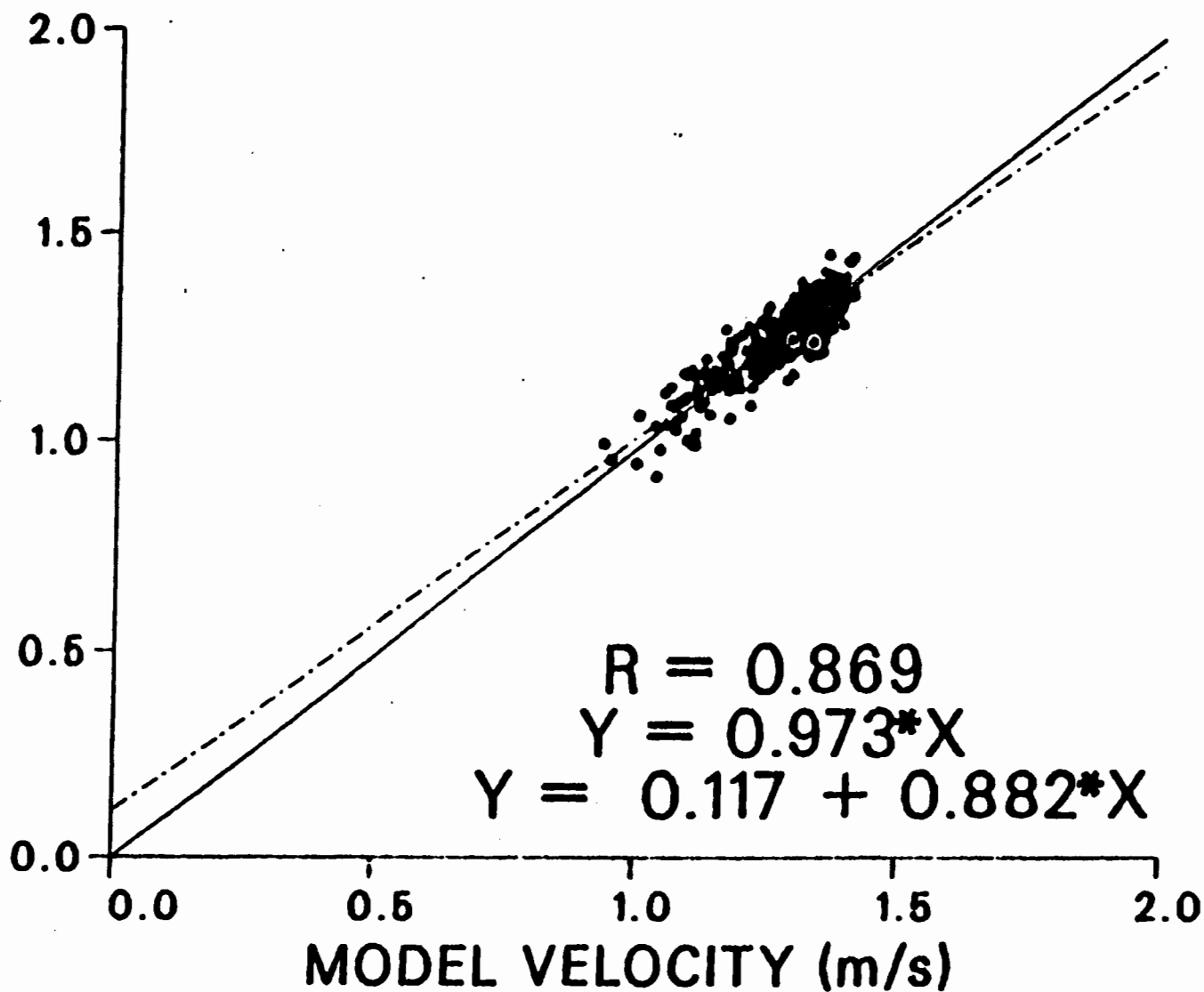


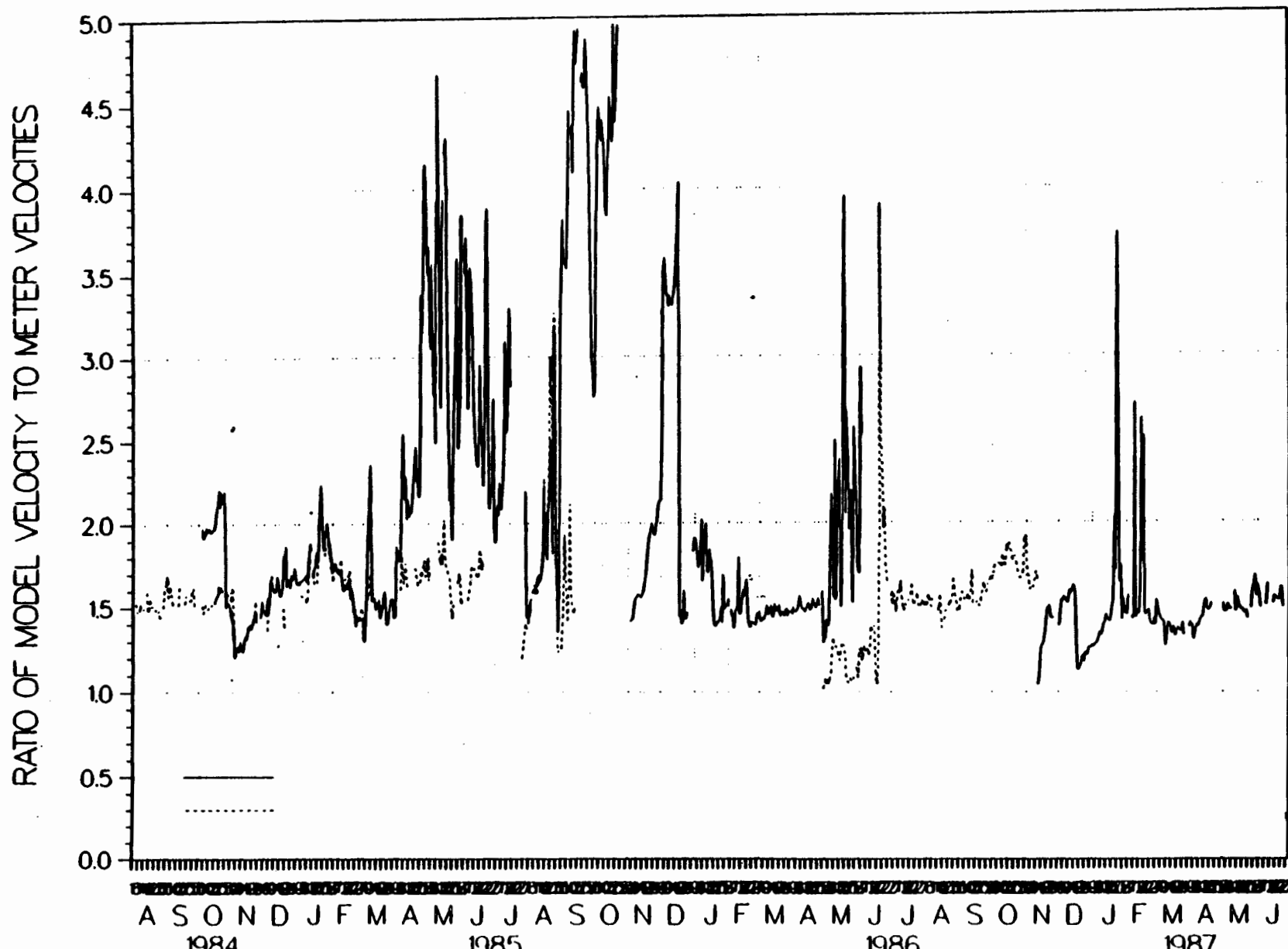


RATIOS

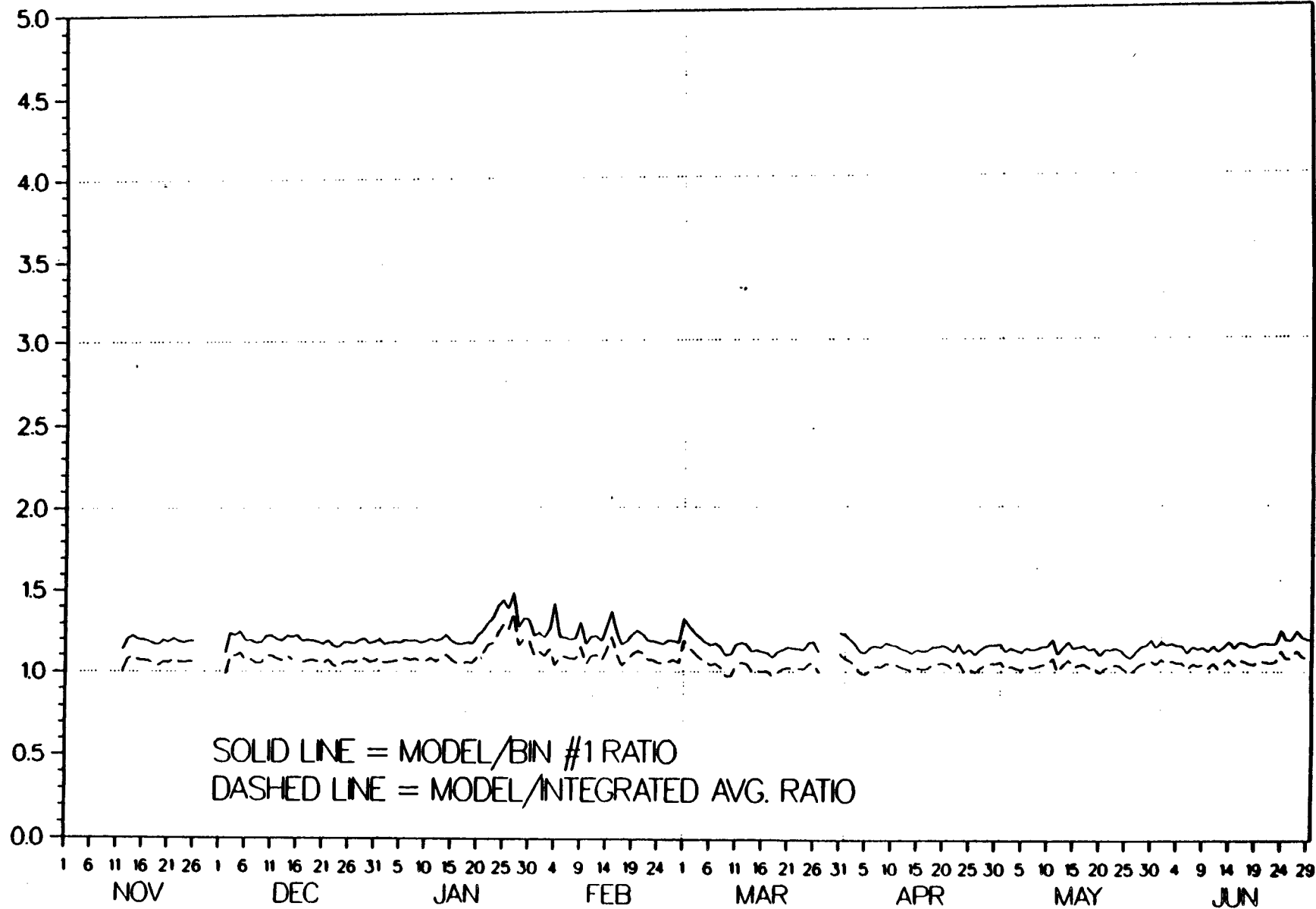


AVG. PROFILER VELOCITY (m/s)





RATIOS: MODEL TO PROFILER VELOCITIES (BIN #1 & NT. AVG.)



DEVELOPMENT OF A SHALLOW WATER NUMERICAL WAVE MODEL FOR LAKE ST. CLAIR

David J. Schwab and Paul C. Liu

In the summer and fall of 1985, the National Water Research Institute (NWRI) and GLERL participated in an extensive field measurement program in Lake St. Clair. The availability of high-quality, over-lake meteorological data and the other physical measurement systems in a relatively flat and shallow basin with sufficient fetch to generate substantial waves provided a perfect opportunity to measure wave dissipation and the effect of waves on resuspension in shallow water. On June 19, 1985, scientists from GLERL, NWRI, and AES (Atmospheric Environmental Service) met and planned a joint program entitled Wave Attenuation, Variability, and Energy Dissipation in Shallow Seas (WAVEDISS '85) for the fall of 1985 in Lake St. Clair to make these measurements.

An inventory of readily available equipment limited the number of recording stations to six, three each from GLERL and NWRI. The GLERL stations consisted of a single Zwarts transmission wave staff and a Datawell Waverider radio transmitter. The NWRI stations consisted of a triangular array of capacitance wave gauges, a cup anemometer, and a SeaData recording package. The instrumentation systems were attached to towers which were guyed to a base anchored with railroad wheels. The towers were deployed along a transect parallel to the prevailing storm wind direction (Fig. 1). One tower was deployed on a perpendicular leg to give an indication of

cross-transect variability. The separation distances between the towers were based on expected differences in energy for a 10 m/s wind compared to the sampling variability of the estimates of wave energy. A sampling rate of 4 Hz was selected based upon expected wave periods. Wave record length was set at 4096 samples, or about 17 minutes at 4 Hz sampling rate. This record length was a compromise between recording capacity of the SeaData recorders and the statistical reliability of wave energy estimates.

The GLERL instruments transmitted continuously to a shore station at Stoney Point, Ontario where a microcomputer stored one wave record from each station per hour. The microcomputer was periodically interrogated by telephone to retrieve the data on the GLERL VAX computer. The NWRI instruments recorded burst samples on even-numbered hours when the anemometer reading exceeded a preset threshold value. The triangular array of capacitance gauges provided wave direction estimates in addition to the wave energy spectrum. The experiment ran from September 20 - December 2, 1985. Nearly continuous measurements of significant wave height and wave period (at hourly intervals) were obtained from the GLERL towers. The NWRI towers recorded data only when the wind speed exceeded a preset threshold (usually 7 ms^{-1}) so the data covers only the higher wave height periods. Meteorological data consisting of hourly values of wind speed, wind direction, air temperature, and water temperature were obtained from the NWRI meteorological buoy at 42.5 degrees north, 82.8 degrees east. The meteorological data was used to drive the GLERL-Donelan numerical wave prediction model on a 1.2 km numerical grid. This model was developed by Donelan (1977) and used successfully to predict wave height and wave

direction in Lake Erie (Schwab et al., 1984) and Lake Michigan (Liu et. al., 1984). The model is a parametric model based on a momentum balance equation for the wave field. The model predicts the two components of the wave momentum vector and the phase speed of the peak energy waves. From these variables, significant waveheight, wave period, and wave direction are derived. In the mathematical formulation of the numerical model, the waves are assumed to obey the deep water dispersion relation. Refraction and bottom dissipation are ignored.

As part of the UGLCCS, the GLERL-Donelan model has been modified to account for the effect of finite water depth on wave propagation by incorporating the Kitaigorodskii et al. (1985) shallow water wave spectrum along with a depth-dependent group velocity and a simple form of bottom friction. This shallow water version of the model was also run with the same grid and same wind input as the deep water version. The results for hourly values of significant waveheight are compared to observations at the six towers in Figures 2 and 3. The statistical comparison in terms of root mean square error and correlation coefficient is presented in Table 1.

As can be seen in Table 1 and Figures 2 and 3, the deep water version of the model provides quite acceptable estimates of waveheight, even for the largest waves at the shallowest stations. The shallow water version of the model tends to underestimate the highest waves at all stations. The shallow water model could be adjusted to better match the observed waveheights by decreasing the bottom friction parameter, but the best it could do would be no better than the deep water model.

Work is underway now to determine why the deep water model works in Lake St. Clair. One possibility is that the wind momentum input function in the model is oversimplified and if it were formulated more realistically, the deep water model would tend to overestimate the highest waves. This possibility is being investigated, but for now, the deep water model appears to be quite acceptable for providing wave height estimates in Lake St. Clair.

LITERATURE CITED

- Donelan, M. A., 1977. A simple numerical model for wave and wind stress prediction. Unpublished manuscript. National Water Research Institute, Burlington, Ontario, Canada. 28pp.
- Kitaigorodskii, S.A., V.P. Krasitskii and M.M. Zaslavskii, 1975: On Phillips' theory of equilibrium range in the spectra of wind-generated gravity waves. J. Phys. Oceanogr., 5, 410-420.
- Liu, P. C., Schwab, D. J. and Bennett, J. R., 1984. Comparison of a two-dimensional wave prediction model with synoptic measurements in Lake Michigan. J. Phys. Oceanogr. 14:1514-1518.
- Schwab, D.J. Bennett, J.R., Liu, P.C. and Donelan, M.A., 1984. Application of a simple numerical wave prediction model to Lake Erie. J. Geophys. Res., 89(C3):3586-3592.

Table 1. Comparison of Deep and Shallow Water Model Predictions with Measured Significant Waveheight

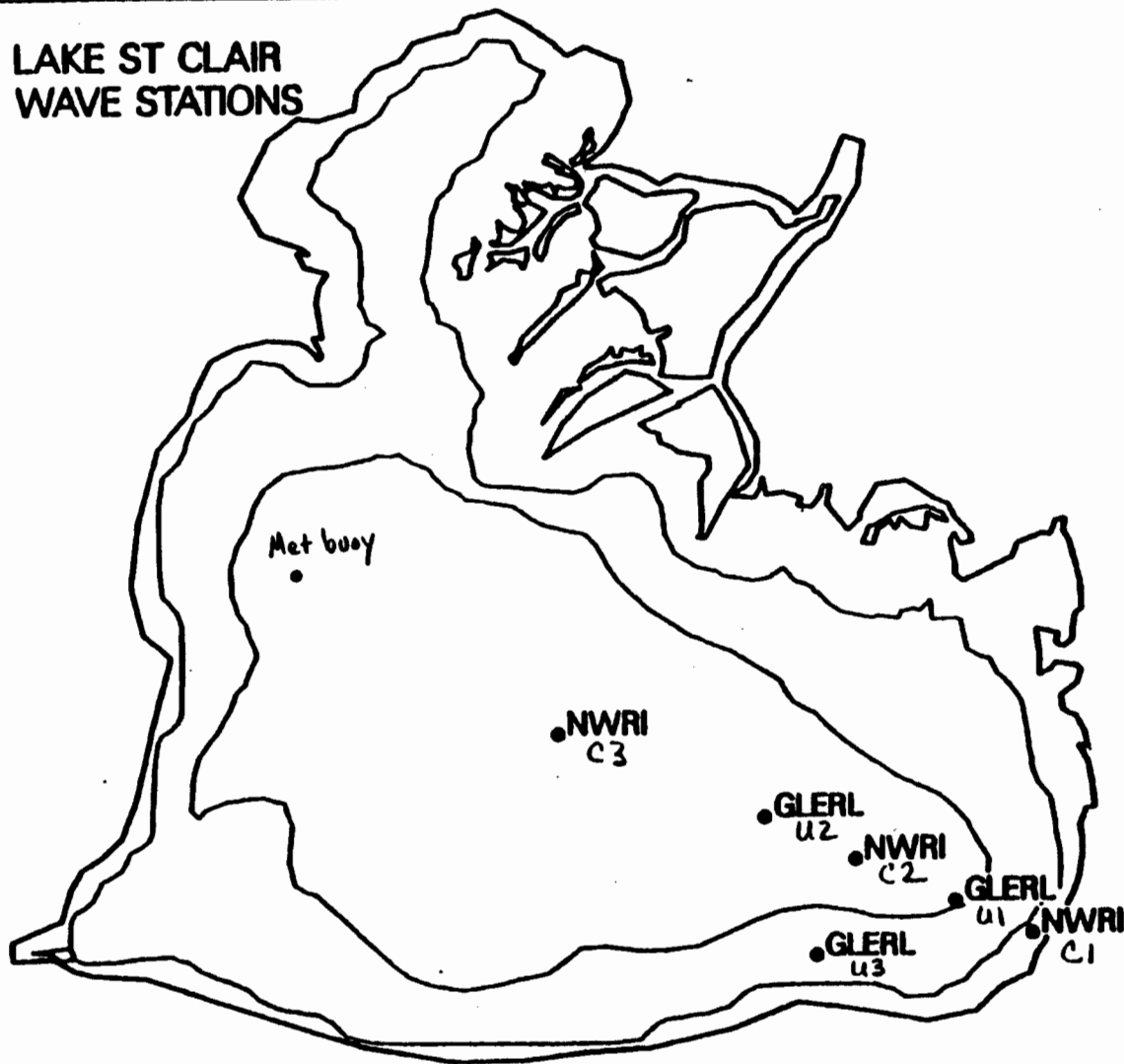
	STATION					
	C3	U2	C2	U1	C1	U3
Depth (m)	6.7	7.0	6.4	5.5	3.7	4.4
Data Points	244	1366	237	1478	153	1539
Deep Water Model						
rmse (m)	0.11	0.11	0.16	0.09	0.10	0.08
corr. coeff. ¹	0.89	0.93	0.88	0.93	0.94	0.94
Shallow Water Model						
rmse (m)	0.13	0.13	0.20	0.11	0.18	0.09
corr. coeff. ¹	0.88	0.93	0.85	0.91	0.92	0.93

¹correlation between predicted and measured values.

LIST OF FIGURES

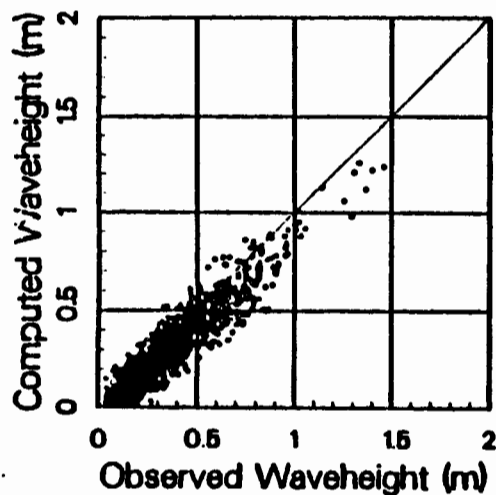
- Fig. 1. Station locations for GLERL and NWRI wave towers during WAVEDISS '85.
- Fig. 2. Comparison of observed and predicted wave height for the deep water model.
- Fig. 3. Comparison of observed and predicted wave height for the shallow water model.

LAKE ST CLAIR
WAVE STATIONS

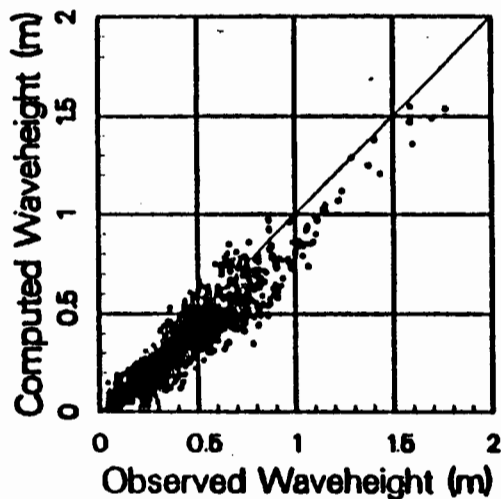


Deep Water Model

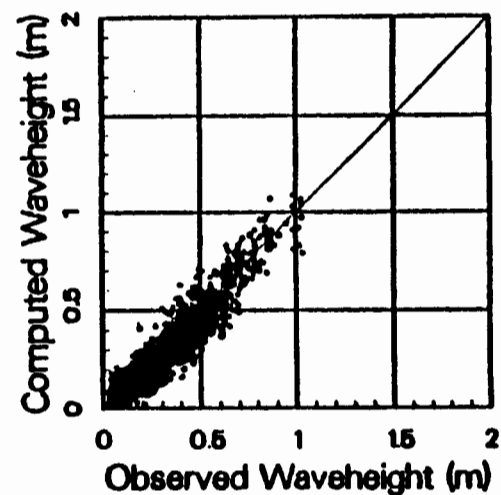
Lake St. Clair 1985 Station U1



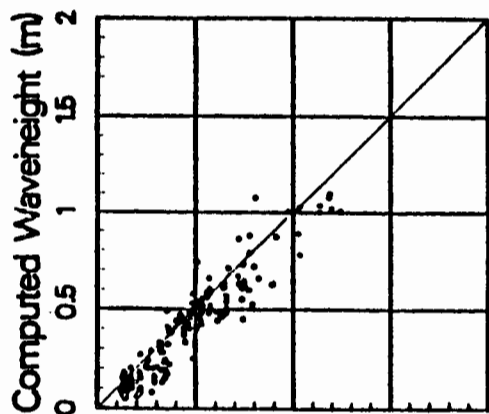
Lake St. Clair 1985 Station U2



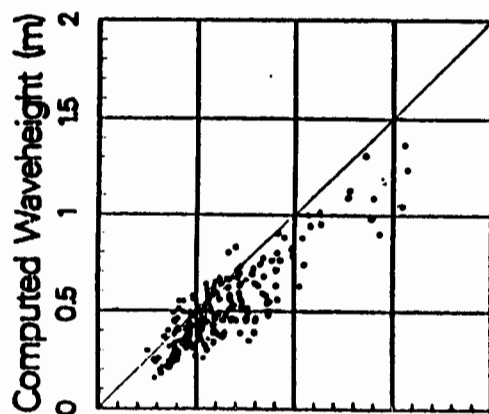
Lake St. Clair 1985 Station U3



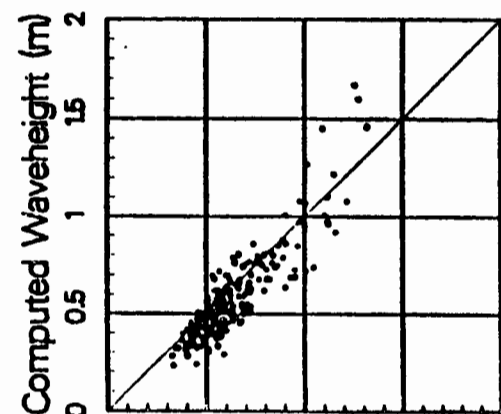
Lake St. Clair 1985 Station C1



Lake St. Clair 1985 Station C2

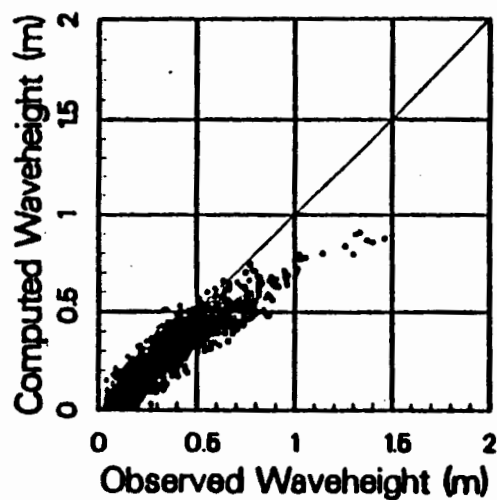


Lake St. Clair 1985 Station C3

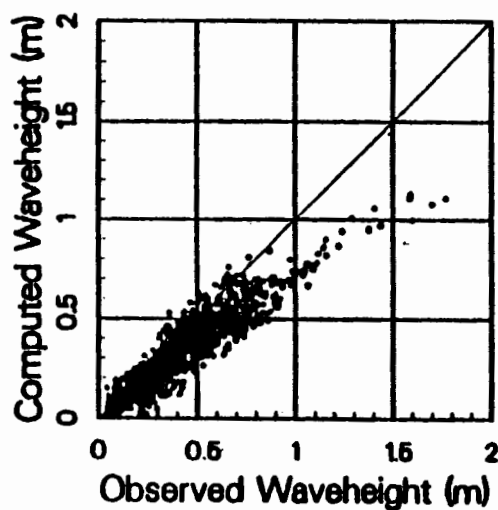


Shallow Water Model

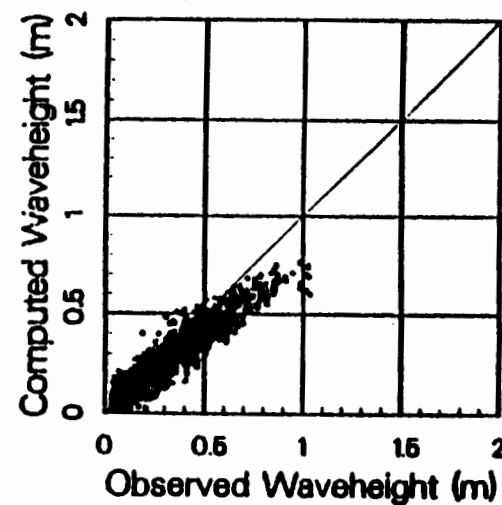
Lake St. Clair 1985 Station U1



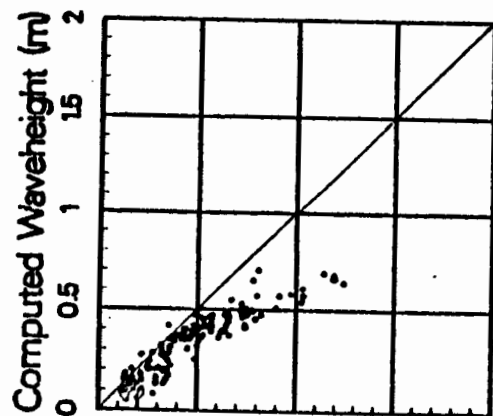
Lake St. Clair 1985 Station U2



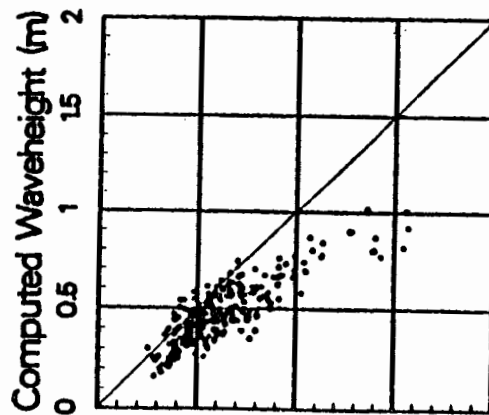
Lake St. Clair 1985 Station U3



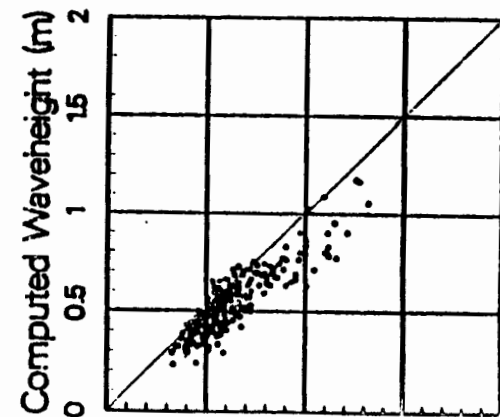
Lake St. Clair 1985 Station C1



Lake St. Clair 1985 Station C2



Lake St. Clair 1985 Station C3



MODELING PARTICLE TRANSPORT IN LAKE ST. CLAIR

D. J. Schwab and A. H. Clites

The results of a numerical circulation model of Lake St. Clair are used to describe particle transport pathways in the lake in terms of residence time and variability due to wind-induced circulation. Specifically, we address the following questions. 1) What path does water entering Lake St. Clair from one of the tributaries follow through the lake before leaving at the Detroit River? 2) How long does it take? 3) How is the path changed by wind-induced circulation in the lake? 4) For the meteorological conditions during the summer and fall of 1985, what are typical statistical distributions of these pathways?

In order to answer these questions, a numerical circulation model of the lake was used. The numerical model is the same time-dependent rigid-lid model developed by Schwab et al. (1981) and used by Schwab (1983) in Lake Michigan and Schwab and Bennett (1987) in Lake Erie. The basic assumptions of the model are that the circulation is barotropic and non-divergent, and that nonlinear acceleration and horizontal diffusion of momentum are negligible compared to first-order acceleration and Coriolis forces. A simple quasi-linear formulation is used to describe bottom friction. The model is forced by the hydraulic flow through the lake and by time-dependent wind stress at the surface. The hydraulic flow is assumed to be constant in time at $5700 \text{ m}^3 \text{ s}^{-1}$ and the inflow is divided

among the tributaries as follows: North Channel, 35%; Middle Channel, 20%; St. Clair Flats, 20%; St. Clair Cutoff, 20%; Bassett Channel, 5%.

Currents are calculated on a 1.2 km grid approximating the shape of Lake St. Clair (Fig. 1). Simons and Schertzer (1986) and Ibrahim and McCorquodale (1985) have also developed numerical circulation models for Lake St. Clair and have obtained essentially similar results for the wind-induced circulation. However, the circulation patterns generated by the numerical models often differ considerably from the results of Ayers' (1964) physical model of the lake for some wind directions.

After currents are calculated for each grid square in the numerical model, another model is used to move tracer particles through the lake. The particles are assumed to follow exactly the vertically uniform currents without sinking or diffusing. The numerical model for particle trajectory calculations was developed by Bennett et al. (1983) and used by Schwab and Bennett (1987) in Lake Erie. The model uses a second-order method to compute particle trajectories and takes special care to realistically represent the currents near the shoreline. As shown by Bennett and Clites (1987), this method is far more accurate than simple first order methods yet is only slightly more complex computationally. This particle trajectory model is also used in the "Pathfinder" trajectory prediction system (Schwab et al., 1984) that is used by the National Weather Service and the U.S. Coast Guard for tracking hazardous spills and search and rescue missions on the Great Lakes.

In order to answer questions about residence time for water entering the lake from the various tributaries, several model runs were carried out with idealized wind conditions. First, the hydraulic flow in the absence of wind was calculated (Fig. 2). This pattern was then used as the initial condition for a series of simulated storms with wind directions from the eight compass points and peak wind speeds of either 10 or 20 ms^{-1} . Figure 3 shows a graph of the time dependence of the wind for the storms. The wind speed increases linearly from zero to its peak value over a period of two days and then ceases. Particles from the five tributaries listed above plus the Clinton River, the Clinton River Cutoff, and the Thames River were released into the resulting circulation pattern starting at the beginning of the second day, when the wind speed was at exactly half its peak value. One particle was released every three hours for one day. These particles were then tracked through the lake and their residence time was compared to the residence time for particles in the absence of wind (purely hydraulic flow). The results for the 10 ms^{-1} storms are summarized in Figure 4. The dashed line in the panel for each tributary represents the residence time for water entering there in the no-wind case. It can be seen that even though the average hydraulic residence time for Lake St. Clair is about nine days (based on hydraulic flow of $5700 \text{ m}^3\text{s}^{-1}$, surface area of 1100 km^2 , and a mean depth of 4 m), residence time for water from the individual tributaries ranges from 4.1 days for the Middle Channel to over 30 days for water from the Thames River. The calculated residence times for all the tributaries in the no-wind case are:

North Channel: 4.5 days
Middle Channel: 4.1 days
St. Clair Flats: 5.0 days
St. Clair Cutoff: 8.3 days
Bassett Channel: 24.1 days
Clinton River: 6.9 days
Clinton Cutoff: 9.5 days
Thames River: over 30 days

The effect of wind on the residence time is greatest for the Thames River and the Bassett Channel where a 10 ms^{-1} wind from the SE, E, or NE can decrease the expected residence time to less than 10 days for Bassett Channel or 15 to 20 days for the Thames. A 20 ms^{-1} wind reduces the residence time even more. Winds from W, NW, or N tend to increase the residence time of water from St. Clair Flats and more considerably from the St. Clair Cutoff and Bassett Channel by moving the water eastward into the relatively stagnant eastern part of the lake. The residence time of water entering the lake from the Clinton River is increased by NE, E, SE, and S winds and decreased by SW, W, and NW winds. Wind from almost any direction except NW tends to decrease the residence time of water from the Clinton Cutoff.

The idealized wind condition calculation give some indication of the variability in residence time that can be expected in Lake St. Clair due to wind-induced circulation, but what kind of variability actually occurs during the summer and fall? To answer this question, hourly values of wind

speed and wind direction recorded at the CCIW met buoy at 42.5 degrees north, 82.8 degrees east for the period 23 May, 1985 - 1 December, 1985 were used to drive the numerical circulation model. The resulting circulation patterns were stored and then used with the particle trajectory model to calculate the paths of tracer particles released at the mouth of each tributary once every six hours during the entire six month period. The calculated tracks of the particles were then used to develop probability plots of the likelihood of a parcel of water emanating from one of the eight tributaries passing through a given area of the lake during this period. These plots quantify the wind-induced variability in the pathway that water from one of the tributaries takes through the lake. The results of these calculations are presented in Figure 5 in terms of probability contours. The outermost line is the 99.9% contour, i.e., 99.9% of the conservative particles released from that tributary remained within this contour for the 6 months simulation. The next contour delineates the area in which 90% of the particles remained. Remaining contours are at 10% intervals.

Most of the water from the St. Clair River enters the lake through the North Channel (35%). According to the calculations, this water tends to flow down the western shore of the lake and never gets into the central or eastern parts of the basin. Water from the Middle Channel tends to remain in the western third of the lake, almost never entering the eastern half. Water from St. Clair Flats and the St. Clair Cutoff can be dispersed almost anywhere in the lake to the south of the shipping channel which connects the St. Clair Cutoff with the Detroit River. A small amount of the St.

Clair inflow (5%) enters through Bassett Channel. This water can pass through any part of the eastern half of the lake depending on the wind conditions. The Thames inflow tends to be confined to the eastern and southern shores before reaching the Detroit River and it can take a very long time to get there (see Fig. 4). Water from the Clinton River and Clinton Cutoff is most likely to follow the western shore of the lake southward with the most probable paths within 3 km of the western shore.

Water quality measurements made in Lake St. Clair by Leach (1972 and 1980) showed two distinctly different areas in the lake. In the southeastern part of the lake, the water quality is dominated by the Thames inflow, which is a major source of phosphate and other dissolved and suspended material. The central and western parts of the lake were more similar to Lake Huron in terms of water quality than to the southeastern part of the lake. The pattern of water mass distribution mapped in Leach's (1980) Figures 1-4 is very close to the combined patterns of the four main St. Clair River inflows and the Thames inflow in our Figure 5. Bricker et al. (1976) examined the distribution of zooplankton in the western half of the lake. They distinguished an area of biological and physiochemical similarity along the western shore of the lake that appeared to be influenced more by the Clinton River than the St. Clair River. The shape of this area matches quite well with the distribution pattern for water from the Clinton River in Figure 5 here.

To verify the circulation model and lend credence to the calculated currents used in this study, the model was tested by comparing model output

to actual current data measured in Lake St. Clair in 1985. Two separate current data bases were gathered. One involved the use of 5 drifting buoys which were repeatedly launched and tracked in the lake. The other was the result of several synoptic current surveys utilizing electromagnetic current meters.

Currents predicted by the circulation model were used to simulate 16 drifter tracks. Most of the tracks are about 2 days in length from various portions of the lake. In most cases, the model simulated the tracks extremely well. For the entire data set, the mean root mean square (rms) of the drifter was 25% greater than that of the calculated current track. The directions compared favorably except for a few tracks near the mouth of the Bassett Channel, where the model prediction was over 90 degrees different in direction when compared with the observed track.

The comparisons between current meter measurements and model-predicted currents were even better. In nearly 100 comparisons, 60% of the variance is explained by the model prediction. The model again seems to under-predict the current speeds, here by about 30%.

The results presented in this report are not water quality calculations. They only track conservative, non-dispersive tracers from the mouths of the tributaries through the lake under various wind conditions. Work in another GLERL UGLCCS project couples the circulation patterns calculated here with the TOXIWASP water quality model for Lake St. Clair. However, based on the comparisons with actual current measurements

presented above, the calculated currents provide a realistic depiction of the wind-induced circulation in Lake St. Clair.

LITERATURE CITED

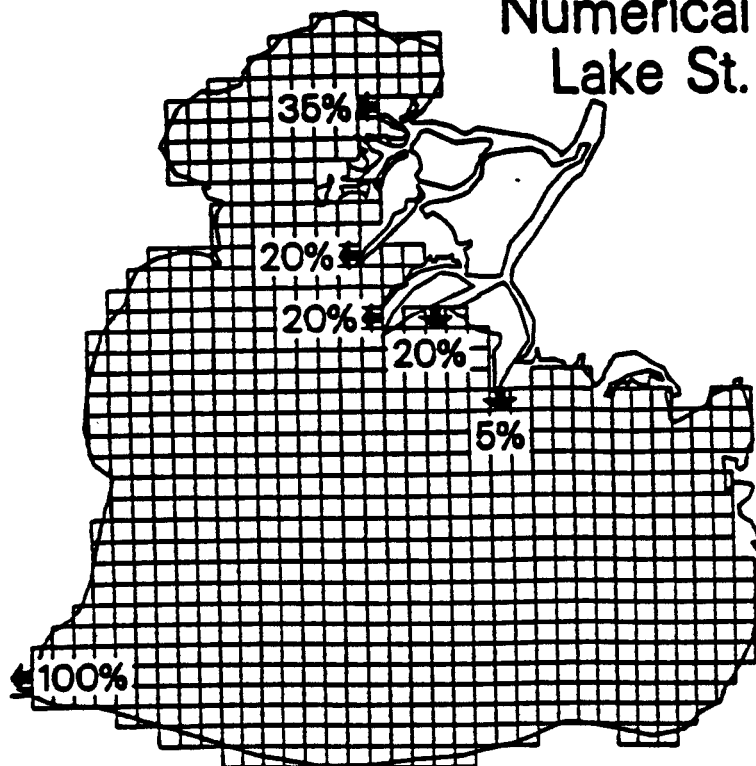
- Ayers, J. C. 1964. Currents and related problems at Metropolitan beach, Lake St. Clair. Great Lakes Res. Div. Spec. Rpt. No. 20, Univ. of Mich., Ann Arbor, Michigan.
- Bennett, J. R. and Clites, A. H. 1987. Accuracy of trajectory calculation in a finite difference circulation model. J. Comp. Physics, 68:272-282.
- Bennett, J. R., Clites, A. H., and Schwab, D. J. 1983. A two-dimensional lake circulation modeling system: programs to compute particle trajectories and the motion of dissolved substances. NOAA Tech. Memo. ERL-GLERL-46, 51pp.
- Bricker, K. S., Bricker, F. J., and Gannon, J. E. 1976. Distribution and abundance of zooplankton in the U.S. waters of Lake St. Clair, 1973. J. Great Lakes Res. 2:256-271.
- Ibrahim, K. A. and McCorquodale, J. A. 1985. Finite element circulation model for Lake St. Clair. J. Great Lakes Res. 11:208-222.
- Leach, J. H. 1972. Distribution of chlorophyll a and related variables in Ontario waters of Lake St. Clair, pp. 80-86. In Proc. 15th Conf. Great Lakes Res. Internat. Assoc. Great Lakes Res.

- Leach, J. H. 1980. Limnological sampling intensity in Lake St. Clair in relation to distribution of water masses. J. Great Lakes Res. 6:141-145.
- Simons, T. J. and Schertzer, W. M. 1986. Hydrodynamic models of Lake St. Clair. NWRI Contribution #86-xxx, National Water Res. Inst., Burlington, Ontario.
- Schwab, D. J. 1983. Numerical simulation of low-frequency current fluctuations in Lake Michigan. J. Phys. Oceanogr. 13:2213-2224.
- Schwab, D. J. and Bennett, J. R. 1987. Lagrangian comparison of objectively analyzed and dynamically modeled circulation patterns in Lake Erie. J. Great Lakes Res. (in press)
- Schwab, D. J., Bennett, J. R., and Jessup, A. T. 1981. A two-dimensional lake circulation modeling system. NOAA Tech. Memo. ERL-GLERL-38, 79pp.
- Schwab, D. J., Bennett, J. R., and Lynn, E. W. 1984. "Pathfinder"--a trajectory prediction system for the Great Lakes. NOAA Tech. Memo. ERL-GLERL-53, 37pp.

LIST OF FIGURES

- Figure 1. The 1.2 km numerical grid for Lake St. Clair. Arrows show the inflows and outflow used in the numerical model.
- Figure 2. Modeled hydraulic flow in Lake St. Clair. Streamlines indicate 10% increments of stream function from -2850 to 2850 ms^{-1} .
- Figure 3. Wind history for residence time calculations.
- Figure 4. Calculated residence time for water from eight tributaries for simulated storm winds of 10 and 20 ms^{-1} from eight compass points. Dashed lines indicate no-wind residence time.
- Figure 5. Probability distributions of water masses from eight tributaries in Lake St. Clair based on model simulations of particle trajectories for the period 23 May - 1 Dec, 1985.
- Figure 6. Verification of circulation model based on drifter and current meter measurements gathered in 1985. Directions compare favorably except near the mouth of the Bassett Channel. Model current speeds seem to be slightly underestimated based on the data.

Numerical Grid for Lake St. Clair



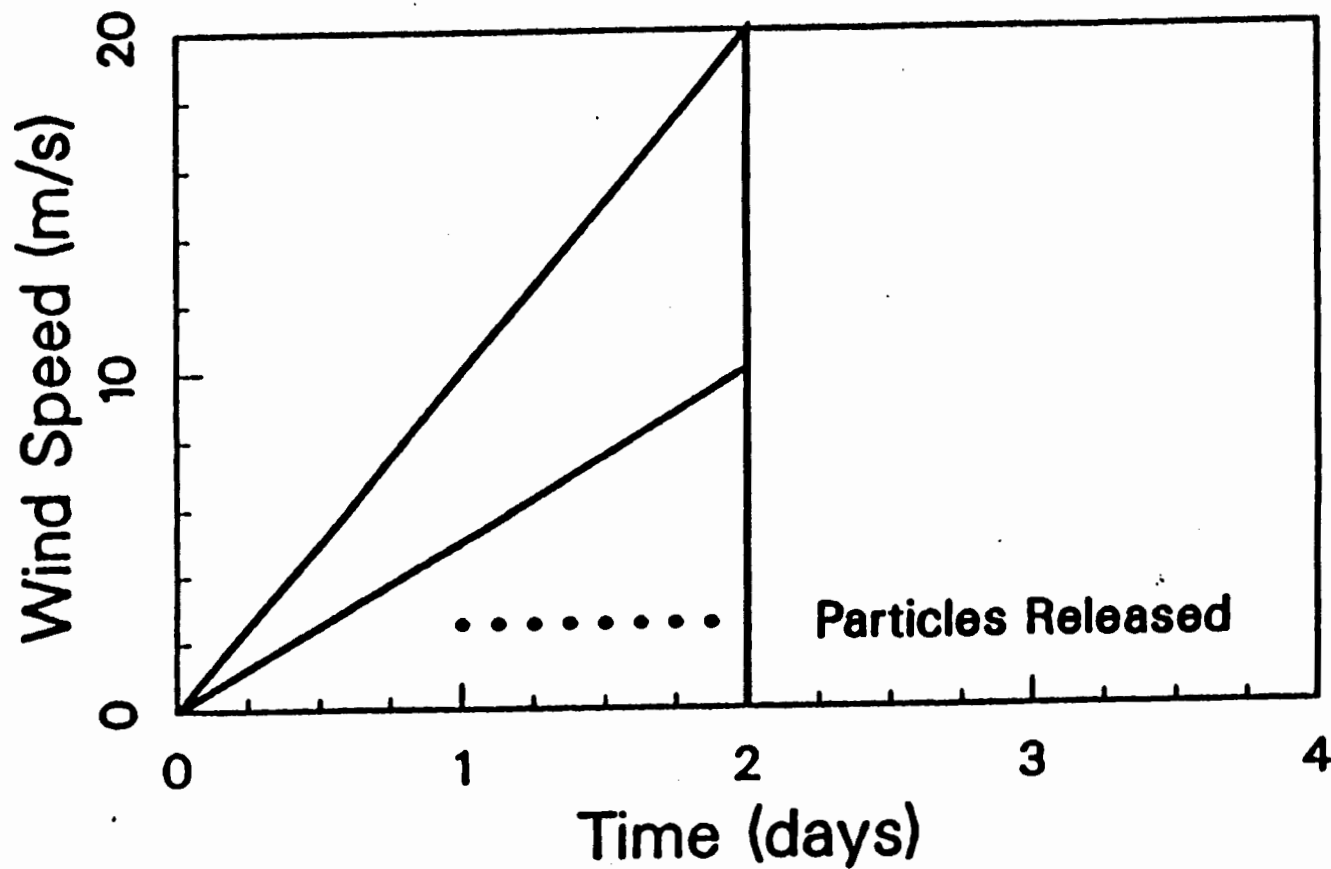
(1)

No Wind



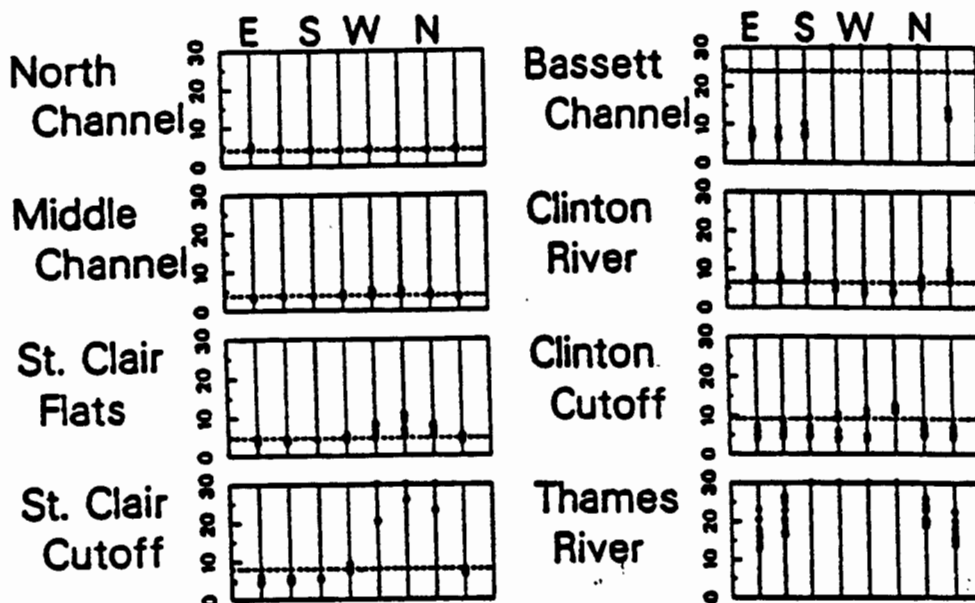
(2)

Wind History for Residence Time Simulations



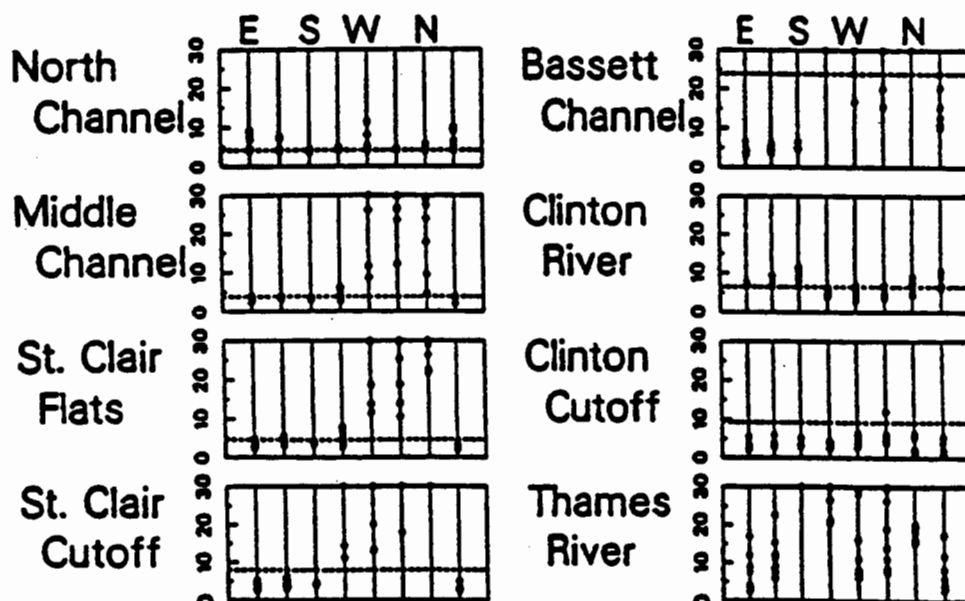
Residence Time (days) in Lake St. Clair for a 10 ms⁻¹ storm

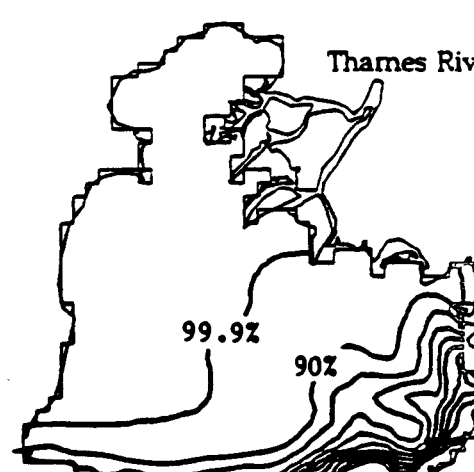
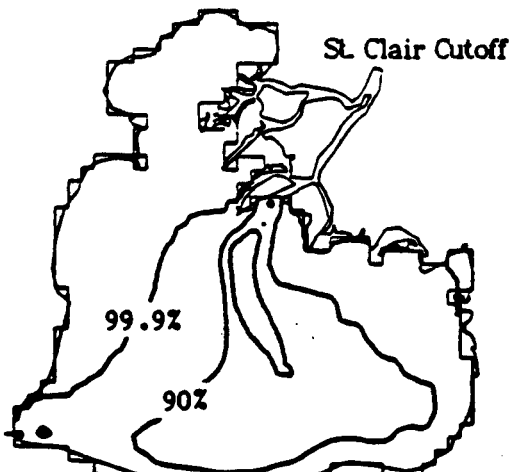
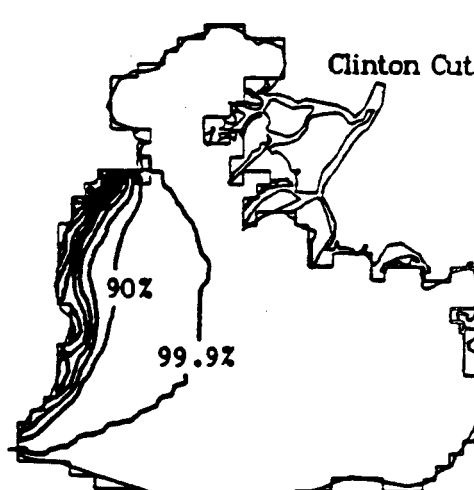
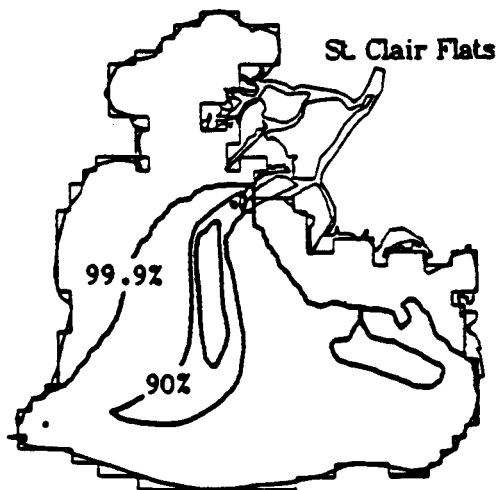
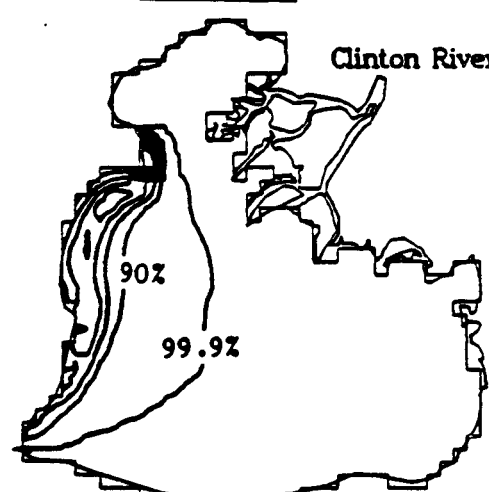
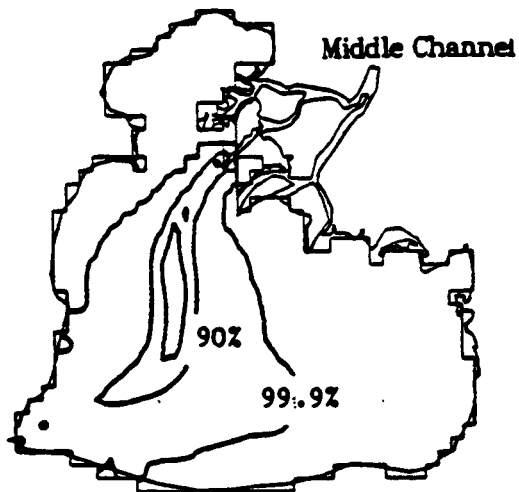
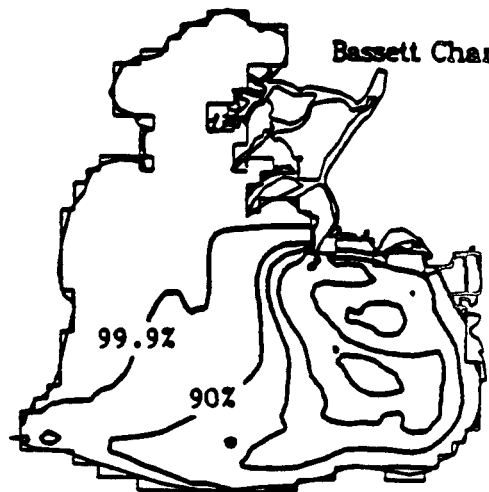
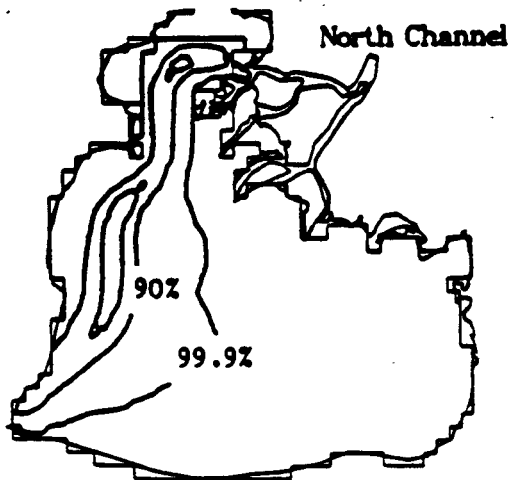
(dashed line indicates no-wind residence time)



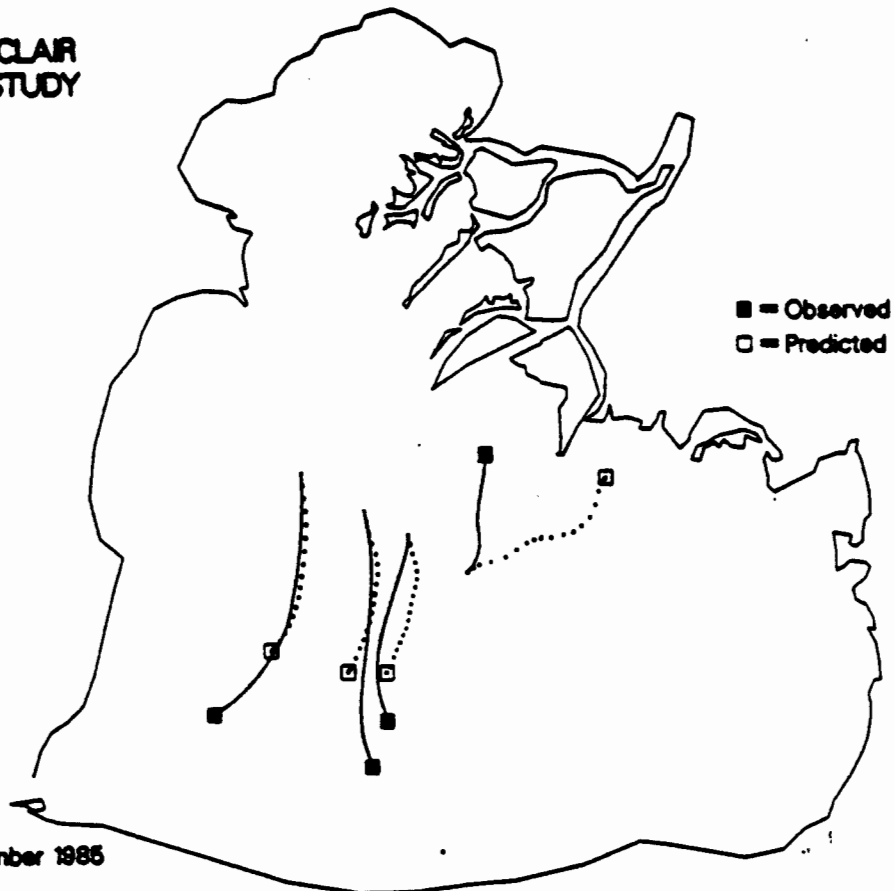
Residence Time (days) in Lake St. Clair for a 20 ms⁻¹ storm

(dashed line indicates no-wind residence time)

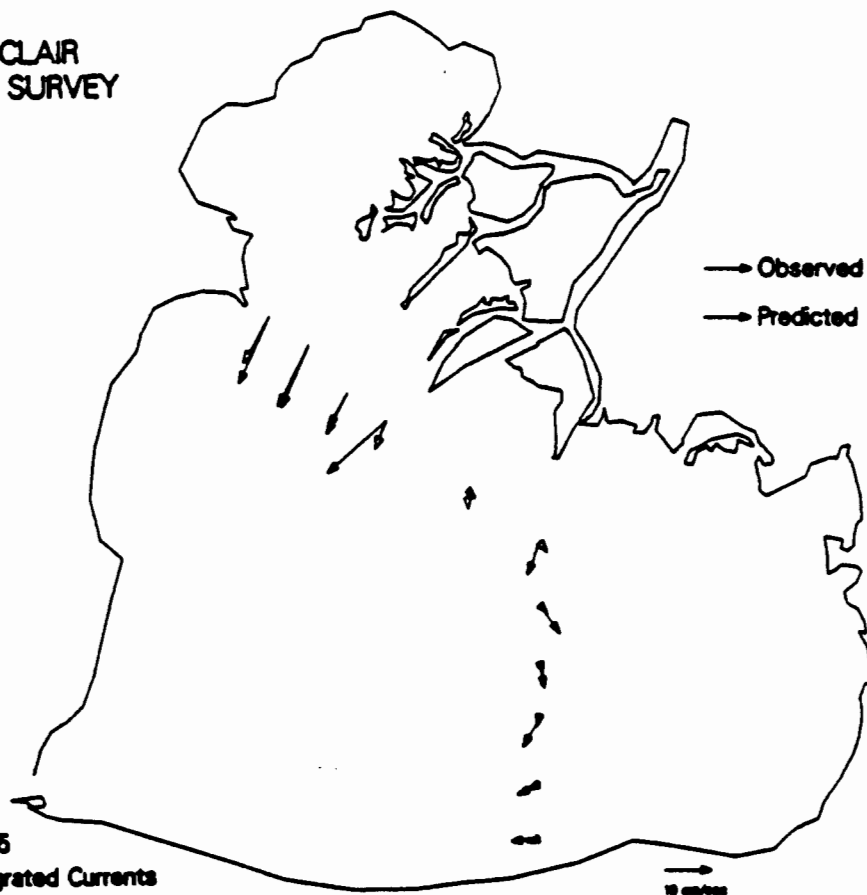




LAKE ST. CLAIR DRIFTER STUDY



LAKE ST. CLAIR CURRENT SURVEY



TOTAL PHOSPHORUS BUDGET FOR LAKE ST. CLAIR: 1975 - 1980

Gregory A. Lang, Julie A. Morton, and Thomas D. Fontaine, III

ABSTRACT

As part of the U.S. - Canadian Upper Great Lakes Connecting Channels Study a total phosphorus budget was developed for Lake St. Clair. An unbiased ratio estimator technique was used to estimate annual loads and variances from monitored hydrologic areas. During the 1975-80 period, Lake Huron was the major source of phosphorus to Lake St. Clair, accounting for approximately 52% of the total annual load. Hydrologic area loads, which include diffuse and indirect point sources, contributed approximately 43% of the total annual load. The remaining 5% came from the atmosphere, shoreline erosion, and direct point sources. Of the hydrologic area loads, 85% could be attributed to diffuse sources. The Thames area contributed 58% of the total hydrologic area load, followed by the Sydenham (17%), the Clinton (9%), the Ruscom (7%), the Black (6%), the St. Clair (3%), and the Rouge (0.4%). Over the entire six year period examined, the lake's total input and output of phosphorus were nearly equal. It was concluded that there was no significant net source or sink of phosphorus in Lake St. Clair during the 1975-80 period.

INTRODUCTION

Phosphorus budget calculations for the Great Lakes have generally overlooked the dynamics of phosphorus transport into and through Lake St. Clair. The sum of Lake St. Clair's point and non-point inputs have simply been included as part of the total load to the Western Basin of Lake Erie; the assumption has been that the entire input of phosphorus to Lake St. Clair is transported, unaltered, through the lake and into the Detroit River. Recent attention to the connecting channels of the upper Great Lakes, however, has served as the impetus for calculating a phosphorus mass balance for Lake St. Clair. The intent of this study was two fold: 1) to estimate the total phosphorus budget for 1975-80, and 2) to determine whether or not the lake is a net source or sink for phosphorus.

Lake St. Clair is unique against the pelagic backdrop of the Great Lakes because it is shallow (average depth = 3.3 m) and has a very short average hydraulic retention time (9 days). Lake St. Clair has a surface area of about 1100 km² and a drainage area of about 15500 km². We calculated the annual phosphorus loads entering this shallow, quick flushing lake from a variety of sources and compared them to the amount of phosphorus leaving the lake through the Detroit River. From these comparisons along with estimates of data and load uncertainty, we were able to draw certain conclusions concerning the likelihood of net sources or sinks of phosphorus in Lake St. Clair.

METHODS

The total phosphorus budget for Lake St. Clair includes external loads, internal sources/sinks, outflow losses, and change in mass storage. At steady state, the sum of the external loads and internal sources/sinks should balance the outflow loss. External phosphorus loads to Lake St. Clair come from Lake Huron, shoreline and streambank erosion, atmospheric sources, direct point sources, and hydrologic area loads. Internal sources and sinks include particle settling and resuspension, groundwater input, bioturbation, and aquatic macrophyte uptake and release. The outflow loss is through the Detroit River.

External Loading Estimates

Lake Huron loads were taken directly from Yaksich et. al. (1982). They estimated the average daily loading for the head of the St. Clair River by multiplying the flow weighted mean yearly phosphorus concentration by the reported average daily flow per month. This daily load was adjusted by the number of days in the month to yield a monthly load. Loading from shoreline erosion was estimated by multiplying the length of Lake St. Clair shoreline by the annual loading rate of phosphorus per kilometer of shoreline for the Lake St. Clair basin (Monteith and Sonzogni 1976). Loading from streambank erosion (along the St. Clair River) was assumed to be negligible because the total loading to the Great Lakes from streambank erosion is < 4% of that contributed by shoreline erosion on the U.S. side of the Great Lakes (Knap and Mildner 1978).

Direct atmospheric loading was estimated to be the average (14.0 MT/yr) of values obtained during the field seasons of 1975 (Delumyea and Petel 1977, measurements made at stations around Southern Lake Huron) and 1981 (Klappenbach 1984, measurements made at Mt. Clemens, Michigan). Direct and indirect point source load estimates were compiled from the International Joint Commission (1982), the Great Lakes Basin Commission (unpub. data), and the Ontario Ministry of the Environment (1985).

Hydrologic Area Loads

Seven hydrologic areas were defined using the convention of Hall et al (1976): the Black, St. Clair complex, Clinton, and Rouge complex (does not include the Rouge River) areas in Michigan, and the Ruscom, Thames, and Sydenham areas in Ontario (Fig. 1). Hydrologic area loads include diffuse loading from land areas that drain into a tributary or directly into Lake St. Clair, and indirect point source inputs. Indirect point source loads are those which discharge upstream of a river monitoring station. Their entire load was assumed to be transported to Lake St. Clair. Direct point sources were defined as those which discharge downstream of a river monitoring station or directly into the St. Clair River or Lake St. Clair. Input from these sources were not included as part of the hydrologic area loads. Several small (< 1 MGD) point source discharges may have been omitted from our hydrologic area analysis since scant information existed for them during 1975-80. However, analysis of recent municipal point source data from STORET (U.S. EPA) and industrial point source data from the Ontario Ministry of the Environment (1985) shows that these sources presently represent about 1% of all of the

point source flows. Therefore, their omission should have little or no effect on calculation of loads from hydrologic areas.

Each hydrologic area load equaled the sum of its monitored and unmonitored area

Monitored areas. Hydrologic area loads from monitored areas were calculated using the unbiased estimate of the daily load at the mouth, adjusted to minimize the variance associated with the flow component, as follows:

$$U_y = U_x \cdot M_y/M_x \cdot \frac{(1 + S_{xy}/(nM_yM_x))}{(1 + S_x^2/(nM_x^2))} \quad (1)$$

where U_y is the unbiased estimate of the daily load at the mouth, U_x is the mean daily flow for the year, M_y is the mean daily loading for the days for which concentration data exists, M_x is the mean daily flow for the days for which concentration data exists, n is the number of days for which concentration data exists, and

$$S_{xy} = \frac{\sum_{i=1}^n X_i Y_i - nM_y M_x}{n-1} \quad (2)$$

$$S_x^2 = \frac{\sum_{i=1}^n X_i^2 - nM_x^2}{n-1}, \quad (3)$$

where X_i is the individual measured flow for each day for which concentration data exists and Y_i is the loading for each day for which concentration data exists (calculated as the product of the individual measured flow and the total phosphorus concentration). Since this load includes any indirect point sources, the diffuse component of the hydrologic area load from a monitored area was estimated by subtracting the indirect point source inputs from the total calculated load.

The estimated mean square error of the estimated load (the square root of which is the estimated standard error of the mean) was also calculated using the ratio estimator method,

$$\begin{aligned} \text{MSE} = M_y^2 \cdot [& 1/n \cdot (S_x^2/M_x^2 + S_y^2/M_y^2 - S_{xy}/(M_x M_y)) \\ & + 1/n^2 \cdot (2 \cdot (S_x^2/M_x^2)^2 - 4 \cdot S_x^2/M_x^2 \cdot S_{xy}/(M_x M_y) \\ & + (S_{xy}/M_x M_y)^2 + S_x^2/M_x^2 \cdot S_y^2/M_y^2)] \end{aligned} \quad (4)$$

where E is the estimated mean square error of the load estimator and S_y^2 is calculated analogously to S_x^2 . In an attempt to quantify some of the uncertainty of these loads and to statistically compare the total annual external load with the outflow loss, the root mean square error (RMSE) is used in a later section to estimate 90% confidence intervals around the individual tributary loads, the total external loads, and the outflow losses.

Three hydrologic areas (Clinton, Thames, Sydenham) were 100% monitored during the entire study period. Percent monitored represents the percent of the hydrologic area that is monitored. The Black area was not monitored for years 1975-77 and 100% monitored for years 1978-80. The St. Clair and Ruscom areas were 36% (Belle R.) and 18% (Ruscom R.) monitored, respectively, during the study period. The Rouge area was not monitored. On an areal basis, 83% of the Lake St. Clair basin was monitored during the study period.

Flow data were obtained from the U.S. Geological Survey (1976-82) and the Water Survey of Canada (1976-81). Flow measurements recorded at gaging stations located upstream of the river mouth were corrected to the river mouth by multiplying the gaged flow by the ratio of the entire drainage area to the gaged drainage area as described in Sonzogni et al. (1978). Phosphorus concentrations were obtained from the U.S. Environmental Protection Agency's STORET system, the U.S. Geological Survey (1976-82), and the Ontario Ministry of the Environment (1975-80). In most cases, water quality monitoring stations were located at or near the river mouth. It was assumed that these phosphorus concentrations equaled the concentrations at the mouth.

Unmonitored areas. Some hydrologic areas and individual tributaries were not sufficiently monitored (fewer than 6 samples per year) over some or all of the 1975-80 period. In addition, some land areas drain directly into Lake St. Clair or the St. Clair River, and therefore cannot be monitored. Diffuse loads for these watersheds were estimated by calculating a diffuse unit area loading (UAL) (the diffuse load per unit area per unit time) for a monitored area with basin characteristics similar to the unmonitored area. The

selection of a representative monitored area was based on soil texture, surface geology, runoff characteristics, land use, and proximity to the unmonitored area. The diffuse load for the unmonitored area was estimated as the product of the diffuse unit area load from the monitored area and the unmonitored area as described in Sonzogni et al. (1978). Indirect point source discharges in unmonitored areas were added to the estimated diffuse load to yield total loads for the unmonitored area.

Total External Load

The total external phosphorus load to Lake St. Clair equaled the sum of loads from the total hydrologic area, atmospheric sources, shoreline erosion, direct point sources, and the Lake Huron. The variance associated with the total external load was not known because some hydrologic areas were partially or totally unmonitored and variance estimates were not available for the atmospheric, erosion, direct point, or Lake Huron loads. However, an estimate of the variance associated with the total external load was made using the following procedure. Annual load probability distributions for each monitored tributary and the outflow from Lake Huron were constructed with means set equal to their estimated annual loads. The variances of the tributary load distributions were calculated from their estimated RMSE (eq. 5). The variance of the Lake Huron load distributions was assumed to be constant and equal to the variance of the Huron load averaged over the six-year period. For each of the six years, values from each distribution were randomly selected and summed to give a single estimate the total annual external load (Figure 2). This

procedure was repeated 12 times to yield a combined probability distribution for each year's total external load. A sample size of 12 corresponds to the average number of times per year that each tributary was sampled. The standard error of the total annual external load was calculated from each year's combined probability distribution for the purpose of statistical comparison with the outflow data.

Outflow Loss

Annual phosphorus loss through the Detroit River and the mean square error associated with this loss were estimated using the unbiased ratio estimator technique. Phosphorus concentrations were measured along a transect at Windmill Point near the head of the Detroit River by the Michigan Department of Natural Resources (DNR) and recorded in EPA's STORET data base. There are ten stations, each representing 10% of the flow of the river. The data from these stations were limited to non-winter months (usually April through October). Phosphorus data for the winter months were measured at the Detroit municipal water treatment facility at Water Works Park and recorded in the U.S. Geological Survey (1976-82). Water quantity data were taken from the results of a hydrodynamic model of the Detroit River (F. H. Quinn, Great Lakes Environmental Research Laboratory, personal communication).

Internal Sources and Sinks

Scant quantitative information exists concerning the annual internal input or loss of phosphorus in Lake St. Clair. It is estimated that some

sources and sinks vary seasonally (e.g., particle settling and resuspension and aquatic macrophyte uptake and release), while others remain more or less constant throughout the year (e.g., groundwater input and bioturbation). For the purpose of annual budget calculations, the amount of phosphorus added to or lost from the lake via internal sources and sinks was estimated as the difference between annual external loads and annual outflow losses.

RESULTS

The annual estimated river mouth phosphorus loads from monitored hydrologic areas to Lake St. Clair as well as the annual estimated Detroit River outflow losses are presented in Table 1. Table 1 also includes the estimated RMSE of the estimated load and the 90% confidence intervals around the estimated load. The RMSE and the Student's t-statistic were used to calculate the 90% confidence intervals (Remington and Schork 1985).

The total annual phosphorus budget for Lake St. Clair is presented in Table 2. On the average, Lake Huron contributed a major portion (about 52%) of the external total phosphorus load. The contribution of hydrologic areas was also significant and equaled approximately 43% of the external phosphorus load to Lake St. Clair. The remaining 5% of the total annual load came from the atmosphere (0.5%), shoreline erosion (2.6%), and direct point sources (1.9%). Average phosphorus dynamics of Lake St. Clair during the 1975-80 period are summarized in Figure 3. In the diagram, the relative proportion of inflows and outflows are approximated by the thickness of the arrow shafts.

Hydrologic area loads originating from Canadian sources averaged 82% of the total hydrologic area load to Lake St. Clair. The Thames and the Sydenham areas contributed 92% of the total Canadian hydrologic area load. The Black and Clinton areas were responsible for 83% of the total U.S. hydrologic area load. The largest individual hydrologic area loads originated from the Thames area. In all years except 1975, loading from the Thames exceeded 50% of the total hydrologic area load (the six-year average contribution was 58%). The Thames area load was followed by the Sydenham (17%), the Clinton (9%), the Ruscom (7%), the Black (6%), the St. Clair (3%), and the Rouge (0.4%).

Over the six year period investigated, about 85% of the total hydrologic area load was calculated to originate from diffuse sources. The remaining 15% came from indirect point sources. The diffuse portion of the Thames and Sydenham area loads accounted for most of the total diffuse load (62% and 20%, respectively). The Clinton and Thames areas contributed a majority of the total indirect point source load (43% and 35%, respectively).

Internal Sources and Sinks

Assuming estimated loads presented in Table 2 are an accurate representation of the actual loads and assuming steady state conditions, then the difference between external loads and outflow losses is a measure of the internal sources/sinks of phosphorus in Lake St. Clair. The total annual incoming load falls within the 90% confidence interval around the Detroit River outflow loss for all years except 1976 (Figure 4). The six-year mean external load (3133 MT/yr) and loss (3148 MT/yr) were not found to be

statistically different at the 10% level of significance (t-test, Remington and Schork 1985). The root mean square difference between annual external loads and outflow losses was only 7% of the mean external load (5% excluding 1976 values). Therefore, given the above assumptions and results, there appeared to be no net internal source or sink of total phosphorus in Lake St. Clair during 1975-80.

DISCUSSION

The second objective of this study was to determine whether or not Lake St. Clair is a net source or sink for phosphorus. The total incoming load fell within the 90% confidence interval around the Detroit River loss for all years except 1976; and, averaged over 6 years, external loads were not significantly different from outflow losses; implying no net internal source or sink of phosphorus in the lake during 1975-80. Because the net internal sources/sinks were calculated as the difference between the incoming loads and outflow losses, their validity is limited by the accuracy and precision of the load/loss estimates. If loads and losses are sufficiently accurate and precise, then the conclusion that net internal sources/sinks were negligible during the study period seems reasonable.

It is difficult to determine how accurate the estimated loads and losses are since actual loads and losses can never be known exactly. Sonzogni et al. (1978) note that the RMSE terms in Table 1 are useful for statistical comparisons, but they do not necessarily reflect how close the estimated load

is to the true load. The RMSE is an estimate of the error determined from a limited number of daily samples, based on the premise that the true annual load can be determined by sampling flow and concentration at the river mouth each day of the year. In addition, the method assumes that instrument and measurement errors can be neglected and that instantaneous flow/concentration measurements are true representations of the tributary conditions on that day.

As briefly stated previously, Dolan et. al. (1981) evaluated 10 tributary load estimator methods and concluded that the ratio estimator method used in the present study was the most suitable for application in the Great Lakes basins. They recommended that this method be used to estimate tributary loads for total phosphorus when concentration data are limited and the daily flow record is available. The accuracy of the streamflow data used in this study was rated "fair" to "good" by the U.S. Geological Survey. "Good" means that about 95% of the reported daily discharges are within 10% of the actual values and "fair" within 15%. Chemical data represent (as much as possible) water quality conditions at the time of sampling, consistent with available sampling techniques and methods of analysis. The phosphorus loads from Lake Huron estimated by Yaksich et. al. (1982), were consistent (trends and magnitude) with other external loads to Lake Erie for 7 water quality constituents, 1970-80 and are thus, for lack of better criteria, considered representative of the true Lake Huron loads. Therefore, given that 90% of the hydrologic area load was from monitored tributaries and that 95% of the total external load was from hydrologic areas and Lake Huron, we conclude that the calculated total external phosphorus loads and losses are at least a fair representation

and at best an accurate estimate of the actual loads and losses to and from Lake St. Clair.

Finally, does this conclusion (i.e., negligible net internal sources/sinks during the study period) seem reasonable given the nature of the internal sources and sinks? Groundwater input of phosphorus is assumed to be insignificant compared to that entering the lake from other sources. The biological release of phosphorus from sediments and mussels to the overlying water has also been shown to be negligible (Nalepa et. al. 1987). Assuming an average apparent settling rate of 16 m/yr (Chapra 1977) and a range of lake-averaged phosphorus concentrations measured during eight cruises in 1975 (US EPA's STORET data base) yields a range of 253-321 MT of phosphorus potentially lost to the sediments annually. These values represent only about 10% of the total external load for any one year and would be lost in the variability between input and output. Given the shallowness and high wave energy of Lake St. Clair, sediment resuspension would reduce the impact of particle settling. Robbins (1987) indicates that the net deposition of particulate matter to the lake's sediments is small; the sediment thickness above post-glacial clay ranges from 0 to 30 cm, corresponding to a net sedimentation rate of only 0.1-0.2 cm/yr. At this rate, a range of 0.01-0.04 MT of phosphorus/year would be lost to the sediments, representing less than 1% of the total incoming load for any one year. Therefore, it does seem reasonable that over a six year period there would be no significant net source or sink of phosphorus in Lake St. Clair.

SUMMARY

The objectives of this study were two fold: 1) to estimate and present the total phosphorus budget for 1975-80, and 2) to determine whether or not the lake is a net source or sink for phosphorus. Lake Huron contributed over half (52%) of the lake's load while the seven hydrologic areas contributed 43% of the remainder. About 92% of the total Canadian hydrologic area load is attributable to the Thames and Sydenham areas of Ontario. The Clinton and Black areas of Michigan were responsible for 83% of the total U.S. hydrologic area load. Were reduction of phosphorus loads to Lake St. Clair deemed desirable, control efforts might be best focused in these four hydrologic areas. Because 85% of the total hydrologic area load is from diffuse sources, a non-point source reduction plan might be most appropriate. Reduction of municipal point sources along the Thames River and the Clinton River may also be important as these sources contributed a majority of the remaining 15% of the total hydrologic area phosphorus load.

Over the six year study period, 1975-80, the mean external load and outflow loss of phosphorus were not found to be statistically different at the 10% level of significance. Assuming accurate estimates of the loads/losses and steady state conditions, we conclude that there was no apparent net source or sink of phosphorus in Lake St. Clair during the study period.

ACKNOWLEDGEMENTS

This is GLERL contribution No. 511. This work was partially funded by interagency agreement DW 13931213-01-0 with the Great Lakes National Program Office, U.S. Environmental Protection Agency, Chicago. We thank Barry M. Lesht, Douglas Salisbury, and two anonymous reviewers for reviewing an earlier version of the manuscript.

LITERATURE CITED

Beale, E.M.L. 1962. Some uses of computers in operational research.

Industrielle Organisation. 31:51-52.

Chapra, S.C. 1977. Total phosphorus model for the Great Lakes. J.

Environmental Engineering Div. ASCE. 103(2):147-161.

Delumyea, R.G, and Petel, R.L. 1977. Atmospheric Inputs of Phosphorus to Southern Lake Huron. April-October 1975. U.S. Environmental Protection Agency, Report number 600/3-77-038, Environmental Research Laboratory, Duluth, Minnesota, 53 pp.

Dolan, D.M., Yui, A.K., and Geist, R.D. 1981. Evaluation of river load estimation methods for total phosphorus. J. Great Lakes Res. 7:207-214.

Hall, J.R., Jarecki, E.A., Monteith, T.J., Skimin, W.E. and Sonzogni, W.C., 1976. Existing River Mouth Loading Data in the U.S. Great Lakes Basin. Pollution From Land Use Activities Reference Group Report, International Joint Commission, Great Lakes Regional Office, Windsor, Ontario, 713 pp.

International Joint Commission. 1982. 1981 Municipal and Industrial Phosphorus Loadings to the Great Lakes. Report of the Great Lakes Water Quality Board to the International Joint Commission, Windsor, Ontario.

Klappenbach, E. 1984. 1981 Atmospheric Loading for Lake Huron. Report to the U.S. Environmental Protection Agency Great Lakes National Program Office, Chicago, Illinois.

Knap, K.M., and Mildner, W.F. 1978. Streambank Erosion in the Great Lakes Basin. Report of the International Reference Group on Pollution from Land Use Activities to the International Joint Commission, Windsor, Ontario.

Monteith, T.J., and Sonzogni, W.C. 1976. United States Great Lakes Shoreline Erosion Loadings. Report of the International Reference Group on Great Lakes Pollution from Land Use Activities to the International Joint Commission, Windsor, Ontario.

Nalepa, T.F., Gardner, W.S., and Malczyk, J.M. 1987. Phosphorus release from sediments and mussels in Lake St. Clair, with notes on mussel abundance and biomass. Upper Great Lakes Connecting Channel Final Report. Great Lakes Environmental Research Laboratory, Ann Arbor, Michigan.

Ontario Ministry of the Environment. 1975. Water Quality Data: Ontario Lakes and Streams. Volume 10. Report of the Water Resources Branch, Toronto, Ontario.

_____. 1976. Water Quality Data: Ontario Lakes and Streams. Volume 11. Report of the Water Resources Branch, Toronto, Ontario.

- _____. 1977. Water Quality Data: Ontario Lakes and Streams. Volume 12. Report of the Water Resources Branch, Toronto, Ontario.
- _____. 1978. Water Quality Data: Ontario Lakes and Streams. Volume 14. Report of the Water Resources Branch, Toronto, Ontario.
- _____. 1979. Water Quality Data: Ontario Lakes and Streams. Volume 15. Report of the Water Resources Branch, Toronto, Ontario.
- _____. 1980. Water Quality Data: Ontario Lakes and Streams. Volume 16. Report of the Water Resources Branch, Toronto, Ontario.
- _____. 1985. Upper Great Lakes Connecting Channels Study: Canadian Point Source Discharge and Combined Sewer Overflow Activities. Report of the Environmental Protection Service, Ontario Region, Environment Canada, Ontario Ministry of the Environment, Windsor, Ontario.
- Remington, R.D. and Schork, M.A. 1985. Statistics with Applications to the Biological and Health Sciences. Prentice-Hall, Inc. Publ., Englewood Cliffs, New Jersey. 415 pp.
- Robbins, J.A. 1987. Accumulation of fallout cesium-137 and chlorinated organic contaminants in recent sediments of Lake St. Clair. Can. J. Fish. and Aquatic Sci. In Press.

Sonzogni, W.C., Monteith, T.J., Bach, W.N., and Hughes, V.G. 1978. United States Great Lakes Tributary Loadings. Great Lakes Pollution from Land Use Activities Reference Group, International Joint Commission, Technical Report, Great Lakes Regional Office, Windsor, Ontario.

U.S. Geological Survey. 1976. Water Resources Data for Michigan. Water Year 1975. Report of the U.S. Geological Survey, Water Resources Division, Lansing, Michigan.

_____. 1977. Water Resources Data for Michigan. Water Year 1976. Report of the U.S. Geological Survey, Water Resources Division, Lansing, Michigan.

_____. 1978. Water Resources Data for Michigan. Water Year 1977. Report of the U.S. Geological Survey, Water Resources Division, Lansing, Michigan.

_____. 1979. Water Resources Data for Michigan. Water Year 1978. Report of the U.S. Geological Survey, Water Resources Division, Lansing, Michigan.

_____. 1980. Water Resources Data for Michigan. Water Year 1979. Report of the U.S. Geological Survey, Water Resources Division, Lansing, Michigan.

_____. 1981. Water Resources Data for Michigan. Water Year 1980. Report of the U.S. Geological Survey, Water Resources Division, Lansing, Michigan.

_____. 1982. Water Resources Data for Michigan. Water Year 1981. Report of the U.S. Geological Survey, Water Resources Division, Lansing, Michigan.

Water Survey of Canada. 1976. Surface Water Data. Ontario. 1975. Report of the Inland Waters Directorate, Water Resources Branch, Water Survey of Canada, Ottawa, Quebec.

_____. 1977. Surface Water Data. Ontario. 1976. Report of the Inland Waters Directorate, Water Resources Branch, Water survey of Canada, Ottawa, Quebec.

_____. 1978. Surface Water Data. Ontario. 1977. Report of the Inland Waters Directorate, Water Resources Branch, Water survey of Canada, Ottawa, Quebec.

_____. 1979. Surface Water Data. Ontario. 1978. Report of the Inland Waters Directorate, Water Resources Branch, Water survey of Canada, Ottawa, Quebec.

_____. 1980. Surface Water Data. Ontario. 1979. Report of the Inland Waters Directorate, Water Resources Branch, Water survey of Canada, Ottawa, Quebec.

_____. 1981. Surface Water Data. Ontario. 1980. Report of the Inland Waters Directorate, Water Resources Branch, Water survey of Canada, Ottawa, Quebec.

Yaksich, S.M., Melfi, D.A., Baker, D.B. and Kramer, J.W. 1982. Lake Erie Nutrient Loads. 1970-1980. Lake Erie wastewater management study. U.S. Army Corps of Engineers District, Buffalo, New York.

Table 1. 1975-80 River Mouth Loadings. The load is presented in metric tons per year, followed by the root mean square error in metric tons per year, followed by the 90% confidence interval in Metric tons per year, followed by the number of phosphorus samples.

Monitored Tributary Name	Year					
	1975	1976	1977	1978	1979	1980
Black	NA ¹	NA ¹	NA ¹	47.4 2.9 [41.9, 52.9] 8	90.8 38.9 [21.0, 160.6] 12	88.4 29.0 [34.5, 142.4] 9
Belle ²	31.1 4.9 [22.2, 40.0] 11	28.7 8.7 [13.1, 44.4] 12	7.1 0.9 [5.5, 8.6] 12	10.4 0.9 [8.8, 12.0] 12	11.9 2.1 [8.0, 15.7] 12	17.4 4.7 [8.7, 26.2] 9
Clinton	198.4 22.3 [158.3, 238.4] 12	143.8 24.0 [100.8, 186.9] 12	118.3 16.9 [88.0, 148.7] 12	112.7 23.3 [70.9, 154.5] 12	77.8 8.9 [62.0, 93.7] 12	114.0 28.9 [62.2, 165.8] 12
Ruscom	3.8 0.1 [3.7, 3.9] 7	6.0 0.5 [5.1, 6.9] 11	16.3 1.3 [14.0, 18.6] 11	22.3 6.0 [11.5, 33.1] 12	9.0 1.8 [5.7, 12.3] 12	36.3 20.7 [0.0, 75.4] 8
Thames	418.3 60.4 [309.9, 526.8] 12	690.8 160.6 [396.5, 985.1] 10	1391.8 427.4 [625.1, 2158.4] 12	643.3 58.1 [537.9, 748.7] 11	917.7 193.3 [587.0, 1248.4] 25	663.8 102.1 [493.8, 833.8] 75
Sydenham	196.0 28.6 [142.9, 249.1] 9	195.5 46.9 [110.5, 280.5] 12	494.3 137.1 [248.4, 740.2] 12	94.4 18.6 [61.1, 127.8] 12	241.1 27.1 [195.0, 287.2] 27	170.3 19.2 [137.7, 202.9] 31
Detroit	2769.3 289.7 [2244.2, 3294.4] 11	3935.9 301.5 [3383.3, 4488.6] 10	3304.7 393.4 [2603.6, 4005.9] 13	3090.2 250.3 [2644.1, 3536.2] 13	2879.7 247.9 [2448.5, 3310.9] 18	2908.7 273.3 [2427.3, 3390.1] 15

¹Phosphorus data not available for years 1975-77,

²Within St. Clair Hydrologic Area.

Table 2. Annual phosphorus budget (MT/yr) for Lake St. Clair (1975-80). Values in parentheses represent percent of total load from diffuse sources. Percent monitored refers to percent of hydrologic area that is monitored.

Source	1975	1976	1977	1978	1979	1980
Hydrological Areas (HA)						
Black	115.5 ^a	84.5 ^a	41.9 ^a	47.4	90.8	88.4
0,100% monitored ^b	(74)	(64)	(28)	(36)	(67)	(63)
St. Clair ^c	75.4	68.7	7.8	17.0	21.2	38.2
36% monitored	(90)	(89)	(3)	(56)	(64)	(80)
Clinton	198.4	143.8	118.3	112.7	77.8	114.0
100% monitored	(48)	(26)	(21)	(37)	(18)	(39)
Rouge ^d	10.8	4.2	2.9	4.7	1.6	5.0
0% monitored	(100)	(100)	(100)	(100)	(100)	(100)
Ruscom ^e	21.8	34.1	92.2	126.4	51.1	205.7
18% monitored	(100)	(100)	(100)	(100)	(100)	(100)
Thames	418.3	690.8	1391.8	643.3	917.7	663.8
100% monitored	(85)	(90)	(94)	(91)	(92)	(90)
Sydenham	196.0	195.5	494.3	94.4	241.1	170.3
100% monitored	(97)	(97)	(99)	(92)	(99)	(99)
Total HA Load	1036.2 (80) ^f	1221.7 (82) ^f	2149.2 (90) ^f	1045.9 (83) ^f	1401.3 (87) ^f	1285.4 (86) ^f
<u>Atmospheric</u>	14.0	14.0	14.0	14.0	14.0	14.0
<u>Erosion</u>	82.5	82.5	82.5	82.5	82.5	82.5
<u>Direct Point</u>	55.8	64.5	58.9	57.7	59.2	54.0
<u>Lake Huron</u>	2022	1373	1187	1613	1703	1827
EXTERNAL LOAD	3211	2756	3492	2813	3260	3263
90% C.I.	[3014, 3408]	[2485, 3027]	[3070, 3914]	[2648, 2978]	[2987, 3533]	[3136, 3390]
OUTFLOW LOSS	2769	3936	3305	3090	2880	2909
90% C.I.	[2244, 3294]	[3383, 4489]	[2604, 4006]	[2644, 3536]	[2449, 3311]	[2427, 3390]
IN - OUT	441	-1180	186	-277	380	354

^aUnit Area Load (UAL) assumed to equal average of UAL of St. Clair HA and UAL of Clinton HA.

b0% for years 1975-77, 100% for years 1978-80.

cUAL assumed to equal UAL of Belle R. within St. Clair HA.

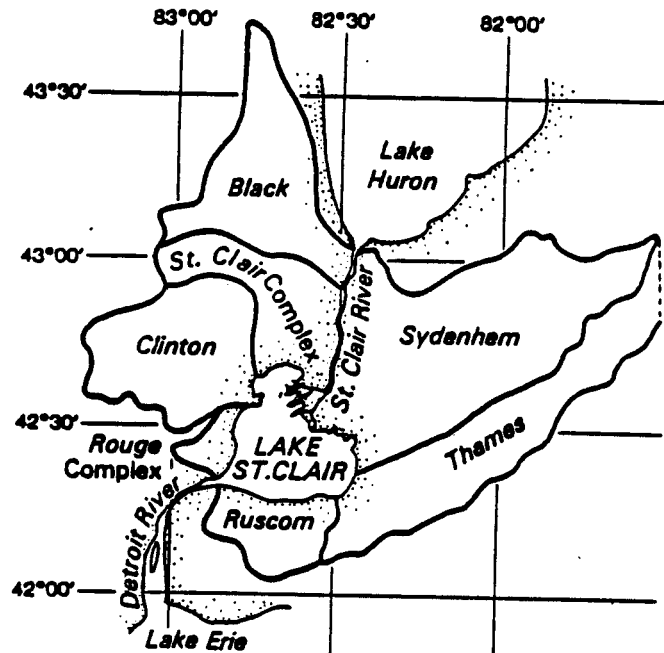
dUAL assumed to equal UAL of Clinton HA.

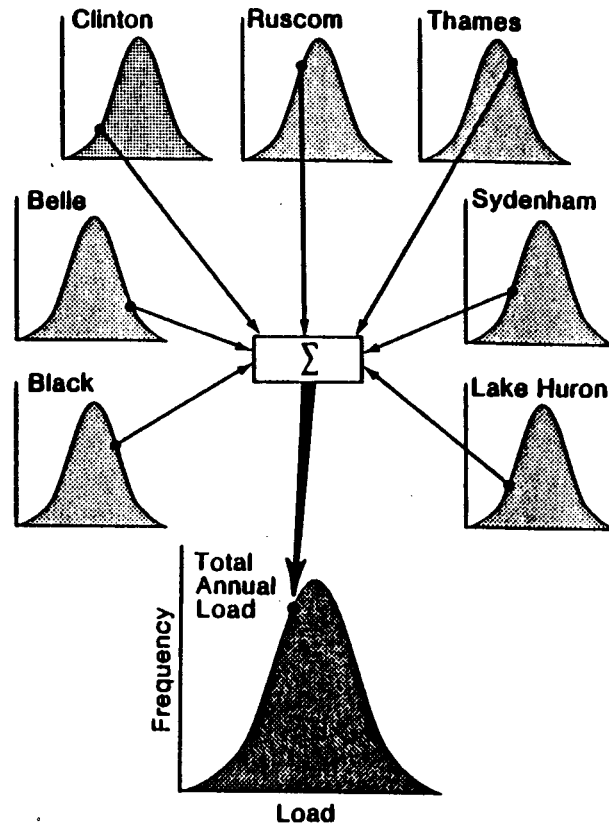
eUAL assumed to equal UAL of Ruscom R. within Ruscom HA.

fPercentages weighted with respect to percent of total annual input that is attributable to a given area.

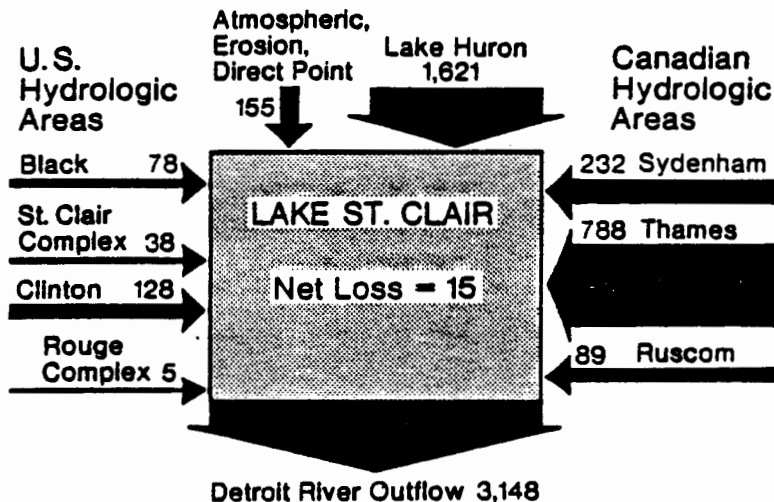
LIST OF FIGURES

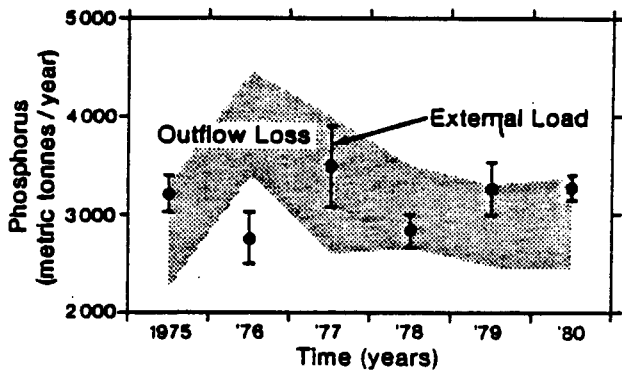
- Figure 1. Lake St. Clair Basin showing hydrologic areas used in calculating load estimates. Note: the Thames hydrologic area extends to approximately 43° 30' latitude, 80° 30' longitude.
- Figure 2. Schematic displaying procedure used to estimate the combined probability distribution for each year's total external load.
- Figure 3. Summary of Lake St. Clair average phosphorus dynamics during the 1975-80 period. Values are in MT/year. The relative proportion of inflows and outflows are approximated by the thickness of the arrow shafts.
- Figure 4. External phosphorus loads to Lake St. Clair (closed circles and vertical bars represent 90% confidence interval around annual load, MT/yr) and Detroit River outflow loss (shaded region represents 90% confidence interval around annual loss, MT/yr).





Lake St. Clair average phosphorus loads and losses during the 1975-'80 period (metric tonnes per year)





PHOSPHORUS RELEASE FROM SEDIMENTS AND MUSSELS IN LAKE ST. CLAIR,
WITH NOTES ON MUSSEL ABUNDANCE AND BIOMASS

T. F. Nalepa, W. S. Gardner, and J. M. Malczyk

INTRODUCTION

Since phosphorus is known to be the critical element in controlling eutrophication, a thorough understanding of phosphorus dynamics is essential for effective control strategies. The sediments play an important role in phosphorus cycling, serving as either a sink or a source of phosphorus to the overlying waters. The processes affecting the net flux of phosphorus from the sediments are complex, depending on such factors as resuspension, sedimentation, sorption, oxygen concentrations, and invertebrate activities. Under oxic conditions, as found in most near-bottom waters of the Great lakes, benthic invertebrates play a major role in phosphorus release from the sediments (Gallepp 1979; Graneli 1979; Holden and Armstrong 1980; Quigley and Robbins 1986). By their constant burrowing and feeding activities, benthic invertebrates increase the rate of exchange between nutrient-rich pore waters and overlying waters. Also, these organisms ingest organic material and subsequently excrete remineralized nutrients in forms readily available for further use by phytoplankton. In nearshore Lake Michigan, excretion by benthic invertebrates was sufficient to account for all the phosphorus released from the sediments (Gardner et al. 1981). Of

the various invertebrate groups, unionid bivalves (mussels) in particular can have a significant impact on nutrient cycling in a given body of water (Lewandowski and Stanczykowska 1975; Walz 1978; Stanczykowska and Planter 1985; Kasprzak 1986; James 1987). These large filter-feeders have the capacity to remove great amounts of organic material from the water. Thus, they enhance nutrient mineralization either directly through excretion, or indirectly by depositing the material on the sediment surface as faeces or pseudofaeces and making it available to deposit-feeding forms.

The purpose of this study was (1) to quantify the rate of phosphorus flux between the sediments and overlying waters in Lake St. Clair and (2) to determine the rate of phosphorus excretion by the mussel population. The significance of both sediment release and mussel excretion was subsequently assessed by comparing these phosphorus sources to other sources of phosphorus into the lake. In addition to measuring excretion, the abundance, biomass, species composition, and production of mussel populations in the lake were also determined. Accurate estimates of mussel biomass were, of course, essential to assessing the importance of phosphorus excretion on a lake-wide basis.

METHODS AND MATERIALS

Intact sediment cores were collected by divers at five sites in Lake St. Clair in May and September, 1985. The sites were chosen to be broadly representative of different areas and sediment types (Fig. 1). The core

tubes (4.2 cm diameter and 10 cm long) were inserted into the sediment about 5 cm, stoppered at both ends, and carefully brought to the surface. The cores were kept upright in a cooler during transport back to the laboratory and then placed in an incubator set at the in situ temperature. Aeration lines were placed through the top stopper and air was slowly bubbled into the overlying waters. This kept the water well-mixed and also kept dissolved oxygen concentrations at near-saturation levels. All core tubes and aeration lines were made of high-density linear polyethylene to minimize phosphorus adsorption. Samples for phosphorus determinations were taken every 3-4 days by drawing out 1 ml of water through a sampling port in the top stopper. Phosphorus concentrations (SRP) were determined with an AutoAnalyzer as described by Gardner and Malczyk (1983). Phosphorus levels in lake-water controls were also measured on each sampling day. The volume of overlying water was kept constant by adding 1 ml of lake water after each sample was drawn. The incubation period lasted between 65 and 70 days.

A total of 6-8 replicates cores were collected at each station on each sampling date. Since Lake St. Clair is shallow and bottom sediments are easily resuspended, the impact of resuspension on sediment phosphorus release was estimated by mixing one-half of the replicates at the beginning of the incubation period to create a sediment slurry with the overlying waters. The sediments were mixed again every 10 days until the end of the incubation period. Phosphorus release rates in these mixed cores were compared to release rates in cores that were left undisturbed.

Mussels for phosphorus excretion determinations were collected on a monthly basis from May to October in both 1985 and 1986. An epibenthic sled was towed behind the vessel until enough individuals were collected. In 1985, mussels were collected from only one site (Station 72) and excretion measured on several different species. In 1986, there were two collection sites (Station 72 and Station 24) and rate measurements were made on only one species, Lampsilis radiata siliquodea. The two sites had contrasting substrate types, with sandy silt the dominant substrate at Station 72 and silt dominant at Station 24. Excretion rates were determined on at least four individuals from each of the two stations except in May when rates were determined on only two individuals from each station. Individual mussels were gently scrubbed and immediately placed in polyethylene containers having 2 liters of low-nutrient culture water (Lehman 1980). The containers were placed in large coolers and the culture water was maintained at the in situ temperature. The incubation period lasted 4 hours with 1-ml samples drawn at 0, 2, and 4 h. Phosphorus concentrations were determined as in the sediment cores. Dry weights of the mussels (soft tissue) were determined after drying at 60 C for at least 48 h.

To determine the density, biomass, and species composition of mussels in the lake, a population survey was conducted in September, 1986. Divers placed a 0.5 m² frame on the bottom and all shells within the frame area were placed in a mesh bag. A total of 10 separate replicate samples were collected at random at each of 28 different stations (Fig. 1). All live mussels were immediately shucked and the soft tissue placed in preweighed aluminum planchets. Dry weights of both the shell and soft tissue were

obtained after drying at 60 C for at least 48 h. Individuals of the two most abundant species, Lampsilis radiata siliquodea and Leptodea fragilaris, were aged by counting the number of annual growth rings on the external shell. The annual production rate of L. r. siliquodea was estimated from the sum of the increase in weight of each of the different age groups (Magnin and Stanczykowski 1971).

RESULTS AND DISCUSSION

Phosphorus Release From the Sediments

Sediment phosphorus release rates at each of the five stations on the two sampling dates is given in Table 1. Rates were calculated from the net increase in phosphorus concentrations in the overlying waters from day 10 to day 65-70 for the May cores, and from day 3 to day 65-70 for the September cores. In some instances, the increase in phosphorus was most rapid at the beginning of the incubation period and then remained relatively constant thereafter. For these cores, rates were recalculated based on the time interval of greatest release and are included in Table 1 to provide an estimate of maximum potential release. The mean release rates in this table include values from all replicates at a given station since there were no significant differences (t-test; $P < .05$) between release rates of mixed and unmixed cores at any of the five stations.

In both May and September, release rates at Stations 71 and 84 were generally lower than release rates at the other three stations (Stations 4, 14, and 24). The former two stations were located in the northwestern portion of the lake near the mouth of the St. Clair River where both nutrient levels and algal productivity tend to be lower than areas more to the southeast (Leach 1972). This portion of the lake is dominated by low nutrient water from Lake Huron, while areas farther south are more influenced by enriched waters from Ontario tributaries (Leach 1980). Also, given the dominant current patterns and wind direction, very little deposition of suspended material occurs in the northwestern portion of the lake (Anne Clites, GLERL, per. commun.). Release rates at Stations 71 and 84 were similar in both May and September, but release rates at the other stations were higher in May than in September. The settling and subsequent mineralization of the spring phytoplankton bloom likely contributed to the higher release rates at these stations in May. Overall, the highest release rates occurred at Station 24; this station was located in the area of greatest deposition.

The release of SRP from Lake St. Clair sediments was generally lower than sediment release rates in other areas of the Great Lakes. The mean release rate in this study was $19 \text{ ugP/m}^2/\text{day}$ with a mean maximum release rate of $47 \text{ ug P/m}^2/\text{day}$. This compares to release rates of 170-570 $\text{ugP/m}^2/\text{day}$ in nearshore Lake Michigan (Quigley and Robbins 1986) and 30-800 $\text{ugP/m}^2/\text{day}$ in Lake Ontario (Bannerman et al. 1974).

To determine the significance of sediment phosphorus release in Lake St. Clair, the annual net release from the sediments was compared to other input sources, i.e. Lake Huron, tributaries, the atmosphere, and direct point sources. The total mean load from these latter sources during the 1975-80 period was about 3,100 MT/year (Tom Fontaine, GLERL, per. commun.). Of this amount, about 40% or 1200 MT can be considered bioavailable; that is, available for algal uptake and not bound to particulates (Sonzogni et al. 1982). Assuming that the mean release rate of phosphorus at the five stations is representative of the entire lake, release from the sediments amounts to about 8 MT/year or less than 1% of the total bioavailable phosphorus load. Maximum sediment release amounts to only about 20 MT/year or 2% of the total bioavailable load. Based on these calculations, the sediments appear insignificant as a source of phosphorus in Lake St. Clair.

Phosphorus Excretion by Mussels

Mean rates of phosphorus excretion on the eleven sampling dates in 1985 and 1986 are given in Table 2. Rates from the two stations sampled in 1986 were combined since significant station differences were not apparent (t-test; $P < .05$) for any of the sampling dates. Seasonal trends in phosphorus excretion were similar for the two years. Rates were high in the spring, declined in the summer, and then increased in the fall to reach peak values. Reasons for this seasonal trend are not clear, but may be related to changes in the gametogenic cycle of the organisms. An increase in ammonia excretion in the summer (Table 2) indicates an increase in gamete production at this time. Active protein catabolism (and hence increased ammonia excretion)

occurs when the glycogen normally used for metabolism is used instead for gamete production (Gabbott and Bayne 1973). While ammonia excretion would increase, phosphorus excretion would likely decrease, since a greater portion of assimilated material would be used for reproductive activities and not metabolism. Seasonal changes in phosphorus excretion were apparently unrelated to the nature of available food; the amount of particulate phosphorus in the near-bottom water was constant throughout the sampling period (Nalepa, unpublished). Mussel excretion rates were generally lower than those of other Great Lakes benthic organisms (Table 3). This may be expected, however, since the rate of phosphorus excretion per unit weight increases as body weight decreases (Johannes 1964). The dry weight of mussels in this study ranged from 1 to 4 g, while dry weights of the other organisms shown in Table 3 have dry weights of less than 2 mg.

Based on estimates of biomass from the September 1986 population survey (see below), the mussels in Lake St. Clair excrete about 59 MT of phosphorus per year or 5% of the annual bioavailable load from other sources. In addition to excreting phosphorus, mussels are active filter feeders and may remove large amounts of particulate phosphorus from the lake water during feeding. Based on preliminary estimates of mussel filtration rates (Vanderploeg and Nalepa, unpublished) and amounts of particulate phosphorus in Lake St Clair water, mussels are capable of filtering 220 MT of phosphorus from the water on an annual basis; this amounts to 7% of the total annual load.

Mussel Population Survey

The overall mean abundance of mussels was $2/m^2$ (range 0-8/ m^2) and the mean biomass was $4.3\text{ g}/m^2$ (range 0-19.4 g/m^2). In general, both abundance and biomass increased from the mouth of the St. Clair River to the head of the Detroit River. This corresponded to previously noted trends in water column productivity. A total of 287 individuals representing 20 different species were collected. The three most abundant species, Lampsilis radiata siliquodea, Leptodea fragilaris, and Proptera alata accounted for 45%, 13%, and 10% of the total population. The former species was the most widely distributed, being collected at 22 of the 28 stations. Abundances found in this survey were lower than abundances reported from other areas in the Great Lakes. For instance, densities of $7/m^2$ (Wood 1963) and $10/m^2$ (McCall 1979) have been reported from western Lake Erie, while Pugsley (unpublished data) reported a mean density of $7/m^2$ in the southwestern portion of Lake St. Clair. A direct comparison can be made between this survey and the Pugsley survey since three of the sampling stations were the same and sampling techniques were similar. Abundances in this survey were significantly lower at two of the three stations (Table 4). It is not clear whether these lower abundances are a result of an actual decline in the population or an artifact of horizontal patchiness. Considering the stability for mussel populations over the short-term, such a decline in abundances over just a 3-year period seems unlikely unless, of course, environmental conditions have recently become unfavorable. Although an unusually high number of dead mussels have been observed on Lake St. Clair beaches over the past few years (Tom Freitag, US Army Corps of Engineers,

per. commun.) only through long-term monitoring efforts can definite trends in abundances be discerned.

In western Lake Erie, mussel density and diversity have apparently declined over the past few decades (Mackie et al. 1980). Unfortunately, historical records of mussel densities in Lake St. Clair are lacking. However, mussel diversity and composition appear little changed since 1893. Reighard (1894) reported finding 20 species in Lake St. Clair with Lampsilis radiata siliquodea being very "widespread and abundant" and Proptera alata, Ligumea nasuta, Anodonta grandis being found "frequently". The most apparent difference between this survey and the 1893 survey of Reighard was the relative abundance of Leptodea fragilaris; this species was reported being "scarce" by Reighard but in this survey, it was the second most abundant species.

The age structure of L. r. siliquodea and L. fragilaris is given in Figure 3. For L. fragilaris, the age structure of the population was quite similar to that found in other freshwater systems (Strayer et al. 1981; Paterson 1985) and reflects low adult mortality and yearly variation in recruitment. However, for L. r. siliquodea, the average individual was almost 10 years of age and few younger individuals were found. The reason for this lack of recruitment is not clear, but may indicate that either the adult population is under some sort of stress (low reproductive capacity) or that mortality of the young is increasing. Populations of fish species which serve as host for the glochidia of L. r. siliquodea (yellow perch, smallmouth bass, largemouth bass, bluegill, and crappie among others) have

remained stable over the years (Bob Haas, Michigan DNR, per.commun.). Because the population is dominated by older individuals, the annual turnover rate (production/biomass) of *L. r. siliquodea* was only 0.13; this value is lower than found for mussels in most other freshwater lakes (Table 5).

LITERATURE CITED

- Bannerman, R. T., D. E. Armstrong, G. C. Holdren, and R. F. Harris. 1974. Phosphorus mobility in Lake Ontario sediments (IFYGL), pp. 158-178. Proc. 17th Conf. Great Lakes Res., Int. Assoc. Great Lake Res.
- Gabbot, P. A. and B. L. Bayne. 1973. Biochemical effects of temperature and nutritive stress on Mytilus edulis L. J. Mar. Biol. Ass. U. K. 53:269-286.
- Gallepp, G. W. 1979. Chironomid influence and phosphorus release in sediment-water microcosms. Ecology 60: 547-556.
- Gardner, W. S., T. F. Nalepa, M. A. Quigley, and J. M. Malczyk. 1981. Release of phosphorus by certain benthic invertebrates. Can. J. Fish. Aquat. Sci. 38:978-981.
- Gardner, W. S. and J. M. Malczyk. 1983. Discrete injection flow analysis of nutrients in small-volume water samples. Anal. Chem. 55:1645-1647.
- Graneli, W. 1979. The influence of Chironomus plumosus on the exchange of dissolved substances between sediment and water. Hydrobiologia 66:149-159.
- Holden, G. C. and D. E. Armstrong. 1980. Factors affecting phosphorus release from intact sediment cores. Environ. Sci. Technol. 14:79-87.

- James, M. R. 1987. Ecology of the freshwater mussel Hyridella menziesi (Gray) in a small oligotrophic lake. Arch. Hydrobiol. 3: 337-348.
- Johannes, R. E. 1964. Phosphorus excretion and body size in marine animals: microzooplankton and nutrient regeneration. Science 146:923-924.
- Kasprzak, K. 1986. Role of Unionidae and Sphaeriidae (Mollusca, Bivalvia) in the eutrophic lake Zbechy and its outflow. Int. Revue ges. Hydrobiol. 71: 315-334.
- i
- Leach, J. H. 1972. Distribution of chlorophyll a and related variables in Ontario waters of Lake St. Clair, pp.80-86. In Proc. 15th Conf. Great Lakes Res., Int. Assoc. Great Lakes Res.
- Leach, J. H. 1980. Limnological sampling intensity in Lake St. Clair in relation to distribution of water masses. J. Great Lakes Res. 6: 141-145.
- Lehman, J. H. 1980. Release and cycling of nutrients between planktonic algae and herbivores. Limnol. Oceanogr. 25: 620-632.
- Lewandowski, K. and A. Stanczykowska. 1975. The occurrence and role of bivalves of the family Unionidae in Miklajskie Lake. Ekol. Pol. 23: 317-334.

- Mackie, G. L., D. S. White, and T. W. Zdeba. 1980. A guide to freshwater mollusks of the Laurentian Great Lakes with special emphasis on the genus Pisidium. EPA-600/3-80-068, Environmental Protection Agency, Duluth, Mn. 144p.
- Magnin, E. and A. Stanczykowska. 1971. Quelques donnees sur la croissance, la biomass, et la production annuelle de trois mollusques Unionidae de la region de Montreal. Can. J. Zool. 49: 491-497.
- McCall, P. L., M. J. S. Tevesz, and S. F. Schweglien. 1979. Sediment mixing by Lampsilis radiata siliquodea (Mollusca) from western Lake Erie. J. Great Lakes Res. 5:105-111.
- Nalepa, T. F., W. S. Gardner, and J. M. Malczyk. 1983. Phosphorus release by three kinds of benthic invertebrates: effects of substrate and water medium. Can. J. Fish. Aquat. Sci. 40:810-813.
- Paterson, C. G. 1985. Biomass and production of the unionid, Elliptio complanata (Lightfoot) in an old reservoir in New Brunswick, Canada. Freshwat. Invertbr. Biol. 4: 201-207.
- Quigley, M. A. and J. A. Robbins. 1986. Phosphorus release processes in nearshore southern Lake Michigan. Can. J. Fish. Aquat. Sci. 43: 1201-1207.

- Reighard, J. E. 1894. A biological examination of Lake St. Clair. Bull. Mich. Fish Comm. No.4. 61p.
- Sonzogni, W. C., S. C. Chapra, D. E. Armstrong, and T. J. Logan. 1982. Bioavailability of phosphorus inputs to lakes. J. Environ. Qual. 11: 555-563.
- Stanczykowska, A. and M. Planter. 1985. Factors affecting nutrient budget in lakes of the R. Jorka watershed (Masurian Lakeland, Poland) X. Role of the mussel Dreissena polymorpha (Pall.) in N and P cycles in a lake ecosystem. Ekol. Pol. 33:345-356.
- Strayer, D. L., J. J. Cole, G. E. Likens, and D. C. Busco. 1981. Biomass and annual production of the freshwater mussel Elliptio complanata in an oligotrophic lake. Freshwat. Biol. 11: 435-440.
- Walz, V. N. 1978. Die produktion der Dreissena-population und deren bedeutung im stoffkreislauf des Bodensees. Arch. Hydrobiol. 82:482-499.
- Wood, K. G. 1963. The bottom fauna of western Lake Erie, 1951-52. Great Lakes Res. Div., Univer. Michigan, Publ. No. 10, pp. 258-265.

Table 1. Mean (\pm SE) rates of phosphorus release from Lake St. Clair sediments at each of the stations on the two sampling dates in 1985. Maximum mean release rates are given in parentheses. Rates are given as $\mu\text{gP}/\text{m}^2/\text{day}$.

Station	Sampling Date	
	May ¹	September ²
4	31.4 \pm 4.9 (40.0)	11.2 \pm 6.3 (32.3)
14	15.5 \pm 6.0 (49.0)	11.2 \pm 1.6 (78.4)
24	31.2 \pm 9.4 (38.2)	22.9 \pm 5.5 (58.5)
71	4.2 \pm 0.8 (18.6)	5.2 \pm 1.2 (16.3)
84	8.3 \pm 3.0 (15.0)	8.0 \pm 3.9 (32.3)

¹Water temperature = 13 C.

²Water temperature = 22 C.

Table 2. Mean (\pm SE) phosphorus and ammonium excretion rates of mussels in Lake St. Clair in 1985 and 1986. Rates given in ug/gDW/h.

Sampling Date	n	Excretion Rate		N:P Ratio
		Phosphorus	Ammonium	
<u>1985</u>				
May 9	5	0.9 ± 0.1	24.6 ± 3.7	27
May 14	7	0.9 ± 0.3	12.8 ± 2.1	14
Jul 16	6	0.7 ± 0.5	49.1 ± 3.2	69
Sep 3	7	3.9 ± 0.9	25.3 ± 2.4	7
Sep 19	7	2.0 ± 0.4	27.6 ± 4.5	14
<u>1986</u>				
Apr 30	9	1.1 ± 0.3	23.3 ± 2.3	20
May 19	4	0.6 ± 0.1	20.9 ± 4.0	35
Jul 10	9	0.5 ± 0.1	50.1 ± 3.7	109
Aug 4	10	1.5 ± 0.3	52.3 ± 8.5	35
Sep 16	10	1.9 ± 0.4	40.8 ± 6.2	21
Oct 15	10	1.9 ± 0.4	21.3 ± 2.2	12

Table 3. Mean (\pm SE) phosphorus and ammonium excretion rates (nmol/gDW/h) for some common benthic invertebrates occurring in the Great Lakes. Data compiled from Nalepa et al. (1983), Gardner et al. (1983), and Gauvin (unpublished).

Benthic Organism	Excretion Rate		N:P Ratio
	Phosphorus	Ammonium	
Chironomidae	690	11,300	16
Oligochaeta	150	8,100	54
<u>Pontoporeia</u>	90	1,090	12
Unionidae	50	1,020	23

Table 4. Comparison of mean mussel abundances (number per square meter) at three stations in Lake St. Clair in 1983 (Pugsley, unpublished) and in 1986 (this study). Standard error in parenthesis. * = Densities significantly different at the 0.05 level (t-test).

Station	1983 (Pugsley 1986)	1986 (This study)
3	13.8 (1.7)	7.8 (1.5)*
21	9.8 (2.1)	2.2 (0.9)*
66	2.4 (0.6)	2.0 (0.7)

Table 5. Turnover ratio (production/biomass) of unionids from various lentic environments.

Water Body	P/B	Reference
Lake Zbechy	0.45	Kasprzak (1986)
Lake Mikolajskie	0.35	Lewandowski and Stanczykowska (1975)
Lac des Deux Montagnes	0.20	Magnin and Stanczykowska (1971)
Morice Lake	0.19	Paterson (1985)
Lake St. Clair	0.13	This Study
Mirror Lake	0.12	Strayer et al. (1981)
Lac Saint Louis	0.10	Magnin and Stanczykowska (1971)

LIST OF FIGURES

- Fig. 1. Sampling stations in Lake St. Clair. Sediment phosphorus release rates were determined at Stations 4, 14, 71, 84, and 24. Mussel populations were sampled at all the stations except the first four stations given above.
- Fig. 2. Age structure of the two most abundant species, Lampsilis radiata siliquodea and Leptodea fragilaris.

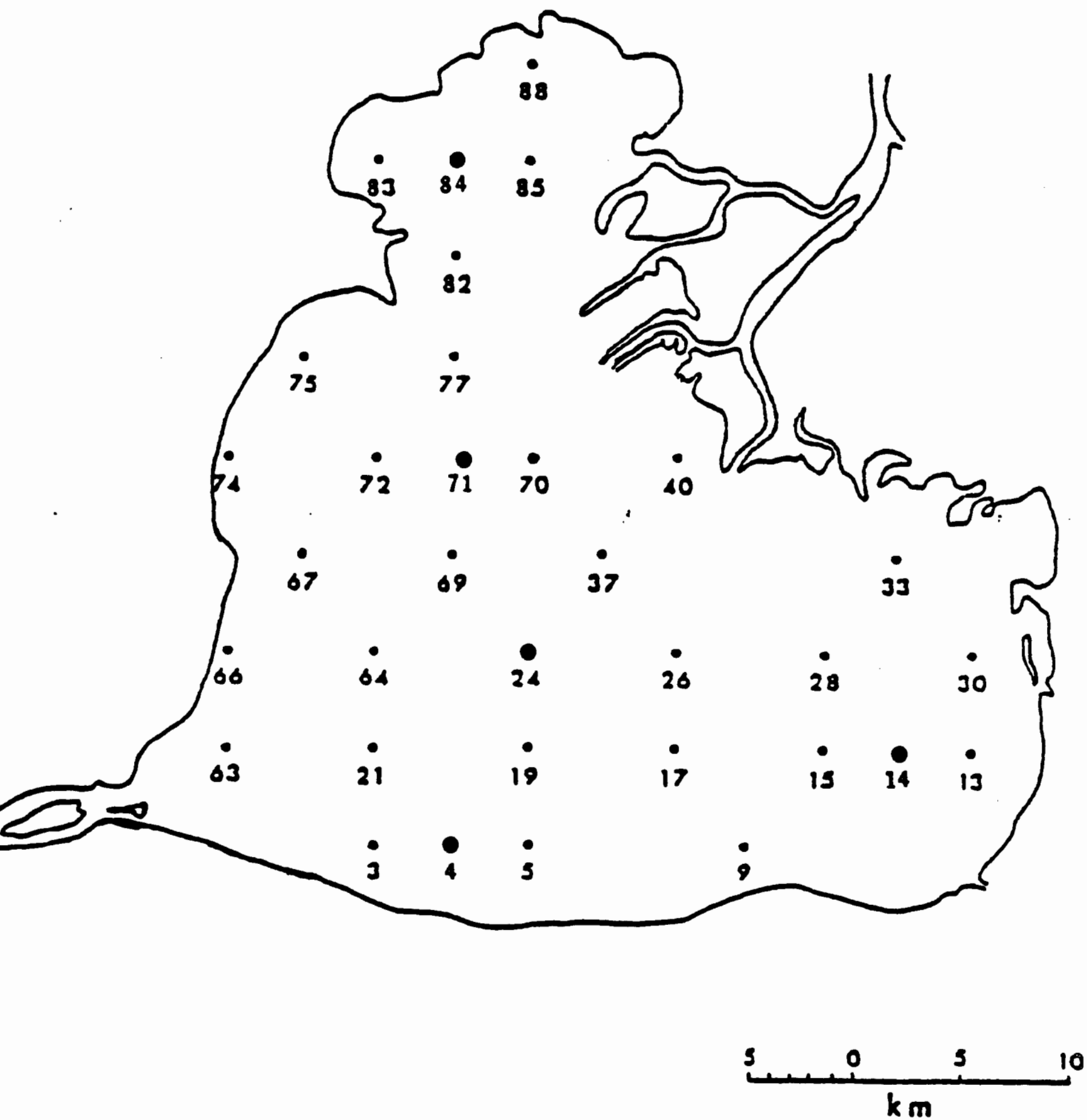


Figure 1.

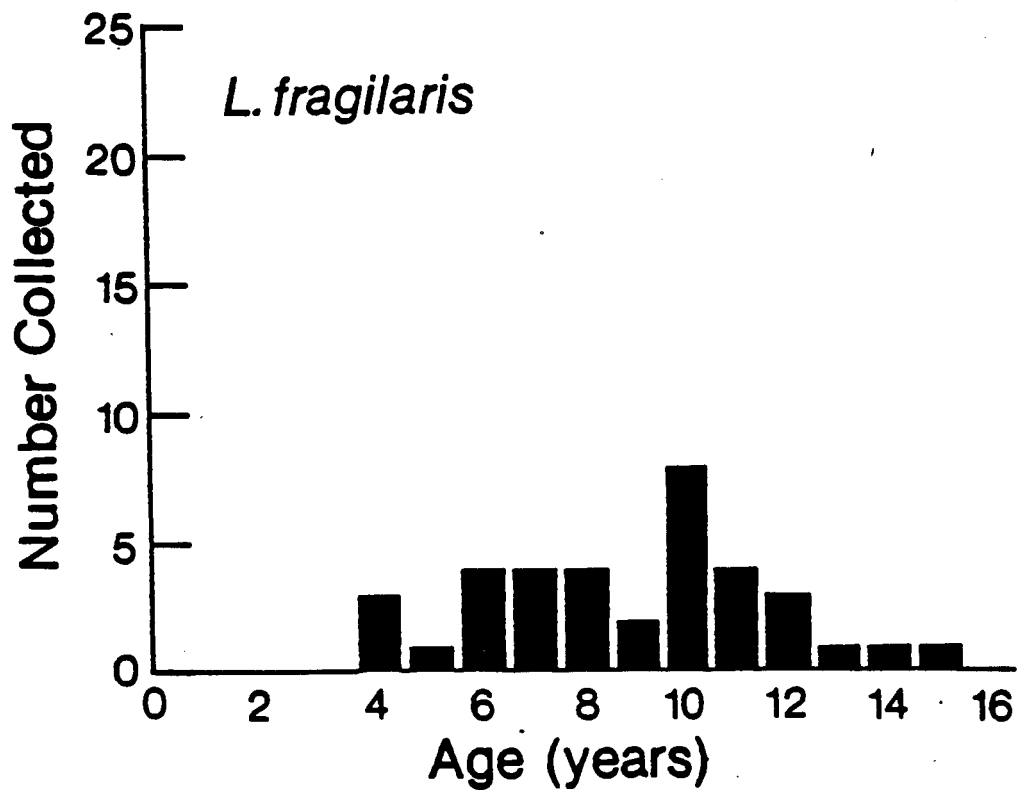
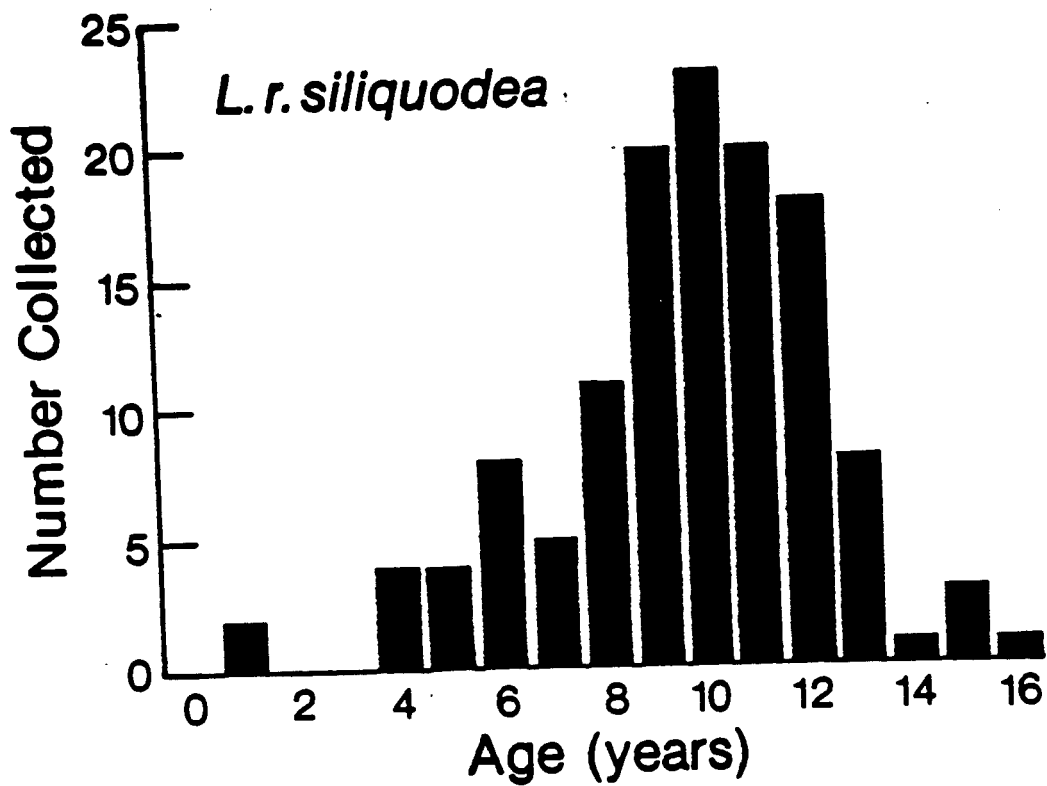


Figure 2.

SEDIMENT TRANSPORT IN LAKE ST. CLAIR

Nathan Hawley and Barry Lesht¹

ABSTRACT

In order to study resuspension in Lake St. Clair, bottom-resting instrumented tripods were deployed at various sites in the lake during 1985 and 1986. The tripods recorded time series measurements of current velocity, temperature, and water transparency. The measurements were then used to calculate the parameters of a simple flux model in order to determine the criterion for sediment resuspension. Since most resuspension in the lake is due to wave action, wave orbital velocity was used as the forcing function. These velocities were calculated by running the GLERL wave model using on-lake wind measurements to determine the wave climate, and then calculating the orbital velocities using intermediate-water wave theory. The pattern of the calculated velocities shows good agreement with both the measured standard deviation of the current velocity (although the magnitudes are somewhat different) and the total suspended material. Critical values of wave orbital velocity (the threshold for resuspension) range from 0.1 to 0.9 cm/s. The model shows good predictive capability and is relatively insensitive to changes in the settling velocity and resuspension coefficient. Some of the variability in the critical velocity may be due to changes in substrate characteristics.

¹Argonne National Laboratory

INTRODUCTION

As part of the Upper Great Lakes Connecting Channels study, we undertook to develop an empirical relation between flow activity and sediment resuspension in Lake St. Clair. To do this we deployed bottom-resting instrument packages in the lake at various times and sites which recorded time series measurements of water transparency, flow velocity, and water temperature. The measurements were then modeled using a relation suggested by Simons and Schertzer (1986) to develop a criterion for sediment resuspension. Measurements of total suspended material (TSM) and vertical profiles of water transparency and water temperature were also made. A meteorological tower measured on-lake weather conditions from July to September, 1986. Plans to use a bottom-resting flume to measure erosion thresholds had to be abandoned because a suitable vessel was not available for its deployment. Several other programs, in particular the wave study by the Great Lakes Environmental Research Laboratory (GLERL) and the Canadian Centre for Inland Waters (CCIW) and the sediment transport study by CCIW have provided valuable supporting data.

Lake St. Clair is a large (approximately 40 km wide), shallow (maximum depth 7m) lake located between Lakes Huron and Erie. As such it receives the entire outflow from the upper Great Lakes - approximately 5300 m³/s. Since the residence time of the water in the lake is only about 7 days, much of the sediment carried into the lake is almost immediately swept out again. However much of the lake is covered by sand and silt which can be resuspended. Because of its shallow depth and large fetch, we felt that

wave action might be a prime cause of resuspension in Lake St. Clair. Thus most of our current velocity measurements were in burst mode. This allowed us to measure not only the mean current, but also its standard deviation, which we felt could serve as a measure of wave action.

DATA COLLECTION

One or more tripods were deployed five times during 1985 and 1986 (Fig. 1). One of these tripods, the one deployed by Barry Lesht of Argonne National Laboratory (ANL), was equipped with a Marsh-McBirney current meter and 25 cm pathlength Seatech transparency meter, as well as with a temperature probe. The other two tripods were deployed by Nathan Hawley (GLERL) and were equipped with only a temperature probe and 25 cm Seatech transparency meter. Although we had planned to have current meters on these two tripods as well, the meters we bought never worked properly. Details of the tripod locations and deployment periods are given in Table 1. In all cases the GLERL transparency meters were 0.9m above the bottom. Both they and the temperature sensor, which was located 1.2m above the bottom, took a 60 second sample at 1 Hz every 15 minutes. The mean and standard deviation of the transparency (TSD) were recorded along with the average temperature. The transparency meter on the ANL tripod was 0.9m above the bottom, the current meter 0.7m and the temperature sensor 1.0m. During all but one of the deployments the current meter recorded a 75 second burst at 3.4 Hz. During July-August of 1985 and May-June, 1986 these measurements were taken every 45 minutes, during July-August, 1986 every 60 minutes, and during

October, 1986 every 30 minutes. For all but the last of these deployments only an average transparency and temperature were recorded. During the October, 1986 deployment transparency was recorded in the same manner as the current velocity. During the September-October, 1985 deployment continuous 5 minute averages of current velocity, water transparency, and temperature were made.

In order to calibrate the transparency meters, measurements of transparency and TSM were made in triplicate at 25 different stations (Fig. 2). For 110 measurements, TSM (measured in mg/l) is related to water transparency (measured as the fraction of the transmittance in air) by

$$\text{TSM} = -8.33 * \text{Ln}(\text{Tr}) - 1.96 \quad r^2 = 0.92 \quad (1)$$

The measurements used to establish this relationship show no geographic or temporal trends. Use of (1) allowed TSM to be calculated from the transparency measurements. Figure 3 shows the predicted values and the measurements used in the regression. The two curved lines represent the 95% confidence interval for the predicted values. It should be noted however, that all of the calibration measurements were made during fairly calm conditions. During resuspension events far more sand-sized material is likely to be in the water column. Because of its high density, a given weight of sand will attenuate the light beam far less than the same weight of more porous, far less dense, flocs which form from cohesive material. Thus, the TSM calculations must be underestimates of the true loading. In

the model we used, however, concentration is essentially a surrogate for transparency. Since the model parameters are all internally estimated, they will still be consistent. However, the actual rates of settling and resuspension measured on a mass basis will probably be somewhat different from those calculated.

MODEL DESCRIPTION

Simons and Schertzer (1986) have proposed a simple model which relates changes in the vertically integrated (assuming vertical uniformity) suspended sediment concentration (C) to changes in the balance between the rates of sediment resuspension and sediment settling. This is just a flux model in which the net flux (the left-hand side of the equation) is equal to the difference between the upward and downward fluxes. The resuspension rate is assumed to be a linear function of the forcing function (F) above some critical value (F_c) and zero otherwise, with R being the resuspension concentration. The settling rate is the product of the settling velocity (S) and the ambient concentration (C_a) which is assumed to always be present. Thus the model is

$$D \frac{dC}{dt} = - S(C - C_a) \quad \text{for } F < F_c \quad (2)$$

and

$$D \frac{dC}{dt} = R(F - F_c) - S(C - C_a) \quad \text{for } F > F_c \quad (3)$$

Using the results from our deployments we could first solve equation 2 for S and C_a for low values of dC , and then use these values in equation 3 to solve for R and F_c . However, we have used the time integrated form of equation (3) to estimate the sets of model parameters that best reproduce the observed time series of sediment concentration. The model results were then evaluated using Wilmot's (1984) criteria. Obviously, since the model does not take advection into account, sediment concentration changes due to advection must at least be identified, and if possible removed from the record, prior to determining the parameters. This requires a set of criteria to differentiate between advection and local resuspension events.

One obvious criteria for local resuspension is that the increase in sediment concentration should occur at the same time as an increase in the forcing function. Thus, if resuspension is due to wave activity, increases in sediment concentration should occur when wave action is greatest (during storms). We have used high values of Speed Standard Deviation (SSD) as an indication of wave activity. Since waves are wind-generated, in the absence of direct or indirect wave measurements wind records might be useful in predicting resuspension activity. There should also be (in the absence of advection) a characteristic decay time of suspended sediment concentrations which depends on the settling speed of the sediment and the height to which the sediment was resuspended. All of the observations in Lake St. Clair indicate that it is vertically well mixed, particularly during resuspension events, so differences in the decay time should depend only on the settling rates. These variations are expected to be small. Chriss and Pak (1976) have also suggested that the standard deviation of water transparency should

be higher during resuspension events than during advection because the water has not had as much time to become well mixed .

Ironically, the data sets that most unambiguously show local resuspension were collected last. Figure 4 shows the sediment concentration record measured at station 42 during October, 1986. The record extends only to day 301 because the other two stations were retrieved at that time. Thus the data collected on days 303-309 are not discussed here. The gaps in the record are due to instrument problems; the recording tape was filled on day 296 and not replaced until day 301. The very high concentrations (off the scale) occurred when the transparency was zero. For zero transparency, equation 1 gives a TSM of of infinity. We have used a value of 68 mg/l - equivalent to the lowest transparency we could measure. The TSM record is very well correlated with both the mean speed and SSD (Figs. 5 and 6). In fact the plots of the mean speed and its standard deviation are almost identical. All three plots show major changes beginning on day 287 and extending until the measurements were interrupted on day 289. The high TSM levels, however, continue for several more days - until day 293 - even though both the mean speed and the SSD are at background levels. Most probably the high TSM values during this time are due to advection of material resuspended elsewhere.

Figure 7 shows wave orbital velocities calculated for the site. These velocities were calculated by running the GLERL wave model using wind data collected by CCIW near the station. The wave model results were then used as input to calculate the maximum orbital velocity one meter above the

bottom. The pattern of the results is very similar to that of the mean measured speed and the SSD, although there is a difference in magnitude of about two. The calculated velocities also decay more quickly than do the measured values. This is probably because the measured parameters also include the effects of currents generated by the storm. In spite of these differences, the generally good agreement suggests that at least most of the TSM record can be accounted for by local wave-induced resuspension. The temperature record (Fig. 8) shows a marked decrease during and after the storm, another indication that advection was present. The standard deviation of the transparency (TSD) in Figure 9 shows a peak during the storm, but also several other peaks when no wave action was present. Apparently, this measurement is not an unequivocal indicator of local resuspension, at least in Lake St. Clair. The very large peak on day 293 is particularly interesting because it does not appear to be related to any measure of flow, either observed or calculated.

Figure 10 shows the results from the model when the calculated orbital velocity data is used as the forcing function. The fit is remarkably good, as evidenced by the high values of Wilmot's (1984) index of agreement (d) and the unsystematic mean-squared error (MSEU, Table 2). Here d is a relative index of agreement between the model and the observations based on the summed square error. MSEU is that portion of the root mean-squared error that is unsystematic. Note that the model predicts a higher concentration than the maximum measured, but recall that the transparency meter was saturated during this period. Also note that the elevated TSM measurements on days 289-301 are not predicted by the model, as would be

true if they are due to advection. Although the main peak (on days 287-299) is predicted quite well, the peak on day 308 is substantially less than the predicted concentration. This suggests that either R is too high or that the resuspension flux is not a linear function of F_c but possibly a power function of some sort. The results agree quite well with those obtained using SSD as the forcing function (Fig. 11), so we have used the wave model results at the other two stations as the forcing function since we have no current measurements at those sites.

Figure 12 shows the TSM record at station 71 for the same period. The large increase on day 287 is also present here, as is the long decay. In addition, however, there is a pronounced peak on day 283. The calculated orbital velocities (Fig. 13) also show a marked peak on day 283, in contrast to the record at station 42, where the peaks in both sediment concentration and wave orbital velocity are much smaller. Again, as at station 42, cooler water is present during the storm and its aftermath (Fig. 14). The TSD (Fig. 15) shows two peaks - one during the storm and the second just prior to the dramatic lowering of the concentration on day 291. Since this second peak is not associated with wave action, it may indicate mixing of clearer water from upstream with the more turbid water in the lake. Comparison of the model results with the observations are shown in Figure 16. Again the model slightly overpredicts the peak concentration, although in this case the transparency meter was not saturated. The model also underpredicts the peak concentration during the storm on day 283, and predicts several small peaks that were not observed. Overall, however, the model does a good job of predicting the actual measurements.

Results of the TSM measurements made at station 1 are shown in Figure 17. The biggest difference between this station and the other two is the two peaks on day 285. It is very reassuring to find that a peak in calculated wave orbital velocities also occurs on that day (Fig. 18), in addition to the peaks on days 283 and 287. The effects of advection after the storm on day 287 are not as evident at this station, and there is no peak in the TSD on day 293 (Fig. 19). There are however several peaks later in the record which are not correlated with wave activity. These may be due to inhomogeneities in the water entering the lake. The temperature record (Fig. 20) is similar to those at the other stations. The observed and modeled results are shown in Figure 21. The model accurately predicts all three peaks, although it either overestimates or underestimates their magnitude, and the decay curves are reasonably close to the observed ones.

Model results for the stations are tabulated in Table 2, along with the percent mud (less than 60 microns) of the bottom sediments as measured by the University of Windsor (1985). The stations for this deployment were, in fact, chosen so that the sand percentages were approximately equal since one of the goals was to investigate the effect of differing wave climates on similar substrates. Although the model results from stations 1 and 71 are in good agreement, the results from station 42 are somewhat different - all the parameters but S are much higher. Some of this discrepancy may be an artifact of the data however. The higher ambient concentrations are probably due mostly to the outflow of the Thames River, which has a high suspended load. If C_a is artificially high, then bottom resuspension may be occurring at lower values of F_c than is evident from the data. An

artificially high value of F_c could in turn lead to a higher value of R , if in fact the resuspension rate is not linear as assumed here but is a power function of F .

The spring, 1986 deployment was designed to examine the effects of changes in substrate on resuspension. During this period the tripods were all located within 8 km of each other in the northwest portion of the lake. We hoped that putting the tripods close together would minimize the differences in wave climate between stations. Since we did not yet have our meteorological tower available, we put the tripods near the St. Clair Shores Coast Guard station, which makes weather observations. However, a comparison of the weather records from St. Clair shores with on-lake observations later in the year showed substantial differences between the two. Until a valid transfer function can be developed, wave climates estimated from the St. Clair Shores weather data are not accurate. This means that we could not use calculated wave orbital velocities as the forcing function in the model for this deployment. Since only the current meter at station 3 worked, only that data set could be analyzed, since we felt that, given the variability in the TSM measurements between the stations, it would not be justifiable to apply the current data from one station to another site. Once a suitable transfer function is developed, we will be able to assess the effects of substrate variability, but this cannot be done yet.

The TSM record for station 3 (Fig. 22) shows several pronounced peaks, one of which lasted for several days. Unfortunately the mean speed record

(Fig. 23) is so noisy that it is hard to see any obvious correlation. The record of the SSD (Fig. 24) shows a correlation with some, but not all, of the TSM peaks and also shows peaks where no TSM increase occurred. We believe the three TSM peaks after day 152 and the one on day 136 are due to wave resuspension since they correlate with peaks in the SSD and decay quickly. The long episode starting on day 142 is probably due to advection since both the speed and SSD are low when it begins. The peak on day 137 is hard to explain because it is not correlated with a peak in SSD but decays quickly. The temperature record (Fig. 25) does not help much in interpreting the results. The model results, using SSD as the forcing function, show a reasonable agreement with the data (Fig. 26) though not as good as for the fall. The most obvious failure is on day 149 (May 29) when the model predicts a non-existent peak in TSM. This is because of a peak in SSD that day. The model parameters (Table 2) are fairly consistent with the results from the fall deployment. C_a is lower, reflecting the relative absence of sediment in the water, and although F_c is higher, it is a different parameter than in the fall. The values of R and S are close to those for the other western stations.

The results from station 5 (Fig. 27-29) are very much like those from station 3. The same TSM peaks are seen, although their form is slightly different, particularly for the (assumed) advection event. The TSD record correlates well with some TSM peaks, particularly those late in the record, but overall TSD does not seem to be a reliable indication of local resuspension. The temperature record show the same general pattern as at station 3.

The tripod at station 1 worked for only part of the deployment. The TSD peaks (Fig. 31) correlate extremely well with the early peaks in TSM (Fig. 30) but not with the TSM peak on day 142. This latter peak, although it looks like the one in the middle of the records at stations 3 and 5, actually begins about a day earlier. The temperature record (Fig. 32) shows a minimum just before the peak in TSM further supporting the hypothesis that it is due to advection.

Stations 1, 5, and 71 were occupied during the summer of 1986. Stations 1 and 5 had been occupied earlier in the year, and station 71 was near both our meteorological tower and a wave rider deployed by NESDIS of Canada. However, several problems complicate the interpretation of the data from this deployment. First, algal growth during the deployment period fouled the transparency meters. We endeavored to calibrate the fouling by taking vertical profiles with a clean meter once a week at each station, but unfortunately two of the tripods stopped during the deployment so we have only one complete calibration curve, and the results vary from station to station. The TSM data shown has been corrected to the best of our ability, but is not perfect. In addition, we also found that although there were very few significant wave events, movement of turbid bottom water occurred fairly persistently, particularly at station 71, which is where our current measurements were made. It is thus extremely difficult to say with any great confidence when resuspension occurred during this deployment.

The TSM record from station 71 is much noisier than that during the fall deployment (Fig. 33) and does not correlate very well with either the

mean speed (Fig. 34) or the SSD (Fig. 35). Nor does it seem to correlate very well with the calculated orbital velocities (Fig. 36). In fact the best correlation seems to be with temperature (Fig. 37) which shows extraordinary variability. In this case, sharp drops in TSM occurred simultaneously with abrupt increases in temperature. These temperature increases are in turn correlated with periods of high wave orbital velocities. Thus, rather than causing resuspension, wave action appears to be associated with minimums in TSM. The explanation appears to be that during the summer there is a thin bottom layer of more cooler, more turbid water underlying the warmer, clearer water. Wave action mixes the two and brings the warmer water down nearer the bottom. Vertical profiles taken during this period frequently show this cooler, turbid layer (Fig. 38). In addition, the water temperature sensor on our meteorological station, which was 3m below the surface, recorded temperatures between 22 and 24 degrees during the deployment. It seems likely then that most of the TSM signal is not due to resuspension but to vertical movement of the upper surface of this bottom turbid layer past the sensor. Not surprisingly, the model does not do very well with this data set.

The results from stations 5 and 1 are somewhat less noisy. At station 5 the TSM (Fig. 39) shows 3 pronounced peaks, and a noticeable minimum beginning on day 201. This minimum correlates with a rise in temperature (Fig. 40) so it may also be due to a thinning of a bottom turbid layer. The first two peaks are associated with peaks in orbital velocity (Fig. 41), but the last is not: it may be due to advection. Again, the TSD record (Fig. 42) is not much help in distinguishing resuspension events.

The TSM record at station 1 (Fig. 43) shows several pronounced peaks which decay very quickly. These peaks are well correlated the the calculated wave orbital velocities (Fig. 44) and also have high TSD values (Fig. 45). There does not appear to be a consistent correlation with temperature (Fig. 46), so it seems likely that these events are in fact due to wave resuspension. We have run the model for this station using the parameters from the fall deployment with the wave orbital velocities as the forcing function. The results, shown in Figure 47) are surprisingly good. The model accurately predicts the occurrence, if not the actual concentrations, for several of the TSM peaks. The most noticeable defect is the overly long decay times, which indicates that S should be increased. The relatively poor values for the index of agreement and MSEU are not too surprising when one considers that most of the summer data is in the range of the ambient concentration for the fall deployment.

Both of the 1985 deployments were exploratory, and neither has been analyzed in any detail. During the summer deployment, one of the axes of the current meter failed, so we have no record of either mean speed or SSD. The transmittance and temperature records are shown in Figures 48 and 49. During the fall deployment, the tripod was placed near one of the wave stations deployed by CCIW. The current meter and transparency meter were both set up to log continuous 5 minute averages. These records and the temperature are shown in Figures 50-52. Although preliminary examination of both data sets shows a correlation between TSM and wave orbital velocities, the model results for these deployments are not yet available.

DISCUSSION

It appears that most, if not all, resuspension in Lake St. Clair is due to wave action. Although it is difficult in some of the records to distinguish between resuspension and advection, those events which can be unambiguously identified are almost always associated with wave activity. The good fits obtained from a very simple model which totally ignores both advection and resuspension due to currents also indicates that wave action is the primary cause of resuspension. The wave orbital velocities calculated from the results of the GLERL wave model serve very well as the forcing function in the model. These velocities are the maximum values calculated using intermediate-water wave theory for a height one meter above the bottom in a total depth of 6.5m. Since the wave model gives significant wave height and period as the output, the orbital velocities are not the absolute maximum velocities, but the maximums for the significant waves, which are somewhat smaller than the peak waves. It is thus not surprising that the calculated orbital velocities are somewhat smaller than the actual measured velocities. The good agreement between the patterns of calculated orbital velocities and the measured standard deviations of the speed indicate that in general the latter is a good analog for the former. However, there are times when high values of SSD are not correlated with high orbital velocities, so the analogy is not exact.

We had hoped that the standard deviation of the transparency (TSD) would be a good indicator of local resuspension, but we found frequent instances of high TSD values which did not correlate with resuspension

events. It appears that in Lake St. Clair the time and length scales for resuspension and advection are too similar for TSD values to serve as a useful distinguishing criterion. This means that resuspension was identified primarily by the simultaneous occurrence of a rise in TSM and in orbital velocity.

The various model results show the most consistency for the values of S and R . However the predicted concentrations are relatively insensitive to the values of these parameters. Examination of the predictions indicate that a higher value of S may improve the fit in several cases by shortening the time required to return to ambient conditions. This in turn would require an increase in R in order to keep the peak concentrations the same. Another solution would be to use a more complicated model, possibly one in which the resuspension rate is a power function of F , as proposed by Lavelle et al (1984). However, given the limitations of our measurements and the good agreement between the model and measured concentrations, a more complicated model may not provide much more insight.

When wave orbital velocities are used as the forcing function in the model, the critical value above which resuspension occurs is less than 1 cm/s (except at station 42 where we believe that the very high ambient concentrations mask the actual initiation of resuspension). Although an extrapolation of F to the bottom is fraught with peril (recall that it is a calculated number - not measured), it appears that sand-sized material is unlikely to be resuspended at these low values. Since sand is resuspended during at least some of the resuspension events (as evidenced by the sand

found in the CCIW traps), there is probably a second, higher value of F , which applies to the coarser material. The value determined from the model is for the finer material which causes the decrease in transparency. The variability in F_c between stations may be due to differences in substrate characteristics, but the only such measures available (% sand, gravel, and mud) are not sufficient to explain the differences. Although there is considerable variation in F_c between stations, the model parameters appear to be fairly constant through time. The good agreement between the model results for the summer deployment at station one, which were obtained using the parameter values calculated from the fall deployment, and the observations, shows that the model has good predictive capability and lends credence to the other results. Further tests of the model using the other summer and spring data will be attempted in the future.

CONCLUSIONS

Our results show that resuspension in Lake St. Clair is due mainly to wave action. When wave orbital velocities are used as the forcing function in a simple model, the agreement between the predicted and observed instances of sediment resuspension is quite good. Critical values of the orbital velocity are less than one cm/s when calculated at one meter above the bottom. These velocities can be calculated from the results of the GLERL wave model if on-lake wind records are available. Variations in the critical velocity between sites may be due to differences in substrate characteristics, but there is no adequate data to test this.

LITERATURE CITED

- Chriss, T.M. and H.J. Pak, 1978, Optical evidence for sediment resuspension-Oregon continental shelf, EOS, 59, p 410.
- Great Lakes Institute, University of Windsor, 1985, A case study of selected contaminants in the Essex Region, Vol 1: Physical Sciences, contract report for DSS contract UP-175.
- Lavelle, J.W., Mofield, H.O., and E.T. Baker, 1984, An in situ erosion rate for a fine-grained marine sediment, Jl. Geophys. Res., 89, 6543-6553.
- Simons, T.J. and W.M. Schertzer, 1986, Modeling wave-induced sediment resuspension in Lake St. Clair, unpublished MS, NWRI.
- Wilmot, C. J., 1984, some comments on the evaluation of model performance, Bull. Am. Meteor. Soc., 63, 1309-1313.

TABLE I

TRIPOD DEPLOYMENTS

<u>Dates</u>	<u>Station #</u>	<u>Location</u>	<u>Tripod</u>
7/11/85 - 8/8/85	42	42°23'45"N 82°42'03"W	ANL
9/10/85 - 10/9/85	71	42°24'55"N 82°41'45"W	ANL
5/15/86 - 5/24/86	1	42°31'18"N 82°44'48"W	GLERL
5/15/86 - 6/6/86	3	42°29'42"N 82°47'42"W	ANL
5/15/86 - 6/6/86	5	42°28'06"N 82°47'24"W	GLERL
7/08/86 - 7/27/86	1	42°31'18"N 82°44'48"W	GLERL
7/08/86 - 7/31/86	5	42°28'00"N 82°47'18"W	GLERL
7/08/86 - 8/8/86	71	42°25'00"N 82°40'48"W	ANL
10/10/86 - 10/28/86	1	42°31'11"N 82°44'49"W	GLERL
10/10/86 - 11/11/86	42	42°23'08"N 82°32'28"W	ANL
10/10/86 - 10/28/86	71	42°24'58"N 82°40'38"W	GLERL

All moorings were in 6-7m of water.

Table 2

Model Results

Station	% Mud	C _a (mg/l)	F _c (cm/s)	S (cm/s)	R (mg/l)	d	MSEU
42-fall	25	6.4	2.8	0.0055	0.17	.947	.999
71-fall	35	3.8	0.9	0.0063	0.05	.969	1.00
1-fall	30	4.3	0.1	0.0100	0.05	.922	.995
3-spring	39	1.3	2.9	0.0033	0.02	.870	.980
5-spring	53						
1-spring	30						
1-summer	30	4.3	0.1	0.100	0.05	.616	.757
71-summer	35						
5-summer	53						

LIST OF FIGURES

- Figure 1. Deployment locations.
- Figure 2. Transparency calibration locations.
- Figure 3. Transparency-TSM calibration curve.
- Figure 4. TSM plot, station 42, October, 1986
- Figure 5. Speed plot, station 42, October, 1986
- Figure 6. Standard deviation of the speed, station 42, October, 1986
- Figure 7. Calculated wave orbital velocity, station 42, October 1986
- Figure 8. Temperature, station 42, October, 1986
- Figure 9. Standard deviation of the transparency, station 42, October, 1986
- Figure 10. Comparison of the observed and calculated TSM using wave orbital velocity as the forcing function, station 42, October, 1986
- Figure 11. Comparison of the observed and calculated TSM using the standard deviation of the speed as the forcing function, station 42, October, 1986
- Figure 12. TSM, station 71, October, 1986
- Figure 13. Calculated wave orbital velocity, station 71, October, 1986
- Figure 14. Temperature, station 71, October, 1986
- Figure 15. Standard deviation of the transparency, station 71, October, 1986
- Figure 16. Observed and calculated TSM using the wave orbital velocity as the forcing function, station 71, October, 1986
- Figure 17. TSM, station 1, October, 1986
- Figure 18. Calculated wave orbital velocity, station 1, October, 1986
- Figure 19. Standard deviation of the transparency, station 1, October, 1986
- Figure 20. Temperature, station 1, October, 1986
- Figure 21. Observed and calculated TSM using wave orbital velocity as the forcing function, station 1, October, 1986

- Figure 22. TSM, station 3, May-June, 1986
- Figure 23. Speed, station 3, May-June, 1986
- Figure 24. Standard deviation of speed, station 3, May-June, 1986
- Figure 25. Temperature, station 3, May-June, 1986
- Figure 26. Observed and calculated TSM using the standard deviation of the speed as the forcing function, station 3, May-June, 1986
- Figure 27. TSM, station 5, May-June, 1986
- Figure 28. Standard deviation of the transparency, station 5, May-June, 1986
- Figure 29. Temperature, station 5, May-June, 1986
- Figure 30. TSM, station 1, May-June, 1986
- Figure 31. Standard deviation of the transparency, station 1, May-June, 1986
- Figure 32. Temperature, station 1, May-June, 1986
- Figure 33. TSM, station 71, July-August, 1986
- Figure 34. Speed, station 71, July-August, 1986
- Figure 35. Standard deviation of the speed, station 71, July-August, 1986
- Figure 36. Calculated wave orbital velocity, station 71, July-August, 1986
- Figure 37. Temperature, station 71, July-August, 1986
- Figure 38. TSM profile, station 71, July 22, 1986
- Figure 39. TSM station 5, July-August, 1986
- Figure 40. Temperature, station 5, July-August, 1986
- Figure 41. Calculated wave orbital velocity, station 5, July-August, 1986
- Figure 42. Standard deviation of the transparency, station 5, July-August, 1986
- Figure 43. TSM, station 1, July-August, 1986
- Figure 44. Calculated wave orbital velocity, station 1, July-August, 1986
- Figure 45. Standard deviation of the transparency, station 1, July-August, 1986

Figure 46. Temperature, station 1, July-August, 1986

Figure 47. Observed and calculated TSM using the wave orbital velocity as the forcing function, station 1, July-August, 1985

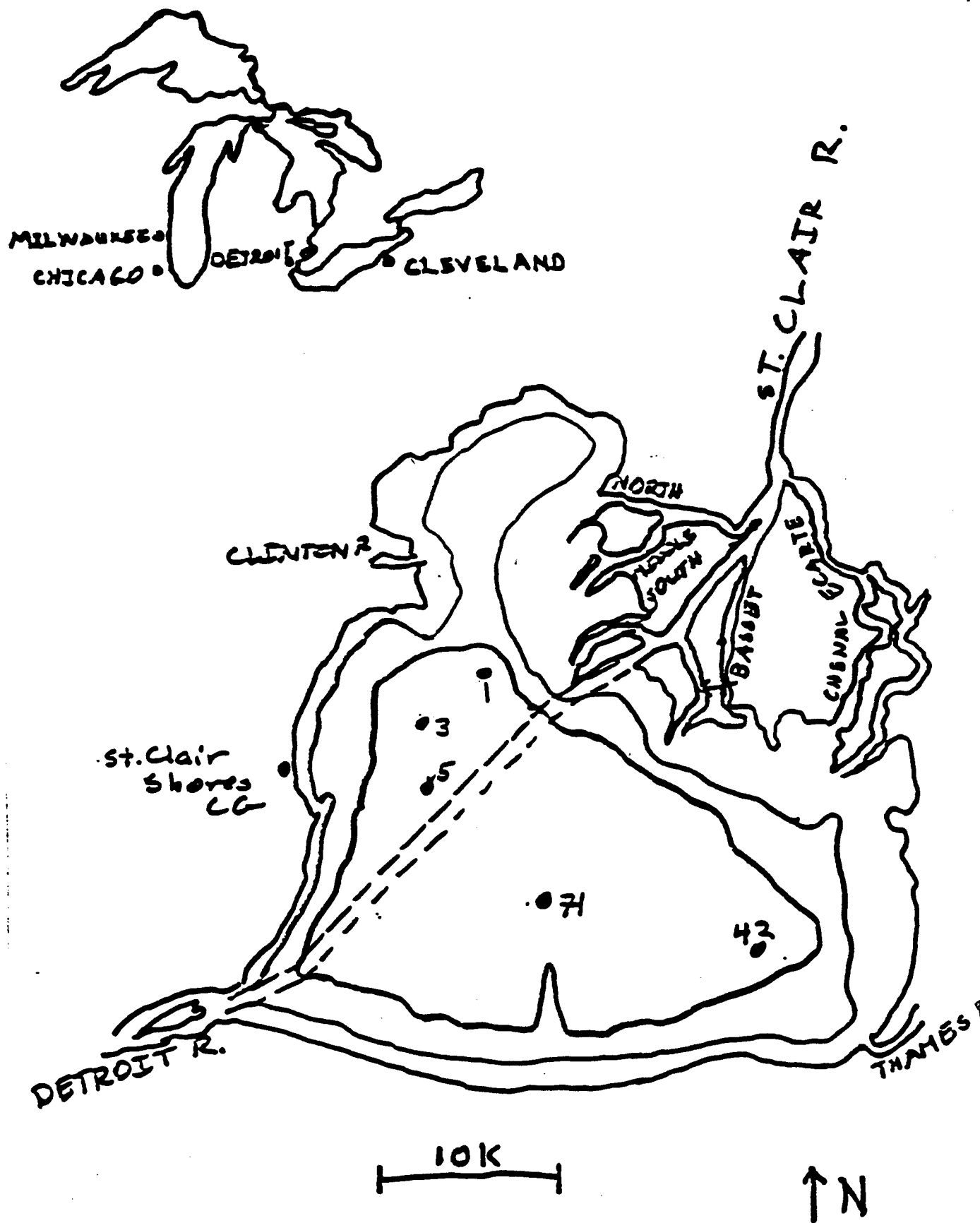
Figure 48. Transparency, station 42, July-August, 1985

Figure 49. Temperature, station 42, July-August, 1985

Figure 50. Transparency, station 71, September, 1985

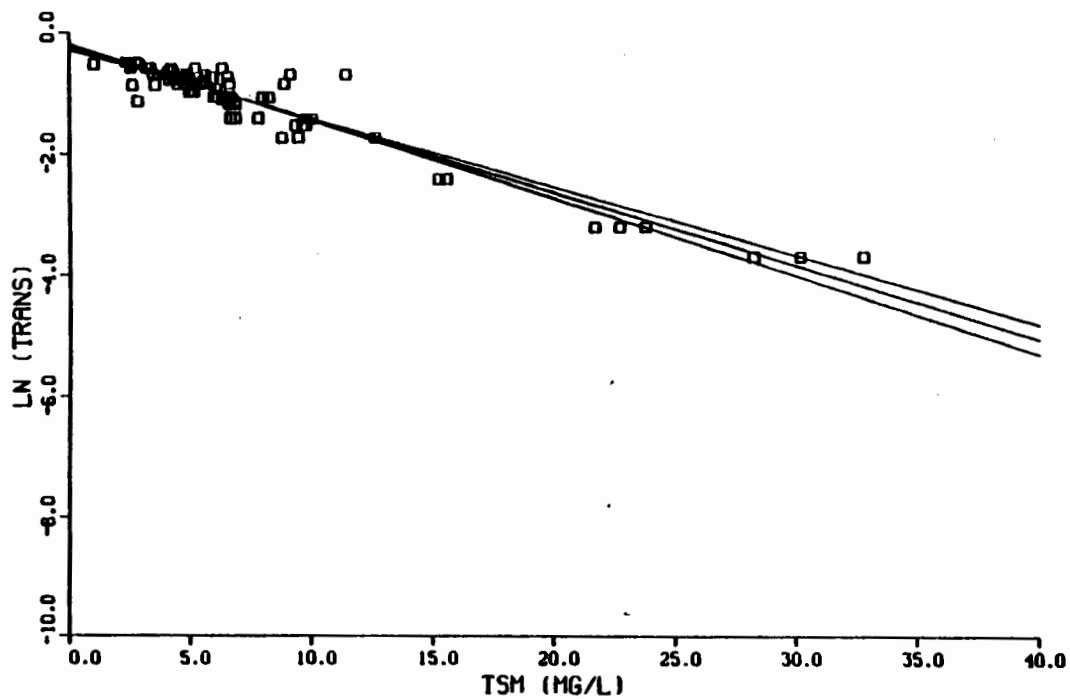
Figure 51. Speed, station 71, September, 1985

Figure 52. Temperature, station 71, September 1985

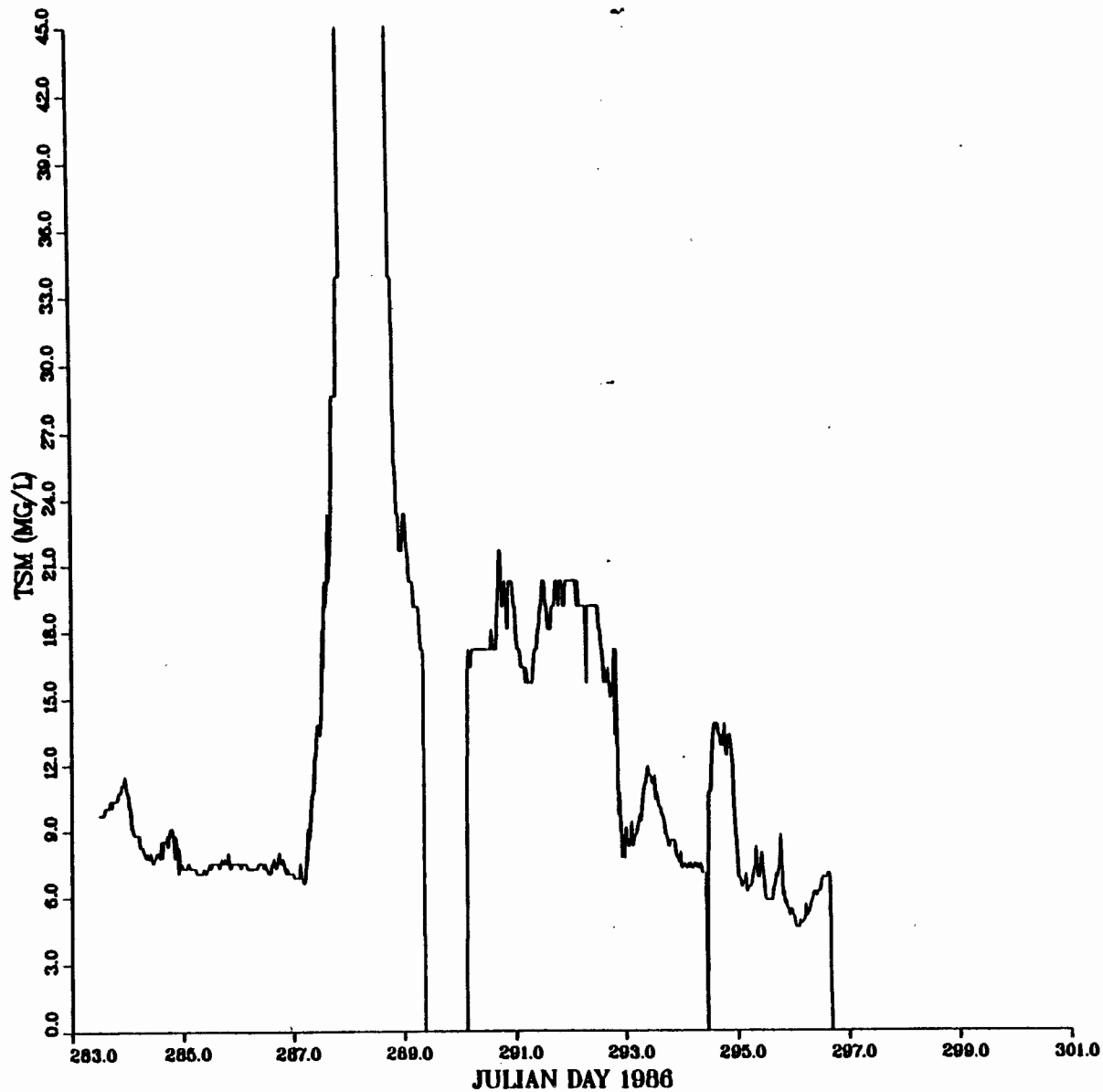




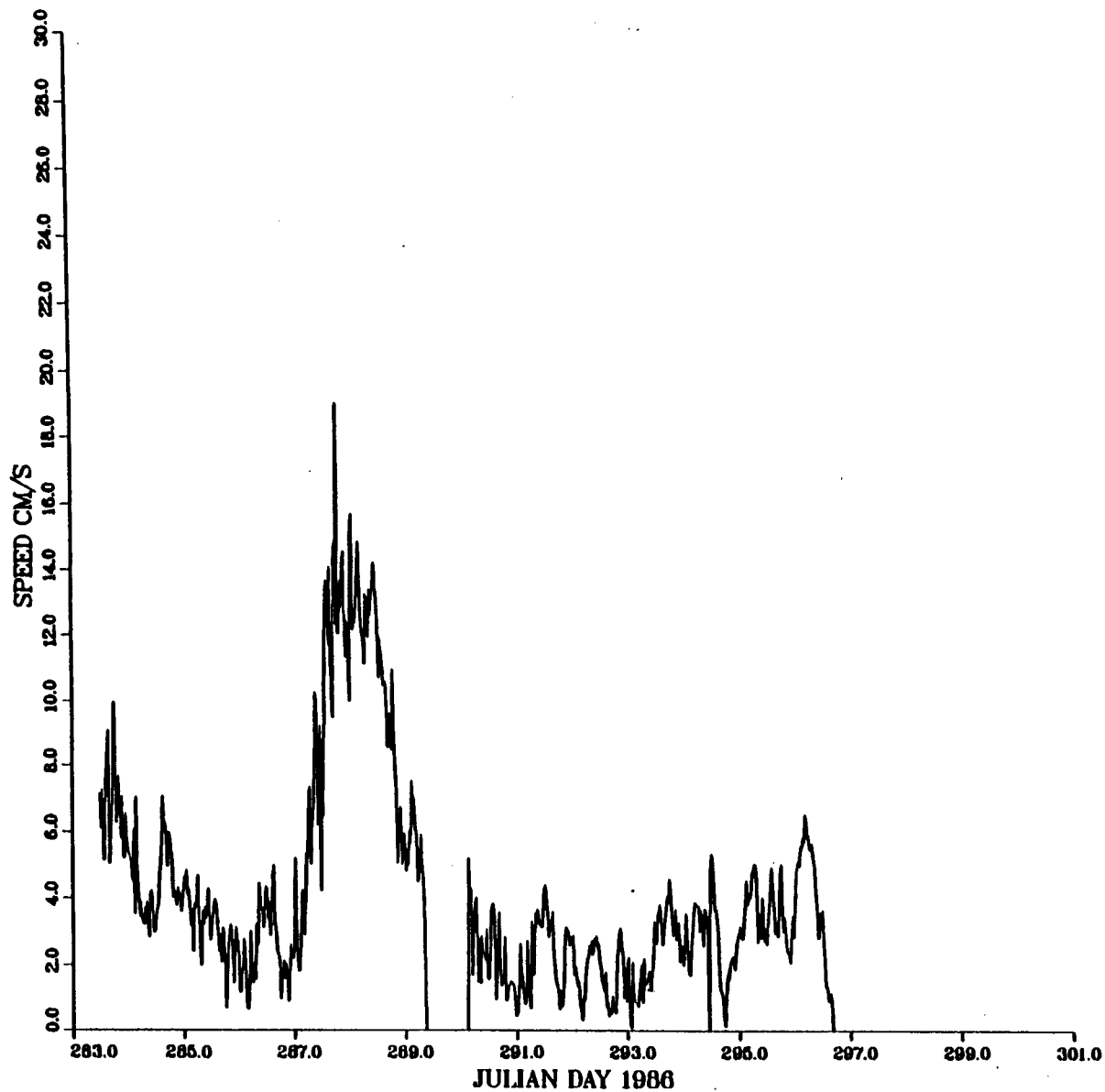
TSM CALIBRATION CURVE



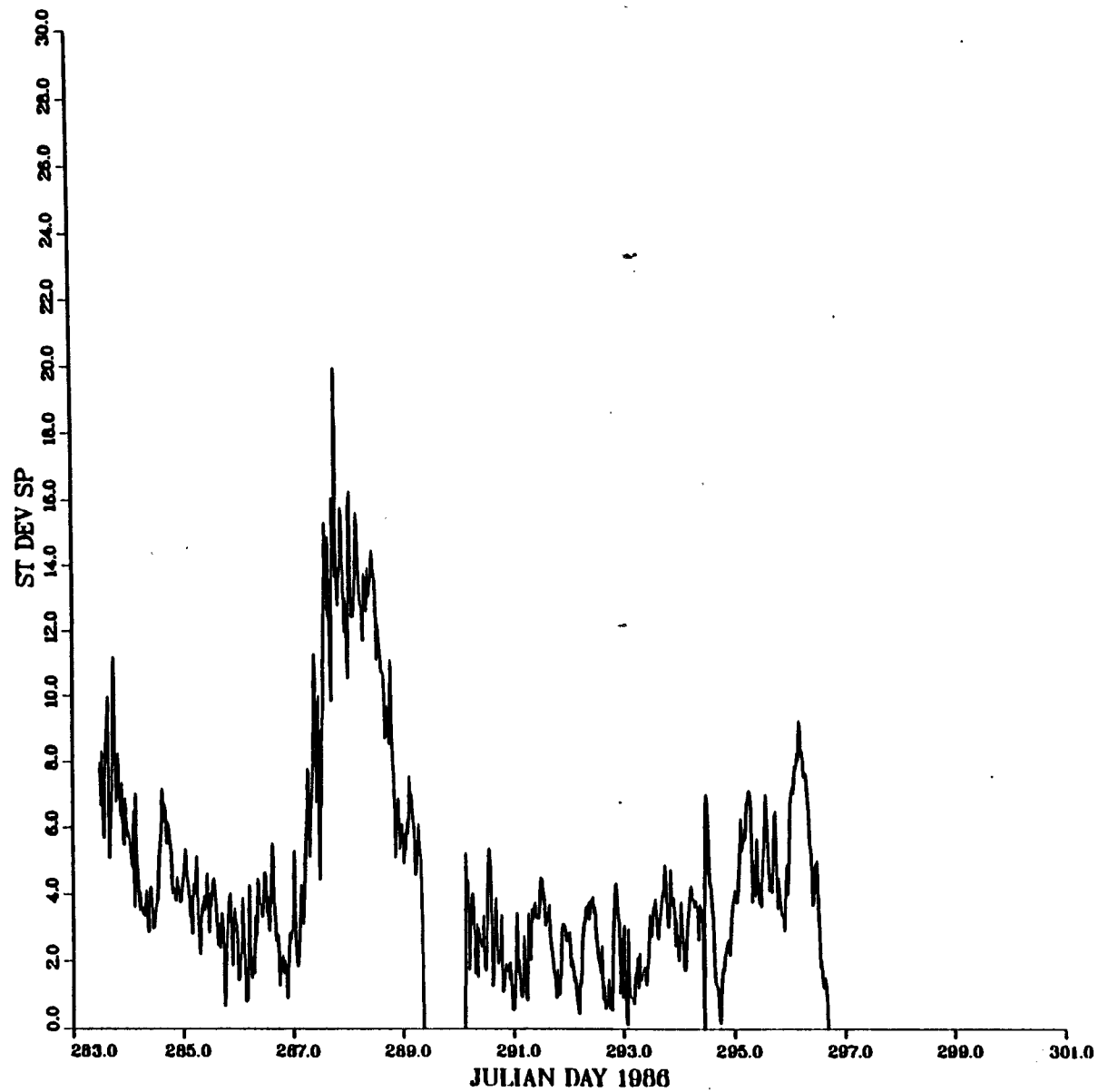
STA 42, OCT 10-NOV 8, 1986



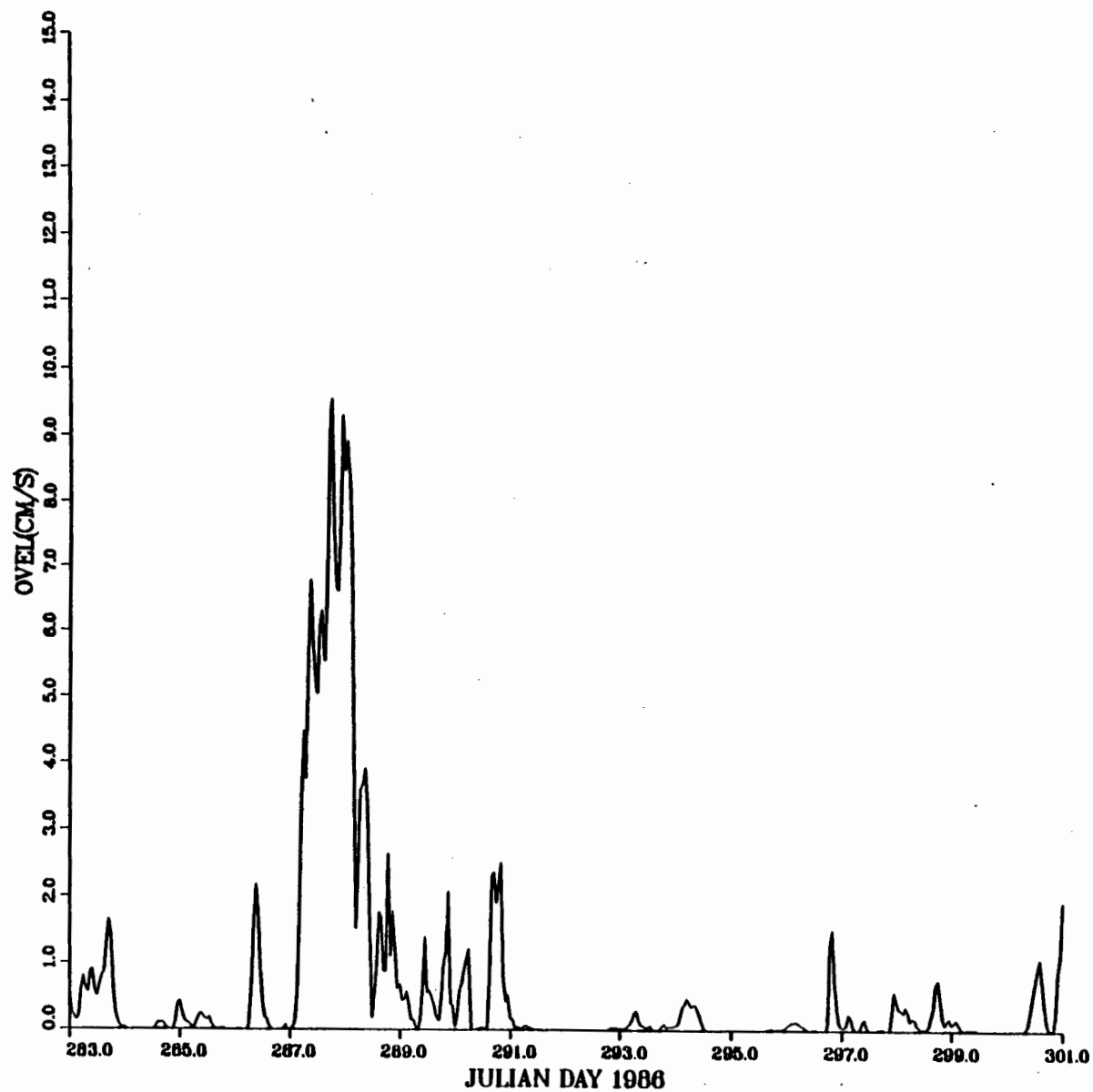
STA 42, OCT 10-NOV 8, 1986



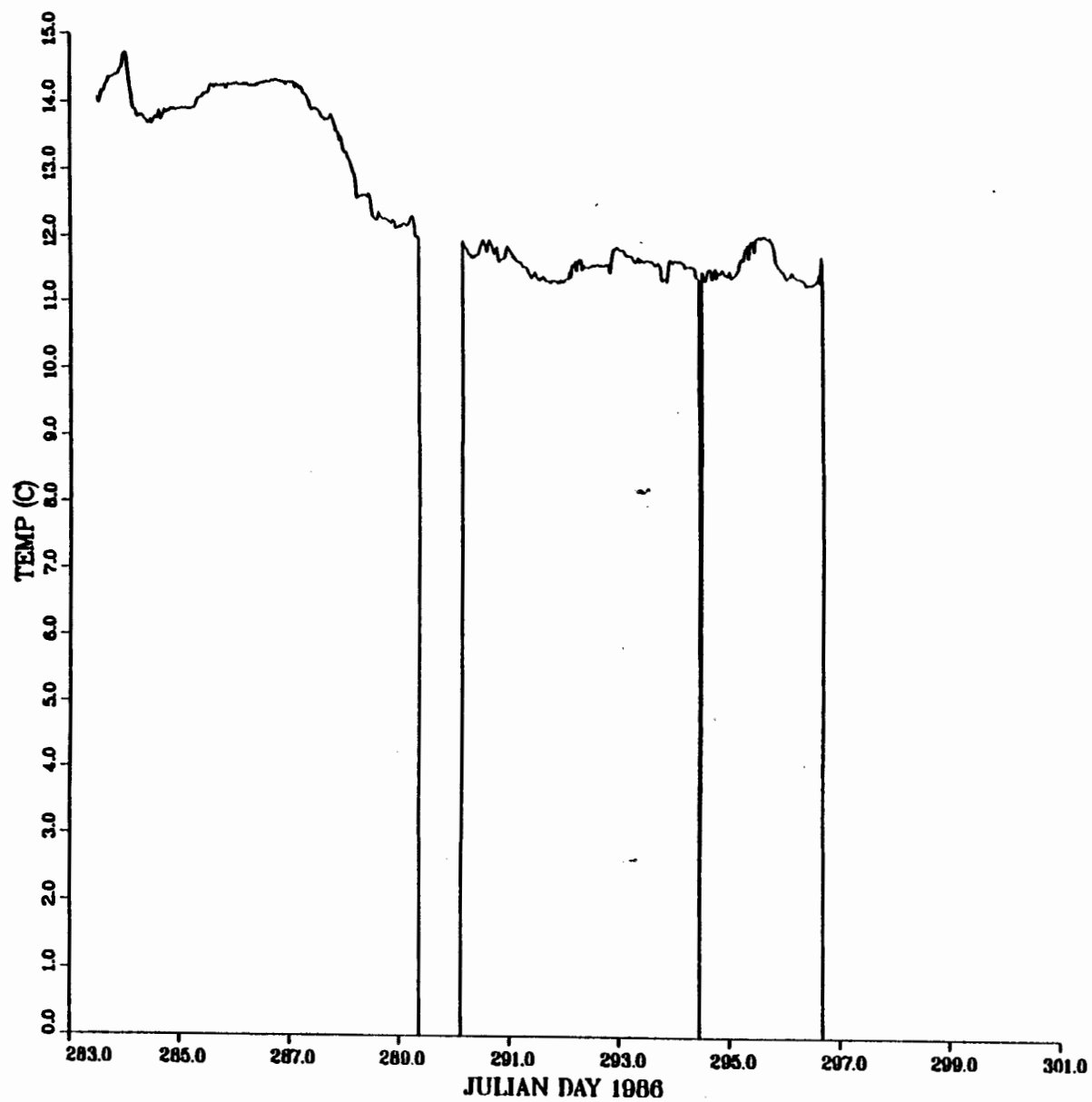
STA 42, OCT 10-NOV 8, 1986



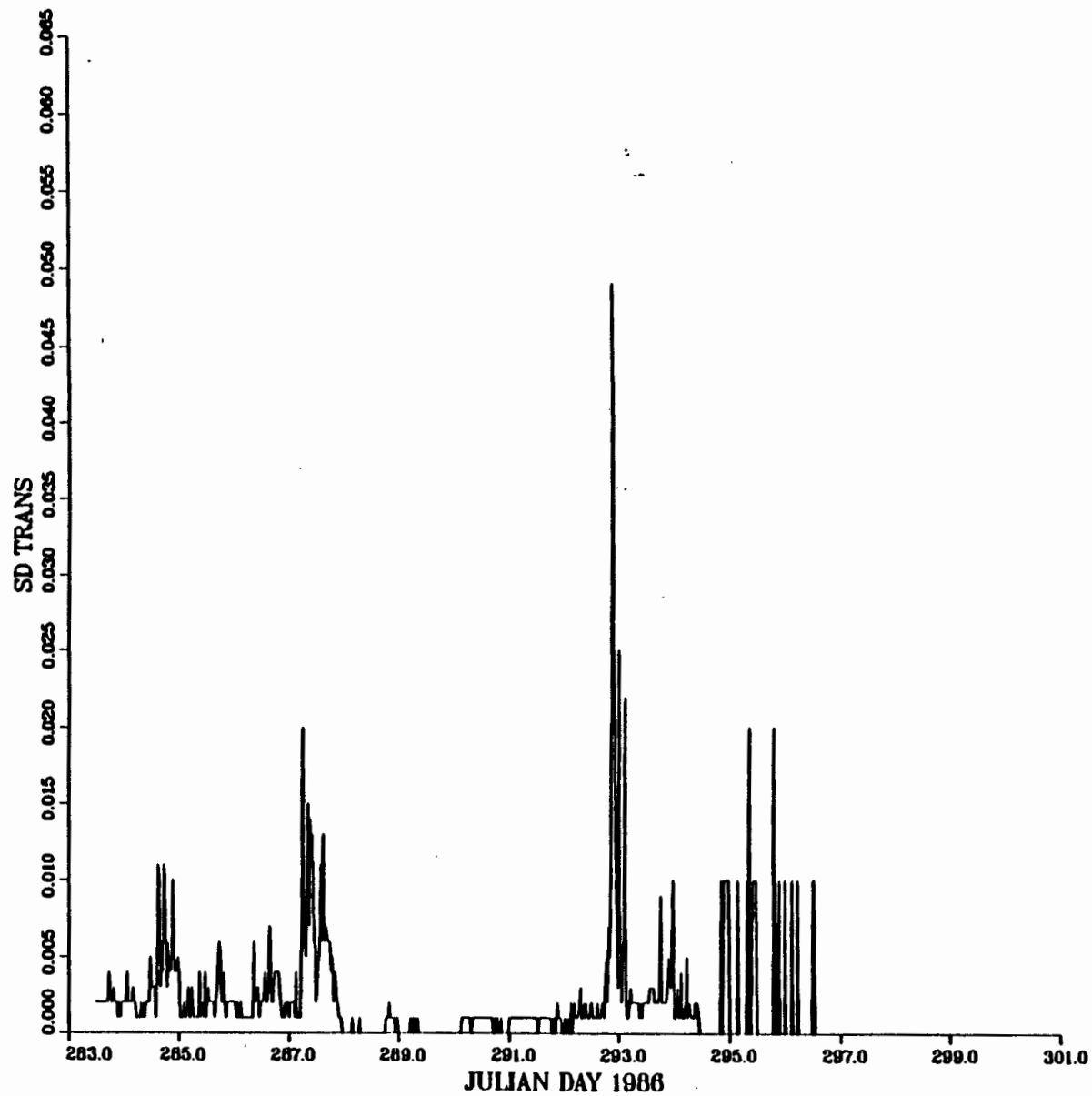
STATION 42 10/1-11/15/86 STARTS AT 0000 EST

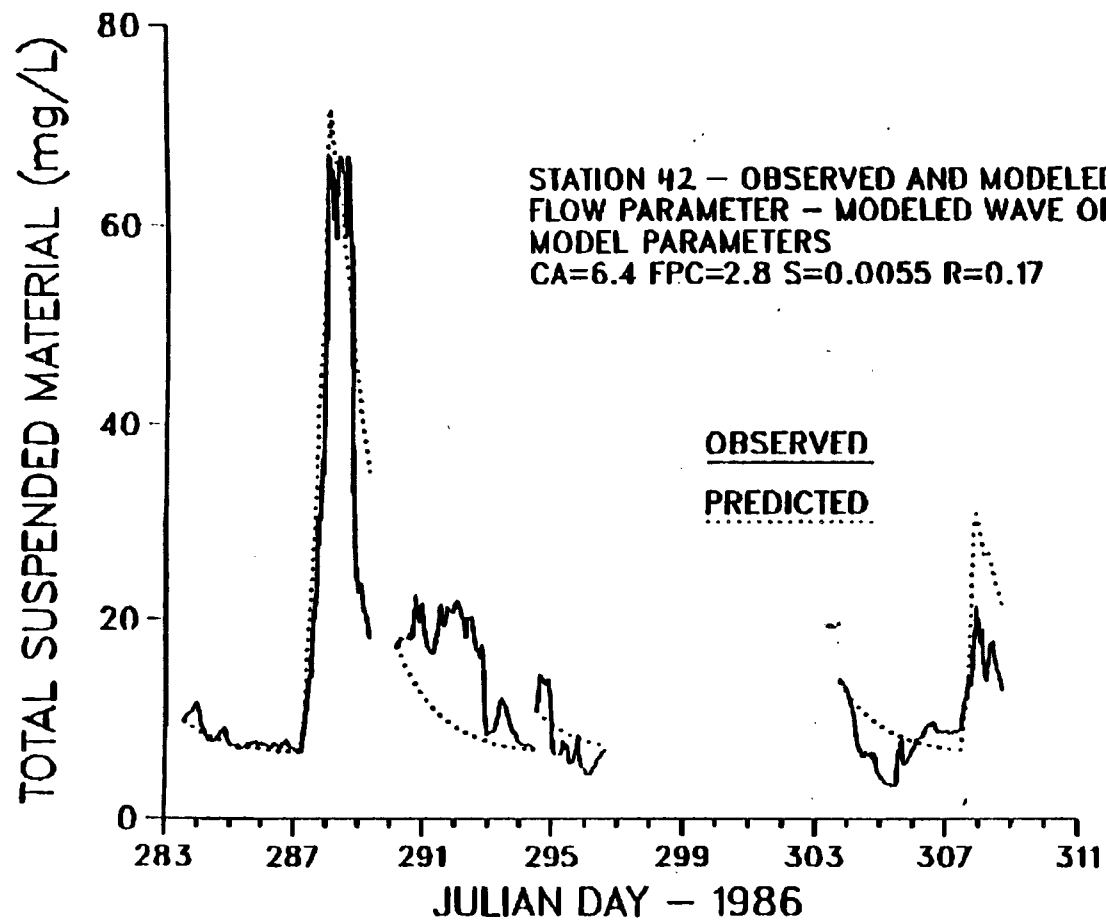


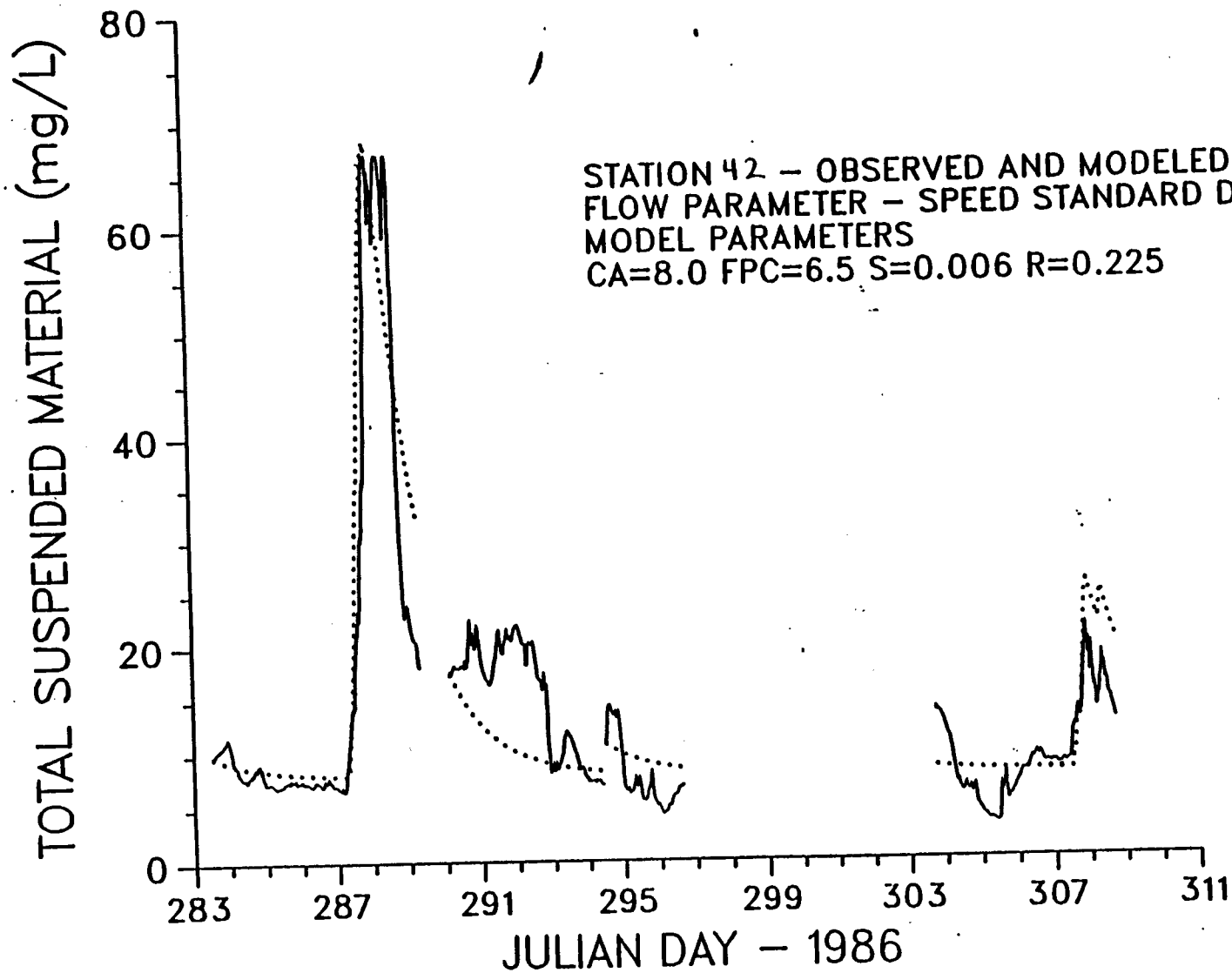
STA 42, OCT 10-NOV 8, 1986



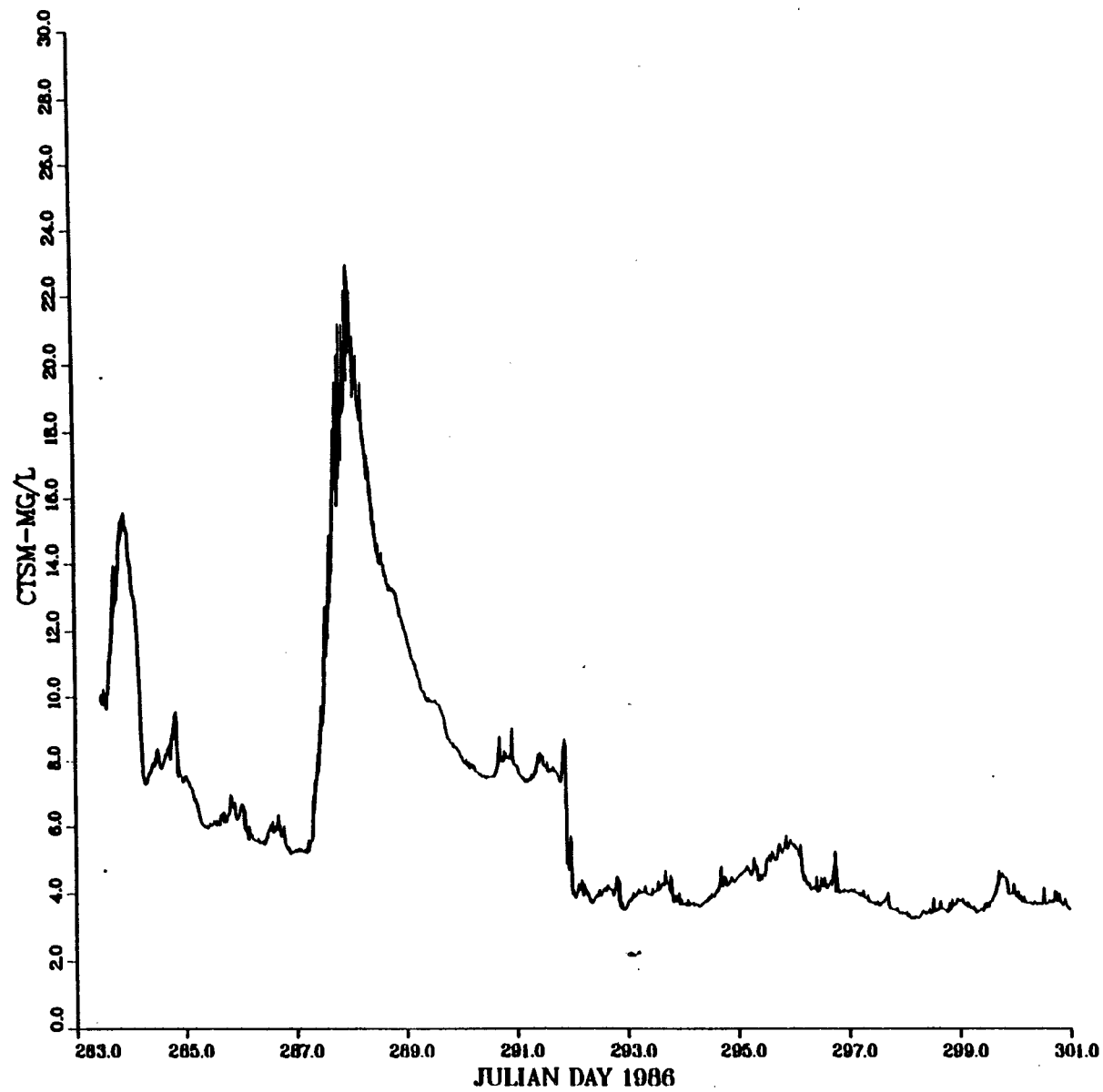
STA 42, OCT 10-NOV 8, 1986



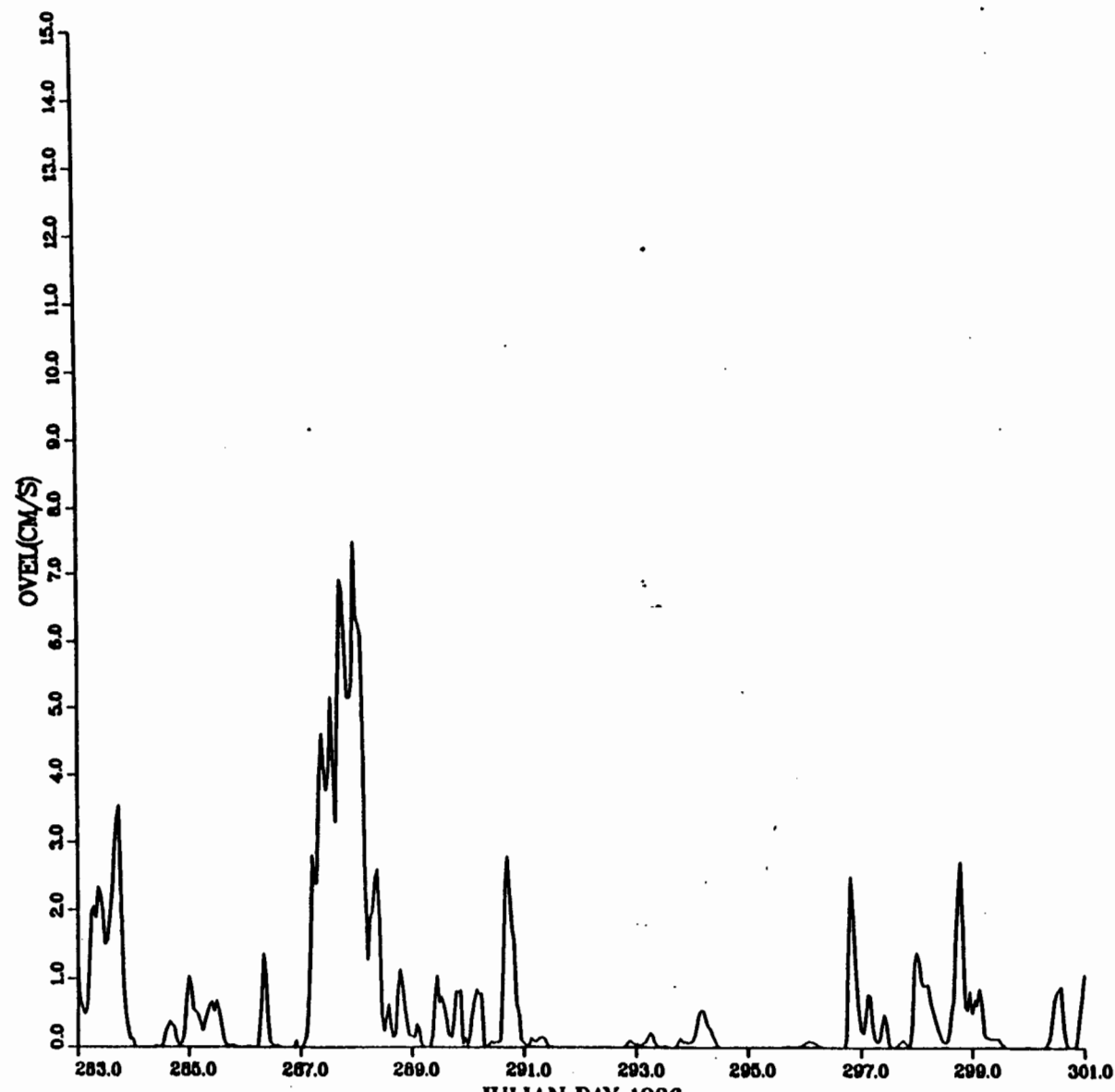




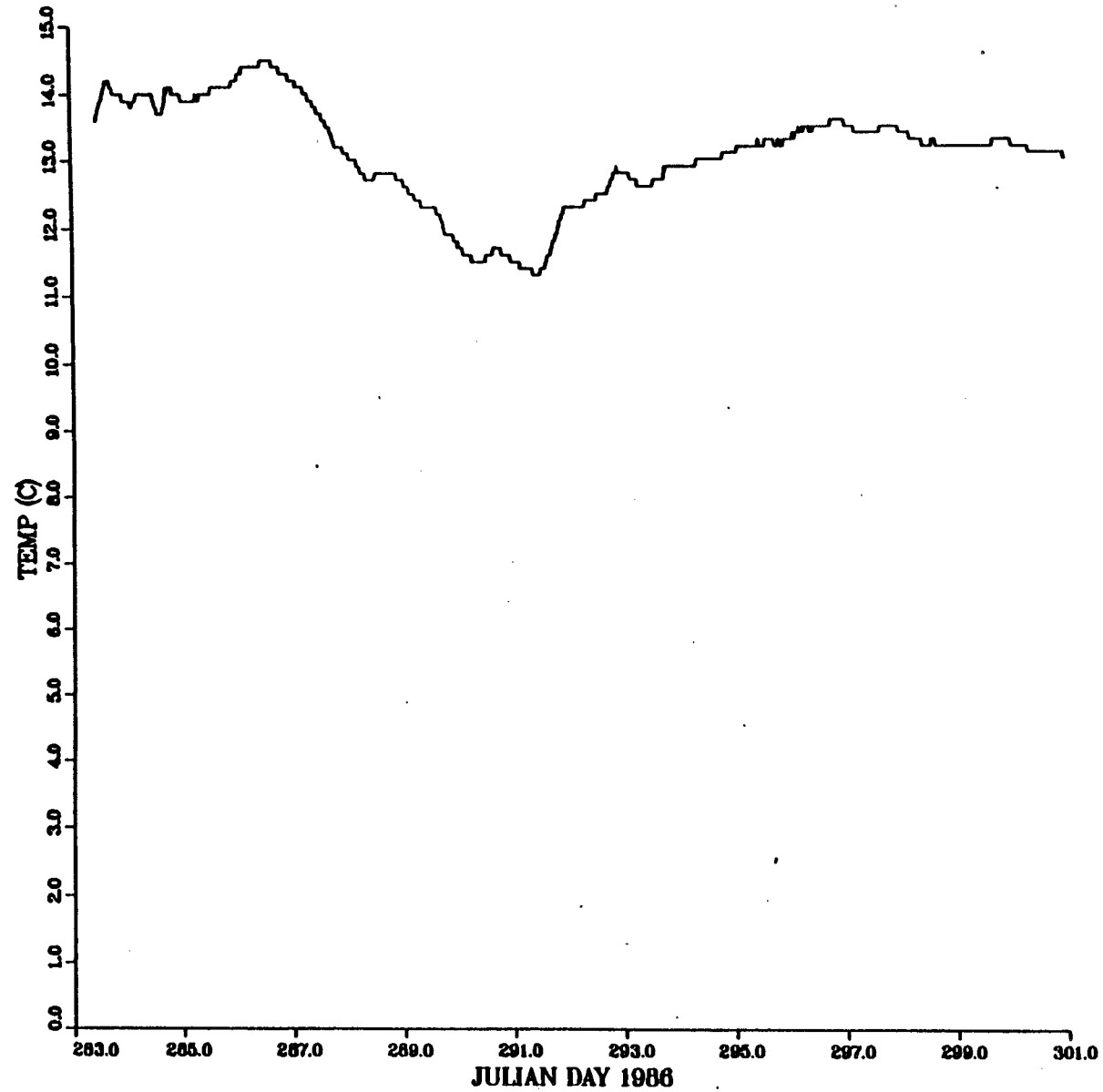
STATION S710CT



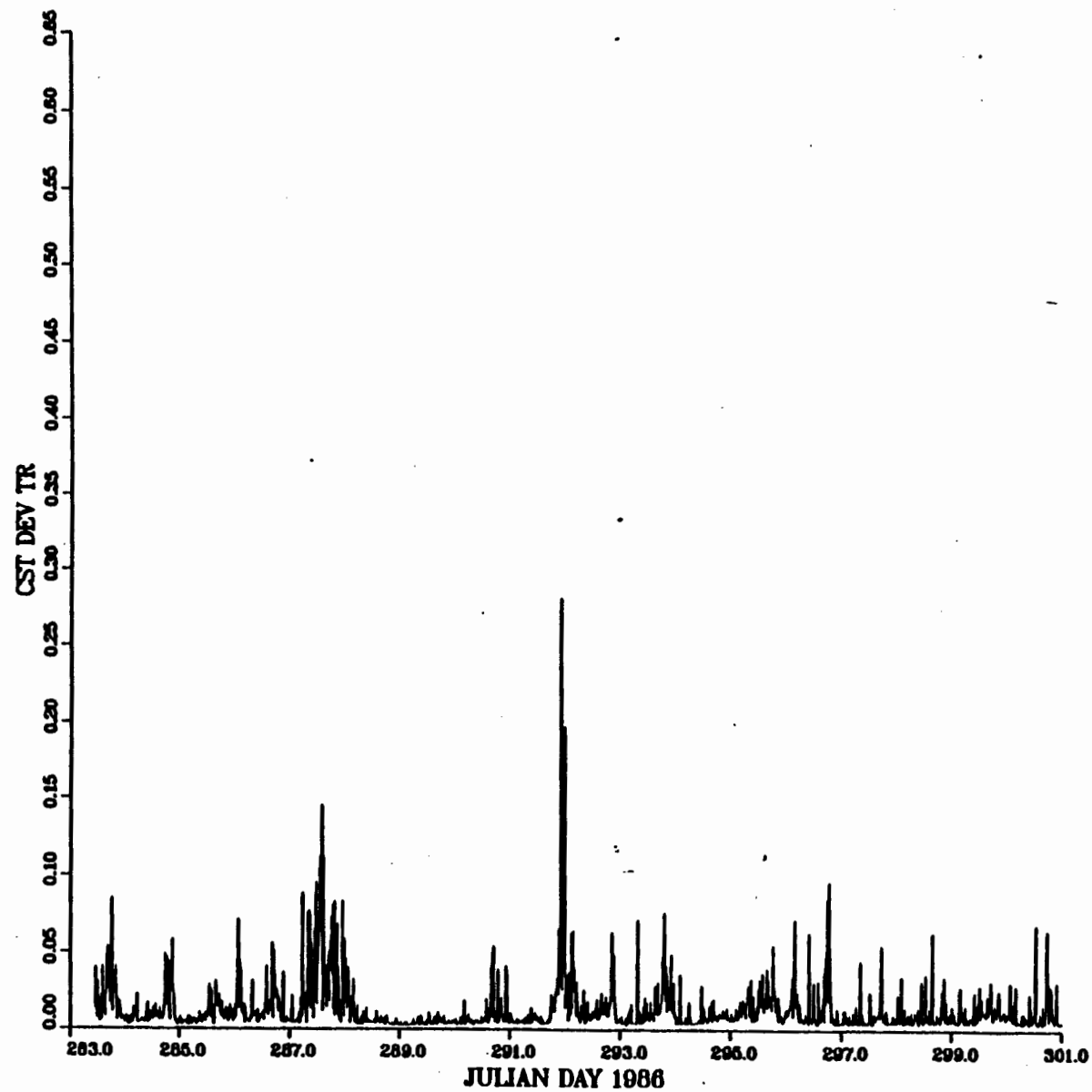
STATION 71 10/1-11/15/86 STARTS AT 0000 EST

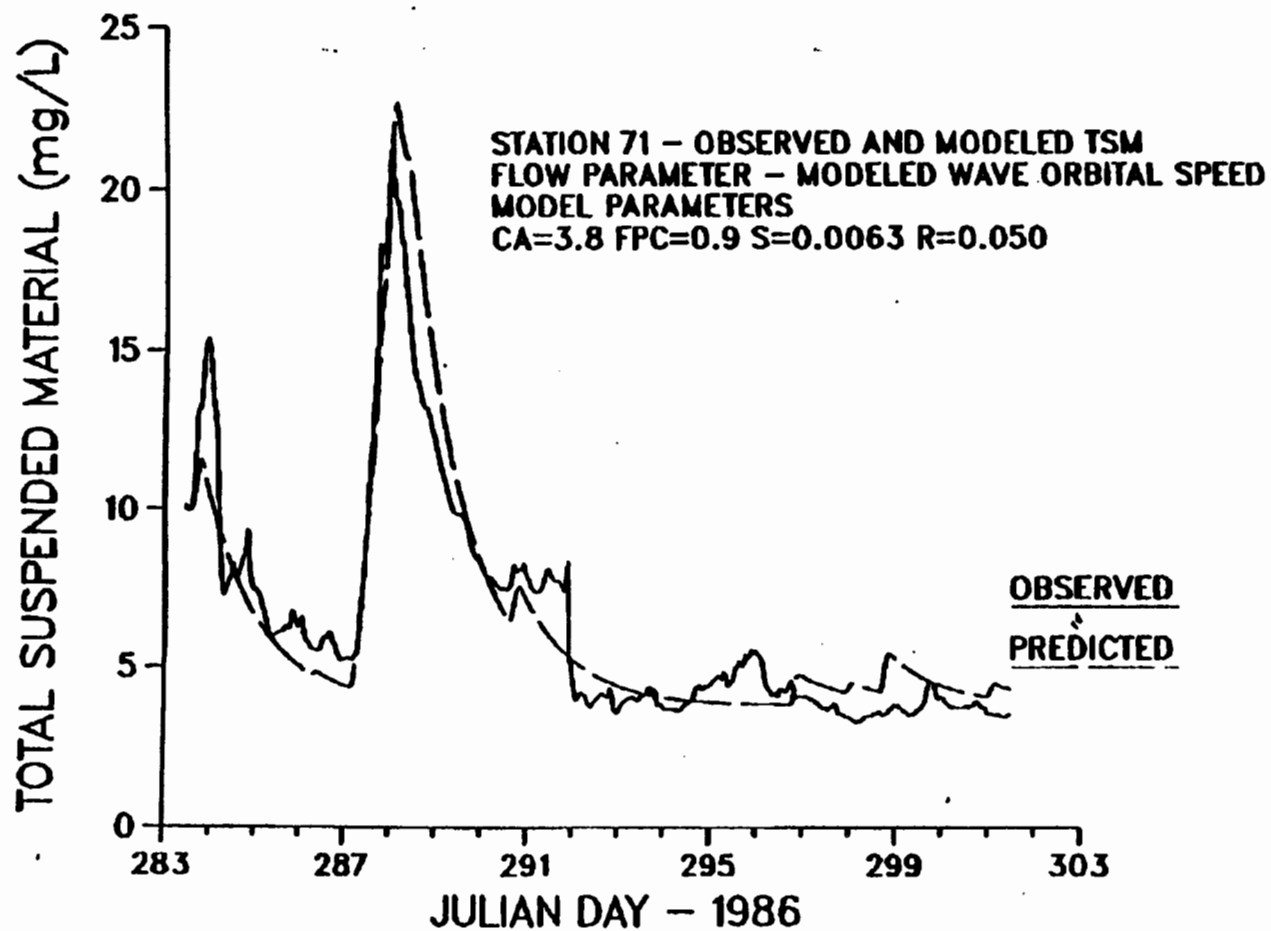


STATION S71OCT

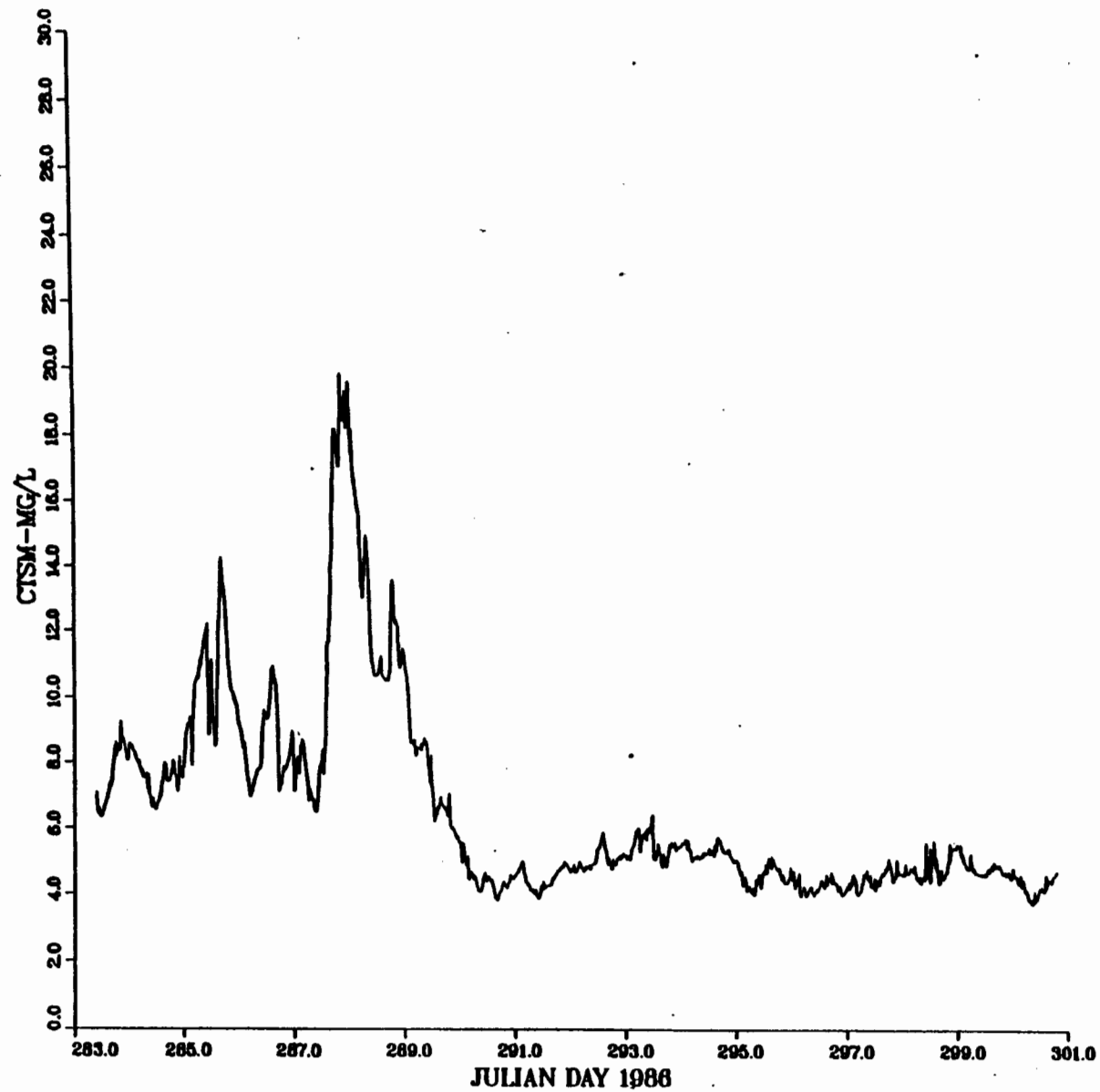


STATION S710CT

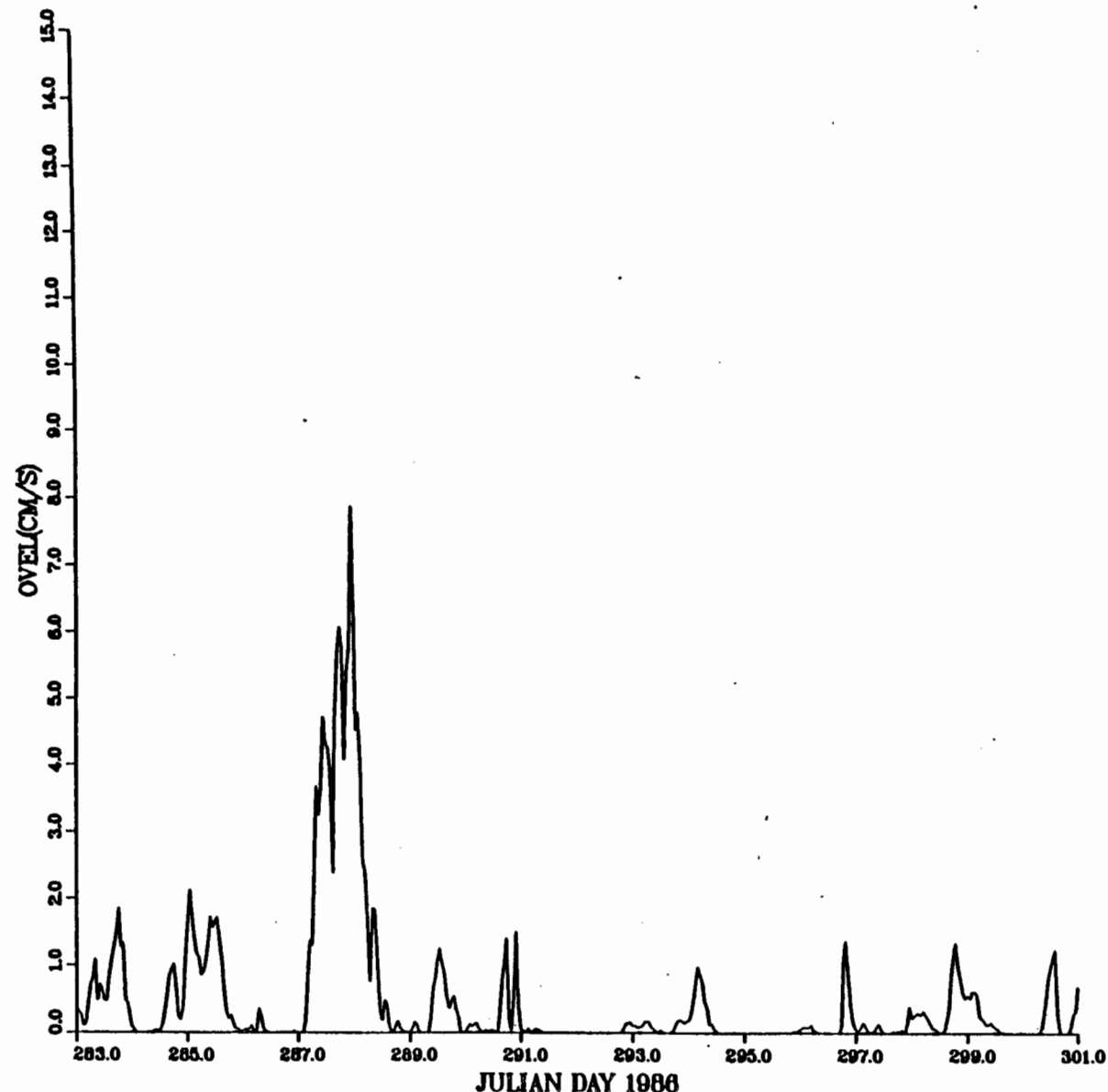




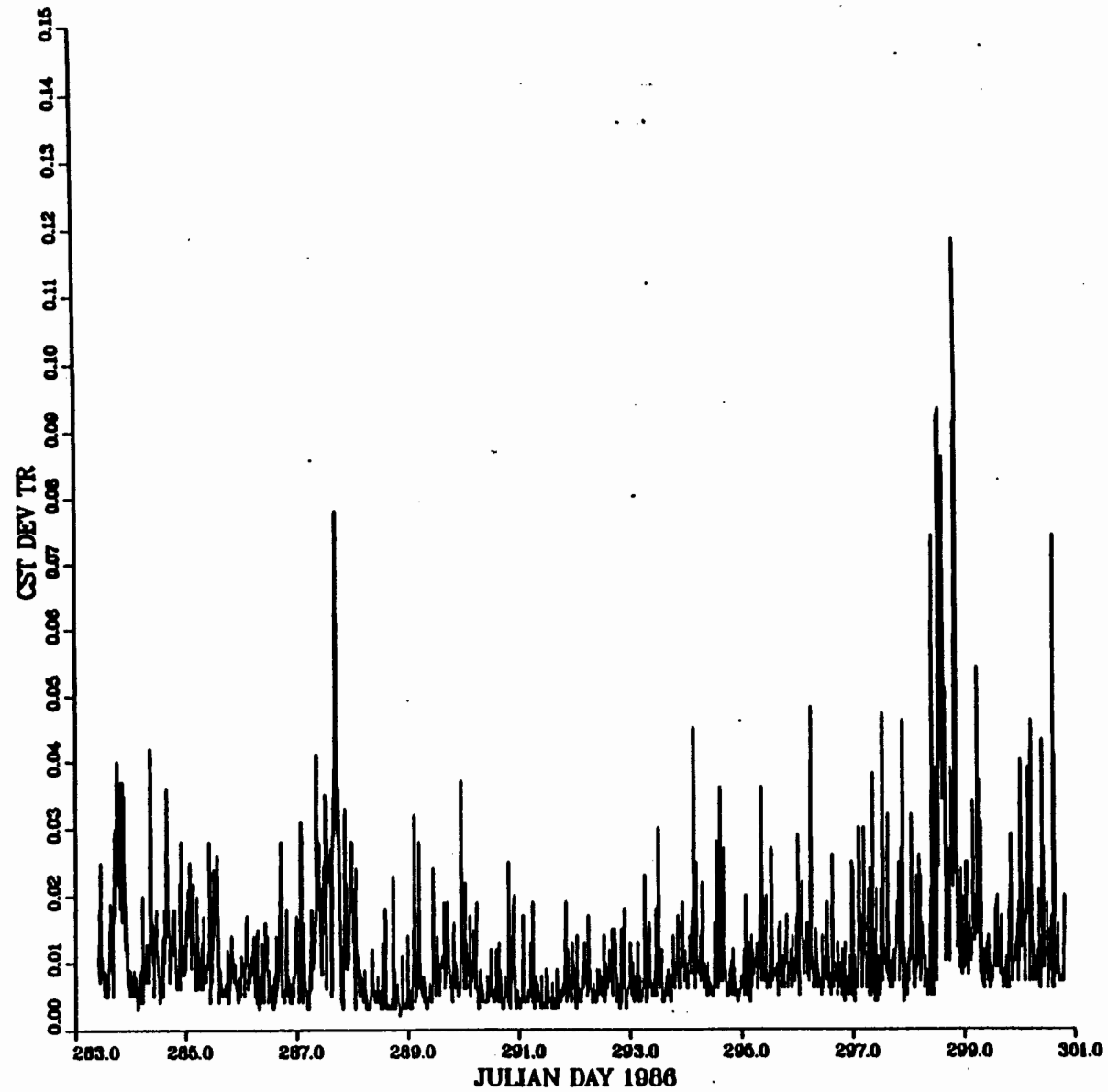
STATION S1-OCT



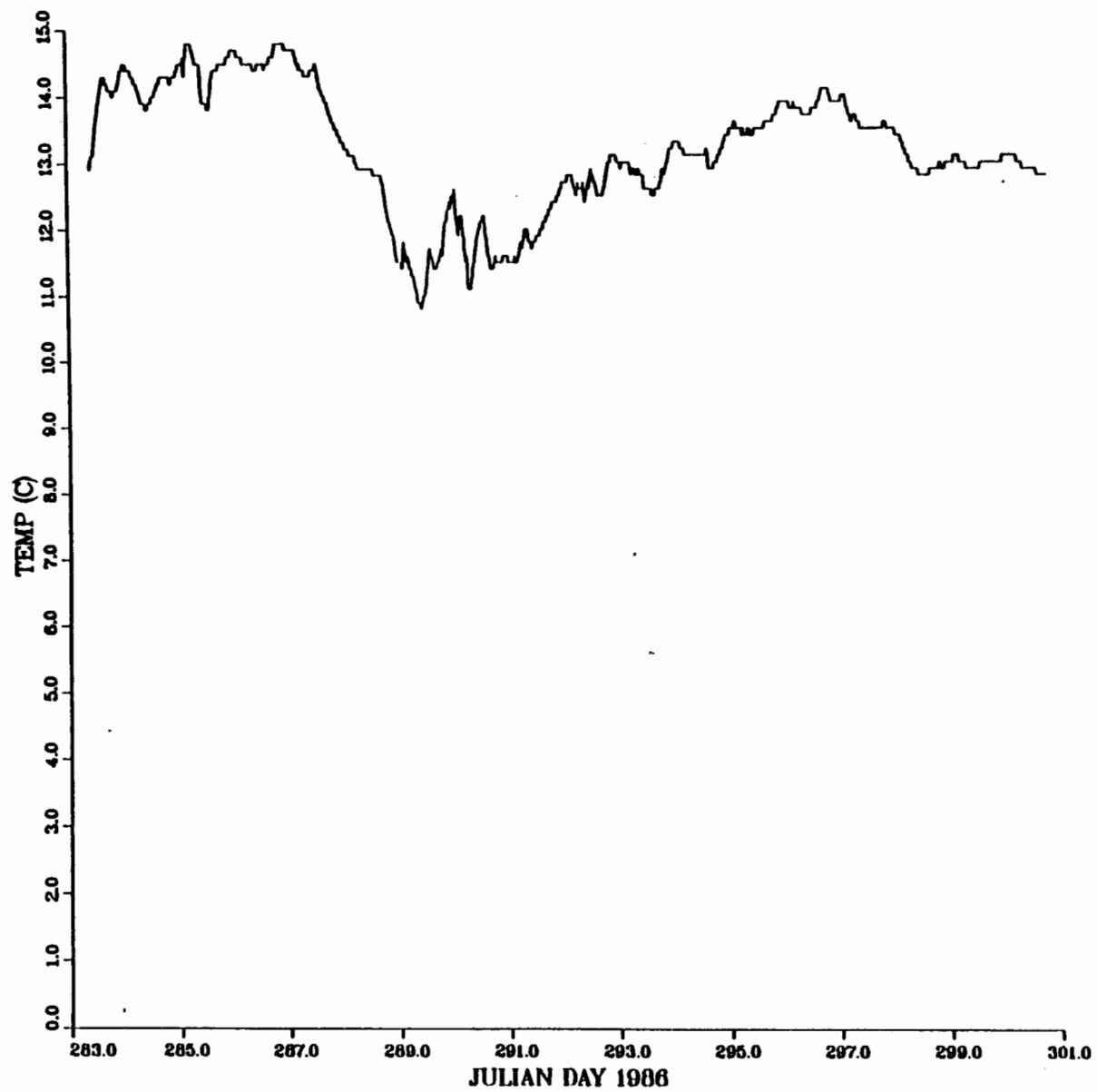
STATION 1 10/1-11/15/86 STARTS AT 0000 EST

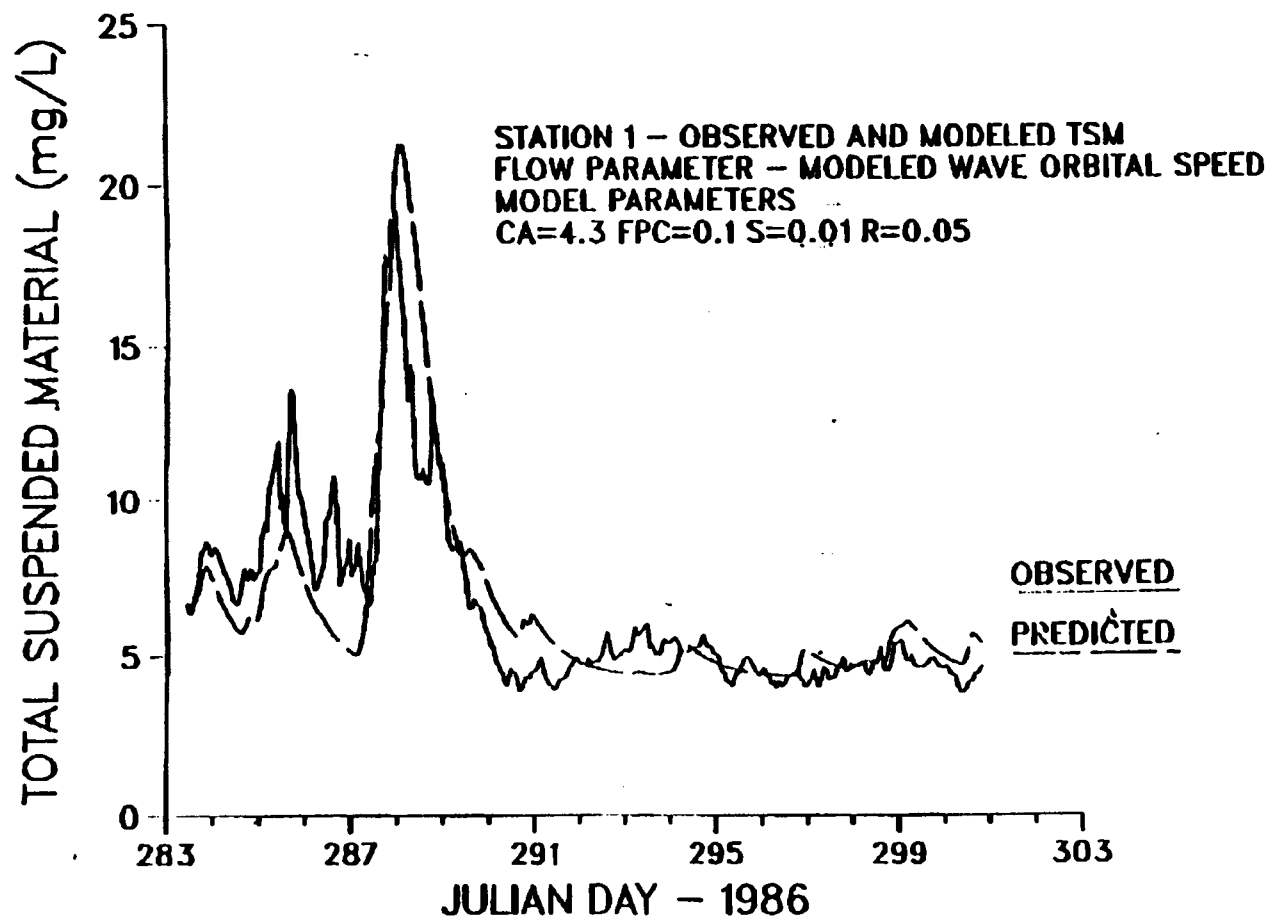


STATION S1-OCT

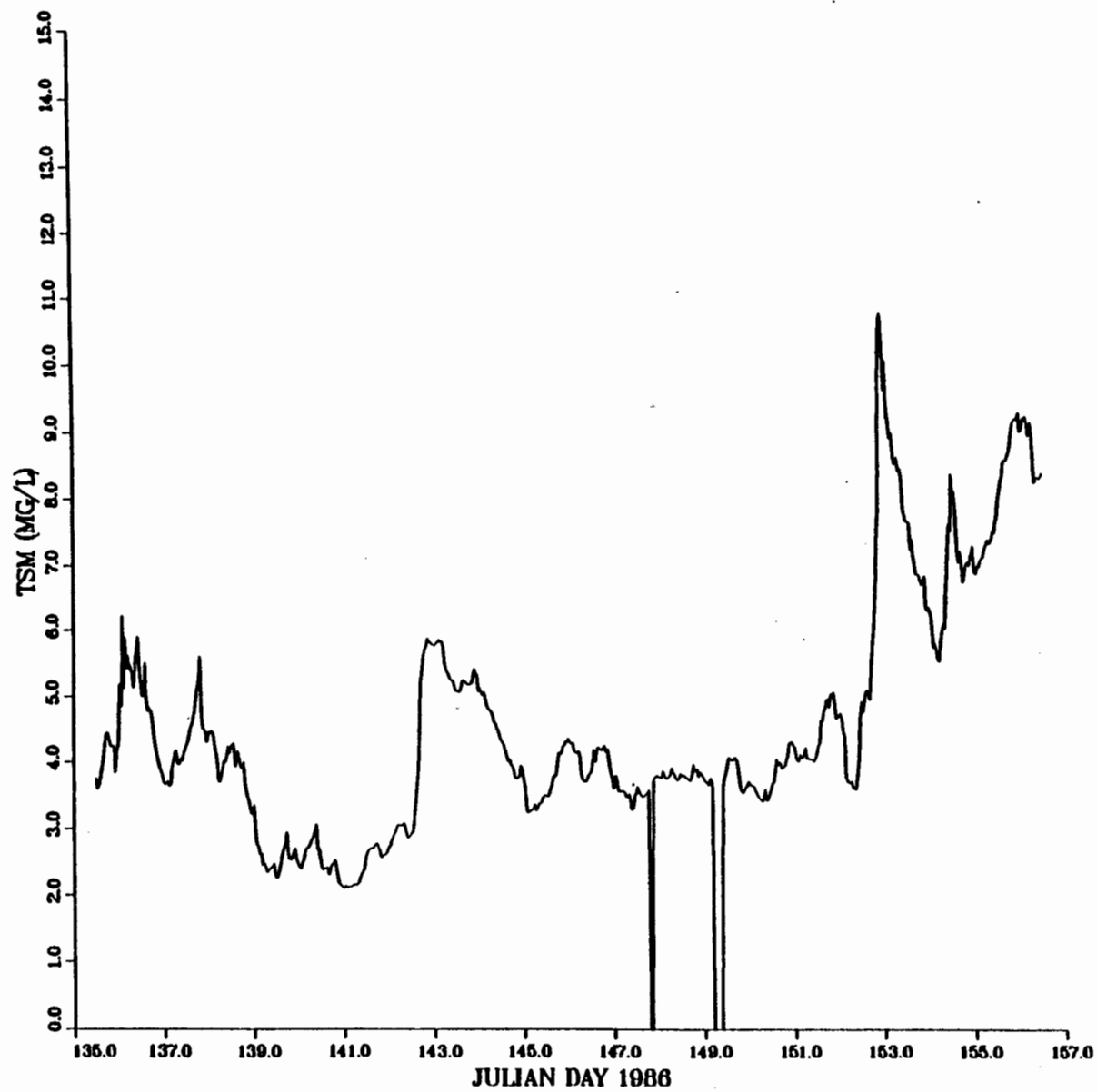


STATION S1-OCT

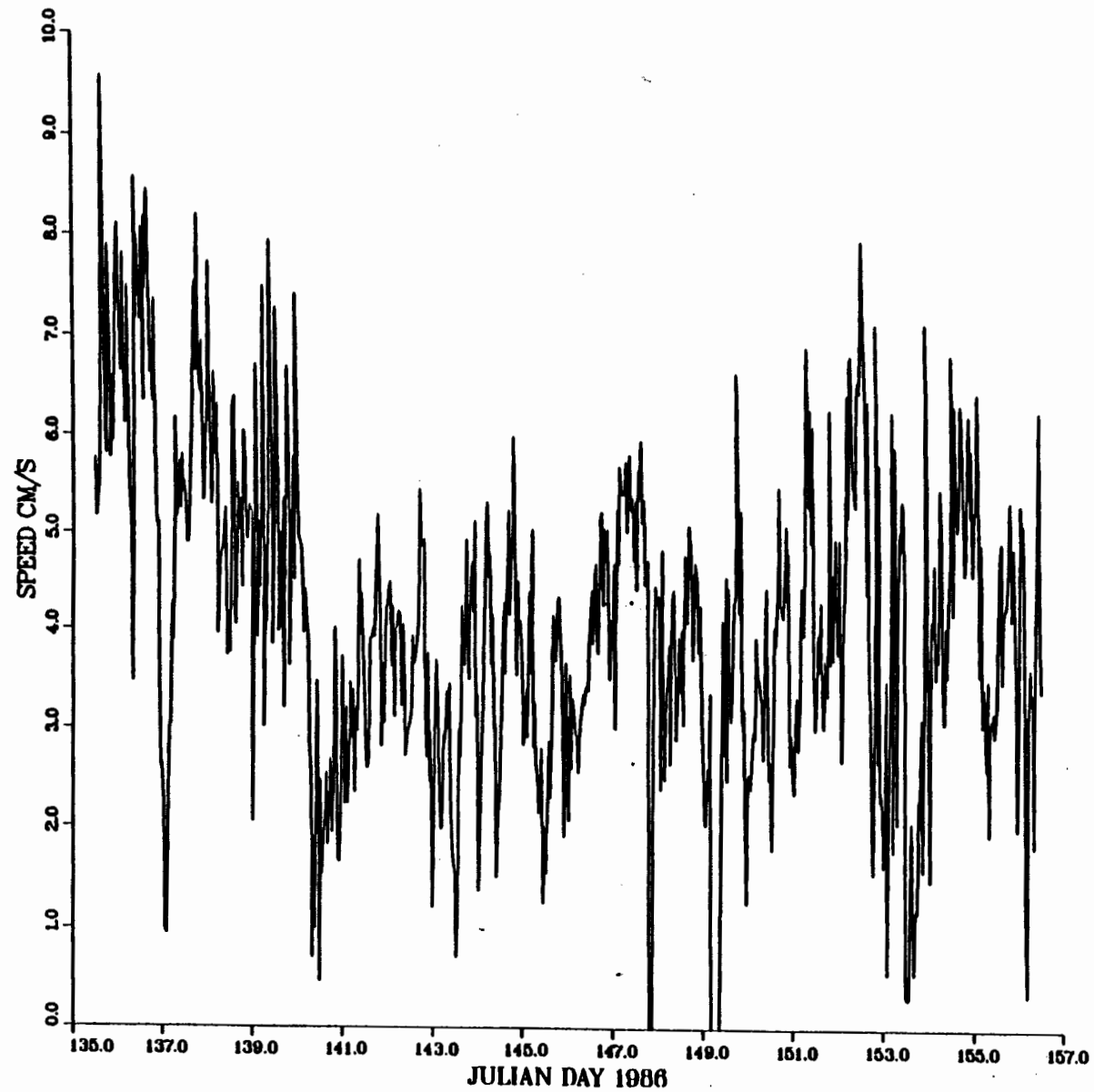




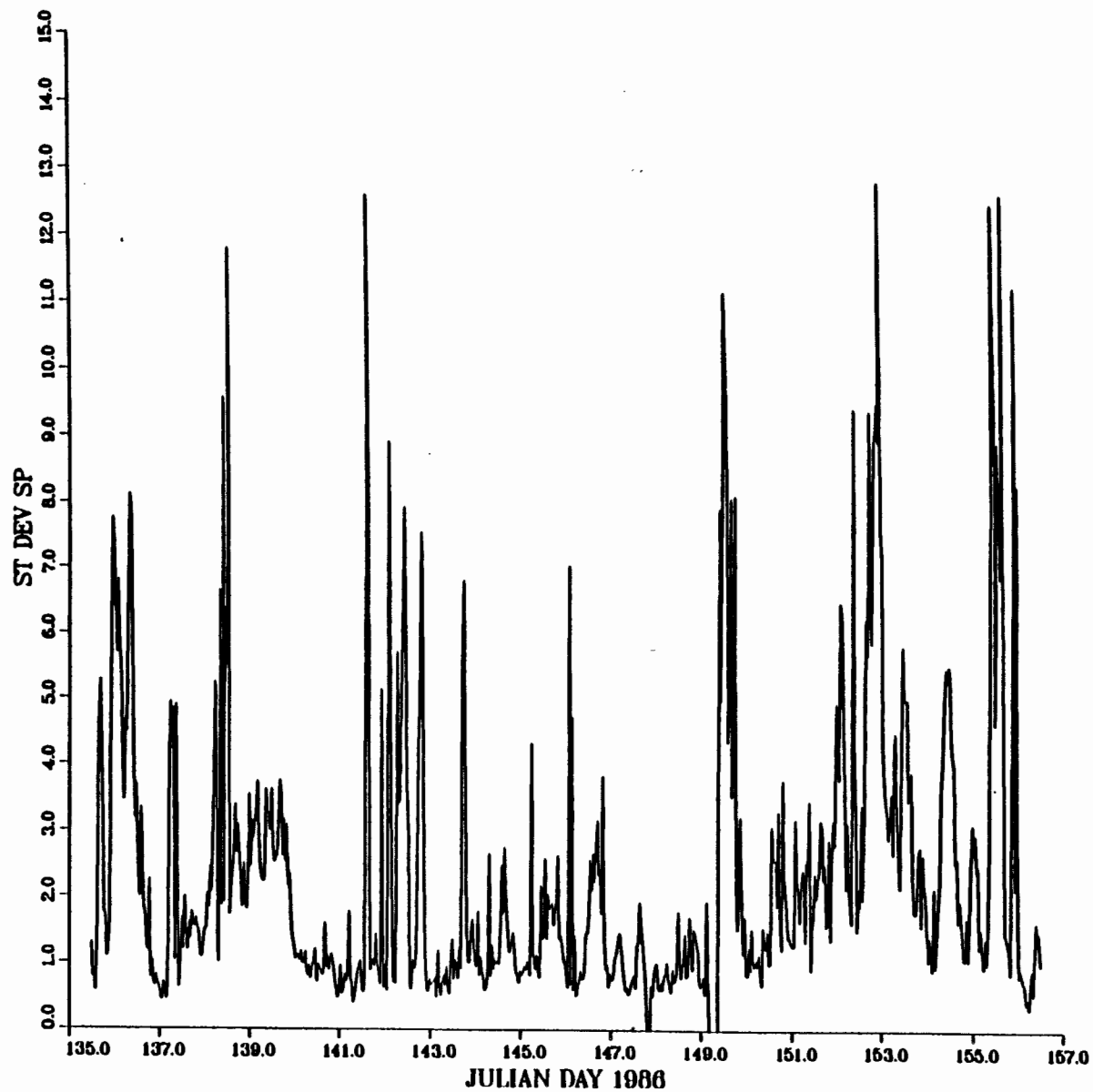
STATION S3 MAY-JUNE, 1986



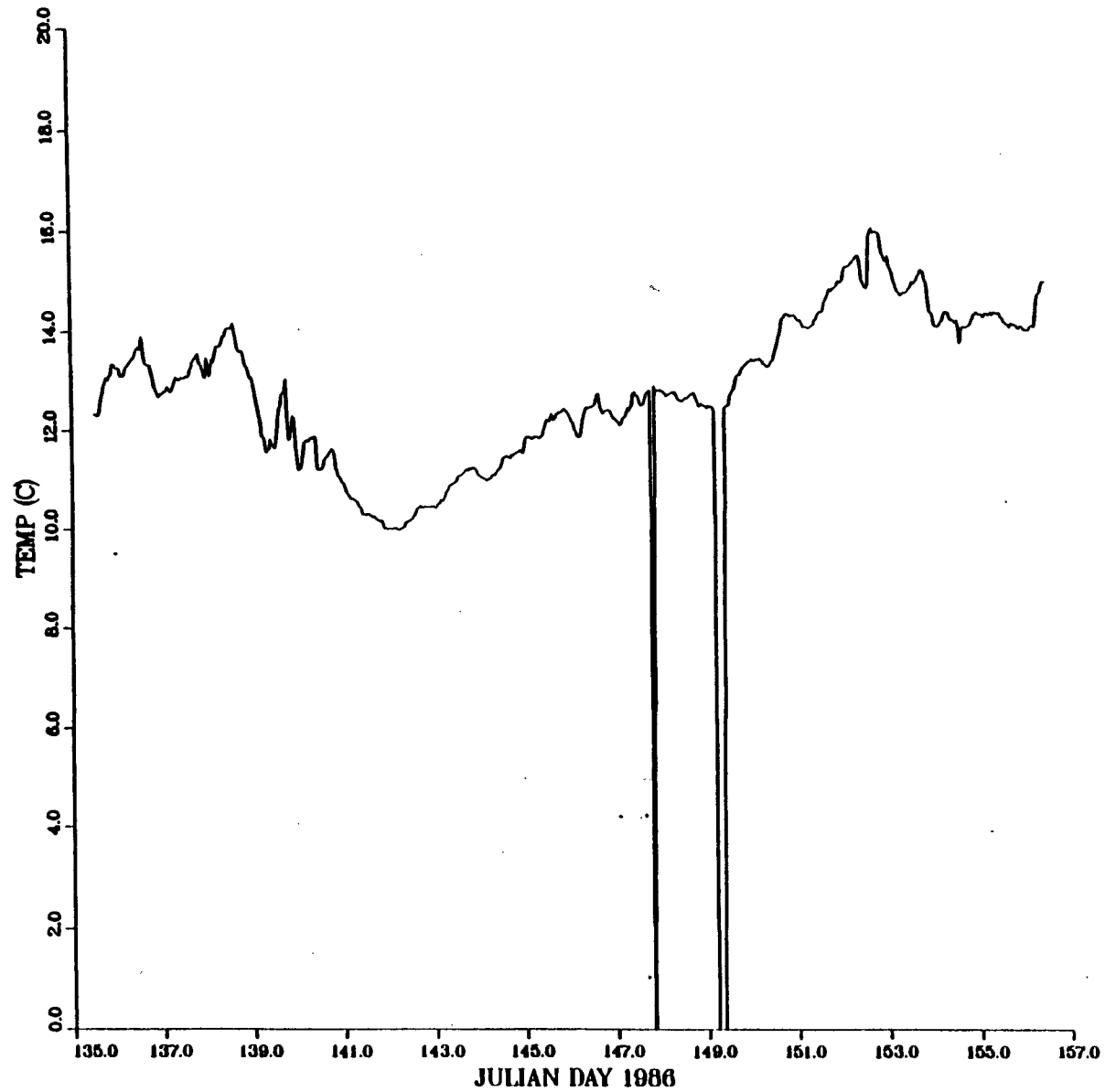
STATION S3 MAY-JUNE, 1986

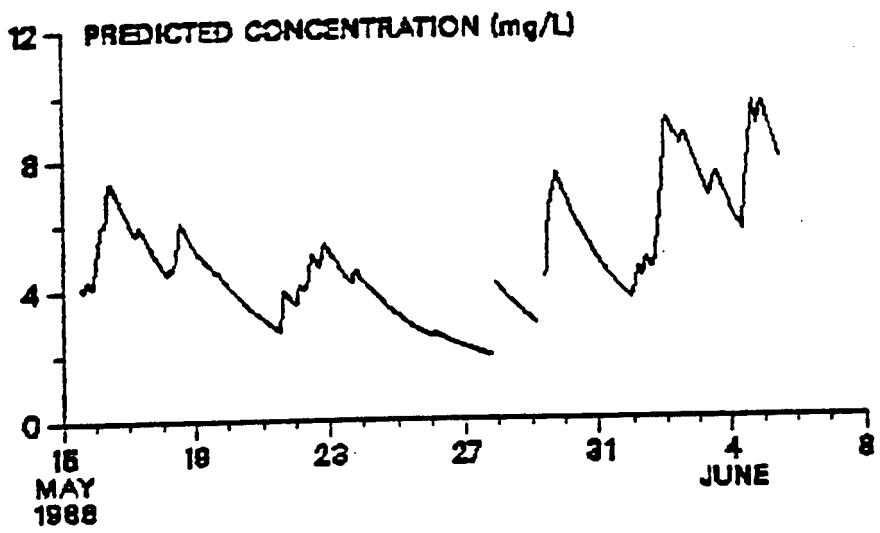
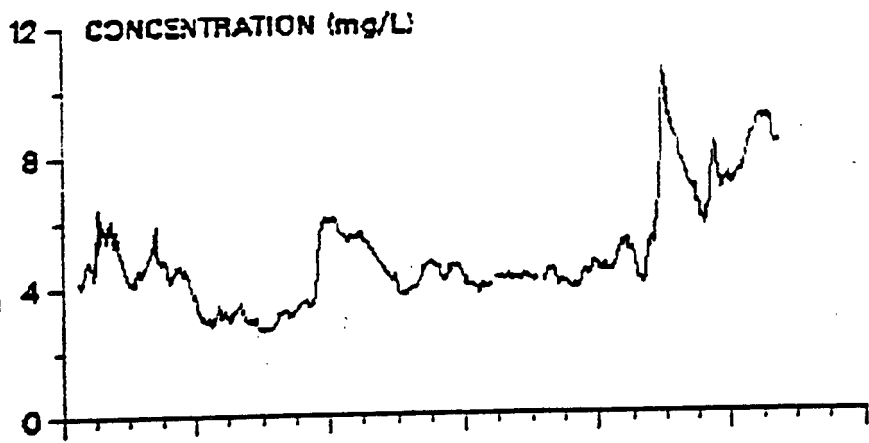


STATION S3 MAY-JUNE, 1986

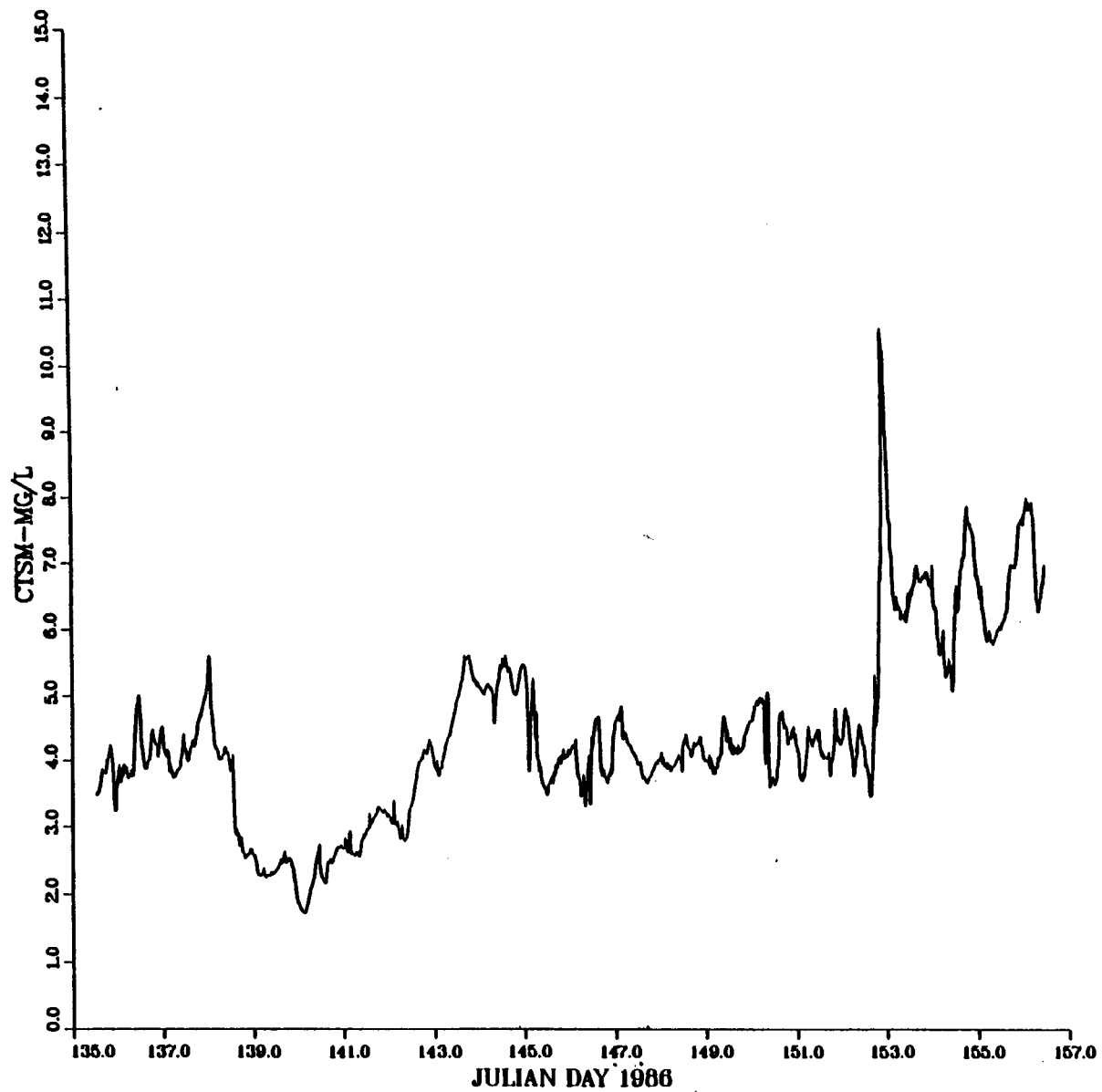


STATION S3 MAY-JUNE, 1986

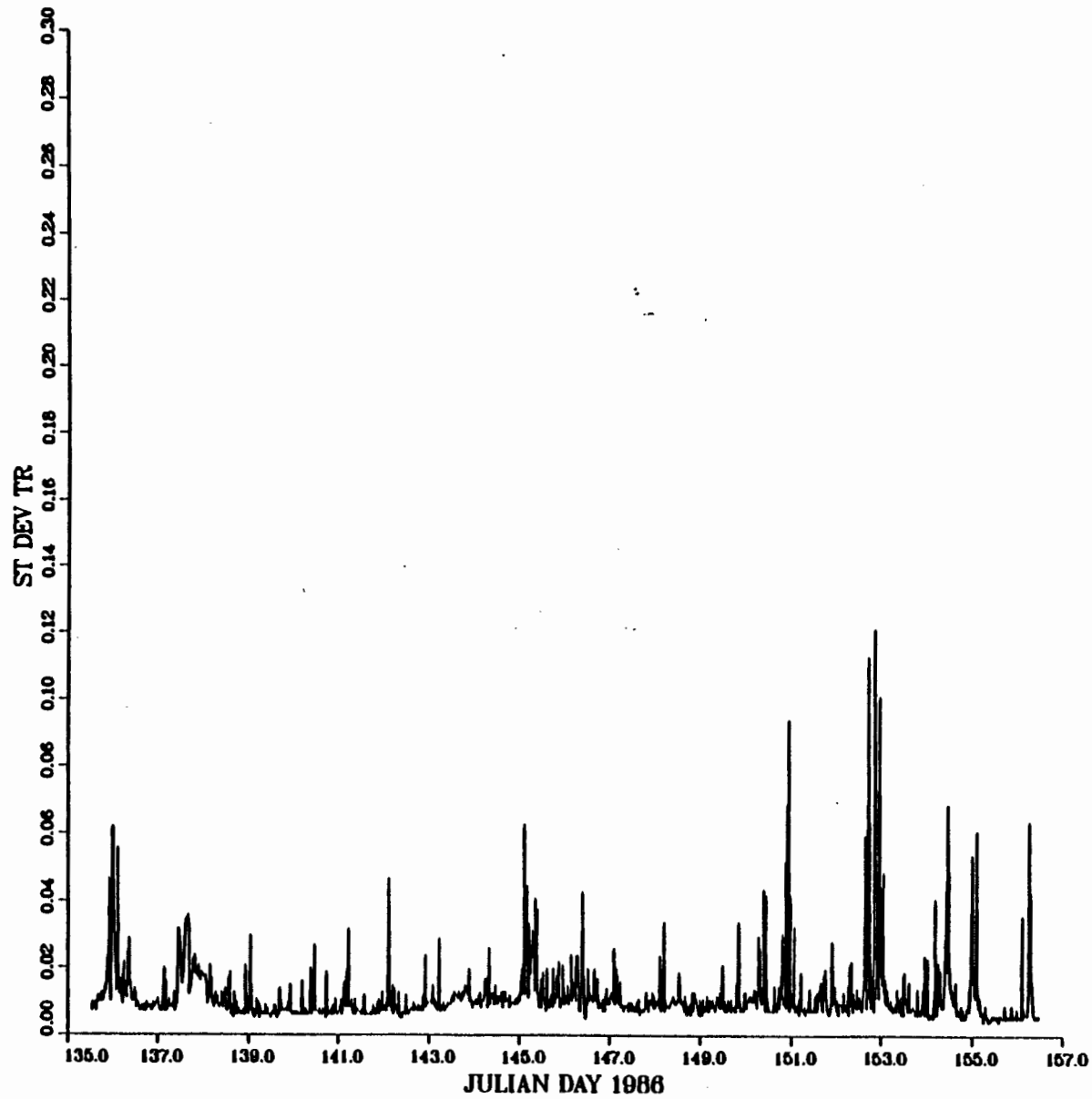




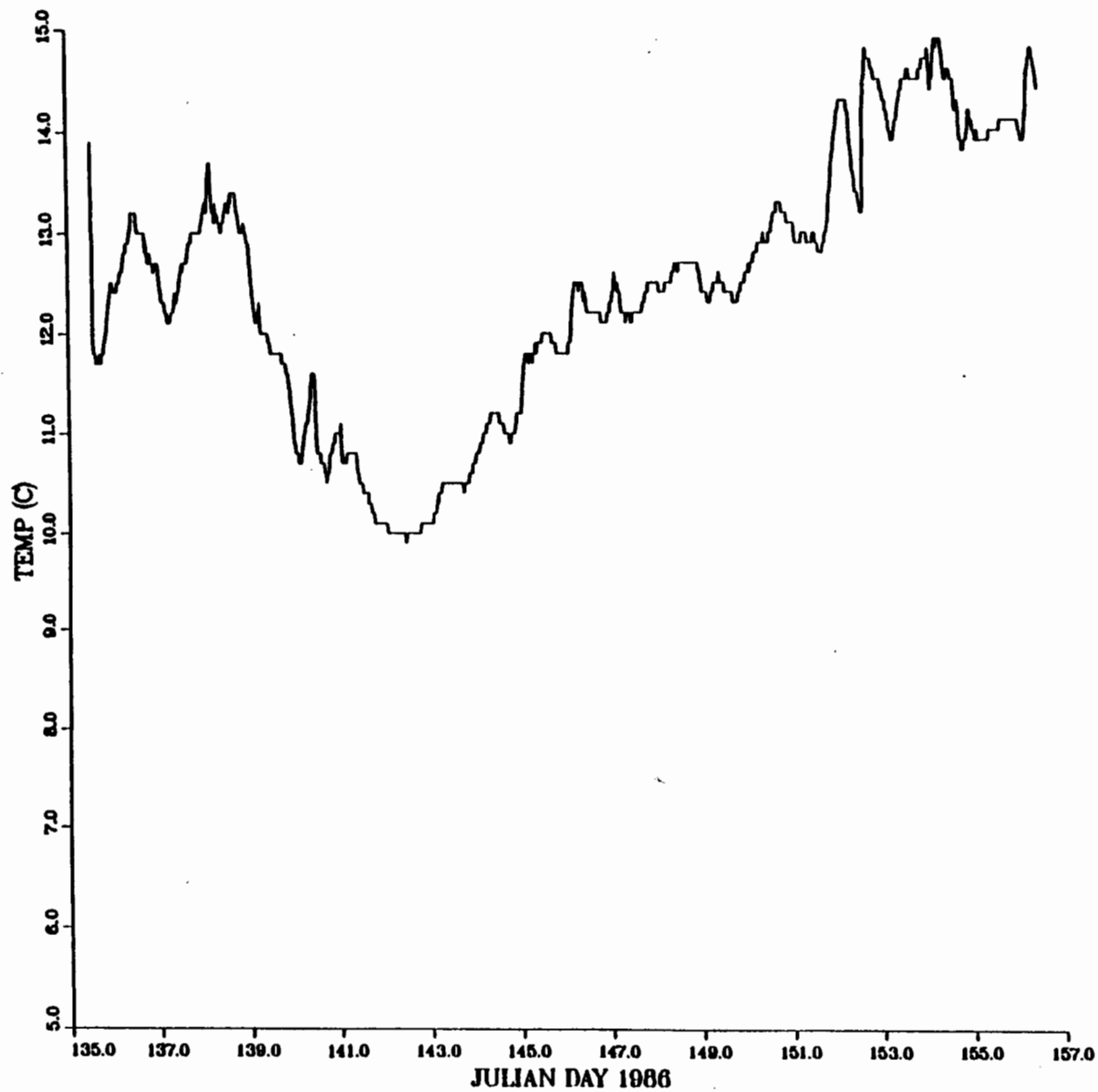
STATION S5-MJ



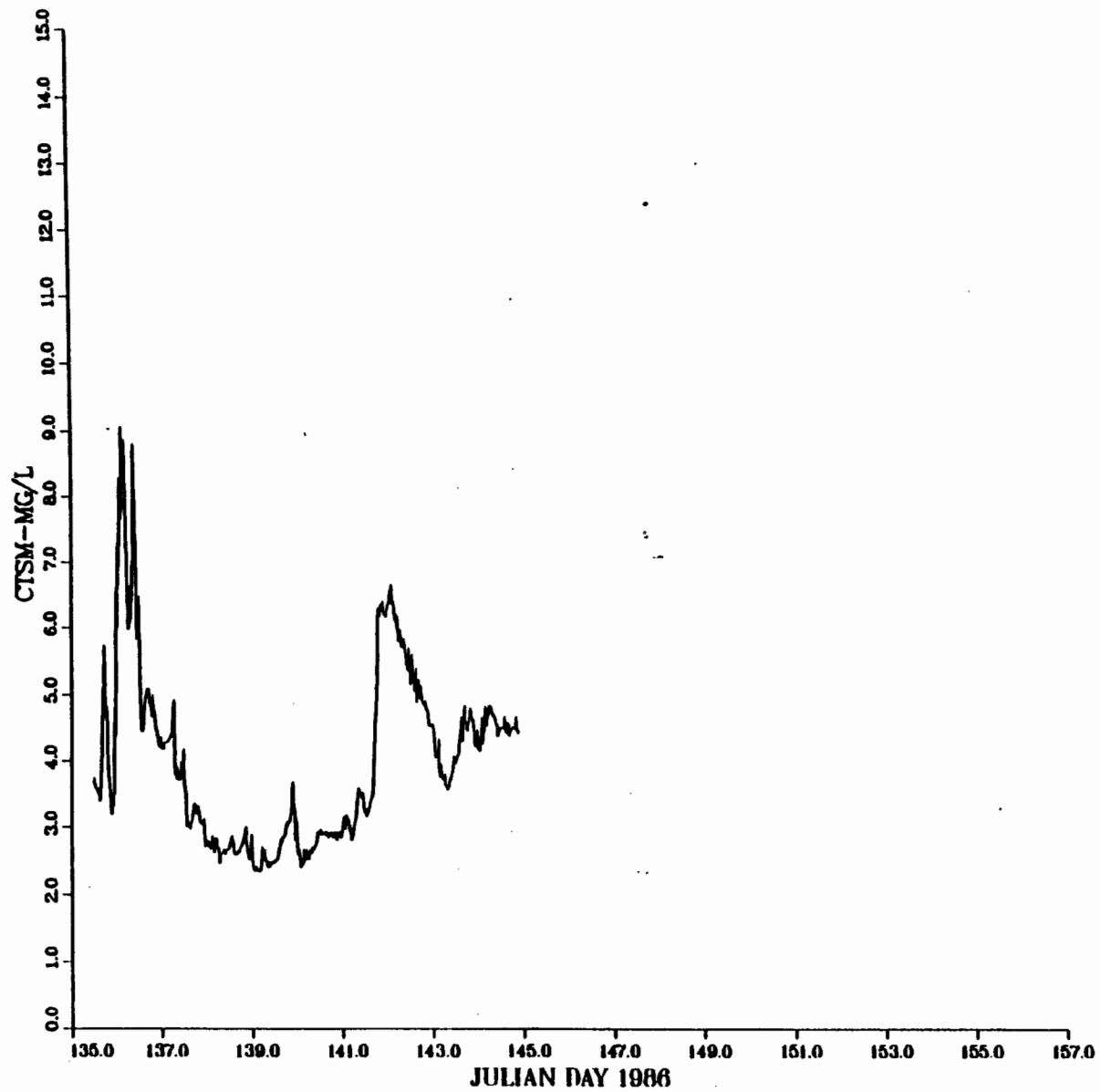
STATION S5-MJ



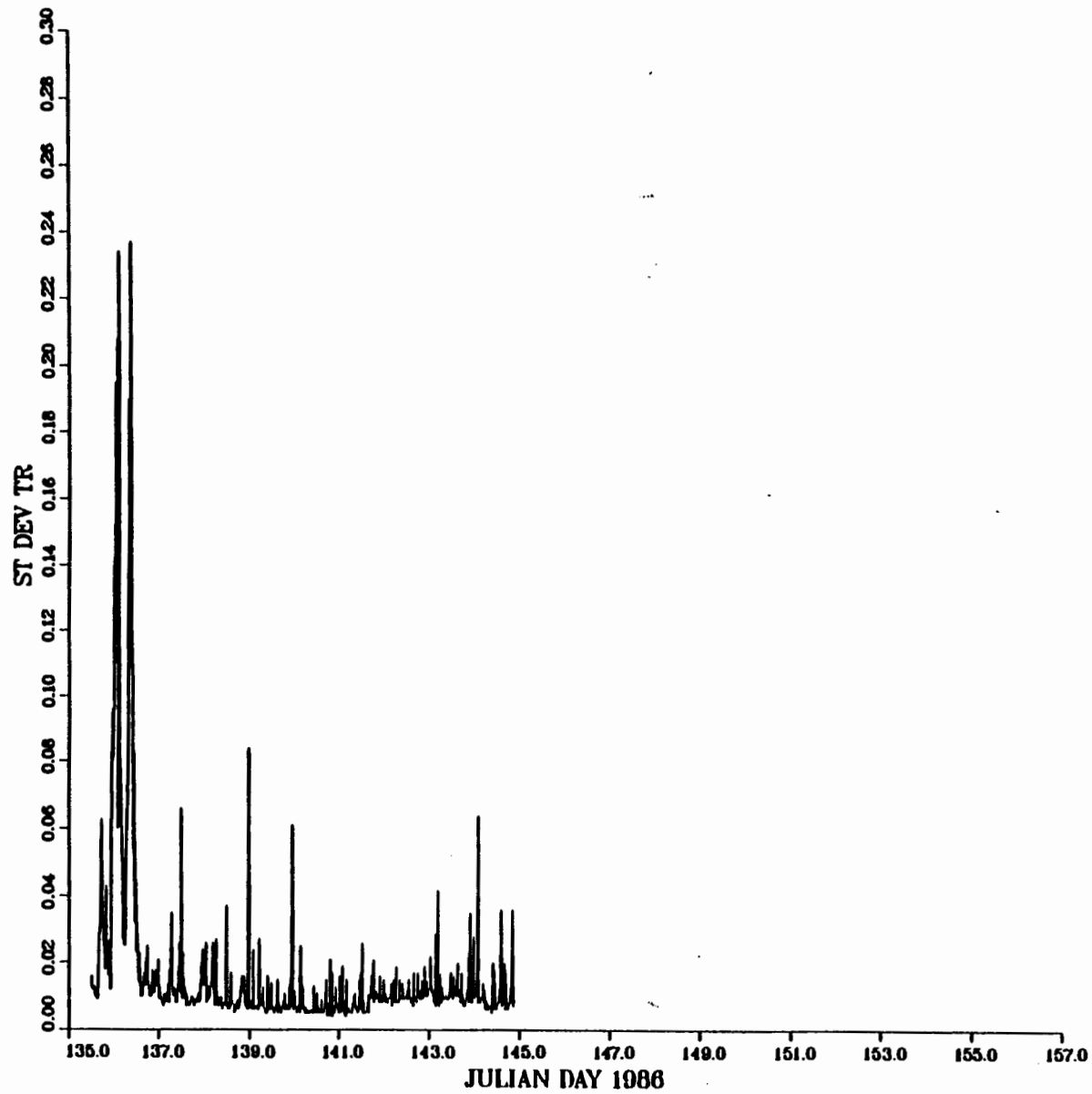
STATION S5-MJ



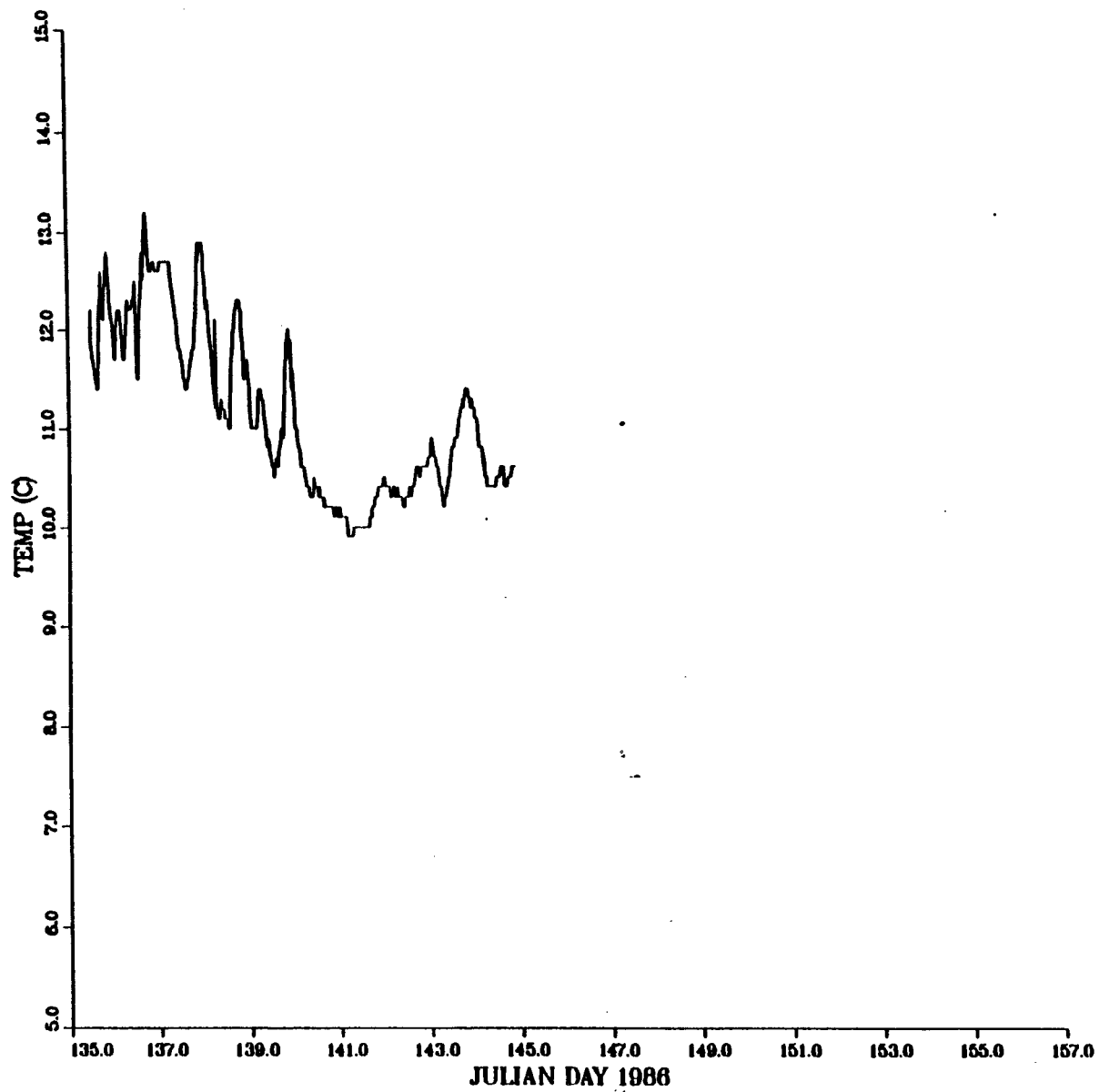
STATION S1-MJ



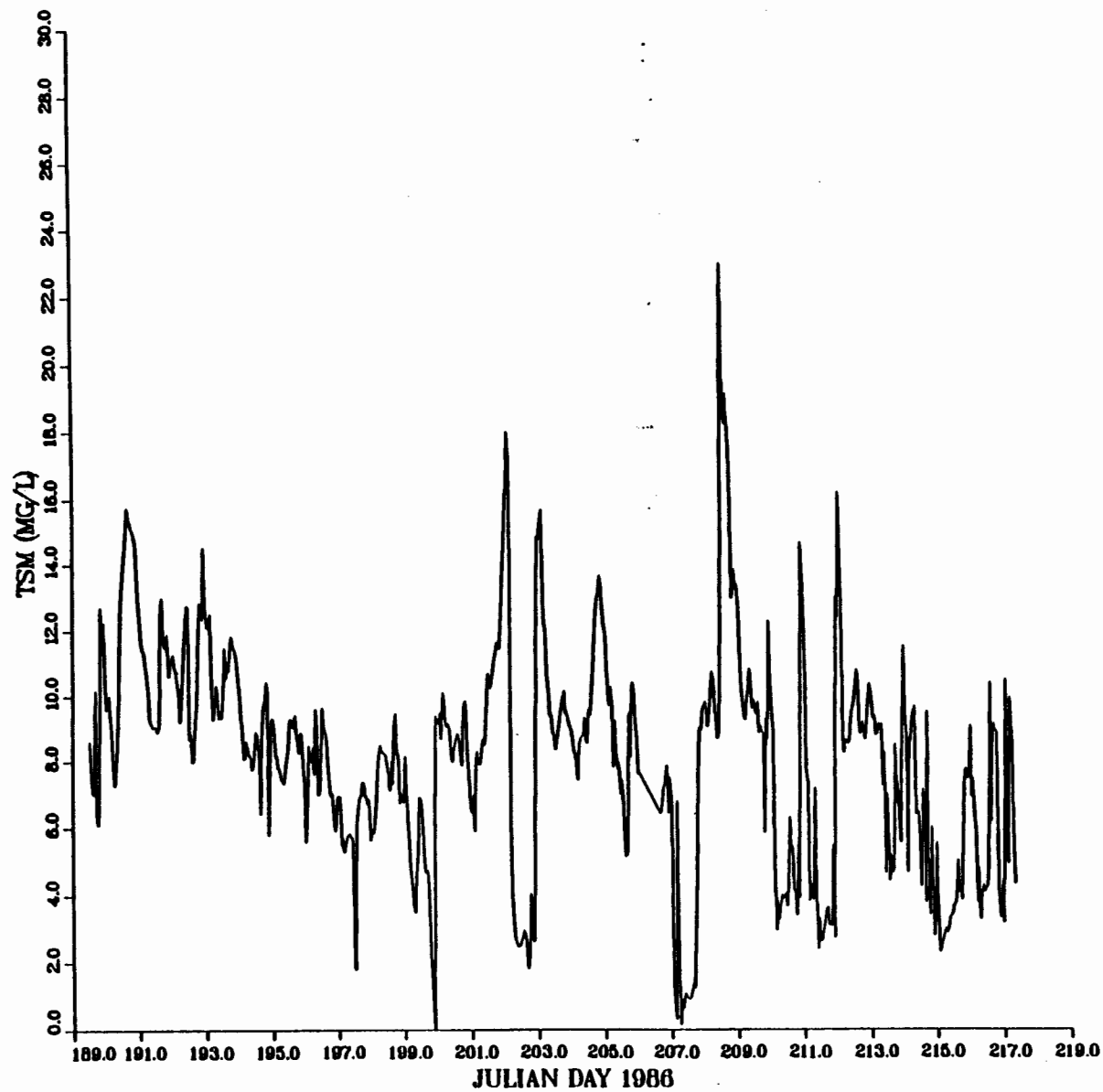
STATION S1-MJ



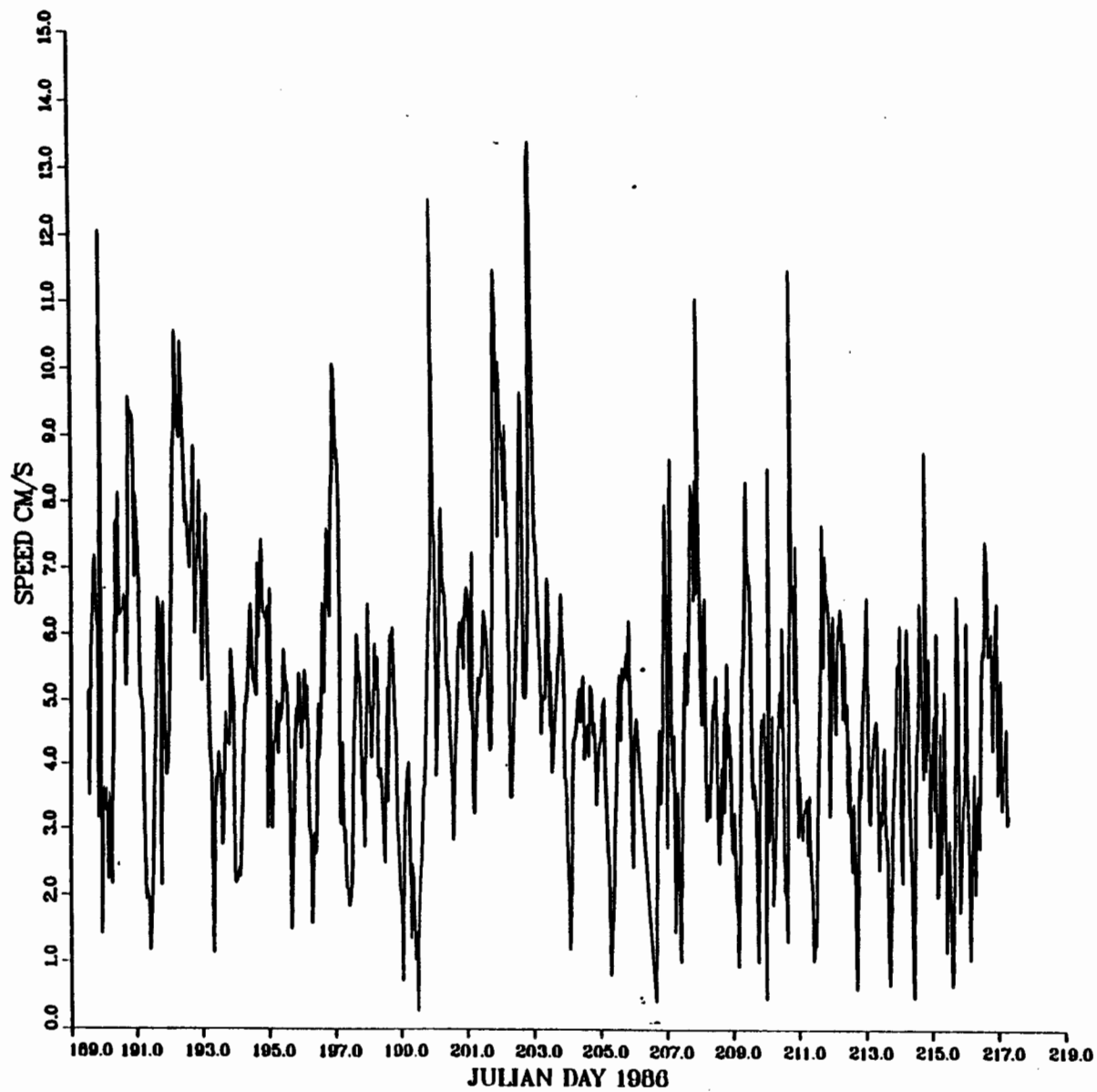
STATION S1-MJ



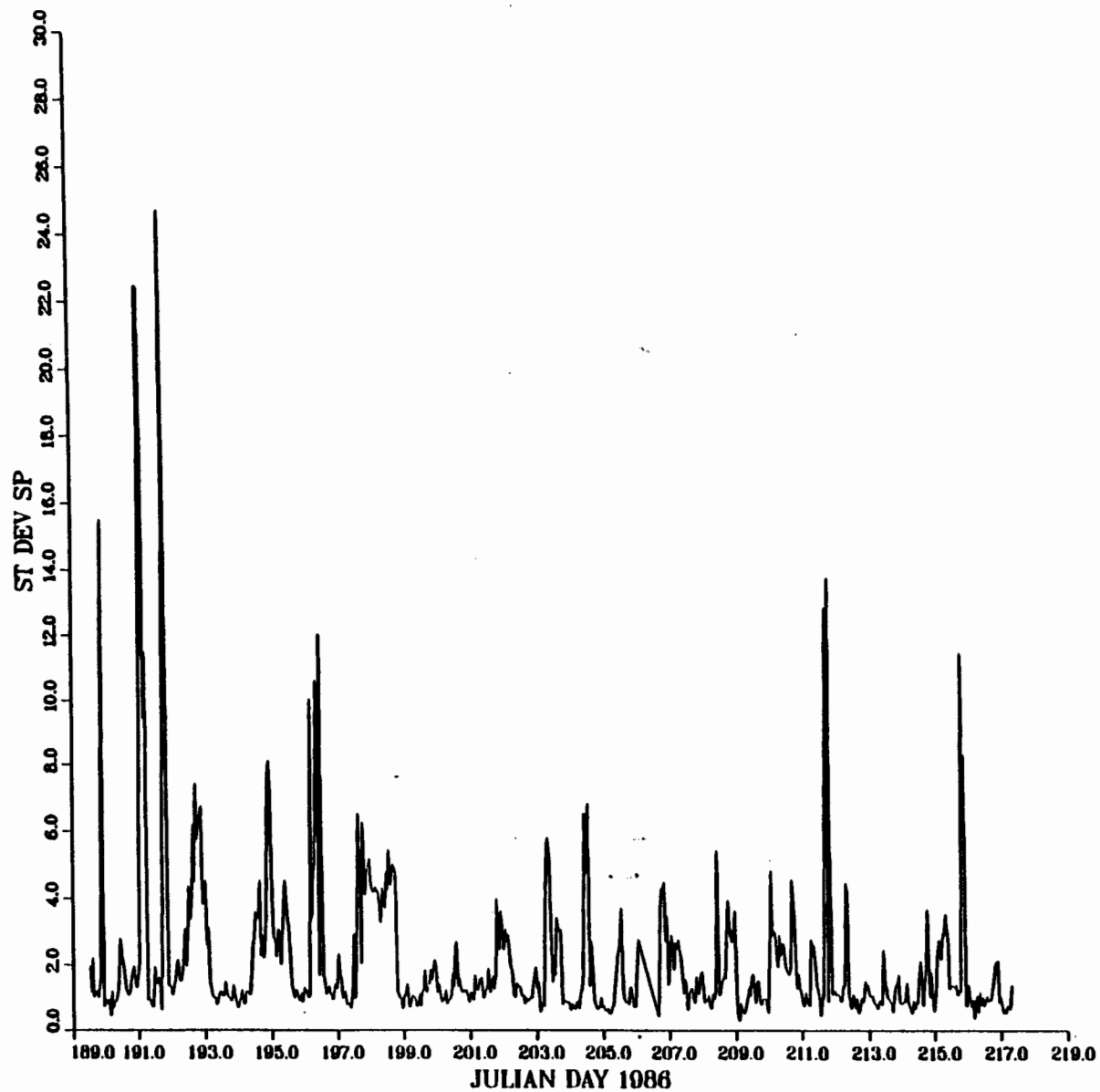
STA 71, JULY 6- AUGUST 7,



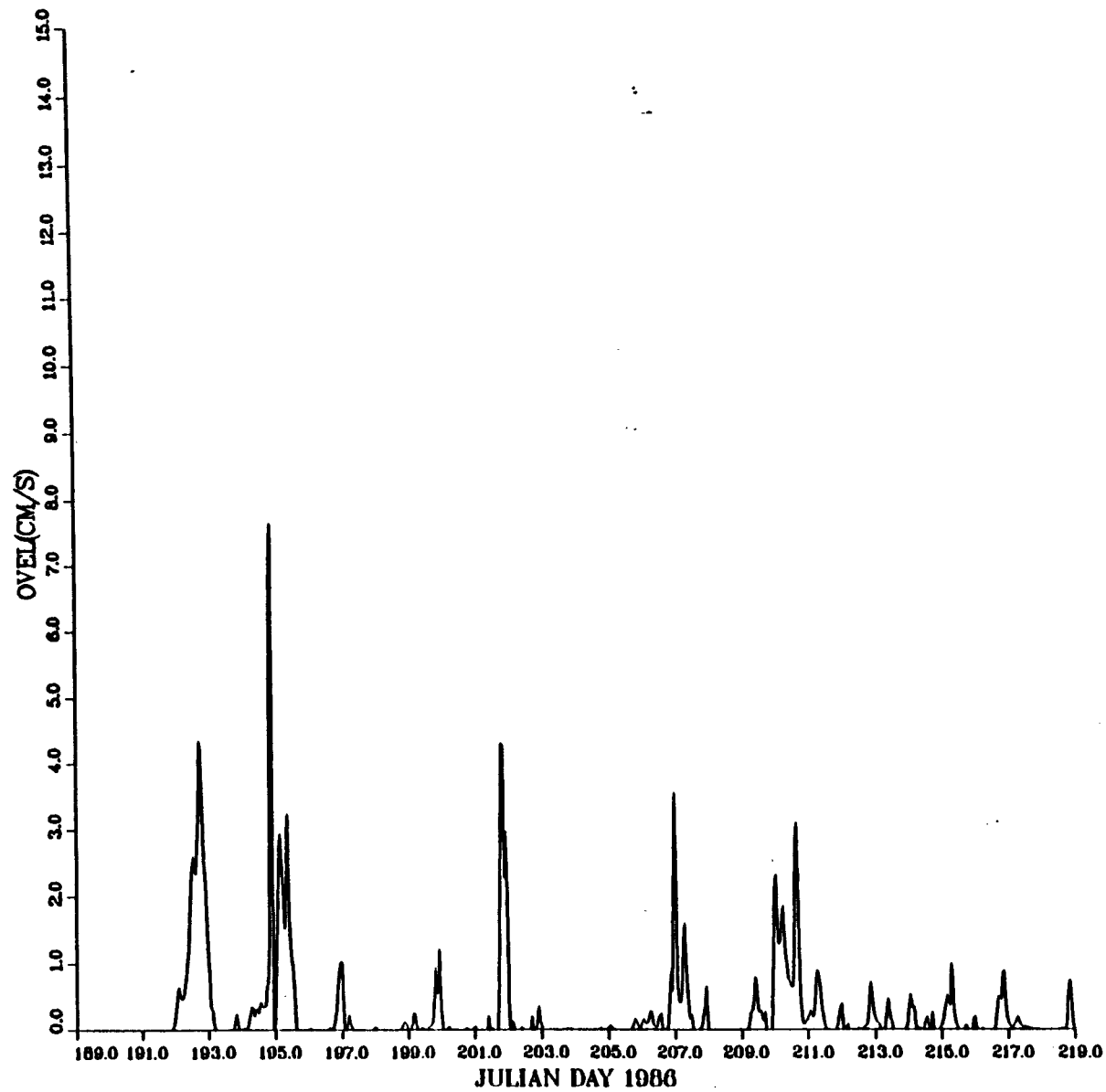
STA 71, JULY 6- AUGUST 7,



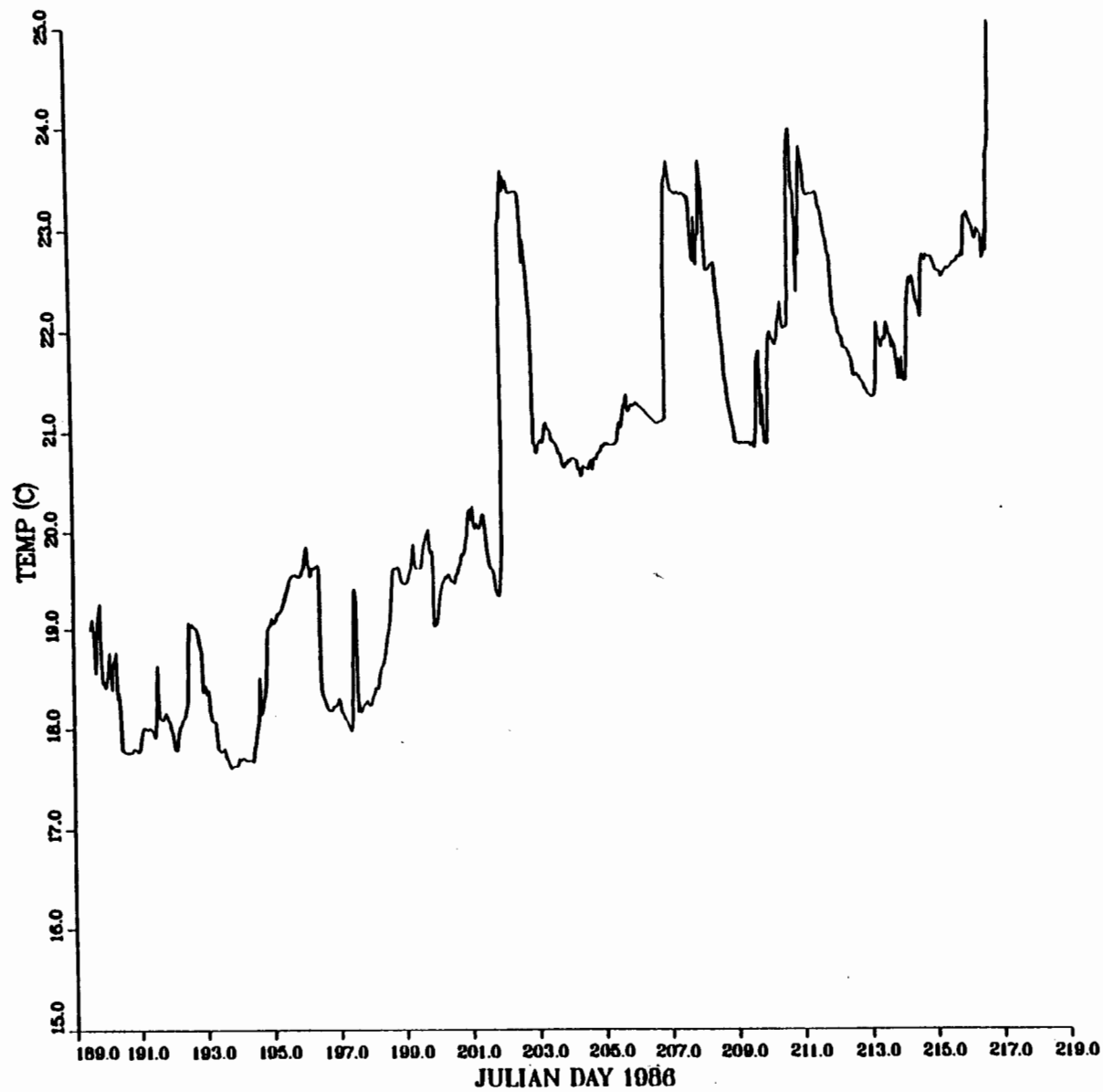
STA 71, JULY 6- AUGUST 7,



STATION 71 7/10-9/27/86 STARTS AT 0600

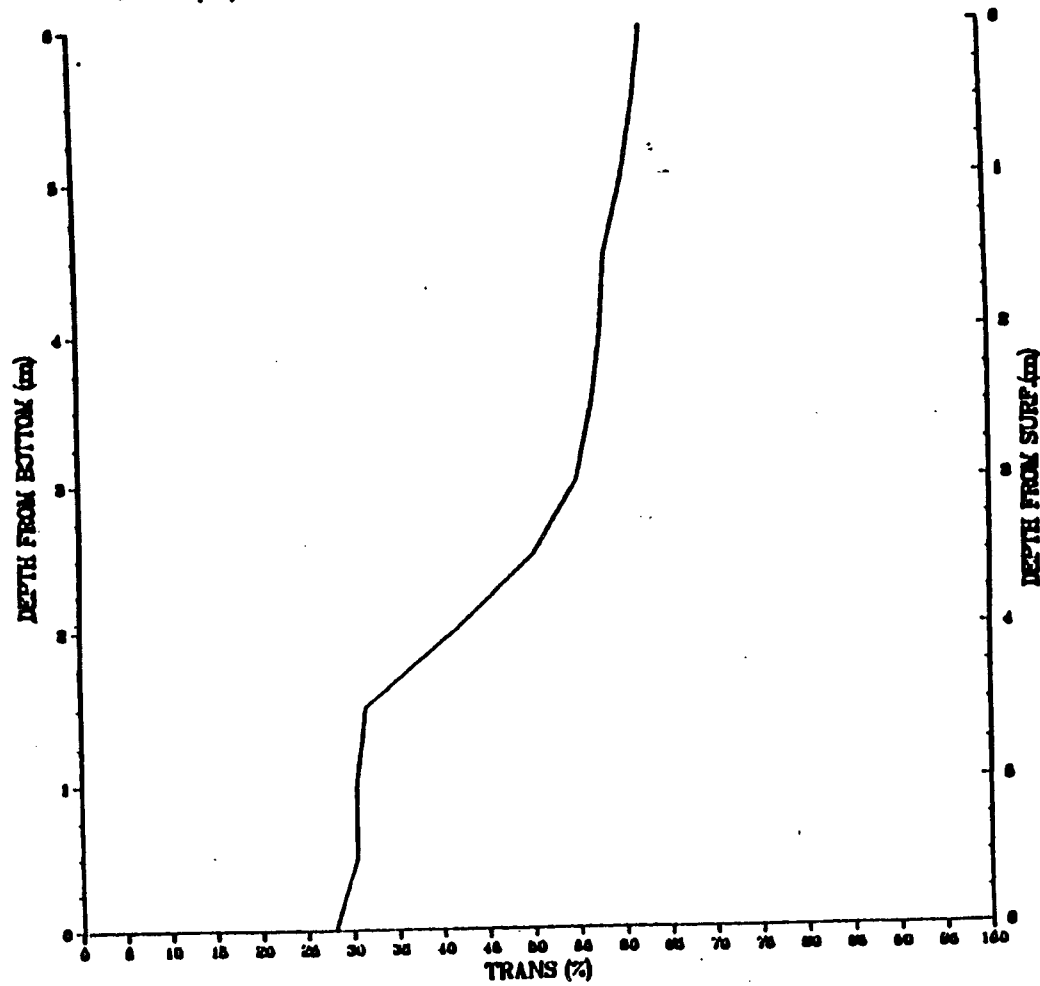


STA 71, JULY 6- AUGUST 7,

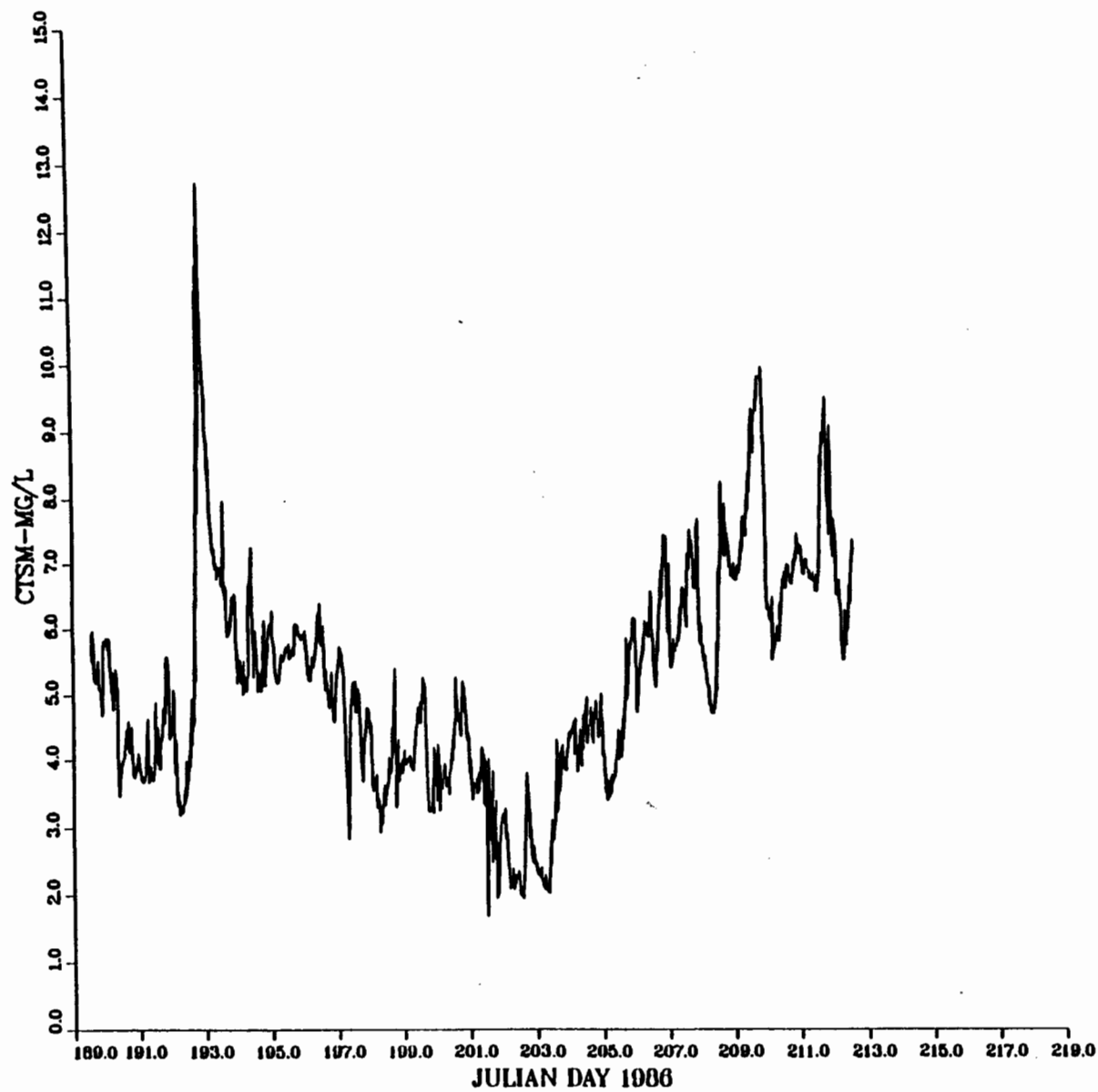


Station: STA 71

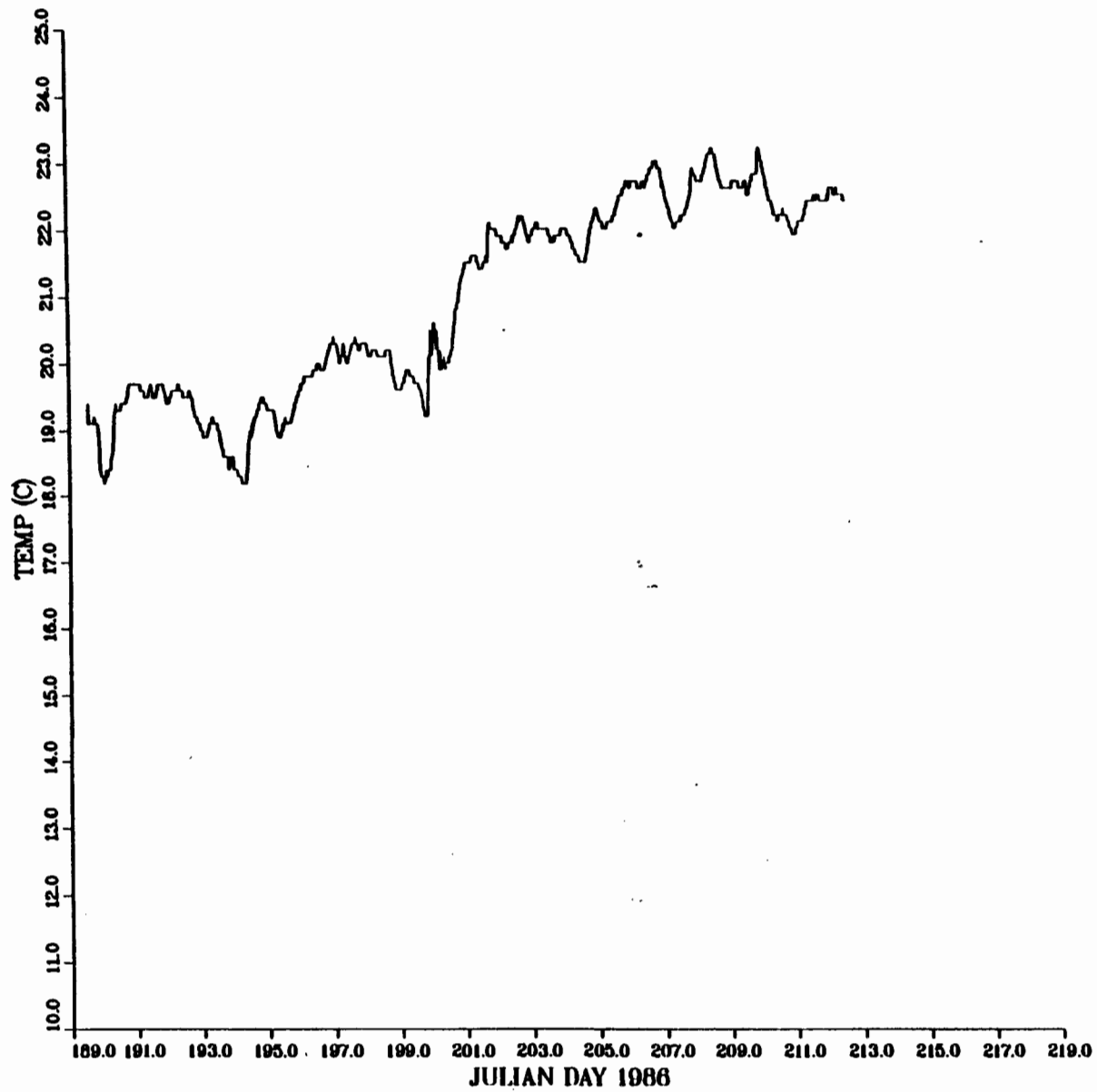
Date: 08/07/22



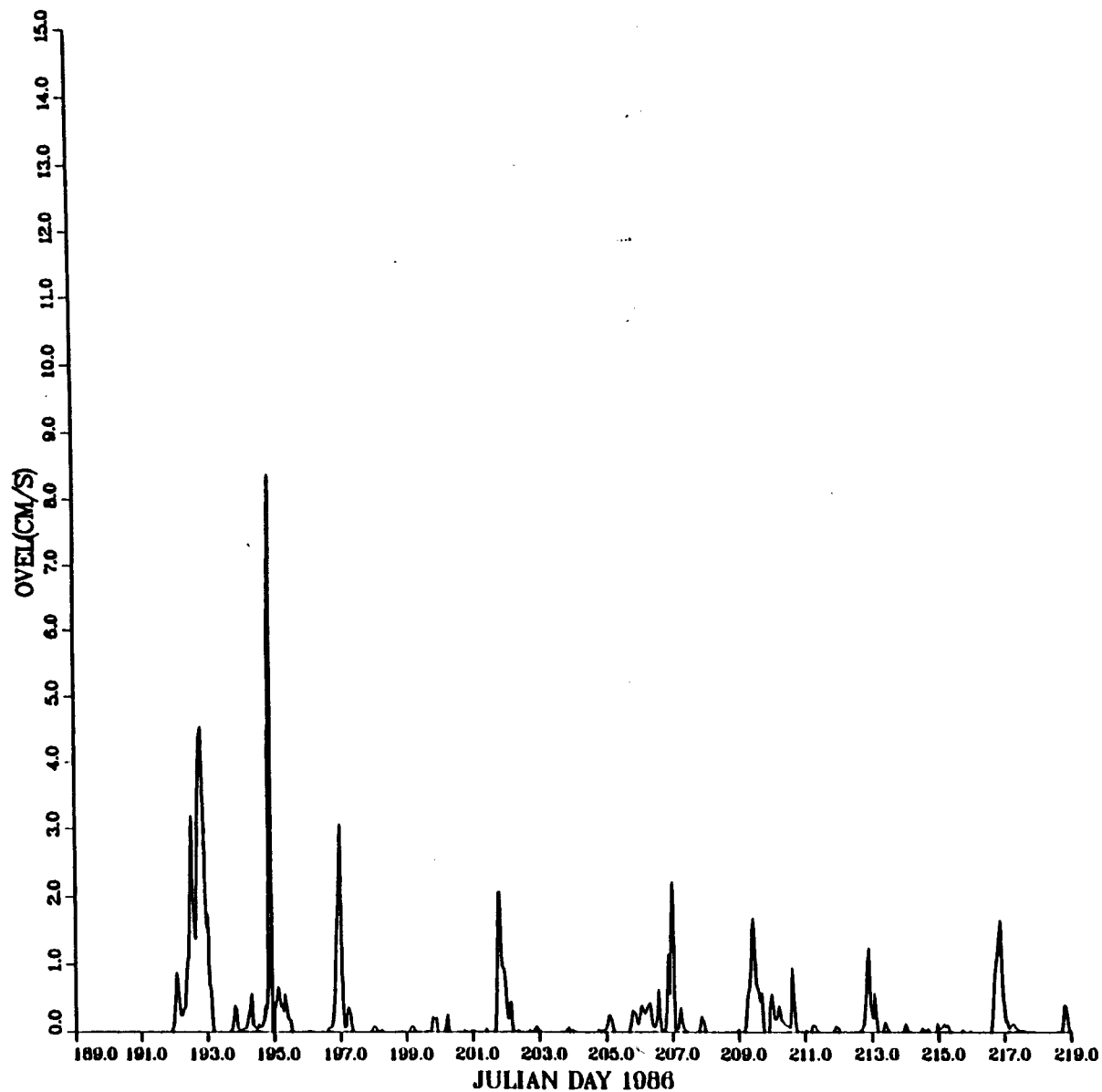
STATION S5JA



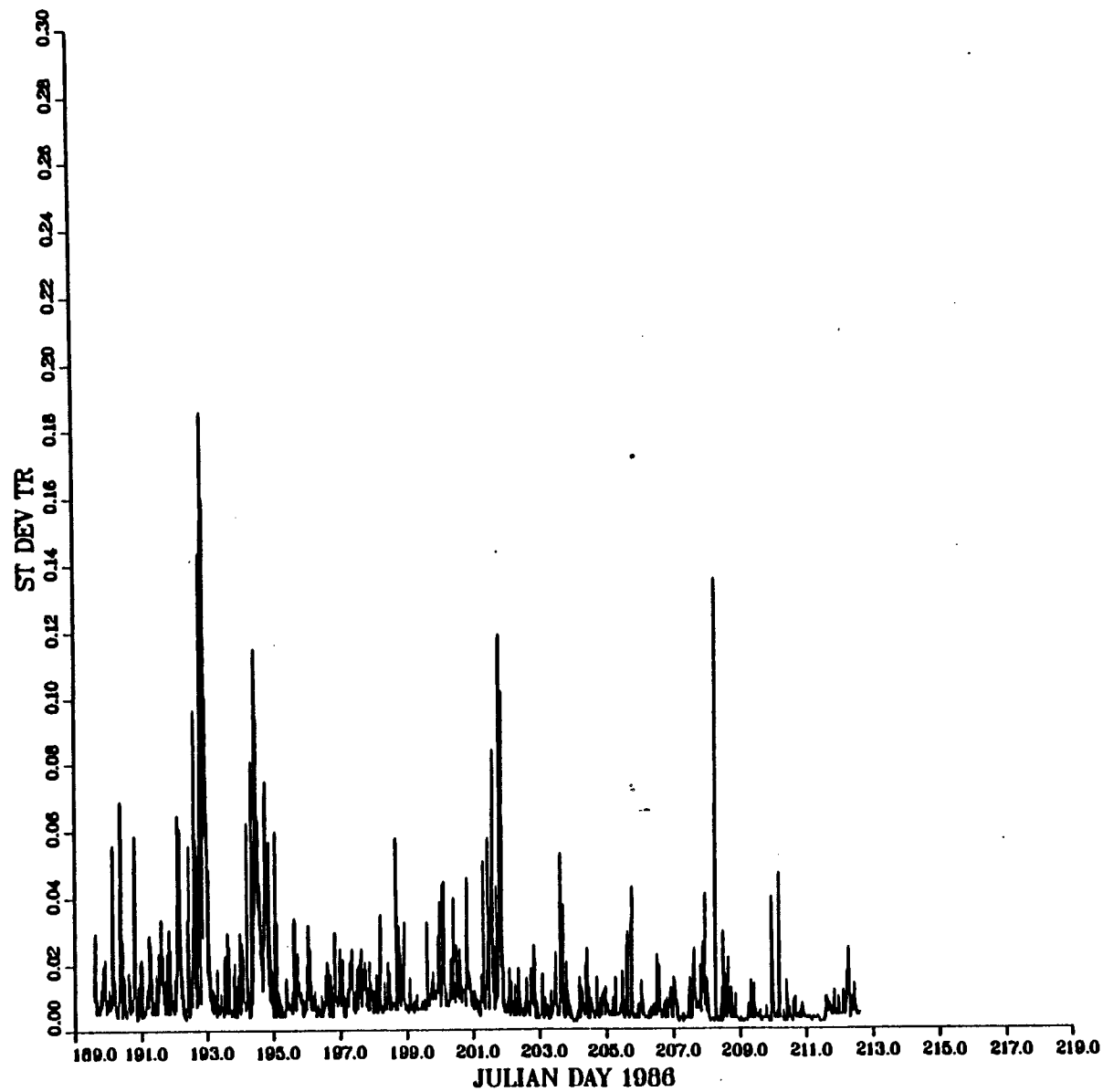
STATION S5JA



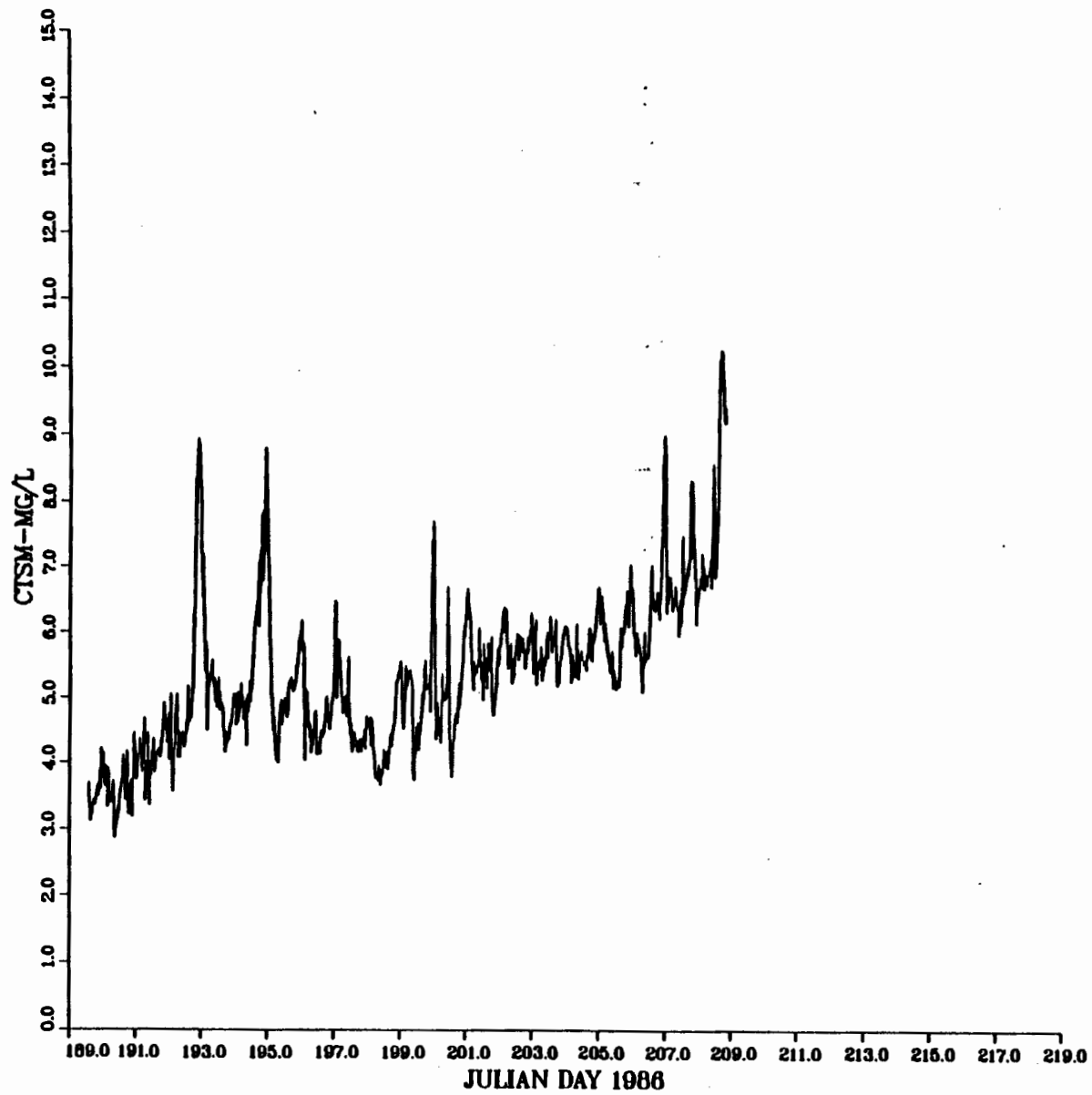
STATION 5 7/10-9/27/86 STARTS AT 0600



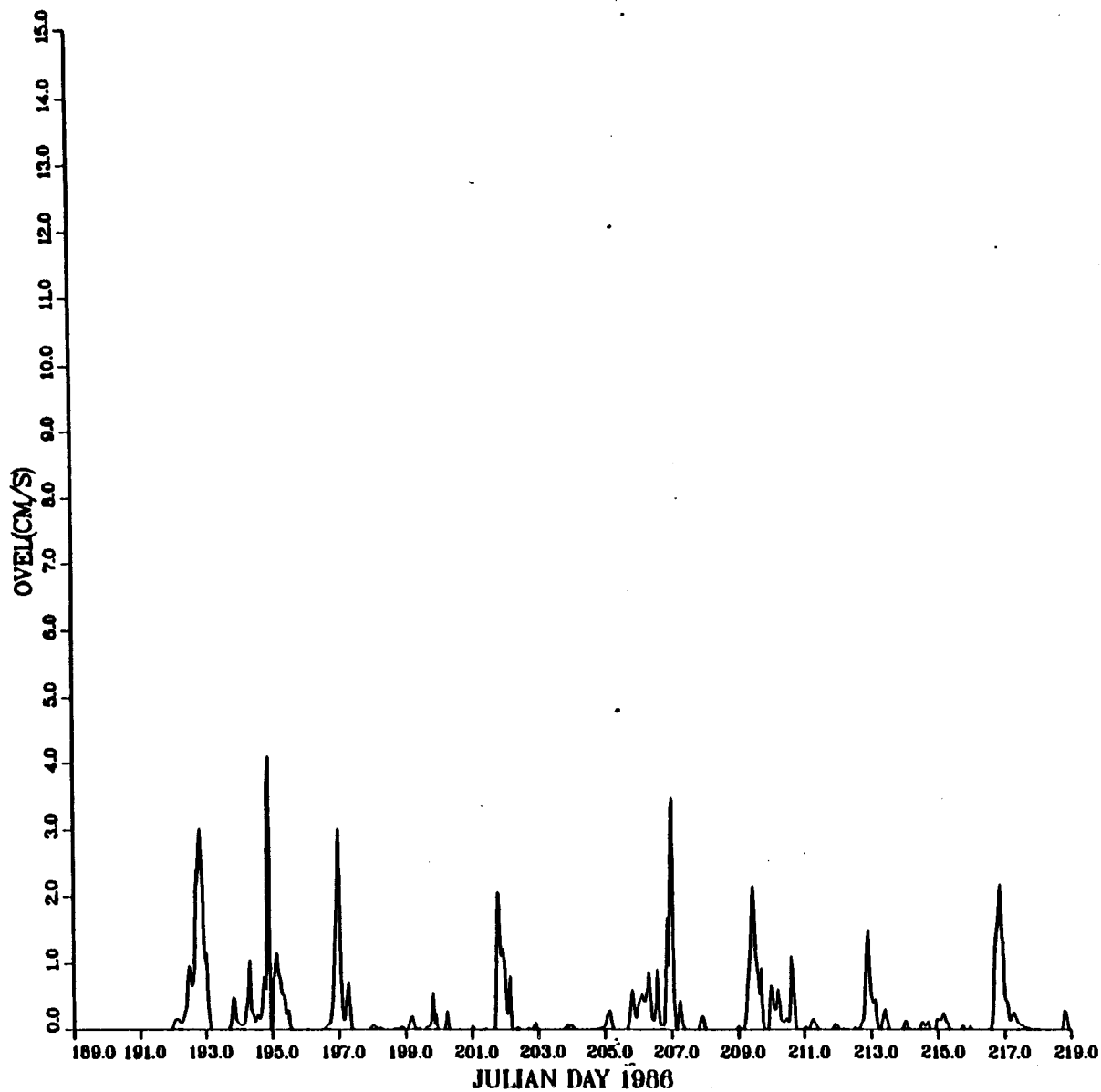
STATION S5JA



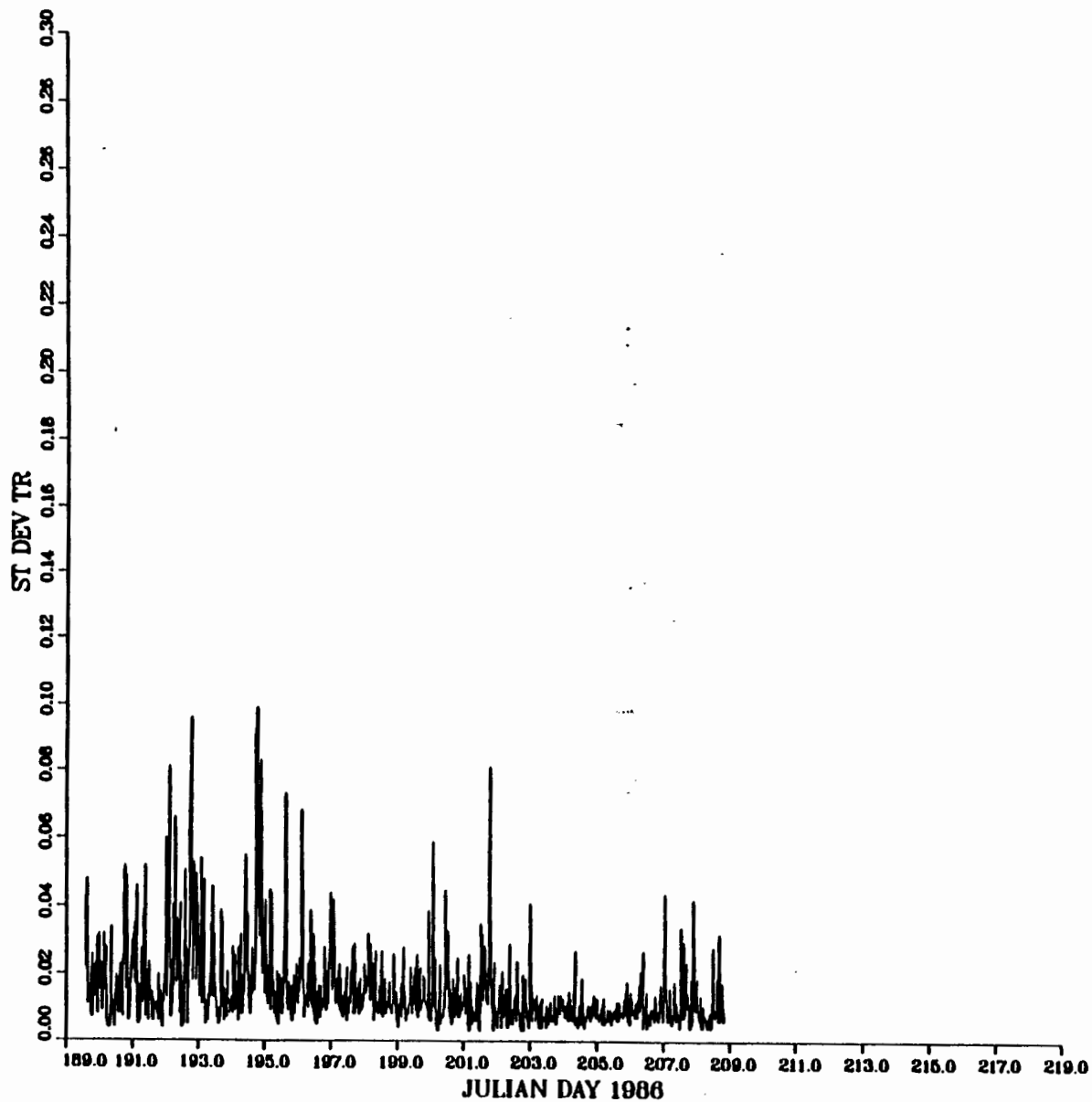
STATION STA1-J



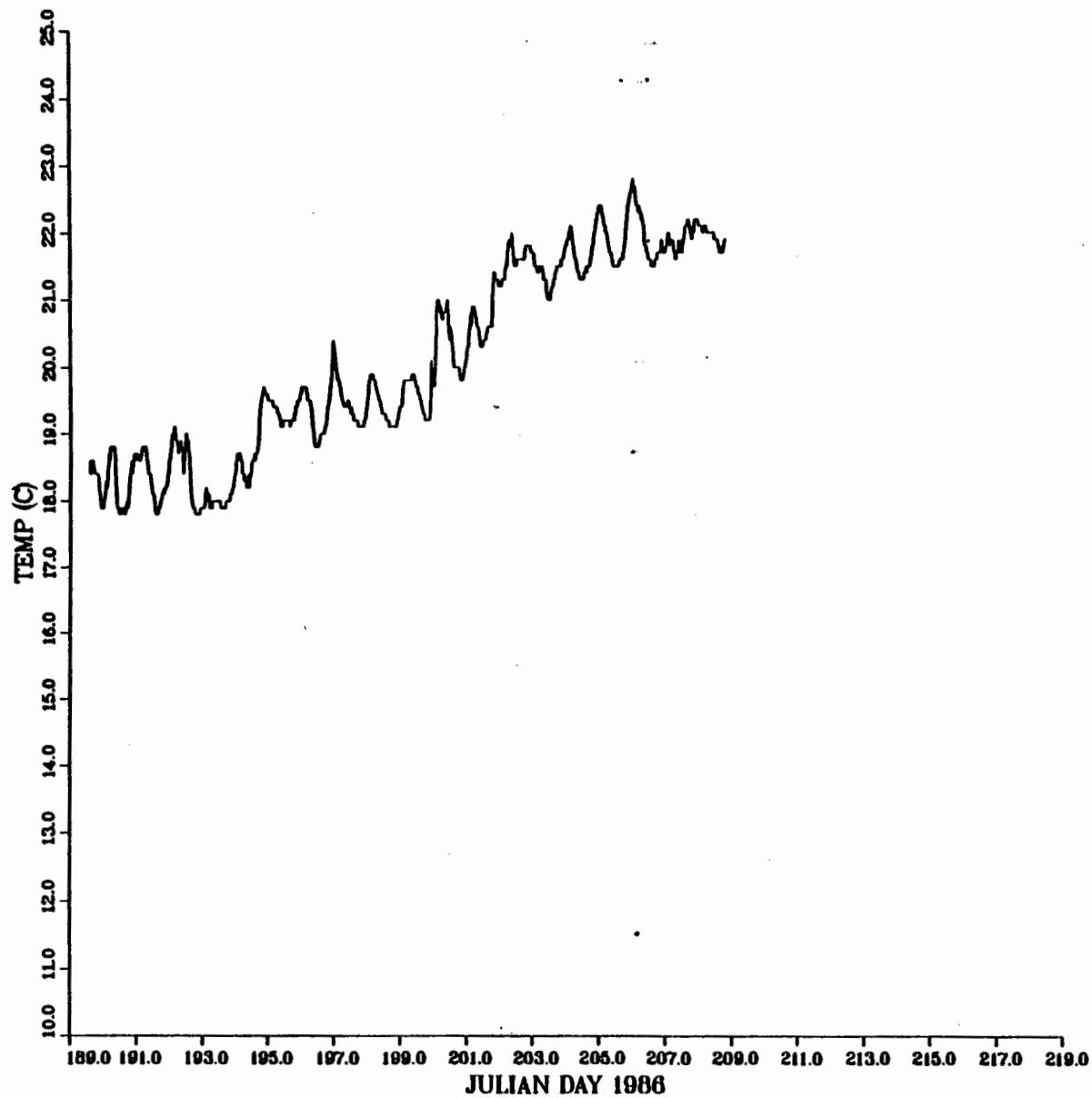
STATION 1 7/10-9/27/86 STARTS AT 0600

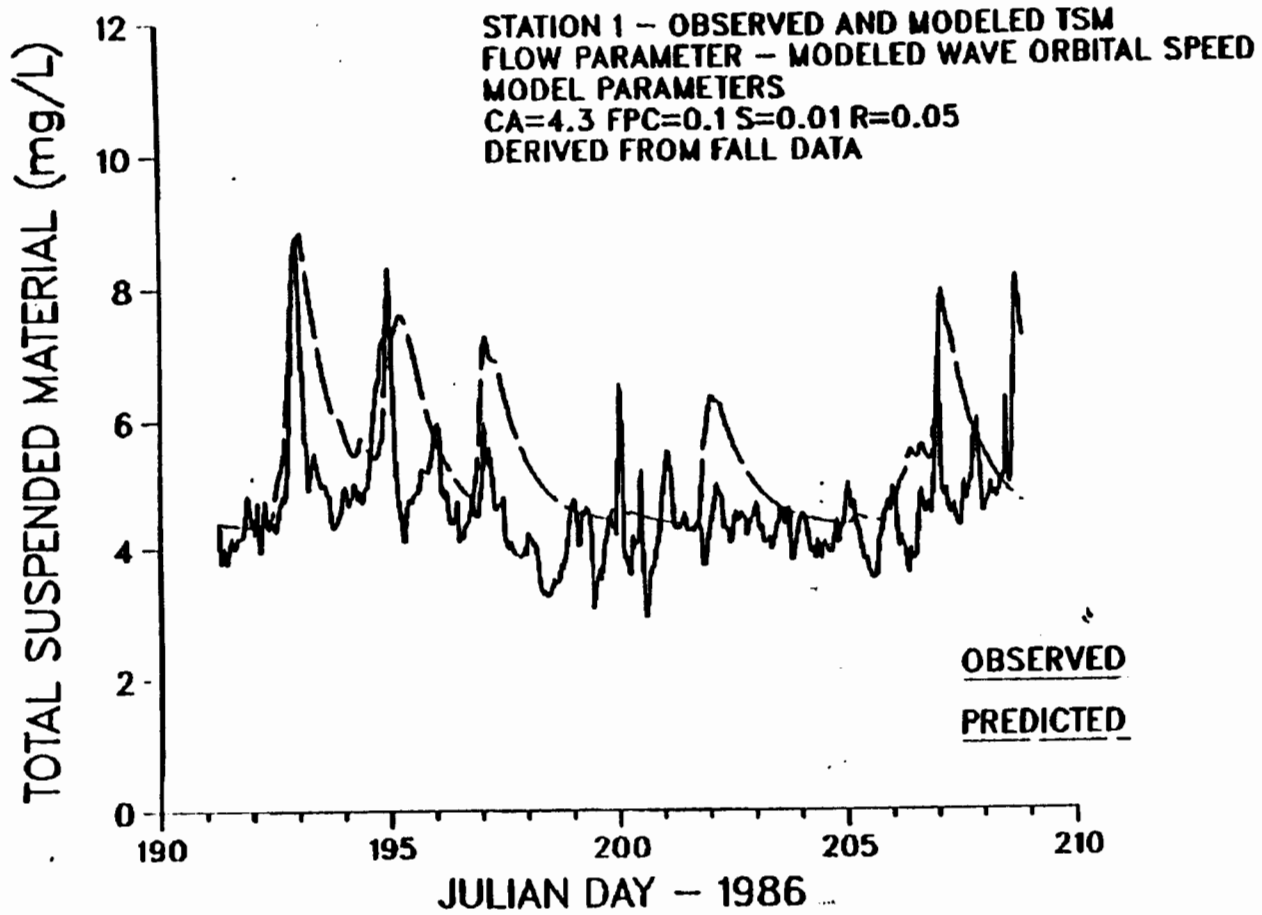


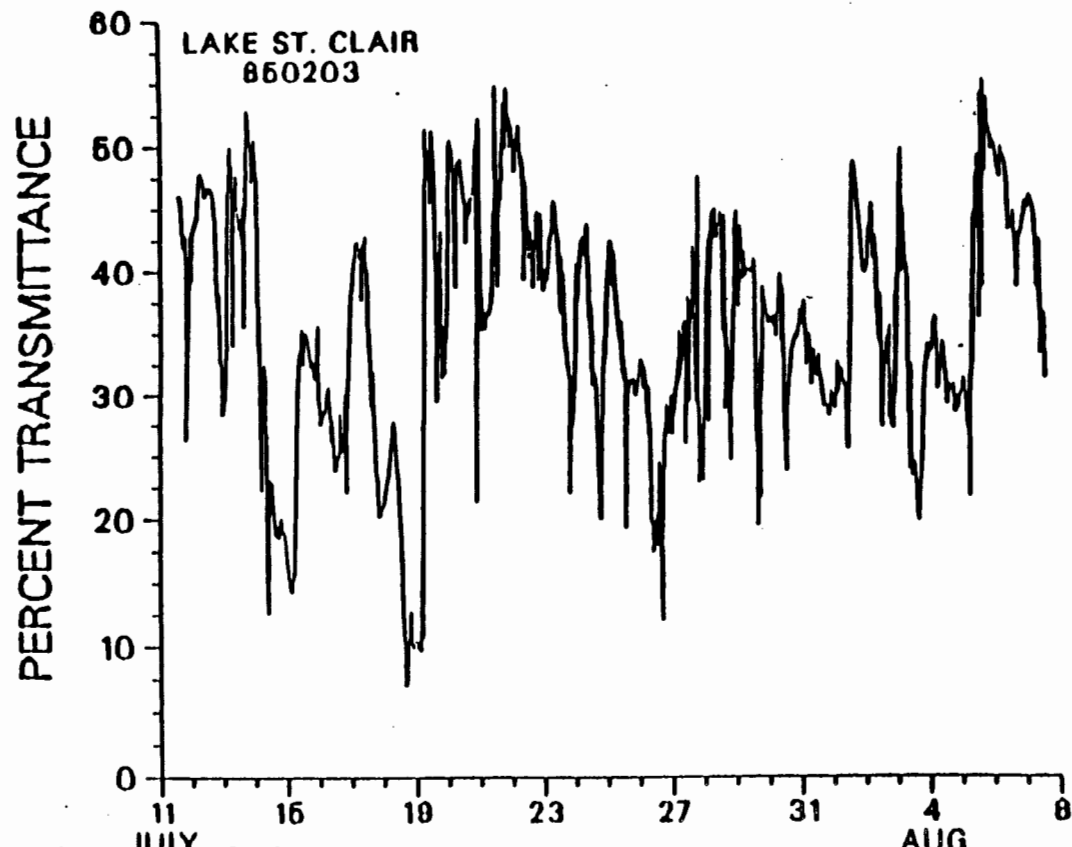
STATION STA1-J

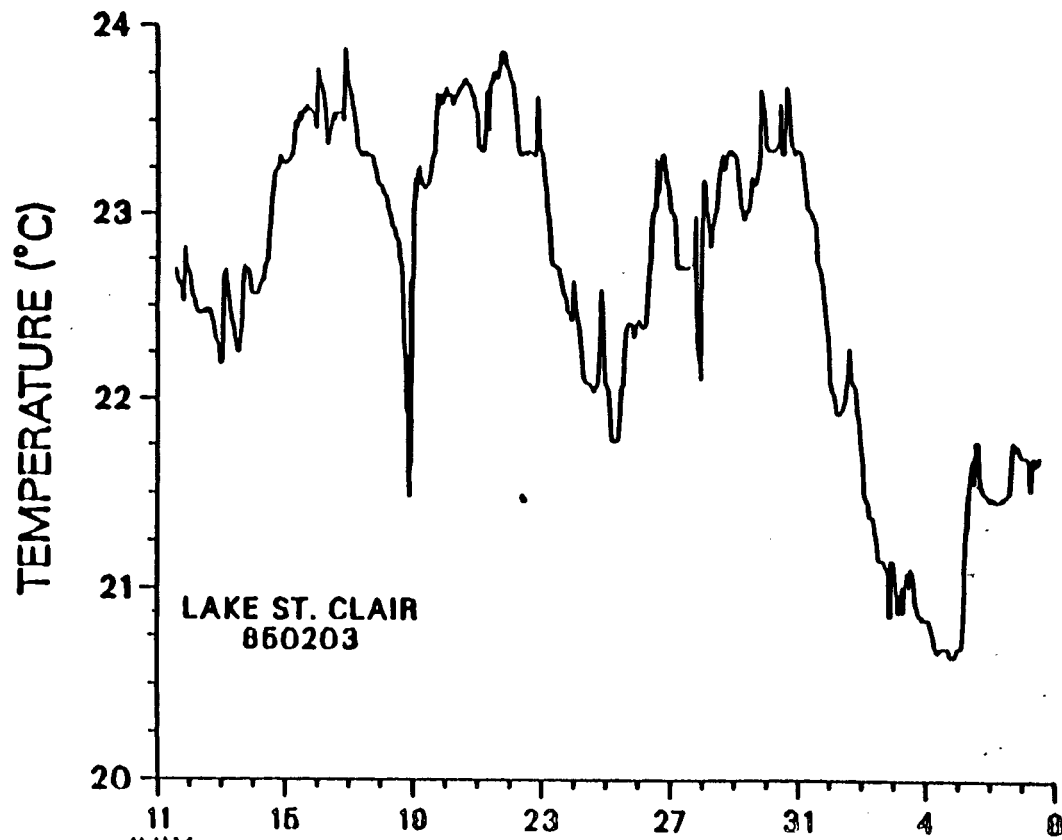


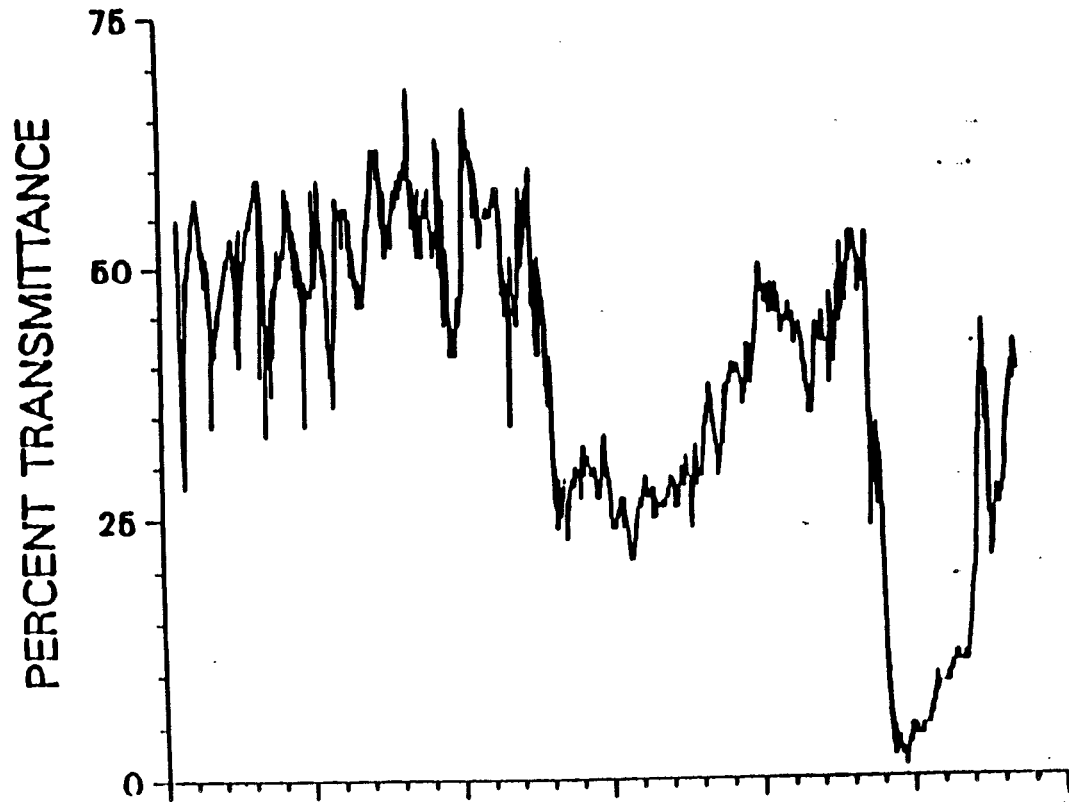
STATION STA1-J

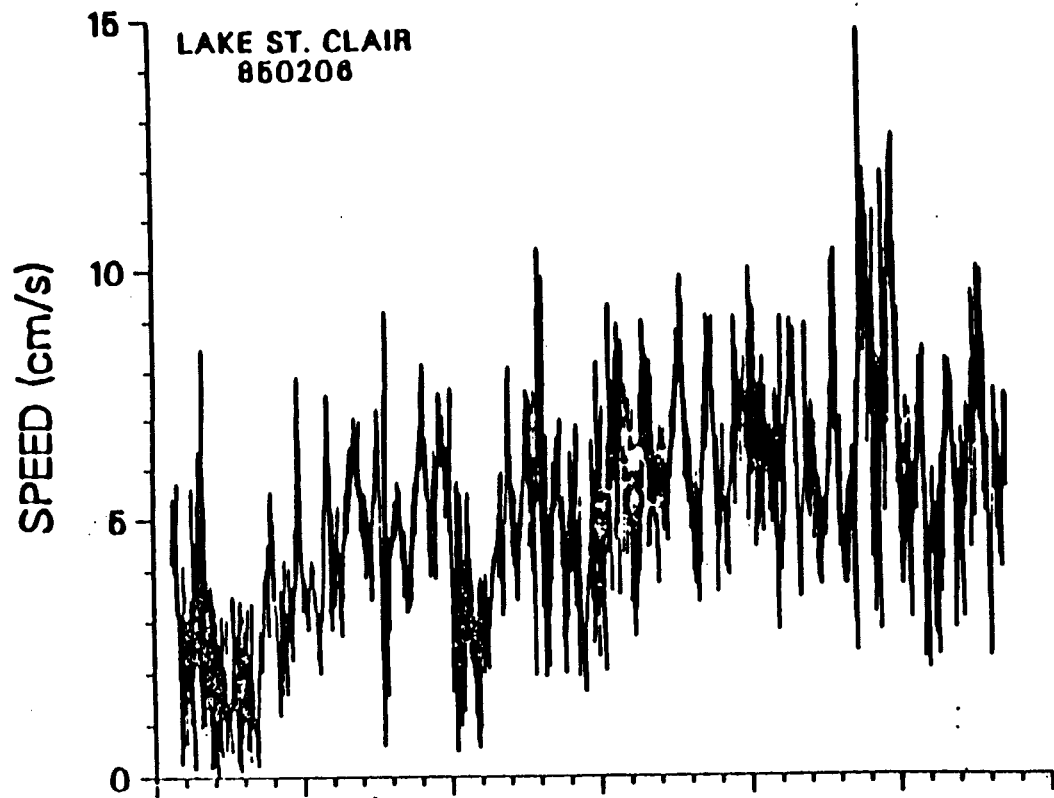


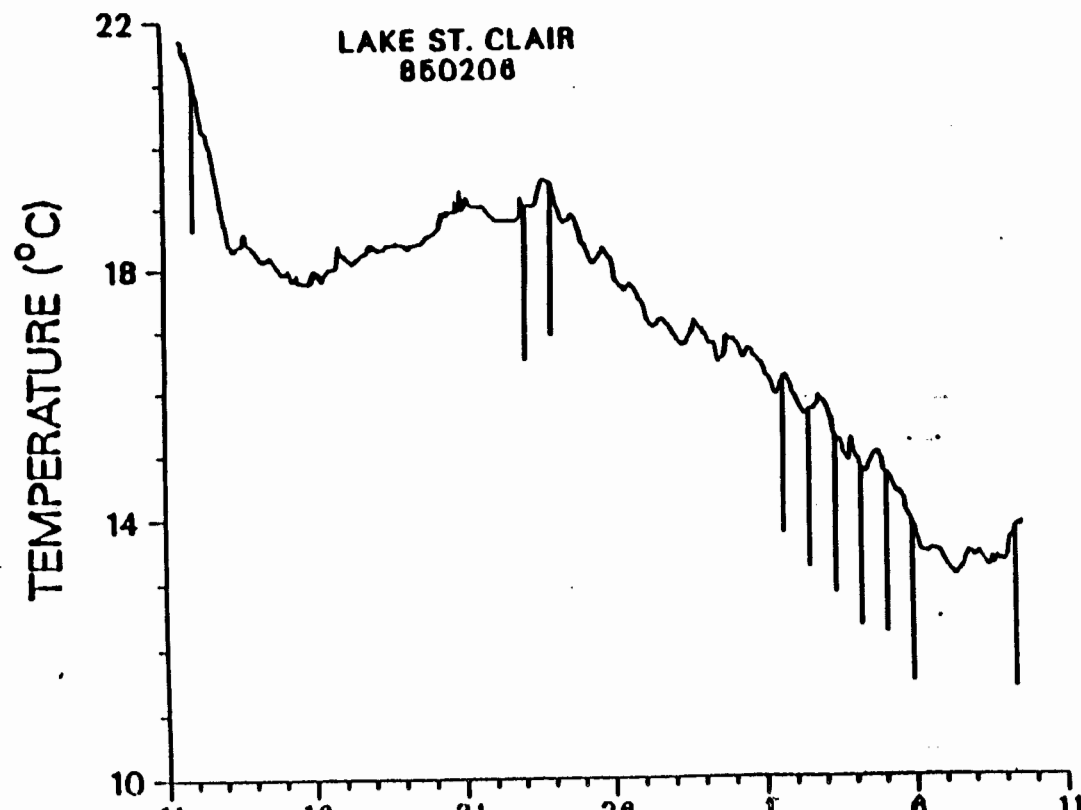












ACCUMULATION OF FALLOUT CESIUM-137 AND CHLORINATED ORGANIC
CONTAMINANTS IN RECENT SEDIMENTS OF LAKE ST. CLAIR

John A. Robbins and Barry G. Oliver¹

ABSTRACT

Cesium-137 originating from atmospheric nuclear testing, lead-210, potassium-40 and several chlorinated organic compounds (HCB, Hexachlorobenzene; OCS, Octachlorostyrene; PCBs, Polychlorinated Biphenyls; HCBd, Hexachlorobutadiene; QCB, Pentachlorobenzene; TCB, Total Trichlorobenzene; TeCB, Total Tetrachlorobenzene, and Total DDT) have been measured in a set of sediment cores collected by diver from Lake St. Clair in 1985. Distributions of Cs-137 often show subsurface peaks which apparently correspond to peak testing in the mid 1960s. Excess lead-210 distributions are similar to those previously encountered elsewhere in the Great Lakes, possessing a zone of constant activity extending about 3 cm down from the surface with exponential fall off below. Mixed depths and sedimentation rates inferred from lead-210 profiles are consistent with Cs-137 profiles and indicate sedimentation rates of the order of 0.1-0.2 cm/yr. Observed profiles can also be correctly predicted by mixing processes (rather than sedimentation) in which mixing below the surface region is

¹National Water Research Institute, Burlington, Ontario, Canada

characterized by constant eddy diffusion coefficients of .2 to 4. cm^2/yr . Because of the evidence of extensive biological activity down to at least 15 cm, mixing is favored as the mechanism producing observed radionuclide and contaminant distributions. Comparison of total loading of Cs-137 to the lake (471 Ci in 1985) to actual storage (37 Ci) indicates a sediment residence time of about 5 years. This value is consistent with that inferred from previously observed changes in surficial sediment levels of mercury and pesticides between 1970 and 1974. Changes in surficial sediment Cs-137 concentrations between 1976 and 1985 are less than expected on the basis of a five year residence time and suggest that the residence time of particle-associated contaminants increases with the amount of time the contaminant has remained in the system. Preliminary measurements of Cs-137 in trap samples collected by others at two sites in the lake indicate that the isotope may be used to distinguish between particle-associated contaminants resuspended from the bottom and new contributions from the St. Clair River. Concentrations of chlorinated organic compounds in surface sediments are well-correlated with each other and the pattern over the lake bottom is closely related to the thickness of recent deposits. In some cores profiles of total DDT and PCBs (as well as compounds with significant local sources such as HCB, QCB and OCS) apparently reflect the history of loading to the lake. Also, profiles of HCB/OCS and HCB/QCB ratios, used to distinguish between alternative industrial sources of the chemicals, indicate the changing history of waste management practices. Total storage of contaminants shows that Lake St. Clair sediments are a significant repository of chemicals passing through the Lake. As of 1985 it is

estimated that 960 Kg of HCB, 870 Kg of PCBs and 210 Kg of OCS are contained in the sediments.

INTRODUCTION

The enormous flow of water from the upper Great Lakes proceeds out of Lake Huron through the St. Clair River and into a shallow heart-shaped body of water, Lake St. Clair. Urban and industrial activity on the shores have made the river and this lake one of the most heavily contaminated regions of the Great Lakes. Although the lake has an extremely short mean hydraulic residence time, about 9 days, sediments manage to acquire significant burdens of contaminants originating from tributary sources, especially the St. Clair River. Previous studies of mercury (Thomas et al., 1977) and chlorinated organic compounds (Frank et. al, 1977) indicated that contaminants passing through the lake are temporarily retained by sediments. The marked reduction which took place during the four year period between 1970 and 1974 in the concentration of these constituents in surficial sediments indicated that the sediment reservoir was not a permanent sink however probably because resuspension in this shallow lake (3 m mean depth) ultimately exports materials out of the lake and down the Detroit river.

These qualitatively characterized properties of the sediment reservoir can be more quantitatively treated by determining the storage and distribution of particle-associated radiotracers whose loading histories, in

contrast to the above contaminants, are well-known. Fallout cesium-137 is especially useful for this purpose since it is a tracer of fine-grained (clay sized) constituents and has an accurately known input history. A second isotope, lead-210 is also of considerable use, since it is delivered to the lakes at a virtually constant, well-determined rate and has no known anthropogenic sources. Thus Cs-137 can serve to illustrate the long-term response of sediments to a pulse of radioactivity passing through the system in the mid 1960s while lead-210 characterizes the steady-state response.

The recent severe contamination of the St. Clair River with chlorinated organics from industrial activity in the Sarnia area has been documented (Environment Canada, 1986, J. Water Poll. Res., 1986). It is known that Lake St. Clair retains some portion of these contaminants since they have been found at significant concentrations in the Lake's sediments (Frank et al., 1977; Pugsley et al., 1985; Oliver and Bourbonniere, 1985). This report also examines the distributions of the contaminants in surficial sediments of the Lake, estimates the mass of contaminants stored in sediments, and discusses contaminant trends in sediment cores.

METHODS

Sediment cores were collected by diver at the sites shown in Fig 1a. during May and September 1985. The locations were chosen to coincide with those occupied previously by Pugsley et al. 1986. Locations possessing sand or coarser materials are unsuited for hand insertion of core tubes and, at

least for cesium-37, are known to possess insignificant amounts of the isotope (cf Robbins, 1986). Two 10.1 cm i.d. cores were collected at each location with no observed disturbance of the sediment-water interface and were suitably spaced from one another (ca 50 cm) to avoid interferences. Cores were extruded hydraulically in the field and sectioned in 1 cm intervals to 10 cm and in 2 cm from 10 cm to the bottom of the core or in many cases to the interface with gray glacial clay. Sections from one core were subdivided for radionuclide and metals analysis while sections from the replicate core were subdivided for organics and additional metals analysis. Because the accuracy of sediment tracer and contaminant inventories depends directly on the extent of recovery of material collected in a tube of known area, care was taken to collect all sediment from each section. Subsamples for organics analysis were stored frozen in precleaned glass jars prior to analysis.

Samples for radionuclide analysis were weighed, freeze dried and reweighed to obtain the fractional dry weight of sediment and the mass of dry sediment per unit area of the core. Dried samples were lightly disaggregated and placed in vials of standard geometry for gamma counting. The activity of Cesium-137 (661.6 KeV) and K-40 (1460.7 KeV) were determined using a lithium-drifted germanium detector coupled to a multichannel analyzer. Absolute detector efficiencies were determined by counting sediment samples of equivalent geometry spiked with a mixture of gamma emitting radionuclides of known activity. Uncertainties in sample activities were generally well under ten percent. Samples for organics analysis were soxhlet extracted prior to analysis by capillary, electron

capture detector, gas chromatographic analysis. Procedure details have been published (Oliver and Bourbonniere, 1985).

In addition, sediment trap samples were analyzed for Cs-137 from two of nine sites occupied during 1985 by Charlton and Oliver (1986). Trap materials were collected at nine (about equally spaced) time intervals during the period from early June to mid-November. The sites 10 and 13 are situated approximately 1 Km north of coring locations 24 and 28 respectively (See Fig 1a.). Samples were freeze dried and lightly disaggregated prior to analysis. Details of the collection and sample preparation as well as supplementary analytical results are given in the above reference.

RESULTS AND DISCUSSION

Characteristics of Sediment Cores

In general sediment cores collected from this Lake evidence significant stratigraphic inhomogeneity. Gelatinous, flocculent material resides on the uppermost centimeter or so of sediment. The surface, particularly in the deepest parts of the Lake is perforated by many circular holes about 0.5 cm in diameter which extend as burrows into sediments as deep as 16 cm. Densities of perforations reached as high as 800 M⁻². The burrows, surrounded by about a 2 cm diameter halo of oxidized sediment were often inhabited by Hexagenia larvae. In regions of the lake with high clay content, the upper 10-20 cm of sediments consisted of brownish gray silty

material with some fine sand and occasional layers of shell fragments. In a few of the cores a transition layer was encountered between 10 and 20 cm consisting of clay with a high water content. An admixture of clay and sand extended below this layer becoming consolidated and possessing increasing sand content. In nearly all cores, at sufficient depths, the sediment composition shifted abruptly to fine post-glacial clay. Sediments above this layer may be considered to be of recent origin. The thickness of the recent sediments, shown in Fig. 1b., corresponds roughly with lake depth and reaches a maximum of over 30 cm in a narrowly defined area. Cores collected in shallower parts of the lake with low clay content occasionally possessed macrophyte fragments and remnants of plants rooted in the sediments collected. A large live clam (Unionid) was found in the region of 2-6 cm depth in a sediment core (discarded) collected at site 39.

Sources of Radiocesium in Lake St. Clair

Cesium-137 in the Great Lakes originates almost exclusively from atmospheric nuclear testing. There is no natural source of the radionuclide and contributions from reactors situated along the shores are many orders of magnitude less than direct fallout loadings. More than two decades of routine monitoring of monthly fallout by U.S. and Canadian authorities have provided the basis for developing estimates of time varying loadings which greatly surpass, both in quantity and quality, our knowledge of any other contaminant entering the lake system. The most detailed records are for Sr-90 which is co-produced with radiocesium in nuclear detonations as a fission product. Cesium-137 and Sr-90 have comparable half-lives (0.2 and 28.1

years respectively) and the ratio of the two isotopes in air and in fallout is well-determined and largely time-invariant. For this reason loadings of Cs-137 may be reliably inferred from Sr-90 records as well as from direct measurement. Data for both Sr-90 and Cs-137 from all monitoring sites in the Great Lakes region have been combined with empirical models relating atmospheric concentrations to over-lake and drainage basin deposition (Robbins, 1985a). This regional source function is used to predict loadings to Lake St. Clair using a lake system response model.

The response of the Great Lakes to fallout radionuclide loadings was first examined by Lerman and Taniguchi (1972) for Sr-90 and subsequently by others for the two long-lived fallout isotopes which are much more strongly associated with particulate matter, Cs-137 and plutonium. Wahlgren et al. (1980) related plutonium isotope loadings to measured aqueous concentrations using a long term fate model which included removal to sediments through an apparent settling velocity. Thomann and DiToro (1983) enlarged the treatment to include the effects of equilibrium partitioning of plutonium between water and suspended matter and included an explicit term for the resuspension of the isotope. Tracy and Prandtl (1983) reported on new Sr-90 and Cs-137 concentration data for several of the Great lakes and illustrated the need to consider resuspension in accounting for the long-term behavior of cesium-137. Recently, Robbins (1985b) has developed an equivalent formalism to calculate the response of the lakes to Cs-137 loadings which includes an improved source function and adds the contributions of the isotope from land drainage. This latter component in the model is based on the semi-empirical relations developed by Menzel (1974) and was calibrated

for the Great Lakes through periodic measurement of the concentration of the isotope in tributary rivers (cf. Nelson et al. 1984). Details of the calculation are given in Robbins (1985b).

The results of the calibrated model calculation are shown in Figure 2. Contributions from the watershed comprise a small (5%) virtually constant fraction of the loading. Direct atmospheric contributions are initially about 40% of the total load but decrease in recent years to less than 20%. Inflow from Lake Huron contributes the largest portion of the loading: about 60% during the period of maximum fallout and increasing to more than 80% at the present time. This increase reflects the persistence of small amounts of the isotope in Lake Huron water. It is fortunate that lake Huron provides the major input to Lake St. Clair as the most comprehensive set of measured concentrations exist for this lake (Barry, 1973; Dasgupta, 1975; Durham and Tamro, 1980; Alberts and Wahlgren, 1981). As a result, the estimate of Cs-137 loadings are only weakly dependent on the assumptions of the long term response model.

The validity of the loading estimate rests on several assumptions. First, it is assumed that measured concentrations (of total Cs-37) adequately represent the concentration in water exiting from the lake Huron. Reported values (especially the pre-1970 data) are provided by Barry (1973) and represent hypolimnetic waters. The values reported by Alberts and Wahlgren (1981) are for the summer when the lake is stratified but no significant difference exists between epi- and hypolimnetic water. This is important because concentrations of some elements (e.g. plutonium) decrease

significantly in the epilimnion as stratification develops. If this were the case for Cs-137, surface waters which presumably exit preferentially from the lake would contribute less to Lake St. Clair during the summer months than predicted by the model. Additionally, it assumed that the river system conveying the radionuclide to the lake has no sinks. This is probably true for the St. Clair river which has a coarse grained, scoured bottom. However the delta and marshy areas which receive inflowing waters could more plausibly store cesium-137. While we were unable to collect suitable cores in these areas there are reasons why the effect should be small. Deposits in the delta are coarse, sand-sized materials which undoubtedly contain negligible amounts of the isotope. Finer grained materials which carry the radionuclide accumulate in the open lake beyond the delta area (Thomas et al., 1975). The marshy areas may trap fines efficiently but the proportion of water which flows through them is very small in comparison with open channel flow.

Vertical Distributions of Cesium-137

Representative profiles of Cesium-137 are shown in Figure 3 for sites along a transect between stations 65 and 28 (see Fig. 1.). Concentrations are generally low in comparison with surface sediments in the main lakes where in Lake Huron values are typically around 20 dpm/g and 5-10 dpm/g in Lake Erie. In most cases there is a peak in the activity which occurs 2 to 10 cm below the sediment surface. The extent of penetration of cesium-137 is generally shallow ranging from 2-4 cm toward the ends of the transect and reaching a maximum of about 14 cm around the transect midpoint. The

occurrence of subsurface maxima suggests that some information about the history of deposition may be preserved in these deposits although the correspondence between loading history and profile shape is generally weak at best.

Profiles of cesium-137 at sites 69 and 38 exhibit the best defined maxima of any from this Lake. As shown in Figure 4, both cores possess high values of cesium-137 at about 10 cm with secondary maxima at about 25 cm and 15 at sites 69 and 38 respectively. If cesium-137 reached these sites by direct transfer without sediment mixing or other integrative processes the expected profile would appear as the dashed line in each case. Sedimentation rates have been chosen to place the theoretical profile at the position of the maximum activity. Inferred rates are 0.54 cm/yr and 0.43 cm/yr respectively for site 69 and 38. In both cases the calculated distribution agrees very poorly with observation. The deeper maximum is not reproduced nor are concentrations predicted successfully elsewhere away from the primary peak region.

These profiles are apparently artifacts of stratigraphic inhomogeneities as can be seen in the companion plots in Figure 4. In each case the valley in the Cs-137 distribution is associated with (1) an decrease in the sediment solids content (FDW=fraction dry weight) as verified both by field observation and measurement, (2) an increase in the amount of material which dissolves on treatment with 10% HCl (FSOL=fraction soluble), (3) a marked increase in the K-40 content over an interval of a few centimeters. Potassium-40 is a direct measure of the total potassium

content of sediments and indicates the amount of clay sized minerals present. These results in combination with field data indicate that such discontinuities as seen in the Cs-137 profiles probably result from interlayering of old fine-grained materials of relatively high water content. As the two sites in question are relatively near the shipping channel (Fig. 1.) it is plausible the such layers as well as the material comprising the secondary peaks could originate from dredging operations. The only other core showing double Cs-137 peaks is 71 (cf Fig. 5f) which is also adjacent to the channel. Adjacent cores 65, 68 and 70 do not have double peaks but the activity of cesium-137 in these cores penetrates only a few centimeters and may be subject to mixing of near surface sediments which might obliterate such structure.

Vertical Distributions of Lead-210

Distributions of excess lead-210 are shown for eleven cores in Figure 5 a-f. Excess lead-210 is computed by subtracting the activity of supported lead-210 from each value. Supported lead-210 is taken as the average of the lowest values of lead-210 in each core, 1.5 ± 0.5 dpm/g. In estimating the supported level, activities of the isotope within glacial clay were not included inasmuch as the supported lead-210 content of the clay may not be representative of background levels in recent sediments. In these cores the K-40 content is essentially uniform down to the gray clay interface indicating that distributions of lead-210 as well as other contaminants are probably not artifacts of grain-size dependent sorting processes. In every case distributions of excess lead-210 are characterized by a zone, extending

down from the sediment water interface to varying depths, possessing a constant activity. Below this depth the activity decreases virtually exponentially. Exceptions to this pattern occur in cores 38, and 69 which exhibit disturbances in the vicinity of the stratigraphic anomalies discussed above.

The remaining distributions have the form seen elsewhere in the Great Lakes, both in the open lake environment (Robbins and Edgington, 1975; Robbins et al., 1978; Robbins, 1980) and in the silty, shallower recent deposits of lower Saginaw Bay. In previous discussions such profiles have been generally treated in terms of the rapid steady state mixing model (RSSM) in which instantaneous mixing of sediment and lead-210 is postulated to occur within a discrete zone at the sediment water interface. Sediments below this zone are free of mixing or other disturbance and accumulate at a constant rate. Details of the mathematical model are provided elsewhere (Robbins et al., 1977). The solid lines shown in Figures 5 a-f are based on the RSSM model, in which values for the depth of mixing (expressed in g/cm^2) and sedimentation rate (expressed in $\text{g}/\text{cm}^2/\text{yr}$) are chosen to yield the best weighted least-squares fit. Inspection of the figures shows that the agreement between observation and the model is excellent except for the previously discussed cores 38 and 69.

Apart from cores 38 and 69 (and 65) mixed depths have a relatively narrow range, averaging about 3.5 (± 1.3) cm. Sedimentation rates are also narrowly confined, 0.19 (± 0.06) cm/yr . If the process is correctly characterized by the RSSM model then the ratio of the mixed depth (g/cm^2) to

the sedimentation rate ($\text{g/cm}^2/\text{yr}$) is a measure of the time resolution for reconstructing time histories from the sediment record. The mean ratio (excluding 38, 65 and 69) is 19 (± 12) yr.

Since the model results refer to sediment processes and not lead-210 per se, a test of the self-consistency of the RSSM model may be developed by applying it to the Cs-137 profiles using the mixed depth and sedimentation rate derived from lead-210. The results of this exercise are shown in the companion plots in Figures 5 a-f. Cs-137 distributions are plotted along with the solid curve which is the unadulterated model fit. In general (with the exception of 38 and 69 as usual) the agreement is good. Dashed curves also shown result from allowing the mixed depth and sedimentation rate to vary so as to produce an optimized fit. In general the predicted distributions are not much better. The effect of unconstraining the solution is to increase the model mixed depth so as to fit the region where the activity of the isotope falls off rapidly. This occurs with a loss of structure in the peak region. In the case of core 65, considerable mixing is implied by the Cs-137 data and no mixing by the lead-210 data. Such an inconsistency would occur if some recent event removed enough surface material either by scouring or by disturbance during collection of the core.

The idea of surface sediment loss in core 65 is further substantiated by the total Cs-137 to total excess lead-210 ratio provided for each core in Table 1. The three cores (38, 69 and 71) with stratigraphic discontinuities have ratios of 1.0-1.6. The remaining cores have ratios ranging from 0.6 to 0.8 while core 65 has a ratio of 0.48. Loss of surface sediment would

measured, (Table 2). This measurement was made only twice due to the time required for performance of the experiments and the analysis of the samples generated.

The assimilation efficiency from sediments can be estimated from literature values of feeding rates (Zimmerman and Wissing, 1978) and the K_s values. Our organisms were generally 20 mm in length or longer and K_s was determined at 15 and 20°C. The feeding rates for the larger nymphs were 0.21 g sediment g⁻¹ organisms h⁻¹ at 15°C and 0.31 g g⁻¹ h⁻¹ at 20°C after converting the feeding rates based on dry weight nymphs to a wet weight basis and converting to hourly averages (Zimmerman and Wissing, 1978). These feeding rates have the same units as the K_s values. Thus, it is possible to compare the feeding rates directly with the K_s values. Since the K_s values are less than the feeding rate the implication is that all of the contaminant is not being removed from the sediment as it passes through the gut of the organisms. Therefore a ratio of K_s to feeding rates should give the fraction of material assimilated or removed. With these feeding rates the efficiency for assimilation for BaP ranged from 11.3 - 21%, Phe from 13.6 - 31.3% and HCB from 14.4 - 29.1%. This estimated assimilation efficiency is in the same range as that determined for obligochaetes for HCB in an elegant dual labeled study (Klump et al., 1987).

Using the same estimates of water and sediment concentrations as used for the simulation model, calculation of the amount of compound accumulated from water versus sediment at steady state was determined by the following equations

$$C_{ss} = (K_w C_w + K_s C_s) / K_d \quad (3)$$

$$C_a^w = K_w C_w / K_d \quad (4)$$

$$C_a^s = K_s C_s / K_d \quad (5)$$

Where C_{ss} is the concentration of the toxicant in the organism from both a water and sediment source at steady state, C_a^w is the concentration in the animal at steady state from water (ng g^{-1}), and C_a^s is the concentration in the animal at steady state from sediment (ng g^{-1}). From these equations the fraction from water can be computed from C_a^w / C_{ss} . Similarly, the fraction from sediment would be computed from C_a^s / C_{ss} .

For the two times that the HCB accumulation from sediment was measured, the fraction of the body burden from the water was estimated to be 0.1 and 0.03. Thus the fraction from sediment was 0.9 and 0.97. The route of HCB accumulation for this organism is apparently via the sediment. Similar comparisons for the PAH yielded ratios for BaP of 0.9 and 0.96 and for Phe 0.95 for both determinations as the fraction of toxicant obtained from the sediments. This determination is very dependent on the ratio of the products of $K_w C_w$ and $K_s C_s$; therefore, changes in environmental concentrations without any change in rate constants would alter the fraction obtained from a particular source.

Comparing the estimated role of sediment as a source with other organisms, H. limbata obtains a greater fraction of its body burden from the

sediment. Using the same water and sediment concentrations as for the projections for H. limbata and the kinetics constants for the oligochaete, S. heringianus, (Frank et al., 1986) and P. hoyi (Landrum et al., 1985), the oligochaetes would obtain 34 to 67% of their BaP body burden from sediment while P. hoyi would only obtain 39% from sediments. This suggests that the role of sediments as a source will depend on the organism as well as the sediment characteristics.

Using the environmental data available, the deterministic simulation model suggests that the highest concentration of the toxicants studied will occur in the winter and early spring. There is a consistent peak in the body burden that occurs in the spring for all the compounds (Figs. 2-4) and is driven primarily by a reduction in K_d resulting in a reduced flux out of the organism (Fig. 5). The organism concentrations then decline during the summer (Figs. 2-4). In general the flux of compound into the organism is primarily from the product of $K_s C_s$ and under the conditions used in the simulation for HCB would be $2.7 \text{ ng g}^{-1} \text{ h}^{-1}$. This flux from the sediment is augmented by the flux in from the water, $K_w C_w$, and is reduced by the flux out of the organism, $K_d C_a$ (Fig. 5). Because of the extremely low water concentrations expected the flux in from the water contributes very little to the overall flux into the organism. Further, because the flux from the sediment is held constant in the simulation and the contribution from the water is small, the seasonal variation in body burden is mainly driven in this simulation by the flux out of the organism as represented by changes in K_d over the course of the season. Thus, the summer decline is generally attributable to the increase in K_d . Changes in K_s would also be expected to

impact the seasonal changes in body burden but there was insufficient data to justify a change with season. The bioaccumulation factor (BAF) (organism concentration/sediment concentration) was based on sediment concentration because it was the predominant source for the organisms. The BAF ranged from about 4.5 to 15.5 for HCB and reflects the generally low elimination rate constant while PAH showed a much lower BAF, Phe 0.9 - 2.2 and BaP 1.5 - 3.8. The change with season of the BAF values tracks the change in organism concentration. The BAF predicted for H. limbata are higher than those found for oligochaetes for HCB in the field (Smith et al., 1985) and BaP (Eadie et al., 1982) but were about the same as oligochaetes for Phe (Eadie et al., 1982). Comparing H. limbata to P. hoyi the range of BAF's are about the same for the two PAH studied (Eadie et al., 1985).

In conclusion, H. limbata exhibits seasonal changes in the toxicokinetics and these changes are expected to result in changes in the BCF and BAF. The organism appears to obtain the preponderance of its body burden for the toxicants examined from the sediment based on the calculations from the toxicokinetics and sediment and water data from the literature.

ACKNOWLEDGEMENTS

This work was jointly supported by the Great Lakes Environmental Research Laboratory, NOAA and by the U. S. Environmental Protection Agency through interagency agreement No. DW13931213-01-01. I wish to thank Tom Fontaine for his critical discussions and suggestions on the kinetics modeling. I also wish to thank Brian Eadie, Tom Nalepa, Mike Quigley and Guy Stehly for their critical review of this manuscript.

Table 1. Oxygen consumption and lipid content for Hexagenia in 1986

Date	Oxygen Consumption $\mu\text{g e}_2 \text{ mg}^{-1} \text{ h}^{-1}$	Oxygen Clearance ¹ $\text{mL g}^{-1} \text{ h}^{-1}$	%Lipid	Temperature °C
May	0.327 ± 0.111 n = 5	23.3 ± 7.9	7.8 ± 1.9 n = 7	10
June	Lost		15.1 ± 2.6 n = 5	15
July	0.667 ± 0.296 n = 5	41.4 ± 18.3	9.1 ± 3.4 n = 8 4.3 ± 1.8^2	15
August	0.435 ± 0.10 n = 5	61.9 ± 13.5	3.6 ± 1.0 n = 7	20
September	0.25 ± 0.06 n = 10	44.5 ± 12	6.0 ± 2.4 n = 6 6.9 ± 1.9^2	20
October ³	0.16 ± 0.10 n = 4	18.6 ± 11.8	3.7 ± 1.2 n = 7 3.3 ± 0.9^2	20
November	ND		6.0 ± 1.4 n = 4	10

1. The n for the clearance determination is the same as the oxygen consumption determination.
 2. Samples collected in 1985.
 3. Sample actually collected on 30 September 1986, Oxygen consumption was run 60 d after collection.
- ND - not determined

Table 2. Seasonal Uptake and Elimination Rate Constants
for Hexagenia limbata

Month		Benzo(a)pyrene	Phenanthrene	Hexachlorobiphenyl	Temp.
May	Ku*	68.5 ± 11.2	131.1 ± 46.8	47.5 ± 23.9	10 ¹
	Kd**	0.011 ± 0.003	0.032 ± 0.004	0.007 ± 0.001	
June	Ku	67.0 ± 28.0	43.3 ± 12.0	44.2 ± 8.0	15
	Kd	0.006 ± 0.002	0.0076 ± 0.0016	0.005 ± 0.002	
	Ks***	0.043 ± 0.005	0.065 ± 0.016	0.030 ± 0.01	
		0.025 ± 0.004 ²			
July	Ku	101.9 ± 32.6	57.5 ± 5.0	40.8 ± 37.3	15
	Kd	0.013 ± 0.002	0.029 ± 0.002	0.005 ± 0.001	
Aug	Ku	65.1 ± 29.1	11.9 ± 4.0	40.8 ± 37.3	20
	Kd	lost	lost	0.007 ± 0.001	
	Ks	0.035 ± 0.005	0.042 ± 0.008	0.09 ± 0.02	
Sept	Ku	149.5 ± 29.0	56.3 ± 6.8	128.7 ± 20.3	20
	Kd	0.016 ± 0.003	0.032 ± 0.004	0.015 ± 0.003	
Sept ³	Ku	76.3 ± 41.0	33.0 ± 8.0	95.0 ± 17.3	20
	Kd	0.028 ± 0.001	0.067 ± 0.008	0.017 ± 0.002	
Nov	Ku	40.9 ± 30.6	34.2 ± 7.2	45.5 ± 16.1	10
	Kd	0.010 ± 0.001	0.026 ± 0.002	0.004 ± 0.0006	

* Ku has been corrected for sorption to dissolved organic carbon and has units of mL g⁻¹ h⁻¹.

** Kd has units of h⁻¹.

*** Ks has units of g dry sediment g⁻¹ animal h⁻¹

1. Temperature is in degrees centigrade.

2. Uptake from sediment was measured twice for BaP

3. This collection was actually made on September 30, 1986.

LITERATURE CITED

- Carr, J. F. and J. K. Hiltunen. 1965. Changes in the bottom fauna of western Lake Erie from 1930 to 1961. Limnol. Oceanogr. 10:551-569.
- Eadie, B. J., W. Faust, W. S. Gardner and T. Nalepa. 1982. Polycyclic aromatic hydrocarbons in sediments and associated benthos in Lake Erie. Chemosphere 11:185-191.
- Eadie, B. J., W. R. Faust, P. F. Landrum, N. R. Morehead, W. S. Gardner and T. Nalepa. 1983. Bioconcentrations of PAH by some benthic organisms of the Great Lakes. In: Polynuclear Aromatic Hydrocarbons: Seventh International Symposium on Formation, Metabolism and Measurement. M. W. Cooke and A. J. Dennis, Eds. Battelle Press, Columbus, OH. pp. 437-449.
- Eadie, B. J., W. R. Faust, P. F. Landrum and N. R. Morehead. 1985. Factors affecting bioconcentration of PAH by the dominant benthic organisms of the Great Lakes. In: Polynuclear Aromatic Hydrocarbons: Eighth International Symposium on Mechanisms, Methods and Metabolism. M. W. Cooke and A. J. Dennis, Eds. Battelle Press, Columbus, OH. pp. 363-377.
- Frank, A. P., P. F. Landrum and B. J. Eadie. 1986. Polycyclic aromatic hydrocarbon rates of uptake, depuration, and biotransformation by Lake Michigan Stylodrilus heringianus. Chemosphere 15:317-330.

- Frez, W. A. and P. F. Landrum. 1986. Species-dependent uptake of PAH in Great Lakes invertebrates. In: Polynuclear aromatic hydrocarbons: Ninth International Symposium on Chemistry. Characterization and Carcinogenesis. M. W. Cooke and A. J. Dennis, Eds. Battelle Press, Columbus, OH. pp. 291-304.
- Gardner, W. S., W. A. Frez, E. A. Cichocki and C. C. Parish. 1985a. Micromethod for lipid analysis in aquatic invertebrates. Limnol. Oceanogr. 30:1099-1105.
- Gardner, W. S., T. F. Nalepa, W. A. Frez, E. A. Cichocki and P. F. Landrum. 1985b. Seasonal patterns in lipid content of Lake Michigan macroinvertebrates. Can. J. Fish. Aquat. Sci. 42:1827-1832.
- Grasshoff, K., M. Ehrhardt and K. Kremling. 1976. Methods of Seawater Analysis. Second Edition, Verlag Chemie, Federal Republic of Germany, pp. 419.
- Henry, M. G., D. N. Chester and W. L. Mauck. 1986. Role of artificial burrows in Hexagenia toxicity tests: Recommendations for protocol development. Environm. Toxicol. Chem. 5:553-559.
- Hiltunen, J. K. and D. W. Schlosser. 1983. The occurrence of oil and the distribution of Hexagenia nymphs in the St. Mary's River, Michigan and Ontario. Freshwat. Invertebr. Biol. 2:199-203.

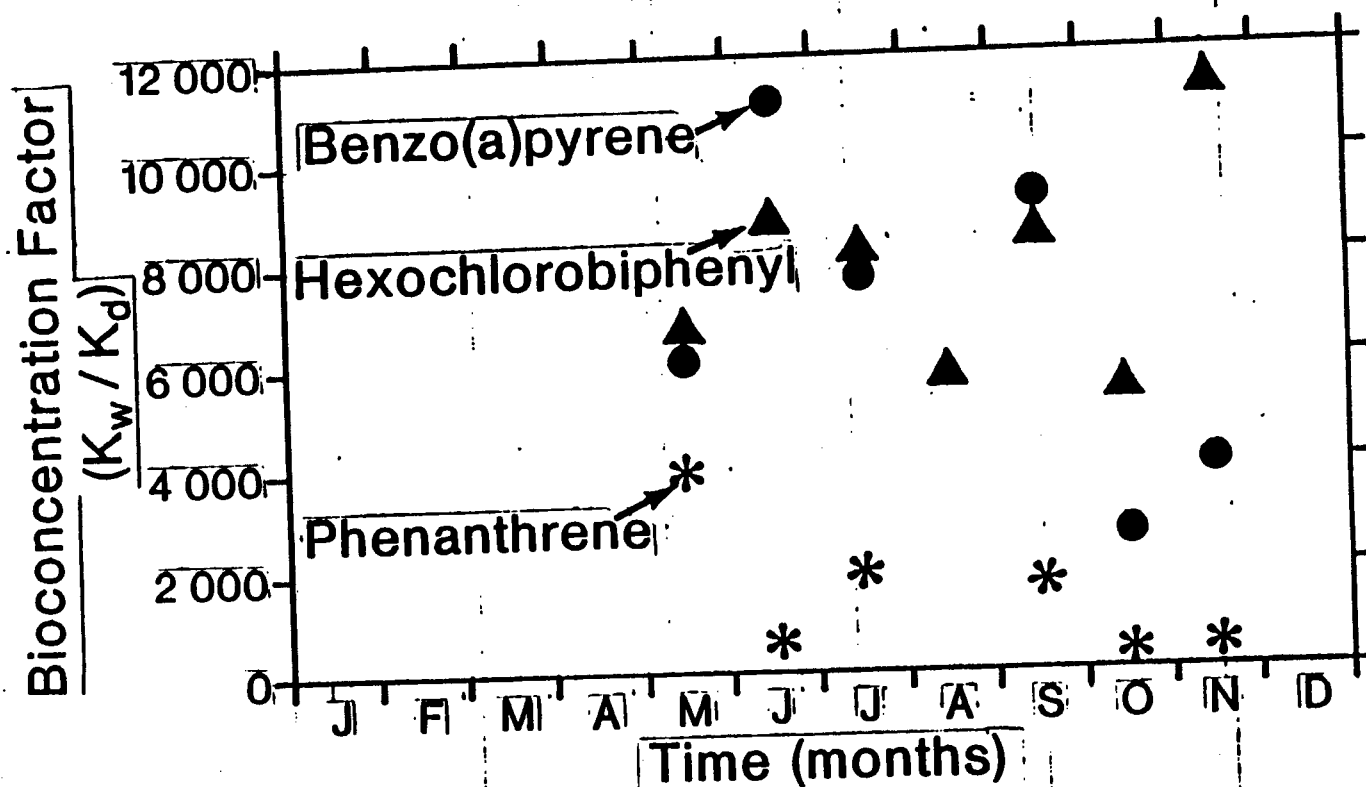
- Howmiller, R. P. and A. M. Beeton. 1971. Biological evaluation of environmental quality, Green Bay, Lake Michigan. J. Wat. Pollut. Cont. Fed. 123-133.
- Hunt, B. P. 1958. The life history and economic importance of a burrowing mayfly, Hexagenia limbata, in southern Michigan lakes. Bulletin of the Institute of Fisheries Research. No. 4. Michigan Department of Conservation, Lansing, MI pp 151.
- Klump, J. V., J. R. Krezoski, M. E. Smith and J. L. Kaster. 1987. Dual tracer studies of the assimilation of an organic contaminant from sediments by deposit feeding oligochaetes. Can. J. Fish. Aquat. Sci. 44:(In press).
- Landrum, P. F. 1983. The effect of co-contaminants on the bioavailability of polycyclic aromatic hydrocarbons to Pontoporeia hoyi. Polynuclear Aromatic Hydrocarbons: Seventh International Symposium on Formation, Metabolism and Measurement, M. W. Cooke and A. J. Dennis eds. Battelle Press, Columbus, OH. pp. 731-743.
- Landrum, P. F., B. J. Eadie, W. R. Faust, N. R. Morehead and M. J. McCormick. 1985. Role of sediment in the bioaccumulation of benzo(a)pyrene by the amphipod, Pontoporeia hoyi. Polynuclear Aromatic Hydrocarbons: Eighth International Symposium on Mechanisms, Methods and Metabolism. M. W. Cooke and A. J. Dennis Eds. Battelle Press, Columbus, OH. pp. 799-812.

- Leversee, G. J., J. P. Giesy, P. F. Landrum, S. Gerould, J. W. Bowling, T. E. Fannin, J. D. Haddock and S. M. Bartell. 1982. Kinetics and biotransformation of benzo(a)pyrene in Chironomus riparius. Arch. Environ. Contam. Toxicol. 11:25-31.
- Schneider, J. C., F. F. Hooper and A. M. Beeton. 1969. The distribution and abundance of benthic fauna in Saginaw Bay, Lake Huron. Proc. 12th Conf. Great Lakes Res. International Assoc. Great Lakes Res. pp. 80-90.
- Smith, E. V., J. M. Spurr, J. C. Filkins and J. J. Jones. 1985. Organochlorine contaminants of wintering ducks foraging on Detroit River sediments. J. Great Lakes Res. 11:247-265.
- Thornley, S. 1985. Macrozoobenthos of the Detroit and St. Clair rivers with comparisons to neighboring waters. J. Great Lakes Res. 11:290-296.
- Zimmerman, M. C., T. E. Wissing and R. P. Rutter. 1975. Bioenergetics of the burrowing mayfly, Hexagenia limbata, in a pond ecosystem. Verh. Internat. Verein. Limnol. 19:3039-3049.
- Zimmerman, M. C. and T. E. Wissing. 1978. Effects of temperature on gut-loading and gut clearing times of the burrowing may fly, Hexagenia limbata. Freshwat. Biol. 8:269-277.

LIST OF FIGURES

- Fig. 1. Calculated bioconcentration factors in Hexagenia limbata over the 1986 field season calculated from the ratio of K_w/K_d .
- Fig. 2. Simulation of the concentration of HCB in H. limbata through one season based on the concentrations of HCB in sediments and water found in the Detroit River..
- Fig. 3. Simulation of the concentration of BaP in H. limbata through one season based on the concentrations of BaP in Lake Erie sediments and water concentrations found in the Great Lakes.
- Fig. 4. Simulation of the concentration of Phe in H. limbata through one season based on the concentrations of BaP in Lake Erie sediments and water concentrations found in the Great Lakes.
- Fig. 5. Simulated flux of HCB into the organism from water and out of the organism through elimination.

Fig 1



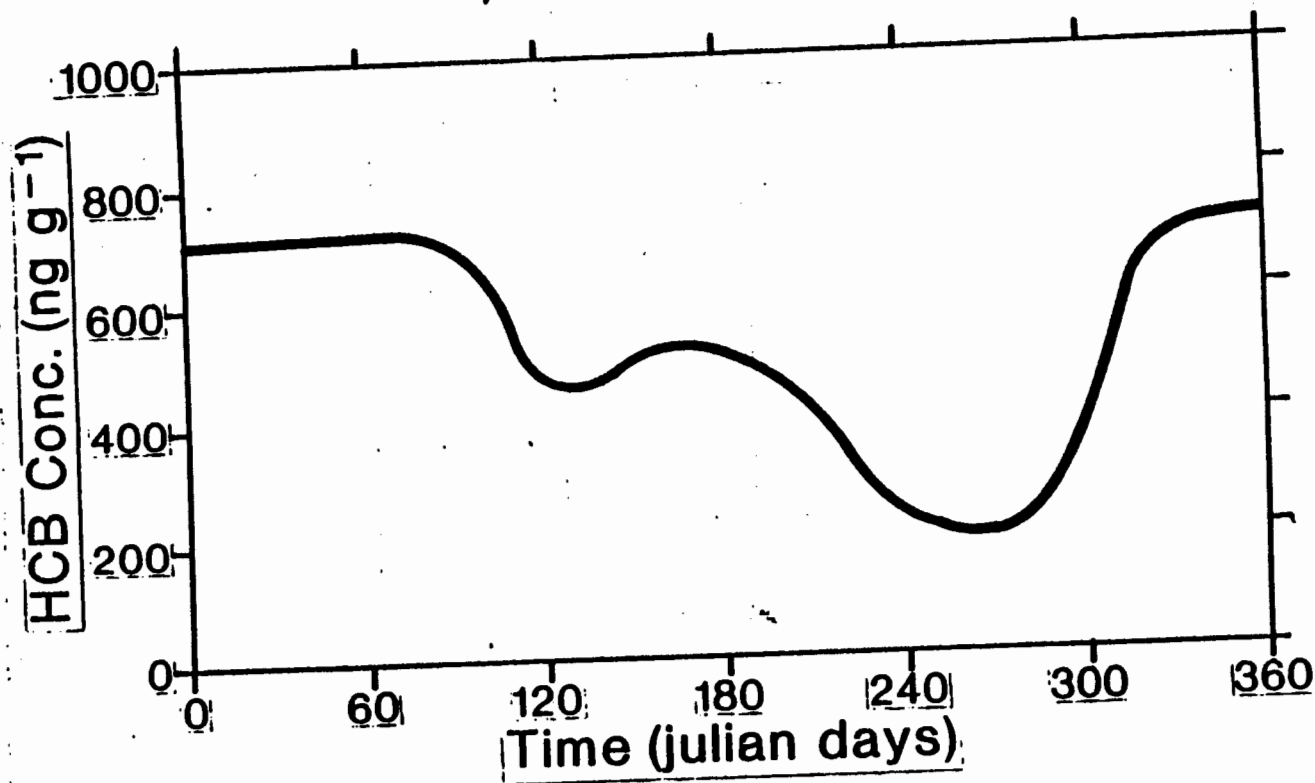
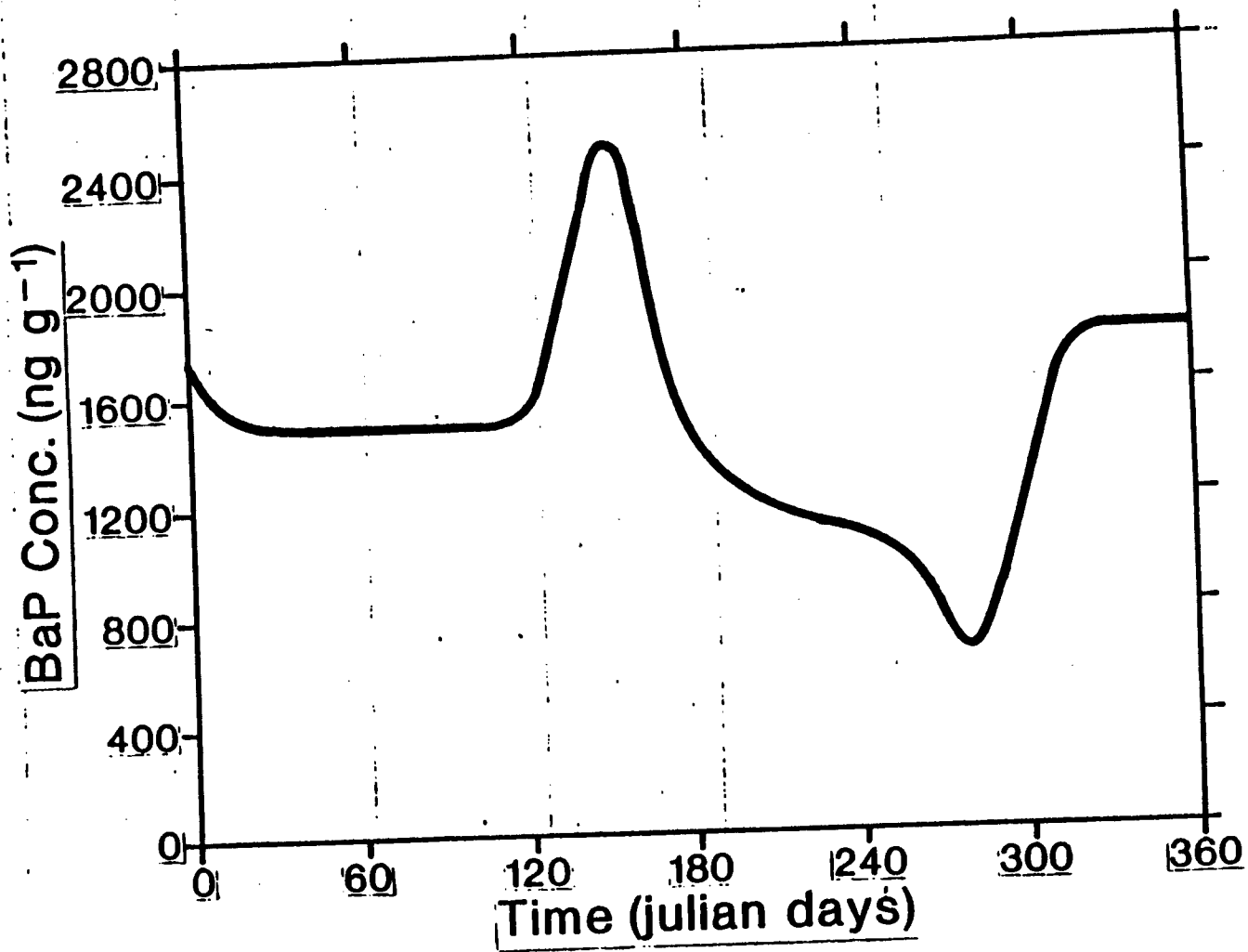
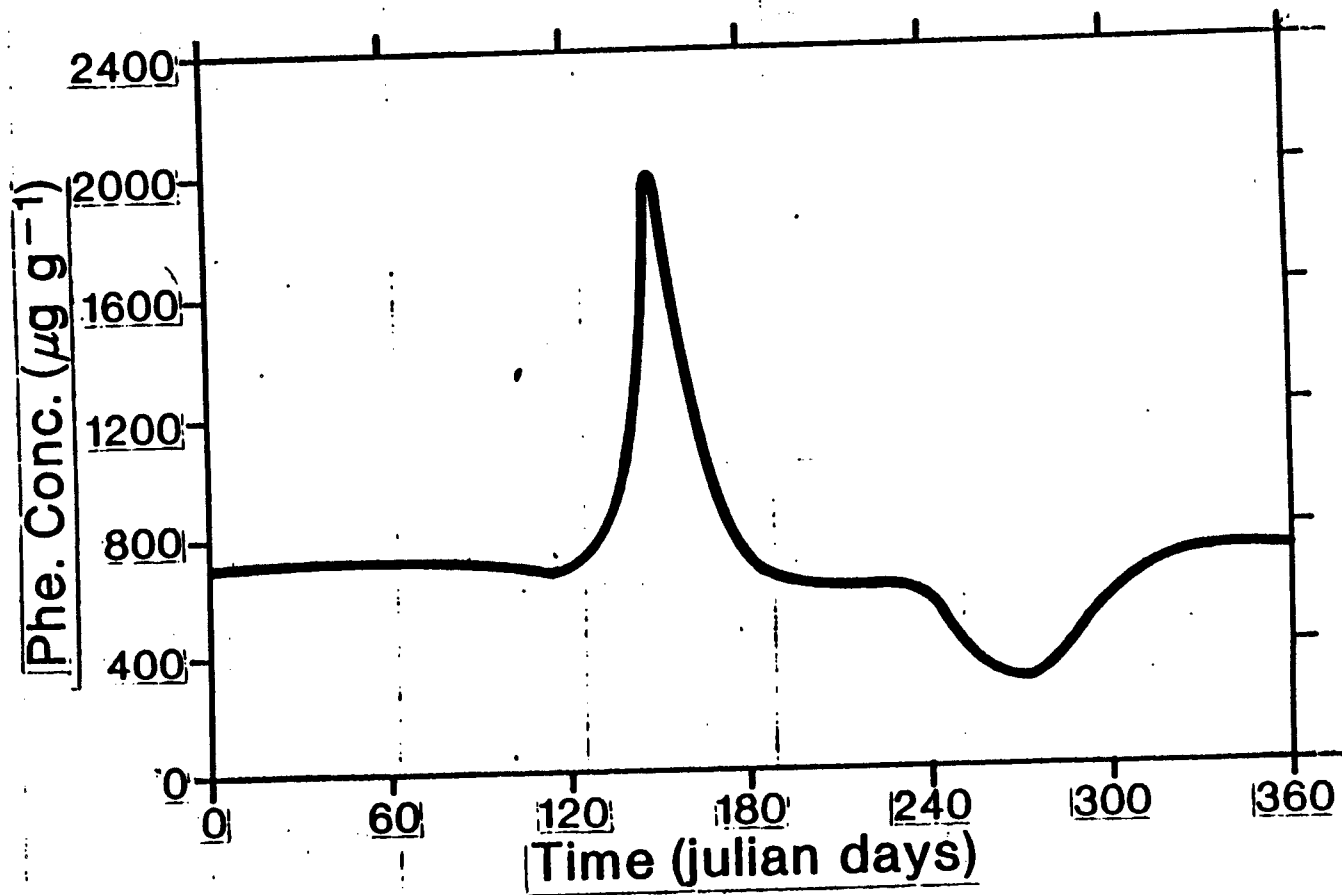
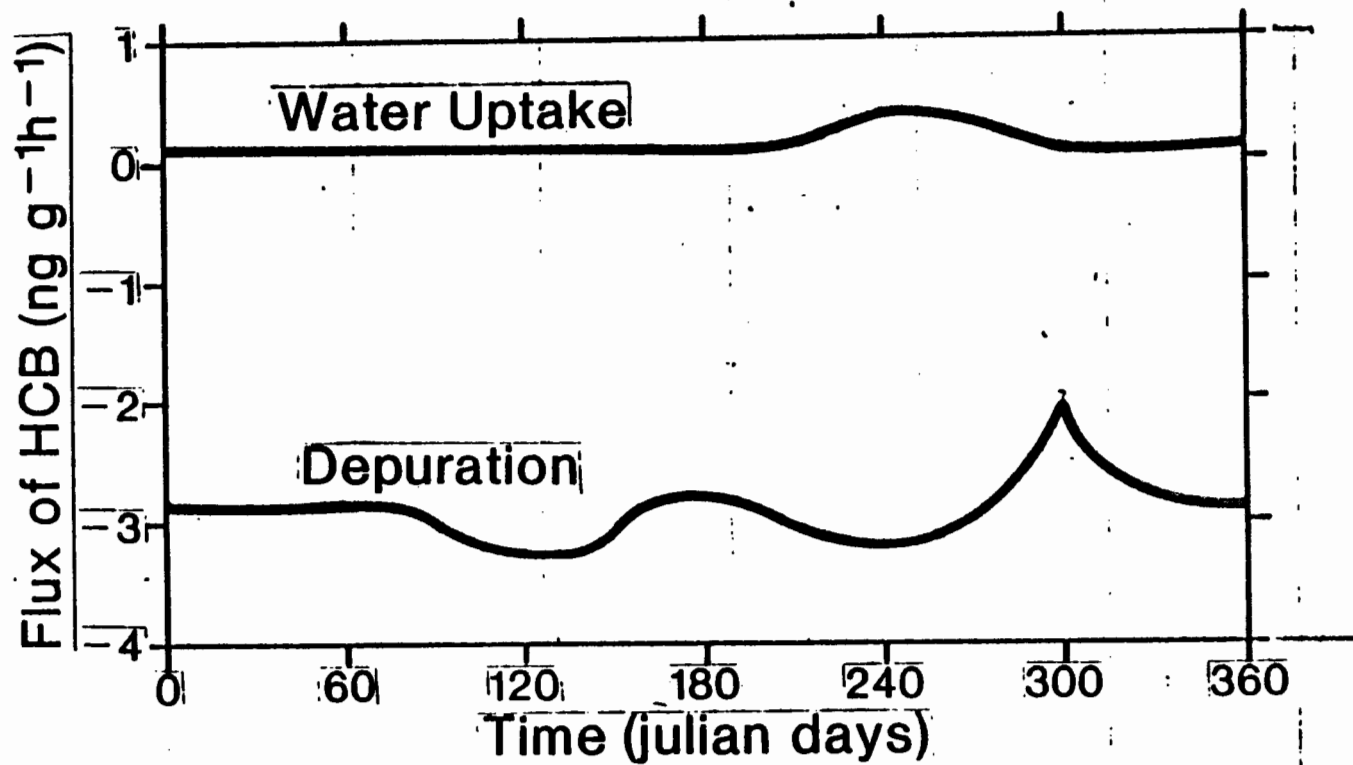


Fig 3



LAVINIA (3)
Fig 4





MODELING THE FATE AND TRANSPORT OF CONTAMINANTS IN LAKE ST. CLAIR

Gregory A. Lang and Thomas D. Fontaine, III

INTRODUCTION

When looking at the Great Lakes System as a whole, two aspects of Lake St. Clair stand out: 1) its average depth is only about 3 m (the next most shallow lake is Lake Erie at 19 m) and 2) its theoretical hydraulic retention time is only about 9 days (again, the next closest is Lake Erie at about 3 years). Lake St. Clair has been described as simply a "wide part of the river" that extends from mouth of Lake Huron to the head of Lake Erie, and past Great Lakes budget calculations have generally overlooked the dynamics of nutrient and contaminant transport into and through Lake St. Clair. Sediment studies of Frank et. al. (1977), Pugsley et. al. (1985), and Oliver and Bourbonniere (1985) document the levels of organic contaminants, including polychlorinated biphenyls and octachlorostyrene, in the surficial sediments of Lake St. Clair and the St. Clair and Detroit Rivers. The concentrated chemical plumes located near the center of Lake St. Clair, between the South Channel and the Detroit River, indicates the ability the lake's sediments to trap particle-bound contaminants.

Recent attention to the connecting channels of the upper Great Lakes and the recognized harmful effects to biota and the extreme environmental

persistence of many of these hydrophobic chemicals have served as the impetus for studying the dynamics of contaminant transport within Lake St. Clair. The objectives of this study were two fold: 1) to develop a multi-segment mass balance model to simulate contaminant fate and transport in Lake St. Clair, based on the Environmental Protection Agency's model TOXIWASP; and 2) to calibrate, verify, and apply the model using available contaminant and tracer data. This report presents the model, briefly describes the model processes affecting chemical and solids concentrations, details the physical lake characteristics and model segmentation, describes the tracer and contaminant input data, and presents the simulation results.

MODELING APPROACH

The mathematical model used in this analysis was based on the Environmental Protection Agency's Chemical Transport and Fate Model TOXIWASP (Ambrose et. al. 1983). TOXIWASP combines the kinetic formulations in the EXposure Analysis Modeling Simulation, EXAMS (Burns et. al. 1982), and the transport processes in the Water Analysis Simulation Program, WASP (DiToro et. al. 1983). The mechanics of TOXIWASP were left relatively unchanged. However, in an attempt to streamline the model, improve its execution time, and to make it more specific to Lake St. Clair's physical and contaminant data, some modifications were made. Numerous programming errors found in the source code (in particular, subroutine SETTLE) were corrected. The EPA-Athens modeling group was informed of all corrections needed.

Two state variables are included in TOXIWASP, total organic chemical and total sediment. Sediment concentrations are affected by advection, dispersion, mass loading, settling, and resuspension. Chemical concentrations are affected by these same processes, plus degradation, sediment-water diffusion, and biological mixing to deep sediments. Chemical degradation is due to hydrolysis, biolysis, photolysis, oxidation, and volatilization. Sorption onto sediments and biota is calculated via equilibrium kinetics using a chemical-specific partition coefficient and spatially-varying environmental organic carbon fractions. These transport and transformation processes are detailed fully in the EPA TOXIWASP Manual (Ambrose et. al. 1983), EPA EXAMS Manual (Burns et. al 1982), and the EPA WASP Manual (DiToro et. al. 1983).

Physical Lake Characteristics

The volume and surface area of Lake St. Clair were taken to be 3.75 km^3 and 1065.7 km^2 , respectively. The study area was segmented into 126 well-mixed segments: 42 water segments, 42 active sediment layer segments, and 42 deep sediment layer segments (Fig. 1). The segment numbers in Figure 1 correspond to water column segments; active layer and deep layer segment numbers are determined by adding one and two, respectively, to the water column numbers. The average segment size was about 5 km on a side. The segmentation scheme was based on the results of two contributing projects. One was an extensive cluster analysis performed on the available chemical, physical, biological, and contaminant data in the water column and sediments of Lake St. Clair (Rybczyk 1986). The other was the 1.2 km grid Lake St.

Clair Rigid Lid Hydrodynamic Model (Schwab and Liu 1987) which generated the wind-driven flow fields used in the present study to transport solids and chemical throughout the water column. The 126-segment grid and the 1.2 km grid were superimposed such that segment interfaces were shared. The hydrodynamic model flows were summed along the larger TOXIWASP segment interfaces yielding 75 net interface flows.

The volumetric inflow and outflow rate was constant at 5700 cms. The depth of the water column segments ranged from 2 m to 5.2 m (areal average = 3.5 m). The depth of the active sediment layer was uniform at 2 or 10 cm, depending on the simulation. The depth of the deep sediment layer was equal to the total depth of the "recent sediments" minus the active layer depth. The "recent sediments" are defined by Robbins and Oliver (1987) as those sediments deposited on top of the post-glacial till and range from 3-30 cm. The rate of horizontal dispersion was assumed to be $1 \times 10^5 \text{ cm}^2/\text{s}$ (Great Lakes Institute 1986). Pore water diffusion was set to $1 \times 10^{-5} \text{ cm}^2/\text{s}$.

Solids

Suspended solids from tributary sources were loaded at a constant rate of 2700 MT/day into 8 water column segments. The St. Clair River load entered segments 16, 25, 37, 49, and 55 (Fig. 1), the Sydenham River load entered segment 58; the Clinton River load entered segment 19, and the Thames River load entered segment 124. The loads were based on average tributary concentrations and flows reported by the Great Lakes Institute (1986). The settling velocity of solids was set equal to 3 m/d, based on

results of an empirical modeling procedure for Lake St. Clair (Simons and Schertzer 1986). The resuspension velocity in each segment was calculated such that the particulate settling and resuspension fluxes across each segment's sediment/water interface were equal (i.e., the net sedimentation rate was assumed zero). The assumption of zero net sedimentation is based on the relatively shallow depth of the recent, post-glacial sediments (Robbins and Oliver 1987).

Under constant wind (and thus constant flow) conditions, the solids concentration in each water column segment could be calculated from the advective flux of solids to and from each segment, the dispersive solids flux between segments, the rate of solids loading into each segment, and the assumption of zero net sedimentation. The suspended solids concentrations resulting from a steady 6 m/s wind from the southwest ranged from 4.7-10.5 mg/l (volumetric average = 6.33 mg/l). These values are consistent with those measured by Bukata et. al. (1987) along ship transects during three separate cruises in Lake St. Clair in September, 1985. They reported a range of 2.5-16 mg/l, with a mean of approximately 5 mg/l. The concentration of solids in the active and deep layer model sediments was set to 1.2×10^6 mg/l, based on the average of 19 10-cm sediment cores from 1985 (Robbins 1986, Great Lakes Environmental Research Laboratory, personal communication). The calculated resuspension rates ranged from 0.42-0.95 cm/yr.

The model does not distinguish between different types of sediment, a particular concern when simultaneously modeling nearshore and offshore

concentrations of organic, hydrophobic contaminants. However, it does provide a parameter for defining the spatially-varying organic carbon content of the sediment. It was assumed that the organic carbon content in each segment would not vary over time; i.e., particulate matter resuspended from the active layer would immediately be available for transport to another segment, but the average organic carbon content of each segment would be maintained over time.

TOXIWASP requires the user to quantify certain model parameters and constants; parameters vary over space but not time, constants do not vary. Ranges and values of Lake St. Clair parameters and constants used in the present study are presented in Table 1. Constants associated with particular contaminants are presented in separate tables.

Chemical

The chemical being modeled was loaded into Lake St. Clair from atmospheric, land runoff, and/or tributary sources. A whole-lake areal atmospheric load was calculated from available flux measurements and then segmented according to each segment's surface area. The tributary chemical loads entered the same segments as the solids loads (segments 16, 19, 25, 37, 49, 55, 58, and 124); although, not necessarily all eight. For example, octachlorostyrene, thought to originate mainly from the Sarnia area, entered the lake through segments 37 and 49 only. The total load from land runoff sources was partitioned to all water segments bordering the shore according to each segment's drainage area.

The model assumed a local equilibrium between the dissolved, sorbed, and bio-sorbed chemical as defined by the organic carbon content of particles and octanol-water partition coefficients, K_{oc} and K_{ow} . K_{ow} , held constant throughout time and space, was multiplied by the varying organic carbon content of the sediment, resulting in a spatial distribution of the solid/water partition coefficient, K_p , that corresponded closely to the distribution of fine-grained, organic-rich sediment. K_{ow} was multiplied by the organic carbon content of the biomass to yield an overall biota/water partition coefficient, K_b .

Vertical distributions of excess lead-210, measured from a set of diver-collected sediment cores from Lake St. Clair in 1985, possessed a zone of constant activity extending down to about 3 cm with exponential fall off below (Robbins and Oliver 1987). Analyses of these distributions plus those of cesium-137 indicate sedimentation rates on the order of 0.1-0.2 cm/yr. Robbins and Oliver state that because of the evidence of extensive biological activity down to at least 15 cm, biological mixing, and not net particulate settling, is favored as the mechanism producing observed vertical radionuclide and contaminant sediment distributions. Because there is no mechanism for biological mixing in TOXIWASP, the model was modified to account for constant, spatially-varying, burial of chemical from the active sediment layer to the deep sediments. This rate was set to 0.1 cm/yr throughout the lake.

SIMULATIONS

A series of simulations were performed during this study for purposes of model calibration, verification, and application. These include simulations of the conservative ion chloride, the radionuclide cesium-137, and the organic contaminants octachlorostyrene and polychlorinated biphenyls. Descriptions of simulation conditions, available chemical observations, loading functions, and chemical constants required for these simulations are presented here; the results are presented in a later section.

Chloride

Chloride, a conservative ion, was chosen to test the efficacy of the transport mechanisms in TOXIWASP. Bell (1980) documents chloride and meteorological data collected during a series of cruises in Lake St. Clair during the summer of 1974. Cruises 3 (19-29 June), 5 (15-24 July), 6 (5-15 August), and 8 (16-25 September) were the most complete and were thus selected for this study. At least 30 stations were monitored during each of the 4 cruises. An average chloride load to the lake was calculated for each cruise as the product of tributary flows and chloride concentrations. The flow fields during each cruise were generated with the hydrodynamic model using the cruise-averaged wind conditions (speed and direction). The model flows were multiplied by a factor of 0.93 to account for the difference in total inflow between the 1974 value (5300 cms) and that used in the

hydrodynamic model (5700 cms). The horizontal dispersion coefficient was set to 1×10^5 cm²/s for all segment interfaces. Chloride is a dissolved conservative substance; thus partitioning, settling, resuspension, and degradation were not included.

Four steady-state simulations were performed, one corresponding to each cruise; each with a different chloride load and wind-induced flow field. The average wind conditions for cruises 3, 5, 6, and 8 were 4 m/s from the northeast, 5 m/s from the north, 5 m/s from the east, and 6 m/s from the west, respectively. The total chloride loads to Lake St. Clair during the four cruise periods were 3.7×10^6 kg/day, 3.4×10^6 kg/day, 3.2×10^6 kg/day, and 3.3×10^6 kg/day, respectively. Eight additional simulations were generated for each cruise; one for each wind direction other than the observed direction and one for the no wind case.

Cesium-137

Cesium-137, a surrogate of many hydrophobic, organic contaminants, was chosen to calibrate and verify the processes associated with sediment-bound contaminant movement. A 35-year history (1950-1985) of Cs-137 loading to Lake St. Clair (Figure 2) was extracted from Robbins and Oliver (1987). During this period, the largest portion of loading has been inflow from Lake Huron. A nearly equal contribution (about 40% of the total load) originated from the atmosphere during the 1950s and early 1960s. Lake Huron presently contributes about 75% of the total load, while the atmosphere contributes less than 20%. The remainder of the load (about 5%) originates from land

runoff sources. Observed cesium concentrations in the upper 2 cm of bottom sediment were available for 1976 and 1985 (Robbins and Oliver 1987). In both years, concentrations were closely related to the thickness of the recent sediments, with the highest concentrations located in the corridor between the mouth of the South Channel of the St. Clair River and the head of the Detroit River. In addition, Robbins and Oliver estimated the total accumulation of cesium-137 over the entire depth of sediments in 1985.

Cesium-137 has a half life of 30.2 years and a partition coefficient, K_p , of about 29000 l_w/kg . The partition coefficient was calculated from the lake-averaged suspended solids concentration in Lake St. Clair and the fraction of dissolved contaminant (0.847), assumed constant for all of the Great Lakes (Robbins 1985). With an average organic carbon content of the open-lake sediments equal to about 2.5%, K_{oc} is calculated to be 1.16×10^6 l_w/kg . The active sediment depth was set to 2 cm to allow direct comparison with the available 1976 and 1985 data.

The model was run for 9700 days, corresponding to the period 1950 to mid 1976, with a constant flow field generated by 6 m/s wind from the southwest. Wind frequency data from meteorological sampling stations in the St. Clair Region during the period 1951-1980 show a predominantly moderate wind speed (5-8 m/s) with a southwesterly flow in all seasons (Great Lakes Institute 1986). Initial 1950 conditions of cesium-137 were set to zero in all segments. The organic carbon content of each segment was adjusted within the range of 0.0% to 5% until the model results matched the 1976 cesium data. This calibration exercise was verified by running the model

for an additional 3300 days (9 years) and comparing the results to the observed 1985 data.

Octachlorostyrene (OCS)

OCS was first reported in the lower Great Lakes in 1980 (Kuel et. al. 1980); however, information regarding its sources and environmental effects is limited. The only documented and recognized regional source of OCS, a by-product of several industrial processes including chlorine and solvent production, appears to be chemical companies in the Sarnia area (Great Lakes Institute 1986, Oliver and Bourbonniere 1985). OCS concentrations in sediments from the St. Clair River indicate that the source is located along the eastern shore of the St. Clair River, possibly from drainage of the Scott Road landfill and Dow Chemical's First Street Sewer discharge (Oliver 1987). Little historical data exists, however, and the magnitude of total loading to Lake St. Clair is unknown. Limno-Tech, Inc. (1985) speculated that OCS was introduced to the lower Great Lakes beginning in the 1970s as industries manufacturing chlorine converted from a process using mercury to one resulting in OCS as a by-product. Concern exists because OCS tends to bioconcentrate and is a chlorinated hydrocarbon. The simulation of OCS in Lake St. Clair is intended as an application of the model.

Pugsley et. al. (1985) presented the distribution of OCS levels in surficial (0-10 cm), diver-collected sediments for 1983. The values ranged from non-detectable to 26.2 $\mu\text{g/kg}$. The distribution of OCS showed a concentrated plume extending from the mouth of the South Channel towards the

the head of the Detroit River, very similar to the pattern of cesium-137 in the surficial sediments. Great Lakes Institute (1986) estimated the total load of OCS to Lake St. Clair to be about 1.9 lbs/day, based solely on model results in which the load was adjusted until predicted sediment concentrations matched the data. In the present study, the load was assumed to enter the lake solely through the South Channel outflow because the source of OCS is believed to be located along the eastern shore of the St. Clair River.

The model was run for 5000 days with a constant flow field corresponding to a 6 m/s wind from the southwest. Initial conditions of OCS were set to zero in all segments based on the assumption that background levels of OCS in Lake St. Clair prior to the 1970s were negligible. The active layer depth was set to 10 cm for direct comparison with the data. The chemical constants used in the OCS simulation, taken from Ibrahim (1986), are presented in Table 2 (e.g., K_{ow} , K_{oc} , molecular weight, etc.).

Polychlorinated Biphenyls (PCBs)

As a final application, the model was used to simulate the fate and distribution of total PCBs in Lake St. Clair. PCBs were first prepared in 1881 and had been manufactured and extensively used since 1930 for industrial purposes where extreme thermodynamic conditions exist such as dielectric fluids, heat transfer agents, and flame retardants (Limno-Tech, Inc. 1985). They are formed by the chlorination of biphenyl in the presence of an iron catalyst. PCBs are relatively nonvolatile, insoluble in water,

soluble in organic compounds, have high dielectric constants, are relatively inert towards acids, alkalies, and other corrosive chemicals, and are stable towards oxidation (Roberts et. al. 1978). They are of particular concern because of their known toxicity to biota, low solubility in water, bioaccumulation, and extreme environmental persistence.

Frank et. al. (1977) measured PCB concentrations of surficial sediments (0-2 cm) collected from Lake St. Clair in 1970 and 1974. They noted that the distribution of PCB in 1970 showed a concentrated plume entering from the St. Clair and Thames Rivers. Great Lakes Institute (1986) estimated the annual load of total PCB to the lake to be 1860 lbs (5.1 lbs/day), based on model simulations in which the load was adjusted to reach the best comparison between model predictions and measured values in 1974. This value is comparable to 1-4 lbs/day, a Lake St. Clair PCB load estimate calculated from Lake Huron outflow concentrations and average atmospheric and tributary loading rates for Lakes Erie and Huron during the late 1970s (Thomann and Mueller 1983). It was assumed that 18% of the total load entered through Thames River, 16% through the Clinton River, and 66% through the St. Clair River. The atmospheric input of PCB was assumed negligible based on an atmospheric loading rate of 1.0×10^{-10} lbs/m²/day which is the average value for Lakes Erie and Huron (Thomann and Mueller 1983).

The model was run for 4 years with a constant flow field corresponding to a 6 m/s wind from the southwest. Initial conditions of PCB were set equal to the 1970 values (Figure 3). The active layer was set to 2 cm for direct comparison with the data. The chemical constants used in the PCB simulation, taken from Mabey et. al. (1982), are presented in Table 3.

RESULTS AND DISCUSSION

Chloride

The magnitude and distribution of simulated chloride concentrations in the water column of Lake St. Clair agree very well with the corresponding data for cruises 3, 6, and 8. Figures 4 and 5 compare the observed concentrations (left frame) and the predicted concentrations (right frame) for all four cruises. The model did especially well in predicting the chloride concentrations in Anchor Bay and in locating the 7, 7.5, and 8 mg/l contour lines. Although it did quite well overall, the simulation corresponding to cruise 3 (Figure 4a) tended to overpredict the concentrations along the northeast and east shores of the main lake (from Figure 1, segments 55, 58, 61, 79, 82, and 103). The simulation corresponding to cruise 5 (Figure 4b) overpredicted the entire eastern half of the main lake. This condition will be addressed in the next paragraph. The simulation corresponding to cruise 6 (Figure 5a) slightly underpredicted the values along the eastern shore between Anchor Bay and the main lake (segments 25, 34, 37, 46, and 49). The simulation corresponding to cruise 8 (Figure 5b) was probably the best of the four, although it slightly underpredicted the concentrations along the northwestern shore of the main lake (segments 28, 40, and 64).

Examining the simulations generated using wind directions other than the observed directions and the no wind case revealed that simulations using the observed winds for cruises 3, 6, and 8 were unique solutions. They more

closely matched the data than simulations using any other wind direction and the no wind case. The simulated chloride concentrations for cruise 5 did not agree well with the data using the observed average wind speed of 5 m/s from the north (Figure 4b). However, simulations generated using winds from the NE, E, and SE agree much better with the data. Looking more closely at the observed wind directions from cruise 5; 13 stations measured winds from the north, 7 from the NE, 3 from the E, 4 from the SE, 1 from the S, zero from the SW, 2 from the W, and 3 from the NW. Therefore, it is not inconceivable that the NW, E, and SE simulations agree well with the data since 14 of the 33 stations reported winds from these three directions. Cruise 5 results may point out the importance of easterly winds in flushing dissolved compounds from the relatively low flowing eastern portion of Lake St. Clair.

In general, considering that the wind conditions were averaged over 10-11 days and over at least 30 stations, the distribution of simulated chloride concentrations in Lake St. Clair were quite close the observed data. The results of the chloride simulations tend to confirm the accuracy of the wind-induced transport mechanisms used in the Lake St. Clair Contaminant Fate and Transport Model.

Cesium-137

Model-simulated 1976 cesium-137 concentrations in surficial (0-2 cm) sediments compare well with observed 1976 values for Lake St. Clair (Figure

6a). Through calibration of the organic carbon content of the sediments, the model was able to match the magnitude and distribution sediment-bound contaminant in the active layer throughout the lake. The calibrated organic carbon content values closely matched the observed distribution of fine-grained surficial (0-10 cm) sediments in 1983 and 1984 and the observed distribution of organic carbon content of surficial (0-10 cm), SCUBA diver collected sediments in 1983 (Great Lakes Institute 1986). However, the magnitude of the calibrated values ranged from 0.14% to 5% (areal mean = 1.27%), while the observed values ranged 0.06% to 1.9% (mean = 0.58%). Kaiser et. al. (1985) and Maguire et. al. (1985) reported values of percent organic carbon in Detroit River sediments which were also consistently higher than those reported in the Great Lakes Institute report. Ibrahim (1986) and Great Lakes Institute (1986) used values of 5% for their model simulations.

The calibrated organic carbon contents, combined with the organic carbon partition coefficient, K_{oc} , and the suspended solids concentrations, yielded water column dissolved Cs-137 fractions of 0.77-0.99; the lower values located in the zones of highest deposition (i.e. fined-grained sediment, rich in organic carbon). The average value for the open-lake segments was 0.84 (n=10). Robbins (1985) reported a constant value of the fraction of dissolved Cs-137 equal to 0.847 for the open-waters of each of the Great Lakes.

Without any further calibration, the model was run for an additional 3300 days, corresponding to 1985. The predicted magnitude and distribution

of sediment-bound Cs-137 in the active layer compare well with observed 1985 values (Figure 6b). Cs-137 was concentrated in the sediments along the South Channel-Detroit River corridor in 1976 and 1985, closely matching the distribution of fine-grained, organic-rich sediments in the depositional zones of Lake St. Clair. Modeled and observed maximum cesium-137 concentrations in the active sediment layer declined during this time period from about 5 dpm/g to about 2 dpm/g due to decreased loading, radioactive decay, particle resuspension, and burial to the deep sediments. In addition, the model predicted the total lake-wide accumulation of Cs-137 in Lake St. Clair sediments to be 41 Ci in 1985 (corresponding to an average of 8.6 dpm/cm²), which agrees reasonably well with the measured 1985 value of 37 Ci (Robbins and Oliver 1987).

During the 35 years of simulation, the model predicted a total Cs-137 loading of 800 Ci. Of the total load, 720 Ci or 90%, exited through the Detroit River, 38.8 Ci or 5%, were lost due to radioactive decay, and 41.5 Ci or 5%, remained in the system. The calibration and verification exercises performed during the cesium-137 simulations provided valuable insight to the processes associated with sediment-bound contaminant movement. Cesium-137 proved to be a unique data set in Lake St. Clair. The loading function was well documented, the initial conditions were known, and two sets of spatially-complete observations were available. The knowledge gained from the Cs-137 simulations (e.g., organic carbon contents) was applied to the following OCS and PCB simulations.

Octachlorostyrene

The simulation of OCS in Lake St. Clair was intended as an application of the model, not necessarily as a further test of the model's ability to predict an observed distribution. A fundamental problem existed: the actual time-variable loading function was unknown. However, on the basis of Great Lakes Institute (1986) estimates, the load was assumed to be constant at 1.9 lbs/day. The model was run until the simulated OCS levels in the active layer (0-10 cm) agreed with the observed 1983 values. This occurred at 4500 days, or just over 12 years (Figure 7), implying that the load was first introduced in the latter part of 1970. This result is consistent with Limno-Tech, Inc.'s (1985) speculation that OCS was introduced to the lower Great Lakes beginning in the 1970s.

Using the sediment organic carbon values from this study, the estimated OCS load, and the constants in Table 2, the model was able to reproduce the observed OCS pattern in the sediments; that of a concentrated plume of OCS extending from the mouth of the South Channel to the head of the Detroit River. However, the model-calculated plume was wider and slightly longer than the measured plume. The model predicted that the mean and maximum sediment concentrations in 1983 were 3.8 and 23.1 $\mu\text{g/kg}$, respectively. These compare with 2.7 and 26.2 $\mu\text{g/kg}$ reported by Pugsley et. al. (1985). The model predicted 1983 active layer bio-bound OCS levels of 0-96 $\mu\text{g/kg}$ dry wt., with a mean concentration of 20 $\mu\text{g/kg}$ dry wt. Pugsley et. al. (1985) reported levels of 2-154 $\mu\text{g/kg}$ dry wt. (mean = 43 $\mu\text{g/kg}$ dry wt.) measured in whole clam tissue (Lampsilis radiata siliquoidea) collected in Lake St. Clair during 1983.

Even though 55% of the St. Clair River flow is directed through the North and Middle Channels, the negligible levels of OCS in the sediments of Anchor Bay tend to verify that the majority of the OCS load to Lake St. Clair entered through the South Channel from its likely source in Sarnia. Model-calculated loss rates ranged from 0.03-0.08 day⁻¹ in the water column and 0.34×10^{-4} - 0.37×10^{-3} day⁻¹ in the sediments.

During the 4500-day simulation period, the model predicted that 3.9 MT of OCS entered Lake St. Clair. Of this total load, 2.6 MT or 68%, were flushed from the system through the Detroit River, 0.7 MT or 18%, were lost due to biological degradation and volatilization, and 0.5 MT or 13%, remained in the system. That which remained in the lake was concentrated in the sediments between the South Channel and the Detroit River. It is worth noting once again that the OCS simulation was performed without prior knowledge of the OCS load to Lake St. Clair. Although we were able to adequately reproduce the 1983 OCS observations using a constant load of 1.9 lbs/day for 4500 days, this solution is not necessarily unique. There is no reason to believe that the load remained constant during the entire simulation period. Any number of time-varying load magnitude and duration combinations could have produced similar results. However, with known initial conditions (zero concentration in all segments), the model was able to predict how much OCS (3.9 MT) had to be loaded into the system to produce the 1983 observations. It also provided some insight on the origin of the OCS load to Lake St. Clair.

Polychlorinated Biphenyls

The simulation of total PCB in Lake St. Clair was also intended as an application of the model. However, as with the OCS simulation, the loading function of PCB was unknown during the period 1970-74. Great Lakes Institute (1986) estimated the load to be about 5 lbs/day, based on model simulations. This load was used in the present study. With initial conditions set equal to conditions in 1970 (Figure 3), and using the constants presented in Table 3, the model was able to reproduce the observed sediment PCB distribution in 1974 fairly well (Figure 8). In general, the model accurately predicted the 1974 PCB sediment concentrations in the Anchor Bay and the open-lake sediments. However, the model tended to overpredict the PCB values along the eastern and western segments of the main lake, which may indicate additional or increased PCB sources in these areas.

The data indicate a decline in mean lake-wide sediment (0-2 cm) concentration of total PCB from 19 $\mu\text{g/kg}$ 1970 to 10 $\mu\text{g/kg}$ in 1974 and in maximum sediment PCB concentration from 40 $\mu\text{g/kg}$ in 1970 to 28 $\mu\text{g/kg}$ in 1974 (Frank et. al. 1977). The model simulated a similar 4 year decline in mean active layer sediment concentration from 19.8 $\mu\text{g/kg}$ to 8.7 $\mu\text{g/kg}$ and in maximum sediment concentration from 39.0 $\mu\text{g/kg}$ to 26.0 $\mu\text{g/kg}$. The model predicted 1974 active layer bio-bound total PCB levels of 31-212 $\mu\text{g/kg}$ dry wt., with a mean concentration of 97 $\mu\text{g/kg}$. No comparable literature estimates of bio-bound PCB were available for the early 1970s. However, Pugsley et. al. (1985) reported mean values of 90.6 and 44.2 $\mu\text{g/kg}$ whole

clam tissue (*L. radiata*) for Aroclors 1254 and 1260, respectively, in Lake St. Clair during 1983.

The model-calculated volatilization rates ranged from 0.11-0.18 m/d. This range compares well with the theoretical rates for Aroclor 1242, 0.21 m/d, and Aroclor 1260, 0.17 m/d (Richardson et. al. 1983). The total loss rate was calculated to be 0.04-0.11 day⁻¹ in the water column and 0.34×10^{-4} - 0.45×10^{-3} day⁻¹ in the sediments.

From 1970 to 1974, the model predicted that the total system mass of PCB decreased from 2.5 MT to 1.5 MT. During this time period, 3.4 MT of PCB were loaded into the system, 2.3 MT were flushed from the lake through the Detroit River, and 2.1 MT were lost due to biological degradation and volatilization. Again, as with OCS, the PCB simulation was performed without prior knowledge of the PCB load to Lake St. Clair. Thus, the 1974 solution, although an adequate reproduction of the data, is not necessarily unique. Any number of time-varying load magnitude and duration combinations could have produced similar results. However, with known initial conditions (1970 values), the model was able to predict how much PCB (3.4 MT) had to be loaded into the system to produce the 1974 observations. It also provided some insight to the possibility of additional PCB sources along the eastern and western main-lake segments of Lake St. Clair.

LITERATURE CITED

- Ambrose, R.B., Hill, S.I., Mulkey, L.A. 1983. User's Manual for the Chemical Transport and Fate Model TOXIWASP. Version 1. EPA Report No. EPA-600/3-83-005. Environmental Research Laboratory, Office of Research and Development, U.S. Environmental Protection Agency, Athens, Georgia. 178 pp.
- Bell, G.L. 1980. Lake St. Clair and St. Clair and Detroit Rivers Chemical and Physical Characteristics Data for 1974. NOAA Data Report ERL GLERL-12. Great Lakes Environmental Research Laboratory, Ann Arbor, Michigan. 10 pp.
- Bukata, R.P., Jerome, J.H., and Bruton, J.E. 1987. Remote and In Situ Optical Studies of Seston and Suspended Sediment Concentrations in Lake St. Clair. Preliminary Report. Rivers Research Branch, National Water Research Institute, CCIW, Burlington, Ontario, Canada.
- Burns, L.A., Cline, D.M., and Lassiter, R.R. 1982. Exposure Analysis Modeling System (EXAMS): User Manual and System Documentation. EPA Report No. EPA-600/3-82-023. Environmental Research Laboratory, Office of Research and Development, U.S. Environmental Protection Agency, Athens, Georgia. 145 pp.

DiToro, D.M., Fitzpatrick, J.J., Thomann, R.V. 1983. Documentation for Water Quality Analysis Simulation Program (WASP) and Model Verification Program (MVP). EPA Report No. EPA-600/3-81-044. Environmental Research Laboratory, Office of Research and Development, U.S. Environmental Protection Agency, Duluth, Minnesota. 145 pp.

Frank, R., Holdrinet, M., Braun, H.E., Thomas, R.L., Kemp, A.L.W., and Jaquet, J.-M. 1977. Organochlorine insecticides and PCBs in sediments of Lake St. Clair (1970 and 1974) and Lake Erie (1971). Sci. Tot. Environ. 8:205-227.

Great Lakes Institute. 1986. A Case Study of Selected Toxic Contaminants in the Essex Region. Volume I: Physical Sciences. Parts One and Two. Final Report. University of Windsor, Windsor, Ontario, Canada.

Ibrahim, K.A. 1986. Simulation of Pollutant Transport Responses to Loading and Weather Variations in Lake St. Clair and the Connecting Channels. PhD Dissertation, Department of Civil Engineering, University of Windsor, Windsor, Ontario, Canada. 436 pp.

Kaiser, K.L.E., Comba, M.E., Hunter, H., Maguire, R.J., Tkaca, R.J., and Platford, R.F. 1985. Trace organic contaminants in the Detroit River. J. Great Lakes Res. 11(3):386-399.

Kuel, D.W., Leonard, E.N., Welch, K.J., and Veith, C.D. 1980. Identification of hazardous organic chemicals in fish from the Ashtabula River, Ohio and Wabash River, Indiana. Association of Official Analytical Chemists Journal. 63:1238-1244.

Limno-Tech, Inc. 1985. Summary of the Existing Status of the Upper Great Lakes Connecting Channels Data. Limno-Tech, Inc., Ann Arbor, Michigan. 157 pp.

Mabey, W.R., Smith, J.H., Podoll, R.T., Johnson, H.L., Mill, T., Chou, T.-W., Gates, J., Waight Partridge, I., Jaber, H., and Vanderberg, D. 1982. Aquatic Fate Process Data for Organic Priority Pollutants. EPA Report No. EPA-440/4-81-014. Monitoring and Data Support Division, Office of Water Regulations and Standards, Washington, DC. 145 pp.

Maguire, R.J., Tkaca, R.J., and Sartor, D.L. 1985. Butyltin species and inorganic tin in water and sediment of the Detroit and St. Clair Rivers. J. Great Lakes Res. 11(3):320-327.

Oliver, B.G. 1987. St. Clair River Sediments. A level II report for the Upper Great Lakes Connecting Channels Study. ELI Eco Laboratories Inc., Rockwood, Ontario, Canada.

- Oliver, B.G. and Bourbonniere, R.A. 1985. Chlorinated contaminants in surficial sediments of Lakes Huron, St. Clair, and Erie: implications regarding sources along the St. Clair and Detroit Rivers. J. Great Lakes Res. 11(3):366-372.
- Pugsley, C.W., Hebert, P.D.N., Wood, G.W., Brotea, G., and Obal, T.W. 1985. Distribution of contaminants in clams and sediments from the Huron-Erie corridor. I-PCBs and octachlorostyrene. J. Great Lakes Res. 11(3):275-289.
- Richardson, W.L., Smith, V.E., and Wethington, R. 1983. Dynamic mass balance of PCB and suspended solids in Saginaw Bay-a case study. In Physical Behavior of PCBs in the Great Lakes. Edited by Mackay, D., Paterson, S., Eisenreich, S.J., and Simmons, M.S. Ann Arbor Science, Ann Arbor, Michigan. 442 pp.
- Robbins, J.A. and Oliver, B.G. 1987. Accumulation of fallout cesium-137 and chlorinated organic contaminants in recent sediments of Lake St. Clair. Can. J. Fish. and Aquatic Sci. Submitted.
- Robbins, J.A. 1985. The Coupled Lakes Model for Estimating the Long-Term Response of the Great Lakes to Time-Dependent Loadings of Particle-Associated Contaminants. NOAA Technical Memorandum ERL GLERL-57. Great Lakes Environmental Research Laboratory, Ann Arbor, Michigan. 41 pp.

Roberts, J.R., Rodgers, D.W., Bailey, J.R., and Rorka, M.A. 1978.

Polychlorinated Biphenyls: Biological Criteria for an Assessment of their Effects on Environmental Quality. Publication No. NRCC 16077. National Research Council of Canada, NCR Associate Committee on Scientific Criteria for Environmental Quality Ottawa, Canada. 172 pp.

Rybczyk, J.M. 1986. Cluster Analysis of Physical, Biological, and Chemical Data of Lake St. Clair. Unpublished Data. Great Lakes Environmental Research Laboratory, Ann Arbor, Michigan.

Schwab, D.J. and Liu, P.C. 1987. Development of a Shallow Water Numerical Wave Model for Lake St. Clair. Upper Great Lakes Connecting Channels Study Final Report. Great Lakes Environmental Research Laboratory, Ann Arbor, Michigan.

Simons, T.J. and Schertzer, W.M. 1986. Modelling Wave-Induced Sediment Resuspension in Lake St. Clair. Preliminary Report. Aquatic Physics and Systems Division, National Water Research Institute, Burlington, Ontario, Canada.

Thomann, R.V. and Mueller, J.A. 1983. Steady state modeling of toxic chemicals-theory and application to PCBs in the Great Lakes and Saginaw Bay. In Physical Behavior of PCBs in the Great Lakes. Edited by Mackay, D., Paterson, S., Eisenreich, S.J., and Simmons, M.S. Ann Arbor Science, Ann Arbor, Michigan. 442 pp.

Table 1. Lake St. Clair parameters and constants required by the TOXIWASP model. Units are consistent with model specifications. Reference in parentheses.

Variable	Description	Units	Value
<u>Parameter</u>			
TEMP	Average segment temperature	degrees C	13(1)
DEPTH	Depth of segment	feet	6.6-17.1(2)
VELOC	Average water velocity	feet s ⁻¹	0.48(2)
WIND	Average wind velocity	meters s ⁻¹	6(3)
BACTO	Bacterial population density	cells ml ⁻¹ (water) cells 100 g ⁻¹ (bed)	10 ⁶ (4) 10 ⁷ -10 ⁸ (4)
BIOMS	Total biomass in segment	mg l ⁻¹ (water) g m ⁻² (bed)	10(4) 1-50(4)
OCS	Sediment organic carbon content	dimensionless	0.14-5.0%(5)
PCTWA	Percent water in sediments	dimensionless	1.67-1.71(5)
PH	Hydrogen ion activity	pH units	8.1(1)
WS	Settling rate in water column	m day ⁻¹	3.0(6)
	Resuspension rate in bed	cm yr ⁻¹	0.45-0.95(5)
	Contaminant burial rate	cm yr ⁻¹	0.1(7)
CMPET	Light extinction coefficient	m ⁻¹	2.0(1)
<u>Constant</u>			
OCB	Biomass organic carbon content	dimensionless	4%(5)
CLOUDG	Average cloud cover	tenths of full cover	4(3)
LATG	Geographic latitude	degrees and tenths	43.2

¹STORET DATA

²Schwab (1987)

³GLI (1986)

⁴Ibrahim (1986)

⁵This study

⁶Simons and Schertzer (1986)

⁷Robbins and Oliver (1987)

Table 2. Octachlorostyrene constants required by the TOXIWASP model. Units are consistent with model specifications. From Ibrahim (1986).

Constant	Description	Units	Value
KOW	Octanol water partition coefficient	$l_w l_{oct}^{-1}$	2.48×10^6
KOC	Organic carbon partition coefficient	$l_w kg^{-1}$	1.20×10^6
MWT	Molecular weight	$g mole^{-1}$	300
HEN	Henry's Law constant	$Atm m^3 mole^{-1}$	10^{-4}
VAP	Vapor pressure	torr	4×10^{-5}
SOL	Aqueous solubility	$mg l^{-1}$	0.02

Table 3. Total polychlorinated biphenyl constants required by the TOXIWASP model. Units are consistent with model specifications. From Mabey et. al. (1982).

Constant	Description	Units	Value ¹
KOW	Octanol water partition coefficient	$l_w l_{oct}^{-1}$	4.14×10^5
KOC	Organic carbon partition coefficient	$l_w kg^{-1}$	2×10^5
MWT	Molecular weight	$g mole^{-1}$	300
HEN	Henry's Law constant	$Atm m^3 mole^{-1}$	3.9×10^{-3}
VAP	Vapor pressure	torr	5×10^{-4}
SOL	Aqueous solubility	$mg l^{-1}$	5×10^{-2}

¹Within range of values for Aroclors 1232, 1242, 1248, 1254, and 1260. They most closely resemble values for Aroclor 1248.

LIST OF FIGURES

- Fig. 1. Lake St. Clair numerical grid used in Lake St. Clair contaminant fate and transport model, based on EPA's TOXIWASP. Segment numbers correspond to water column segments. Active layer and deep layer segment numbers are determined by adding one and two, respectively, to the water column numbers.
- Fig. 2. Loading of Cs-137 to Lake St. Clair during the period 1950-1985 from three principal sources: inflow from Lake Huron, direct atmospheric fallout, and land runoff from the watershed. Reprinted from Robbins and Oliver (1987).
- Fig. 3. Observed distribution and model initial conditions of PCBs ($\mu\text{g}/\text{kg}$) in surface (0-2 cm) sediments in Lake St. Clair, 1970. Data from Frank et. al. (1977).
- Fig. 4. (a) Comparison of observed and model-simulated concentrations (mg/l) of chloride in the water column of Lake St. Clair during cruise 3, 19-29 June 1974. Wind speed: 4 m/s NE. (b) Comparison of observed and model-simulated water column concentrations (mg/l) of chloride during cruise 5, 15-24 July 1974. Wind speed: 5 m/s N. Data from Bell (1980).
- Fig. 5. (a) Comparison of observed and model-simulated concentrations (mg/l) of chloride in the water column of Lake St. Clair during cruise 6, 5-15 August 1974. Wind speed: 5 m/s E. (b) Comparison of observed and model-simulated water column concentrations (mg/l) of chloride during cruise 8, 16-25 September 1974. Wind speed: 6 m/s W. Data from Bell (1980).
- Fig. 6. (a) Comparison of observed and model-simulated concentrations (dpm/g) of Cs-137 in surface (0-2 cm) sediments of Lake St. Clair in 1976. Model was calibrated by adjusting the spatially-varying sediment organic carbon content until the model results matched the data. (b) Comparison of observed and model-simulated 0-2 cm concentrations (dpm/g) of Cs-137 in 1985. The 1985 simulation verified the 1976 model results. Data from Robbins and Oliver (1987).
- Fig. 7. Comparison of observed and model-simulated concentrations ($\mu\text{g}/\text{kg}$) of octachlorostyrene (OCS) in surface (0-10 cm) sediments of Lake St. Clair in 1983. The simulation was run until the model results agreed with the 1983 data, which occurred at day 4500; implying that the load was first introduced during the latter part of 1970. Data from Pugsley et. al. (1985).
- Fig. 8. Comparison of observed and model-simulated concentrations ($\mu\text{g}/\text{kg}$) of total PCBs in surface (0-2 cm) sediments of Lake St. Clair in 1974. Simulation was run for four years using initial conditions presented in Figure 3. Data from Frank et. al. (1977).

